AMBULATORY MONITORING AND ANALYSIS OF ECG SIGNALS

A THESIS

submitted in fulfilment of the
requirements for the award of the degree
of
DOCTOR OF PHILOSOPHY
in
ELECTRICAL ENGINEERING

By

P. K. KULKARNI

DEPARTMENT OF ELECTRICAL ENGINEERING
UNIVERSITY OF ROORKEE
ROORKEE-247 667 (INDIA)

SEPTEMBER, 1997

CANDIDATE'S DECLARATION

I hereby certify that the work is being presented in the thesis entitled **"AMBULATORY MONITORING AND ANALYSIS OF ECG SIGNALS"** in fulfillment of the requirement for the award of the Degree of Doctor of Philosophy submitted in the Department of Electrical Engineering of the University of Roorkee, Roorkee is an authentic record of my own work carriedout during the period from **December,1994 to September,1997** under the supervision of *Dr. H.K.Verma and Dr.Vinod kumar, Professors in the Electrical Engineering Department, University of Roorkee, Roorkee.*

The matter embodied in this thesis has not been submitted by me for the award of any other degree.

(P.K. KULKARNI)

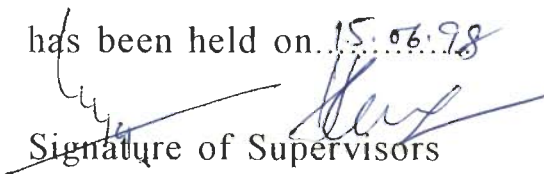This is to certify that the above statement made by the candidate is correct to the best of our knowledge.

ROORKEE
Date September, 29,1997

(Dr. H.K.VERMA)	(Dr.VINOD KUMAR)
Professor	Professor
Dept.of Electrical	Dept. of Electrical.
Engineering.	Engineering
University of Roorkee	University of Roorkee
Roorkee (INDIA)	Roorkee (INDIA)

The Ph.D.Viva-voce examination of Shri P.K. Kulkarni Research scholar has been held on.15.06.98

Signature of Supervisors   Signature of External Examiner

Signature of Head of Department.
Electrical Engineering Department
University of Roorkee, Roorkee
U.P. (India)

ABSTRACT

Ambulatory monitoring of ECG signals is an important topic of research in the area of Biomedical Engineering. The basic concept lies in providing medical service to the cardiac patients away from the hospital. A complete computer based management of the ambulatory monitoring of ECG forms the basis of the present work. Two improtant aspects, namely development of ambulatory monitoring system for arrhythmia analysis and data compression techniques for both, on-line and off-line, applications were identified for the development of this concept by the author.

A good number of ambulatory monitoring systems are available for arrhythmia analysis of ambulatory patients. Various techniques and algorithms for arrhythmia analysis and data compression are available. More important once are briefly reviewed in the thesis.

A prototype ambulatory monitor has been developed based on 8088 microprocessor system. There are five modules in the ambulatory monitoring unit. The first one is the data acquisition module capable of recording three channels simultaneously. The input ECG signal is conditioned using instrumentation amplifier and highpass, notch and lowpass filters in cascade for eliminating baseline wander, power line interference and high frequency noise contents, respectively. The second module consists of 8088 microprocessor and accessories, including EPROM which is loaded with the software. The module acts as the controller of the ambulatory monitor. The digital input/output module consist of different programmable peripheral chips for providing timing signals, parallel to serial data communication and pushbutton / keyboard controls. The memory module consists of three banks of read/write memories , each bank providing 256 k bytes for ECG data storage. The indication and display module gives a visual indication of different events and alarms and a numerical display of the crrent values of ECG parameters, such as heart rate, intervals etc. All the five modules interfaced to each other through a mother board are controlled by a sophisticated and efficient software package developed using assembly level programming .

Having developed the hardware for ambulatory monitor, two important algorithms were developed for processing the ECG signal. The first algorithm is for eleminating various types of noise present in the ECG signal. but not completely eleminated by the hardware . The second algorithm developed provides ECG wave recognition to measure amplitudes (P, Q, R, S and T waves) and the characteristic points (P_{on} , P_{off} , QRS_{on}, QRS_{off} and T_{end}) of the ECG. The detection of QRS complex has been obtained through slope-threshold method. The baseline estimation is made according to the recommendations of the Common Standards for Quantitative Electro-cardiography (CSE) Working Party. The parameters obtained through this software are stored in a file for further processing and use.

For arrhythmia analysis, the commonly used ECG features are intervals and segments; these are derived using the parameters obtained from the software developed for the ECG wave recognition and characteristic point location. Diagnostic criteria are then applied for classifying the arrhythmia. The five different types of arrhythmias for which diagnostic rules are clearly known namely, Normal sinus rhythm, Atrial premature contraction, Sinus arrhythmia, First degree AV block and Sinus bradycardia, are identified from the derived features of ECG based on these rules. A six - step logical procedure has been adopted in the algorithm for arrhythmia classification. The algorithm thus developed has been tested on different records of Massa-chusetts Institute of Technology/Beth Israle Hospital (MIT/BIH) arrhythmia database. These results are then compared on a beat-by-beat basis, each beat being individually examined and verified against the results available in the database.

Another aspect of the thesis is data compression, transmission and reconstruction of the original signal. Data compression becomes neces-sary to reduce the memory requirement for storage and to speed-up data transmission in real-time. Various direct data compression techniques exist in the literature; five out of these techniques have been selected for compari-son and evaluation. The performance of these techniques have been mea-sured using two indices, namely, compression ratio and percent root-mean-square difference besides fidelity of the reconstructed signal. The major contribution in this work is the study of the effect of sampling frequency on

the performance of direct data compression techniques and the clinical acceptabilty of such schemes. In order to know the clinical acceptable quality of the reconstructed signal, peak, boundary and interval measurements were made both on the reconstructed and the original signals of the same record and the results were compared.

Data compression techniques have also been proposed for offline storage as database. Two transform based methods namely, fast Fourier transform (FFT) and fast Walsh transform (FWT) based on the principle of successive doubling, have been developed for the purpose. The performance of these compression schemes are evaluated using compression ratio and PRD ,besides fidelity of the reconstructed signal. Further, to know the extent to which the clinical information is preserved in the reconstructed signal, peak, boundary and interwave measurements were made on both the original and reconstructed signals and compared.

The algorithms for real-time implementation in ambulatory monitor have been selected on the basis of simplicity and speed of execution to implement on microprocessor. Algorithms for data acquisition, data compression, QRS detection and arrhythmia analysis have been developed and implemented using assembly language. The performance of the algorithms have been tested individually. The data acquisition algorithm has been tested by acquiring the ECG signal from the normal human beings. The ECG recorded is of good quality and can be used straightaway for further analysis. Other algorithms namely data compression, QRS detection and arrhythmia interpretation have been tested on standard MIT/BIH Arrhythmia database. The performance of all these algorithms is found to be satisfactory.

The results obtained from different algorithms tested on the standard CSE & MIT/BIH database are critically examined in the thesis. The conclusions in respect of the work presented are given at the end of the thesis and finally the scope for future improvements is brought out.

ACKNOWLEDGMENT

CONTENTS

CHAPTER - 1

INTRODUCTION

CHAPTER - 1

INTRODUCTION

1.1 Background

Continuous monitoring of electrocardiogram of ambulatory patients is common clinical practice, as there exists a correlation between ventricular arrhythmias and mortality in this class of patient. This type of monitoring includes both the measurement of heart rate, so as to compare it with the limits of normality and identification of isolated ventricular ectopic beats, which calls for continuous beat- by - beat analysis.

Direct visual monitoring of ECGs by human being is a tough task whose monotony increases the loss of clinical information. Over the last four decades great efforts have been made in this direction to develop automatic analog or digital system to carry out this function. Computer-based ECG analysis system have proved to be more efficient , having made possible rapid retrieval of data for storage and techniques of data presentation whose clinical utility is evident. The great majority of these systems follow conventional techniques to extract parameters from the raw ECG signal for statistical or heuristic classification algorithms. The basic problem is the identification and selection of characteristics containing sufficient clinical information to discriminate between the different categories which it is desired to classify. Although computerized ECG analysis started in the early 1960's, a review of the state of art of automated ECG analysis reveals that, both on-line and off-line techniques have not made any major improvement as far its diagnostic performance is concerned [16]. While existing commercial systems are generally effective in processing the ECG signal starting from data acquisition to parameter extraction, interpretation of the signal is still referred to the cardiologist. This is because of two reasons, first, interpretation is generally performed at a rudimentary level by clinical computing systems compared with the performance of experienced physician. Secondly, medical decision support tools are hardly accepted as such [34]. However, when the

role is clearly support in situations where repetitive and extenuating decisions are to be made, medical decision tools can be accepted at large.

The introduction of microprocessor technology, although reducing cost and space requirements, has also put restrictions on the size of the extraction algorithms used for such applications. This is owing to the conflict between the limited speed of calculation of microprocessor systems and the demand for real-time processing inherent in monitoring. A minimum number of parameters must be obtained which differentiate between different class of cardiac arrhythmias and whose real-time implementation on microprocessor systems is feasible.

The main goal of electrocardiographic processing and analysis using computers is to record the ECG signal and process the signal for extracting few parameters of interest from the signal for further diagnosis. This is achieved through the following processing stages:

(1) Data acquisition
(2) Filtering and analog to digital conversion
(3) Identification of waves and characteristic points
(4) Parameter extraction
(5) Disease classification

In the first step (1) the classical methods of ECG signal acquisition are still followed and are used to pick up the signal generated by the cardiac muscles from the body surface. The acquired ECG signal is amplified and conditioned in the processing stage. In the next step (2) noise in the acquired signal is minimized so as to improve signal to noise ratio. Further, the analog signal is digitized through A/D convertor and fed to the microprocessor or computer as well as to display and storage devices. The digitized data is then processed for wave recognition and delineation in step (3). After the wave has been identified, a baseline estimation for establishing time and amplitude references are marked. This forms the basis for parameter measurement. Recognition of the ECG wave starts with the QRS complex identification which is the most significant even in the ECG signal [18,55,109,133]. Here after, the onward processing is application dependent. In step (4)

depending on the application for which the processing is to be done, a few relevant parameters are extracted from the measured parameters. For ambulatory monitoring ,the ECG features that are commonly used for classification of arrhythmias are based on timing data [2,22]. In the final step (5) these features are grouped to form patterns, which are, then used for classifying the arrhythmias.

Holter recorder is used for continuously recording the ECGs from ambulatory patients and it does not perform on-line analysis for detecting the arrhythmias. On the other hand ambulatory monitor is one which not only records the ECGs but also performs the on-line arrhythmia analysis and generates alarm in case of lethal arrhythmias. In the present application ambulatory monitoring system has been developed for arrhythmia analysis. The unit will be placed in the ambulance to record the ECGs on way to the hospital and generates alarm to alert paramedical staff to provide necessary preliminary rescuitation to in cardiac patient. The ECGs recorded during this period are transmitted to the cardiac center for expert opinion and also stored in the RAM for the detailed arrhythmia analysis off-line.

1.2   History of Ambulatory ECG Monitoring

In 1961 Holter invented a taperecorder for continuously recording the ECG from ambulatory patients [56]. The Holter recorders are commonly employed for recording ECGs up to 24 hours. Developments in Holter taperecorder and their clinical use was reviewed by Webster [149]. High speed analysis of ECG was usually performed manually by a trained nurse but occasionally semiautomatically or automatically by a computer [115]. This has lead to improved health care and improved clinical investigations. Use of computer made a drastic change in Holter data storage, data reduction and analysis. The subject of automated arrhythmia detection was reviewed by Oliver et. al. 1974 [108]. The design of the ambulatory arrhythmia monitor really become possible after the invention of the microprocessor. Previously, large mainframe computers were used [115]. Microprocessor technology permitted the design of a compact even portable device that analysed the ECG signal in real-time. Walters developed a microprocessor based bed side monitor [146].

Portable microcomputer based arrhythmia monitoring system was first attempted in 1978 [133,136,149]. Thakor et al presented the detailed design implementation and evaluation of an ambulatory monitor [131]. Fancott and Wong (1980) reported a system for the analysis of 24 hours ambulatory ECG 60 times real-time [35]. Craig (1980) described a microprocessor based recorder for the generation of histograms of beat-to-beat heart rate during daily physical activity [30]. A simple microprocessor system for the on-line analysis of electrocardiograms was proposed by Mahoudeaux et.al. in 1981 [90]. Tompkin's (1982) discussed the trends in portable arrhythmia monitoring towards portable computer that travels with the patient to do real-time data analysis and capture the arrhythmias [137]. Arrhythmia detection algorithm was developed for intensive care unit by Ruiz et.al. [119]. Method involved mapping cardiac arrhythmias in real-time using 8 bit microprocessor system. Thakor (1984) presented the techniques of ambulatory ECG signal acquisition, processing, arrhythmia detection and performance evaluation of automated arrhythmia detectors [131]. Design of a portable battery powered microcomputer based monitor for recording ambulatory ECG and its analysis was described in 1984 by Thakor [132]. Tompkin's in 1983 reported a patient - worn intelligent arrhythmia system [138]. The micro-monitor is a miniaturized data processing systems which was developed by Wiesspeiner and Xu in 1992 for the requirement in the ambulatory patient monitoring [150]. Blazek and Janecek (1995) described the design of a simple low cost device for surgeries and ambulance monitoring [17]. De-maso et al reported the ALTER DISCS developed for use in an ambulatory clinical environment [32].

Large amount of noise is often superimposed during ECG recording. Both high frequency electromyographic (EMG) noise and low frequency baseline wander are present.Removal of these noise is a significant step in the ECG processing. Filtering of ECG is to enhance signal discrimination and is used in a multitude of circumstances. Broadly speaking filtering improve visual quality of the signal. The most common filters used are low-pass, highpass and bandpass or notch filters[100]. These filters have fixed corner or centre frequencies and operate on each lead of multilead ECG independently. Recently, variety of adaptive digital filters for the removal of

powerline interference are reported in the literature [4,37,42]. Several approaches to the problems of baseline wander removal have been presented. Most common among them are linear interpolation and cubic splines used by MacFarlane et. al. 1977; Meyer and Keiser 1975, Bartoli et. al. 1983 [14,88,95]. Another approach for eliminating the baseline wander is by means of linear phase filtering have been described by Van - Alste and Schilder; 1985, Makivirta et.al. 1985; Van Alste et al 1986, Mortara 1981 [91,101,143,144].

The performance of ambulatory monitor heavily depends on the accurate and reliable detection of the QRS complex. During last two decades, software QRS detectors have become an integral part of the ambulatory monitor. Conceptually, most QRS detectors are grouped into two broad categories. The first is the preprocessors and the second being the decision rule. Preprocessing can be further subdivided into linear filtering and nonlinear transformation. Linear filtering is based on the analysis of the first derivative of the ECG [13,19,29,145]. Others have used a filter, capable of giving symmetry to the QRS complex, and then select the control point within a specific threshold detector [141]. Yet, other approach used is the contour limiting technique [97]. Goovaerts et. al. 1976 presented a technique that yield good results when signal to noise ratio value is high [46]. Conversely the cross-difference technique is more adequate in the presence of particularly noisy ECG signal [82]. Other algorithms make use of cross-correlation technique and ECG signal envelope maximum [1,33,106]. For the measurement of RR interval algorithms improving sensitivity have been developed [38,53,93,107,111]. The averaging technique has been proposed by Barbaro et. al. in 1983 [13]. The most recent approach for QRS detection makes use of Wavelet transform [81,121].

Wave recognition and parameter extraction is a classical problem in the analysis of the ECG signal. A number of papers have been reported for the detection of ECG wave characteristics points. Kyrkos et.al. demonstrated the usefulness of time recursive prediction for event detection[77]. A complete solution to the fundamental problem of ECG analysis, viz, delineation of the signal into its components using discrete cosine transform (DCT) was presented by Murthy et.al. [103]. An automatic ECG analysis program

DECGAP was described by Gritzali et. al. [47] for detection, recognition and parameter extraction of the ECG waves. Laguna et.al. presented a method to automatically detect the characteristic points [78]. Fundamental problem of delineation of ECG signal into components waves using Fast Fourier Transform (FFT) was developed by Murthy et.al. [104]. A simple non iterative method for complete wave delineation of the electrocardiograms is derived by modelling its discrete cosine transform is reported by Niranjan [105]. Recently an algorithm based on Wavelet transform have been developed for detecting ECG characteristic points [81]. Real-time online implementation using wavelet transform for detecting ECG characteristic points was presented by Sahambi et.al. [121].

Automatic monitoring of arrhythmias can be broadly classified into two groups. In the first group, the only characteristic analyzed is heart rhythm, in the form of RR interval, on the basis of which classification and/or display algorithms are framed [89,116,135]. The second line of approach are based on algorithms, taking into account both rhythm and features reflecting the morphology of the ECG waveform. Further, this approach is subclassified into two types. First among these makes use of extracting multiple features for the morphological characterization of the QRS complex. Such features include duration, offset, the area under the curve, maximum slope etc. [26,35]. Inconjuction with RR interval data, these parameters are very useful for training the classification. The second sub group employs a single feature to characterize QRS morphology. The most frequently used is the cross-correlation coefficient, which quantifies the similarity between a given waveform and previously stored template [36,69]. A new approach to classify the cardiac arrhythmias makes use of artificial neural network (ANN) Classifier based on adaptive resonance and fuzzy theory have been investigated for identifying normal and abnormal beats by Ham et al 1996 [49].

Data compression methods for ECG signals have gained popularity in recent years, to meet the requirements of digital storage as database, for subsequent and several comparisons besides the transmission of these signal over a communication line. The main goal of any such technique is to derive maximum data compression without loosing the clinically significant information. There are three signal domain in which ECG data compression can

be performed, the first one is compression in time domain, which consists in approximating the signal by a sequence of straightlines and slopes. Cox et. al. 1968 reports ECG data compression using amplitude- zone time epoch coding (AZTEC) [27]. Muller (1978) developed turning point technique for real-time ECG data compression [102]. In 1982, Abenstein and Tompkins described a hybrid method for ECG data compression called CORTES, which is the combination of AZTEC and TP technique [2]. A modified AZTEC method for real-time application was suggested by Furht & Perez (1988) [41]. Scan-along-polygonal approximation technique (SAPA) was presented by Ishijima et.al. 1983 [64]. The second category of algorithms to compress data involves extraction of the different frequency components using suitable transform and storing the coefficients in the compressed form, Fourier transform [11,114], Walsh transform [72], cosine and Haar transform [5]. The latest is the Wavelet transform [20,23,54,81,121]. The third method of compression is parameter extraction in which a set of parameter is extracted from the signal, which are then used for reconstructing the signal, Peak picking [25] Linear prediction [120] and neural network approach [50].

1.3 Objective and Plan of the Present Work

Present work investigates the various technical aspects of the development of a microprocessor-based ambulatory monitoring system. The proposed system has been developed with an objective to provide efficient medical care to cardiac patients, while being shifted to hospital. A complete computer based management of the ambulatory monitoring of ECG forms the basis of the work presented here.

The work started with the development of intelligent ambulatory ECG monitoring system. The monitor is built around 8088 microprocessor. It consists of five modules. The first one is the data acquisition module which records three channel ECG simultaneously. Hardware filtering is carried out to suppress the noise present while recording the ECG. The second module being 8088 microprocessor which forms the heart of the system, controls the whole system functions. The third module is the memory module which is used for storing the data during the transit period and will be used for

further analysis off-line. Digital input/output module is the fourth one which provides interfacing between processor and other modules. Last one being the indication and display module which will provide necessary indication and display during monitoring. The hardware developed is completely software controllable.

In the next stage of the work if, the recorded signal contains the unwanted noise such as powerline interference and baseline wander these are eliminated through software filtering using digital filters off-line. Algorithm has been developed for the simultaneous removal of powerline interference and baseline wander. After this, ECG wave detection and its characteristic point location is done. The process of wave recognition starts with the identification of most important event which represents ventricular depolarization that is QRS complex. This has been achieved using slope threshold criteria. An upper and lower thresholds have been set to discriminate between noise and P and T waves. Followed by this, R peak is detected as a point where the slope changes from positive to negative. Further P and T wave are identified and their onset and offsets are determined using the slope threshold and search criteria. The parameters such as PR interval, RR interval, QRS duration etc. are derived from the measured parameters and stored for further processing.

In the ECG processing final task is to classify the disease. Algorithm for disease classification based on decision logic approach has been developed. The parameters which have been obtained in the previous stage are used here for interpretation of the arrhythmia. Developed algorithm checks for different criteria given in the disease classification table for each class of disease. If any of the conditions are satisfied a particular class of disease is identified accordingly.

In addition to the above automation data compression techniques have been developed to reduce the memory requirement both for storage and transmission of the ECG signal to cardiac care centres and also used for storage as database. Direct and transformation data compression algorithms have been developed along with their validation for clinical acceptability. Direct

data compression techniques are useful in the real time application and on the other hand transform based techniques will be used for compressing the large amount of data for storage as database for future reference.

1.4   Thesis Organization

The work embodied in the thesis is organized in nine chapters. The current chapter presents introduction to computer processing of ECG signals. State of art of ambulatory monitoring from the days of simple Holter recorder for recording ECGs upto 24 hours to the present days ambulatory monitor. Subsequently the objective of the proposed work is highlighted.

The second chapter introduces the concepts of electrocardiography, starting from the anatomy of heart, to mechanical and electrical activity of the heart. An ECG cycle demonstrating the waves and intervals which reflects the functioning of the heart are briefly explained. A brief explanation about the different types of electrodes is given in this chapter. For the purpose of recording the ECG, generally three and twelve leads systems are used and are presented here. Brief descriptions of standard database namely CSE and MIT/BIH are covered in this chapter. These database have been used in the present work for evaluating the performance of the algorithms developed for ECG signal processing.

Hardware of ambulatory monitor is described in chapter 3. The monitor is built around 8088 microprocessor and has fiye modules. The basic design considerations, selection of microprocessor and choice of ADC are presented in this chapter. Descriptions of each module are also detailed in this part of the thesis.

Chapter 4 deals with the problem of noise, ECG wave recognition and characteristics point location. After hardware filtering, the signal may still contain noise. Therefore off-line preprocessing is required to suppress the noise if any present in the ECG signal. For this purpose digital filtering technique is developed and presented in this chapter. This chapter also presents the algorithms for ECG wave recognition and characteristic point location.

The subject matter of chapter five covers the arrhythmia disease classification. The output file generated from the ECG wave recognition and characteristic point algorithm has been used as the input file for the arrhythmia classification program. The algorithm developed for arrhythmia interpretation uses six step logical procedure. The parameter used for classification are RR, PP, QRS, PR, P-duration and rhythm. Then the diagnostic rules were applied for classifying the arrhythmias. The software developed for this purpose is very simple and efficient.

Chapter 6 describes different techniques of ECG data compression suitable for on-line real-time applications. Five direct data compression techniques have been proposed in this chapter. Their performance has been tested using different parameters such as compression ratio, PRD, fidelity and diagnostic acceptability. In addition to this an important study has been made to show the effect of sampling frequency on the performance of the direct data compression algorithms.

Chapter 7 deals with off-line data compression techniques for the purpose of off-line storage of ECG data for future use as database. Two transformation methods namely fast Fourier transform and fast Walsh transform methods have been proposed for data compression. Both algorithms performance are tested using important indices, namely, compression ratio, PRD, fidelity and diagnostic acceptability. A compression between FFT and FWT based on execution time, compression ratio and fidelity is presented in this chapter.

The software for ambulatory monitor has been covered in chapter 8. It includes four softwares, for data acquisition, data compression, QRS detection and arrhythmia interpretation. Each algorithm has been tested for their performance independently and the results are given in this chapter.

Chapter 9 presents the conclusions drawn from the presented work and finally, the scope for future improvements is suggested in this chapter.

CHAPTER - 2

THE ELECTROCARDIOGRAPHY

CHAPTER - 2

THE   ELECTROCARDIOGRAPHY

2.1   Introduction

Electrocardiogram (ECG) has become a diagnostic tool almost as popular as stethoscope and blood pressure measuring instrument. It's purpose is well known in the non-medical community as well. The main advantages of this instrument are its simplicity and non-invasive characteristic, which provides faithful representation of the function of the heart. It's immense importance lies in the detection of the cardiac arrhythmias and conduction defects. It is essential to know the fundamentals of anotomy of the heart to understand the characteristics of the ECG signal..

2.2   The   Heart

Heart forms one of the most important and critical organs of the human body. The basic function of the heart is to circulate the blood through two major circulating systems namely, the pulmonary circulation in the lungs and the systemic circulation in the rest of the body ; this is carried out by the co-ordinated rhythmic contraction and relaxation of the different chambers of the heart [21].

The walls of the heart comprises of several layers. The inner most layer is known as endocardium made up of smooth lining of cells. Next to this is the myocardium which consists of muscular cells and constitutes the major part of the heart mass. It is their co-ordinated contraction and relaxation which causes the chambers of the heart to pump the blood. The

myocardium is covered by a layer of fat called epicardium. The pericardial sac which encloses the heart is formed by the outer most two layers of the pericardium which have a small amount of lubricating fluid between them. Though the heart consists of several layers, it is only the myocardium which is responsible for generating large amount of current, sufficient to be detected and recorded on the surface of the human body [12,44,87].

The heart consists of four chambers. The upper two chambers are named as, the left and right atria, are synchronized to act together [21,31,112]. Similarly the lower two chambers called the ventricles, operate together. Right atrium and right ventricle are coupled through a valve called tricuspid valve and similarly the left atrium and left ventricle are connected through mitral valve as shown in Fig. 2.1.

2.3   Mechanical Activity of the Heart

Basically the heart acts like a two stage pump, comprising of four chambers. The incoming oxygen deficient blood enters the heart through superior and inferior Venacavas and fills the right atrium. When filled, it contracts and forces the blood through the tricuspid valve into the right ventricle; this in turn, contracts to pump the blood into the pulmonary circulation system. When ventricular pressure is more than the atrial pressure, the tricuspid valve closes and the pressure in the ventricle forces the semilunar pulmonary valve to open, there by causing blood to flow into the pulmonary artery, which then divides into the two lungs.

From the pulmonary vein, the blood enters the left atrium, and from there it is pumped through the mitral valve or bicuspid valve into the left ventricle by contraction of the atrial muscles. When the left ventricular muscles
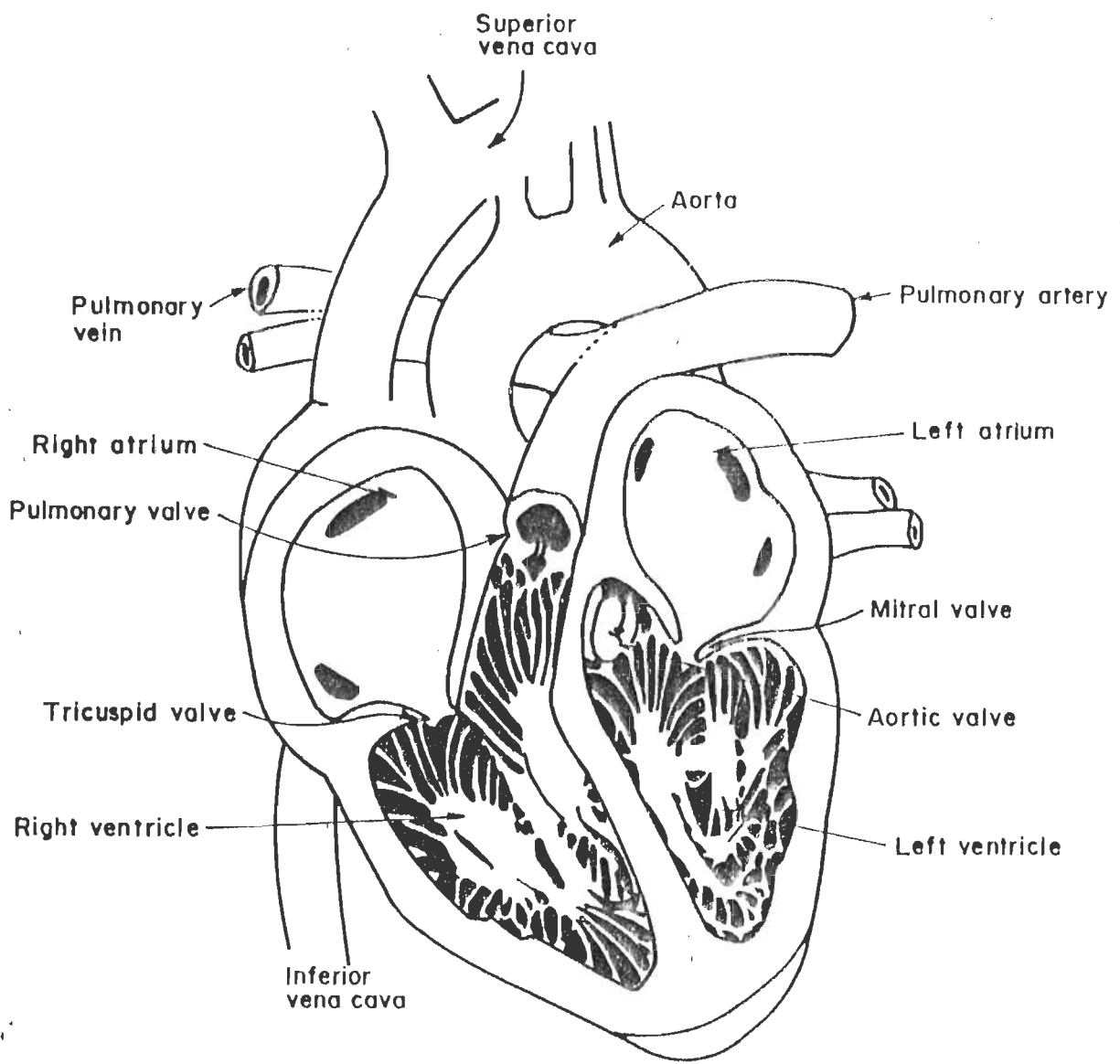
Fig. 2.1 Cross section of heart

contract, the pressure produced by the contraction, mechanically closes the mitral valve and the build of pressure in the ventricles forces the aortic valve to open, causing the blood to rush from the ventricle into the aorta [31,87,112]. First two atria are synchronized to pump together followed by the two ventricles.

2.4 Electrical Activity of the Heart

Fig. 2.2 shows the electrical conduction system of the heart. The electrical activity in the heart originates at the sinoatrial (SA) node [31,112]. It is a group of specialized cells that generate action potential at a regular rate and is also named as pacemaker. The action potential generated by the pacemaker spreads in all directions along the surface of both the atria towards the junction of the atria and ventricles and terminates at a point near the heart called the atrioventricular (AV) node. At this node, some special fibers acts as delay line to provide proper co-ordination between the action of the atria and ventricles. From here, the impulse travels through "bundle of His", which further separates into left and right bundle branches. The fibers in the bundle called Purkinje fibers further divide into branches in their respective ventricles.

2.5 Electrocardiogram (ECG)

The electrical activity associated with the depolarization and repolarization of cardiac muscle can be recorded and analyzed by means of ECG. The electrical activity during the cardiac cycle is characterized by five separate waves of deflections designated as P,Q,R, S and T. A normal ECG consists of a series of five successive waves. The P-wave represents electrical activation of the atria, the QRS complex represents depolarization of the ventricles and the T-wave reflects recovery of the ventricles. The atria

Fig. 2.2 Electrical conduction system of the heart

Labels on the figure:
- SA node
- AV node
- Bundle of His
- Right bundle branch
- Left bundle branch
- Left septal fibers
- Purkinje fibers
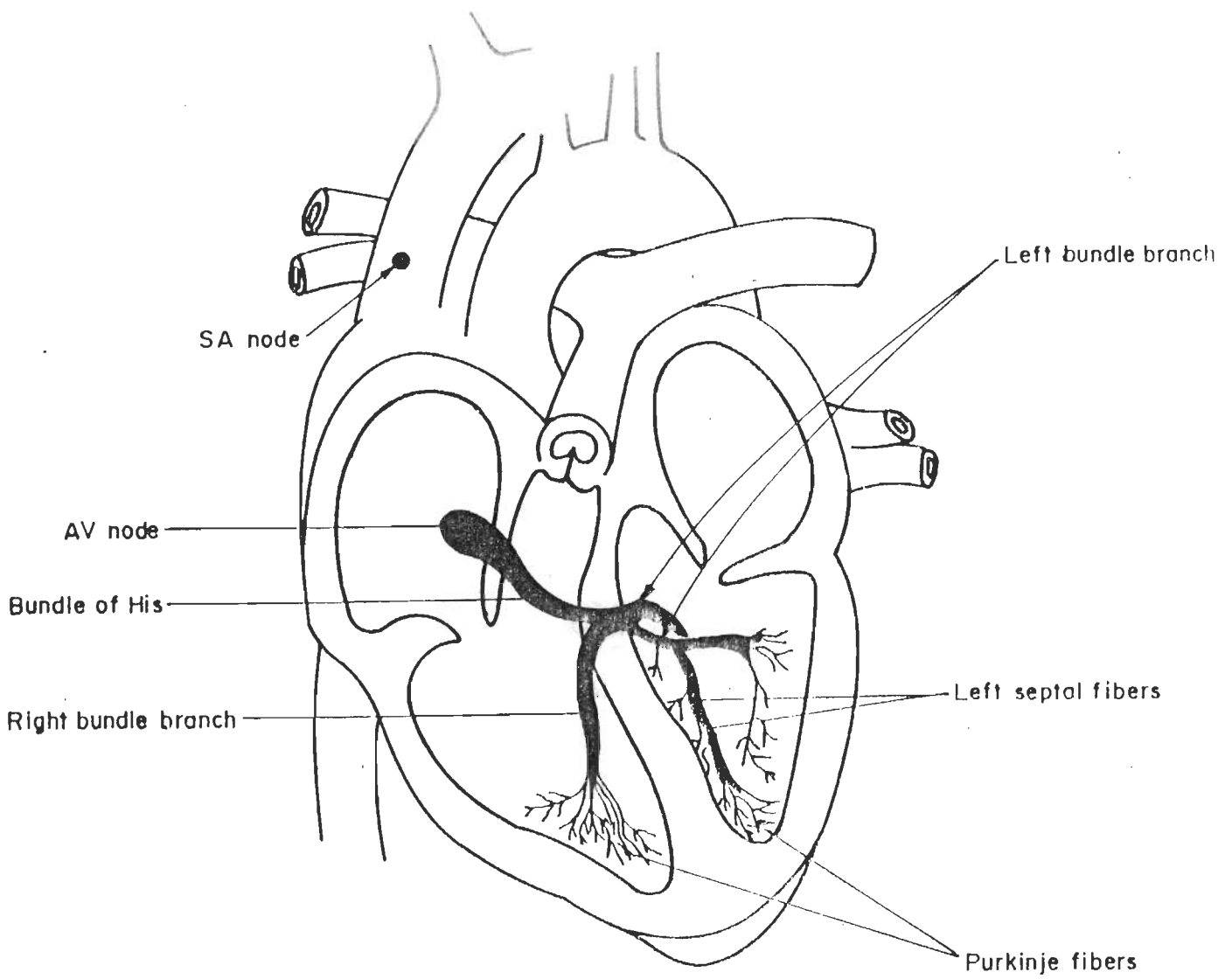
also have a recovery period but the wave for atrial repolarization is hidden in the QRS complex. The distances between the waves in the ECG are called intervals or segments [31,68]. The configuration of one complete ECG cycle demonstrating the waves intervals, and segments normally seen in the ECG is shown in Fig. 2.3 .

2.5.1   P Wave

The P wave is the first wave of the electrocardiogram represents the electrical activity associated with the original impulse emanating from the SA node and its passage through the atria. The presence of P wave with normal shape and size, it can be assumed that the impulse for cardiac contraction begins in the SA node. Absence or abnormal positioning of P wave indicates that the impulse is originated outside the SA node. It is normally upright in lead I & II but it is frequently diphasic or inverted in lead III. It is normally inverted in aVR and upright in aVF. It is variable in other leads. Its amplitude should not exceed 0.2 to 2.5 mV in any lead, and its normal contour is gently rounded - not pointed or notched (leads system is discussed in section 2.7).

2.5.2   PR Interval

The period lapsed from the beginning of P-wave to the beginning of QRS complex is represented as PR interval. It represents the time taken for an original impulse to travel from the SA node through the atria and AV node to the ventricles. With normal conduction, the duration of this interval ranges from 0.12 to 0.20 sec. If the duration of the PR interval is more than 0.2 sec it can be reasoned that a conduction delay (block) exists in the area of AV node. In some situations, the PR interval is unusually short (less than 0.1 sec). A shortened PR interval may indicate that an impulse reached
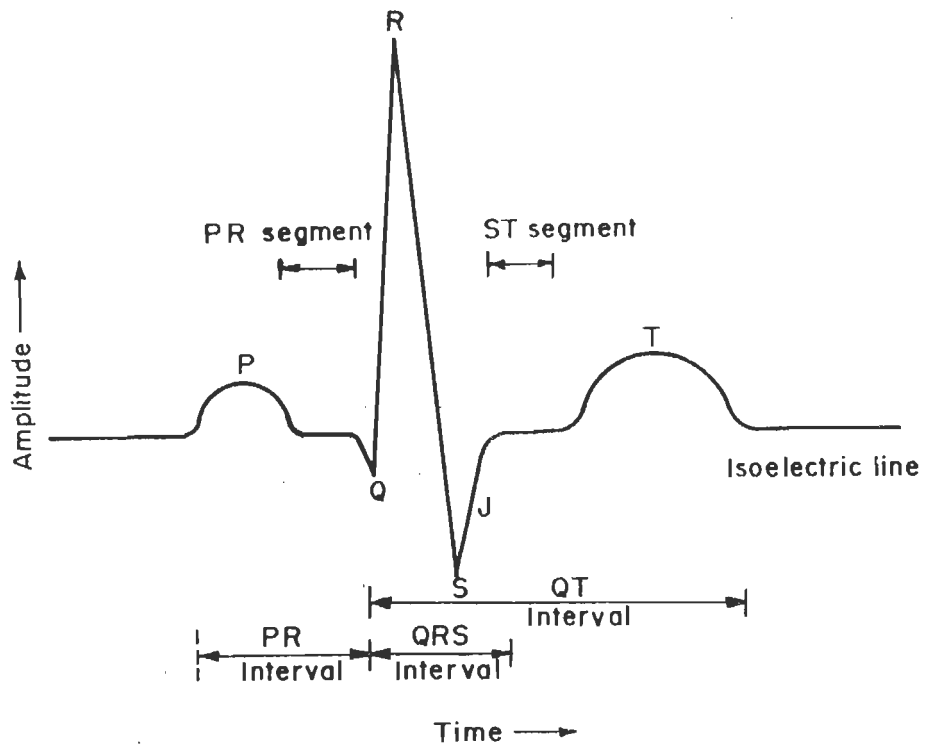
Fig.2.3 Normal cardiac cycle on the ECG.

the ventricle through a shorter than normal pathway. Abnormally short PR intervals are the most common features in the Wolffparkinson - White syndrome. This path provides a connection between the atria and ventricles that bypasses the AV node and therefore ,stimulates the ventricles prematurely. A junctional rhythm is generated in the area of the AV node instead of the SA node. In the case of junctional rhythm, the atria are depolarized in a retrograde direction. The P wave may be inverted or buried in the QRS complex. Depending on where in the AV node it generated a junctional rhythm, it can cause a shortened PR interval.

2.5.3 PR Segment

The P-R segment is a subset of PR interval. This segment is referred to as the baseline between the end of P wave and beginning of QRS complex. Usually isoelectric, it may be displaced in atrial infraction and in acute pericarditis. The normal value lies in the range from 0.04 to 0.16 sec.

2.5.4 QRS Complex

This complex is the most important event in the ECG as it represents depolarization of the ventricle muscle. The process of depolarization begins at the endocardium of the ventricle and progresses outward to the epicardial surface. This results in a complex consisting of an initial downward deflection (Q-wave), a tall upward deflection (R-wave) and a second downward deflection (S-wave). These three deflections comprising the QRS complex vary in size according to the lead being recorded. If the QRS complex contains only an R-wave, the points at which the complex starts and ends are marked as 'Q' and 'S' respectively, though , there are no actual 'Q' or 'S' waves. On the other hand if the QRS complex consists of only 'Q' wave, it is described as QS complex.The J point is defined as the offset

point of the S wave [8]. Its location is determined by the occurrence of a significant reduction in slope.

For interpreting the QRS complex, there are at least six common features that should be routinely examined i.e. duration, amplitude, presence of Q-wave electrical axis in the frontal plane (limb leads), relative prominence of the component waves in the precordial leads, and the general morphology including the presence and location of the notch. The QRS duration is measured from the beginning of the 'Q' wave to the end of 'S' wave. The normal value of QRS duration lies in the range from 0.05 to 0.10 sec. in case of standard limb leads. The chest leads frequently display, a slightly longer QRS duration 0.06 or 0.12 sec than the standard leads. If the QRS duration is greater than 0.12 sec. is indicative of abnormal intraventricular conduction. The amplitude of the QRS complex has wide normal limits.

2.5.5   ST Segment

This segment of the ECG reflects the period between the completion of depolarization and the beginning of the repolarization of the ventricular cells. Normally, this segment is isoelectric, meaning that, it is neither elevated nor depressed, because the positive and negative electrical forces within the ventricular myocardium are equal to one another during this period. Elevation or depression of the ST segment indicates an abnormality in the onset and recovery of ventricular muscle.

2.5.6   T Wave

The T wave represents the major portion of the recovery phase after ventricular depolarization. For the interpretation of T wave, normally, three

features are examined, namely direction, shape and height. Normally, T wave is upright in lead-I and II and in precordial leads, but it is normally inverted in aVR. The morphology of the T wave is normally flat and slightly asymmetrical. In some diagnosis, T wave amplitude is also important.

2.5.7 QT Duration

It defines the total duration of the combined phases of depolarization and repolarization of the ventricular muscle. This interval, is measured from the beginning of the QRS complex to the end of T wave. It varies with heart rate, sex and age and its normal values can be obtained directly from the standard table. A useful rule of thumb is that, the QT interval should be less than half of preceding RR interval. This holds good for normal sinus rates. The QT interval is lengthened in congestive heart failure, myocardial infraction and hypocalcemia [40,44,68,94]. The normal values of the various parameters of ECG (lead II) are summarised in Table 2.1.

2.6 Electrodes for ECG Recording

Almost every patient monitoring system is concerned with the ECG and hence the selection of the electrodes is a matter of general concern. The type of electrodes employed mainly depends on the application. Modern ECG recording electrode designers generally prefer silver-silver chloride (Ag-Agcl) recording element, that makes electrical contacts with skin through an electrode gel [130]. Usually, the gel consists of electrolytes such as NACL or KCL in isotonic concentration. The electrode body is most often made from porous form or fibric that does not impede respiration. The electrode adhesive should resist respiration and wetting, and at the same time should not cause irritation.

Table 2.1   Normal Values of ECG (Lead II) Parameters [31]

Wave Peaks (mV)	Intervals (sec)	Segments (sec)
P-wave=0.25	PR=0.12 to 0.2	PR=0.04 to 0.08
Q-wave 25% of R wave	QRS=0.05 to 0.12	ST=0.12 to 0.16
R-wave = 0.5 to 1.5	QT=0.35 to 0.4	
S-wave=0.2	Pwave=0.11	
T-wave=0.1 to 0.5		

Different types of electrodes have been in common use for recording the ECG signal from the subject [43]. A few of the more familiar types are shown in Fig 2.4. The earliest ECG measurements used immersion type of electrodes. A great improvements over the immersion electrodes were the plate electrodes, introduced for the first time in 1917. Commonly used electrodes for ECG recording consists of two rectangular or circular plates of German-silver, nickel-silver or nickel plated steel as shown in Fig. 2.4(a). When these electrodes are applied to a patient with electrode jelly, typical d.c. resistance values are in the range of 2 to 10 k ohms.

A very useful type of electrode is the suction -cup electrode as illustrated in Fig. 2.4(b). This type of electrode is commonly used in practice as an ECG chest electrode and as well suited for attachment to flat surface of the body and to regions where the underlying tissue is soft. Although the electrode looks to be physically large, this electrode has a small area because only the rim is in contact with the skin.

Yet, another type of ECG electrode which allows quick application is contained in a strip of adhesive tape. This electrode is shown in Fig. 2.4(c) consists of a lightweight metallic screen backed by a pad for electrolyte paste. Measuring approximately one and half inches square, it adheres well to the skin and exhibits a relatively low resistance. The adhesive backing holds the electrode intact and retards evaporation of the electrolytes. These electrodes are commercially available.

A most interesting and very practical ECG electrode designated as the multipoint electrode shown in Fig. 2.4 (d) consists of a 6x5 cm segment made of stainless steel or tin-plated soft iron. It is slightly curved to fit over fleshing parts of the body; the abrasive side is placed against the skin.
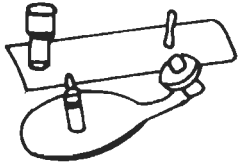
(a) Metal plates
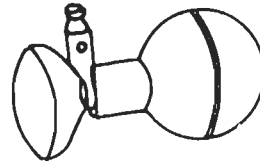
(b) Suction electrode
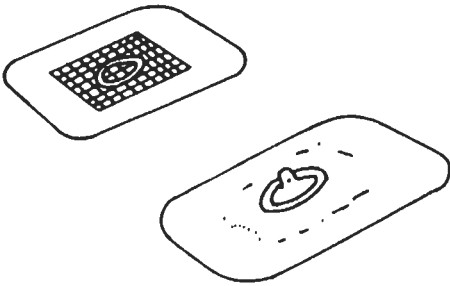
(c) Adhesive Type electrode

(d) Multipoint electrode

(e)

(f)

Ag/AgCl

(g)

Lead wire
Electrode paste
Wire screen
Rubber support
Body surface

(h)

Resin seal
Rubber suction cup

Lead to amplifier
Silver/Silver chloride contact pole
Space for soline jelly
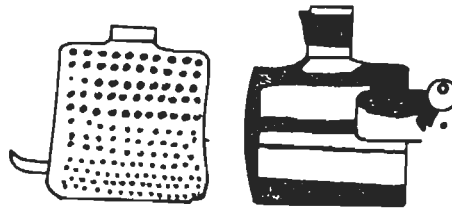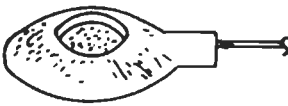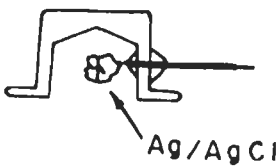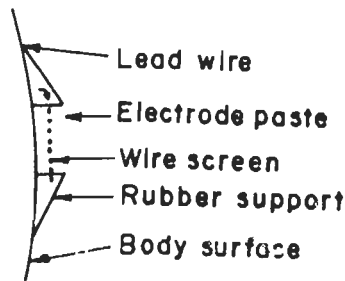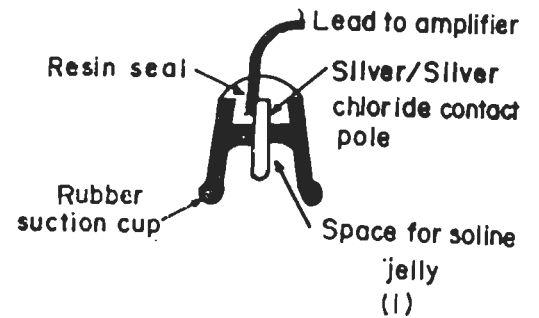
(I)

Floating or liquid junction electrodes

Fig. 2.4 Types of ECG electrodes

Multipoint electrodes are of special value in some unusual recording circumstances; for example, for screening the ECG in large number of human subjects, the short time required for application and removal is a most attractive feature. Multipoint electrodes are also useful in extreme environmental condition. In situations of low temperature and barometric pressure, it is difficult to store electrode pastes and jellies in their containers. The use of multipoint electrodes eliminates the need for these substances and permits easy recording under field conditions.

An electrode frequently used for recording exercise ECG is the floating electrode, sometimes referred to as the liquid junction electrode. In this type, the metal does not contact the subject; contact is made through an electrolyte bridge. The modern versions of floating electrodes takes different forms. One form, consisting of a zinc electrode recessed in a holder and contacting the palm via a film of jelly. Another type of floating electrode consists of a silver-silver chloride rod mounted centrally in a rubber cup filled with electrode jelly. This electrode, shown in Fig. 2.4(e) was found to have remarkably high electrical stability despite movement of the cup on the skin. A similar high-stability electrode, consisting resembling a top hat is illustrated in Fig. 2.4(f). This type of floating electrode which has become more popular in aerospace medicine and is now commonly used for recording ECG signals on moving subjects. In another type of floating electrode shown in Fig. 2.4 (g), the metalic conductor is mounted in a flat rubber or plastic washer which is cemented to the skin by special adhesives, the washer holds the electrode away from the skin, and contact is established via a thick film of electrolytic paste. Two more floating type of electrodes made of silver disks chlorided silver screen and plates, and disks of a compressed mixture of silver and silver chloride have been employed with

greater success and are shown in Fig. 2.4(h) and 2.4 (i) respectively. In general, these floating electrodes are of disposable type.

In the present application, metal plate cup type electrodes have been used for recording ECG. This electrode is selected because, they are commonly available and they make good contact with the skin. Another advantage being, they can be easily placed on the subject and will not cause any irritation.

2.7   Electrocardiographic   Leads

The electrical impulses generated within the conduction system of the heart, results into weak electrical currents that flows through out the entire body. By placing electrodes on the different locations of the body and connecting these electrodes to ECG machine, the ECG is recorded [31]. In electrocardiography, the amplitude, polarities and even timing and duration of the ECG are dependent to a larger extent upon the location of the electrodes on the body. So it is conventional to use a series of different electrode positions to record the ECG. It helps to view the conduction of electrical signal in the heart from different angles and directions. Each set of electrode locations from which the ECG is recorded is called lead. Depending on the application, ECG recording commonly uses two different lead systems namely, "three lead and twelve lead system". Three lead system is useful in ambulatory monitoring and the twelve lead system is extensively employed for detailed analysis and diagnosis for other cardiac diseases [94]. These lead systems can be classified as

(i)   Bipolar standard limb leads

(ii)   Unipolar leads

(iii)   Unipolar chest leads for precordial leads

(iv)   Orthogonal leads

2.7.1   Bipolar Standard Limb Leads

The bipolar standard limb leads I, II and III are the original leads selected by Einthoven to record electrical potential in the frontal plane as shown in Fig. 2.5. Electrodes are placed on the left arm (LA), right arm (RA) and left leg (LL) (In practice a fourth electrode is placed on the right leg (RL) and it serves as a ground electrode). The LA, RA and LL leads are then connected to their respective electrodes.

Each of the three ECG lead records the difference between two electrode sites. These potentials are as shown in the Fig. 2.5 (a), (b) and (c).

Lead-I   =   Potential difference between the left arm and the right arm

=   LA-RA

Lead-II   =   Potential difference between the left leg and right arm

=   LL-RA

Lead-III   =   Potential difference between the left leg and the left arm

=   LL-LA

Bipolar limb leads

(a) Lead I (b) Lead II (c) Lead III
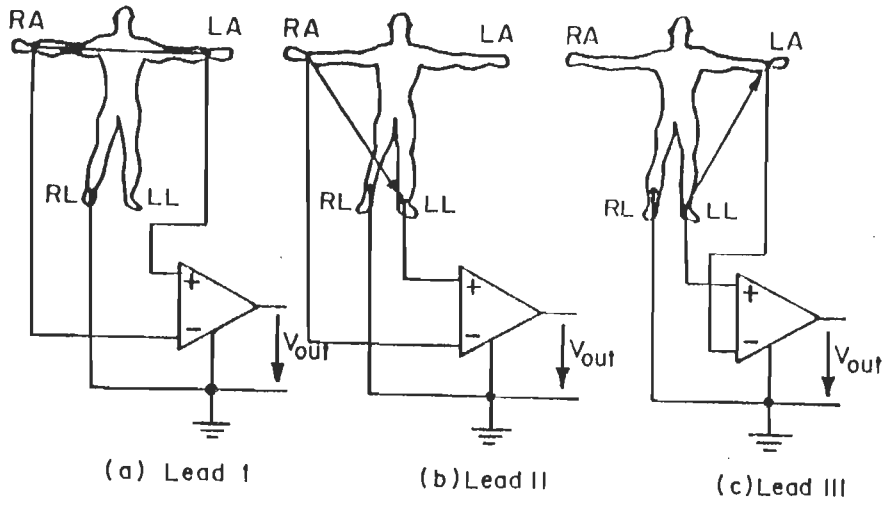
(Augmented) Unipolar limb leads

(d) Lead aVR (e) Lead aVL (f) Lead aVF
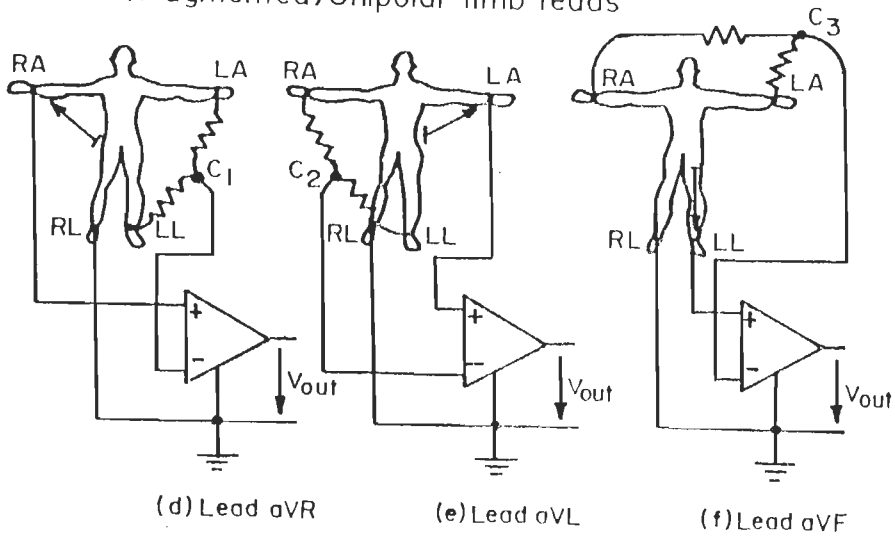
Precordial chest leads

$V_1 - V_6$
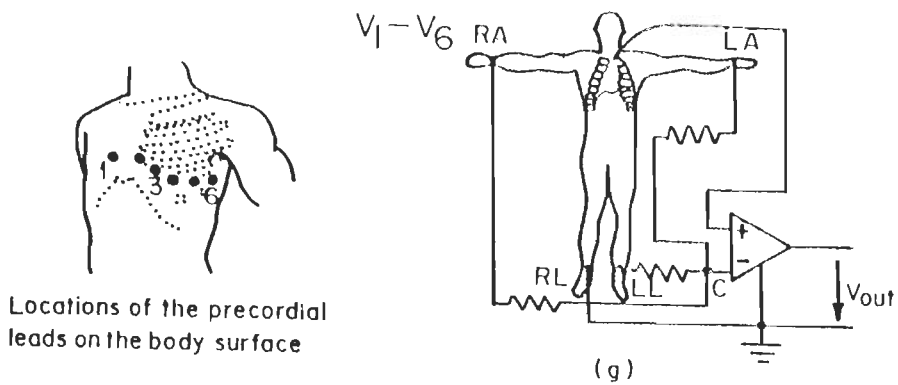
Locations of the precordial leads on the body surface

(g)

Fig. 2.5 Lead configuration of E.C.G. [31]

The relationship between the three bipolar limb leads is expressed algebraically by Einthoven equation as

$$\text{Lead II} = \text{Lead I} + \text{Lead III}$$

This is basically well known Kirrchoff's current law.

2.7.2 Unipolar Leads

Fig. 2.5 (d), (e) and (f) shows the unipolar augmented leads aVR, aVL, and aVF are introduced by Wilson in 1944. The potential difference measured by these leads are as follows:

Lead aVR = Potential difference between the right arm and the central terminal c_1 (junction of two equal resistors connected to left arm and left leg)

$$= RA - \left[\frac{LL + LA}{2} \right]$$

$$= 3/2\ RA.$$

Lead aVL = Potential difference between left arm and the central terminal c_2 (junction of two equal resistors connected to right arm and left leg).

$$LA - \left[\frac{RA + LL}{2} \right]$$

$$3/2\ LA$$

Lead aVF = Potential difference between left leg and the central terminal c_3 (junction of two equal resistors connected to right arm and left arm).

$$= LL - \left[\frac{RA+LA}{2} \right]$$

$$= 3/2 \ LL$$

If the axis of the bipolar and unipolar limb leads are superimposed a hexaxial reference system for six terminal plane leads is formed and is shown in Fig. 2.6.

2.7.3 Unipolar Chest Leads or Precordial Leads

The chest leads V_1-V_6 are shown in Fig. 2.5. A junction at central terminal 'c' is formed by connecting right arm, left arm and left leg electrodes connected through resistors of equal value. The potential at the junction 'c' of the resistors corresponds to the average potential of the three electrodes. Chest leads V_1-V_6 are the potential difference between the electrodes placed at the six different locations of the chest (as indicated on the diagram as 1,2,3,4,5 and 6 respectively) and the central terminal 'c' shown in the figure 2.5(g). The locations of electrodes for recording chest leads V_1, V_2, V_3, V_4, V_5 and V_6 are defined as below:

V_1 = Fourth intercostal space, at right sternal margin.

V_2 = Fourth intercostal space, at left sternal margin.

V_3 = Midway between V_2 and V_4.
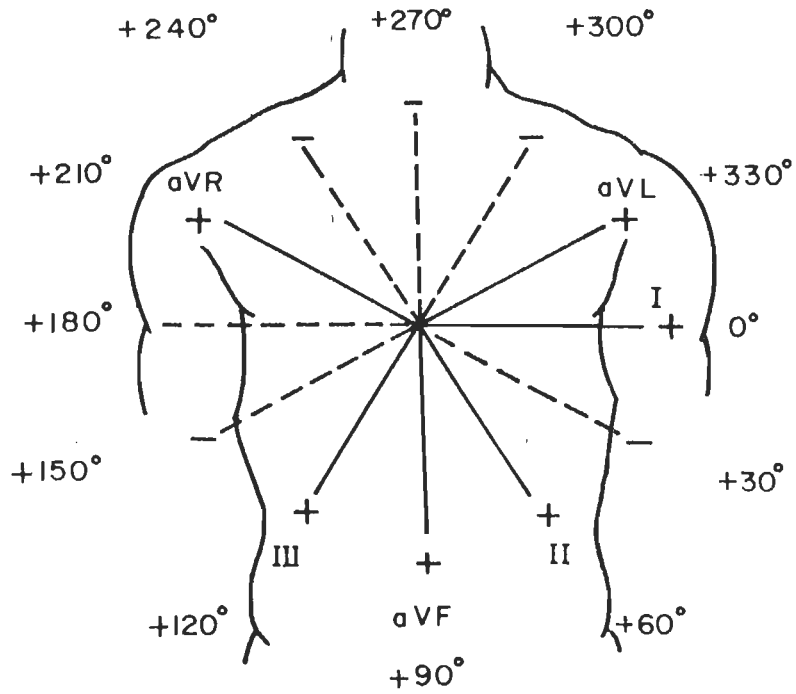
Fig. 2.6 Hexaxial reference system for six frontal plane leads

V_4 = Fifth intercostal space, at mid-clavicullar line.

V_5 = Same level as V_4, an anterior auxiliary line.

V_6 = Same level as V_4, an mid-auxiliary line.

Similar to standard and unipolar extremity leads a reference diagram may be drawn for the axis of the unipolar precordial leads and is shown in Fig. 2.7. The axis of the limb leads are located in the frontal plane, on the other hand those of precordial leads are located in the horizontal plane. The axis of the unipolar precordial leads is on a line extending from the location of the exploring electrode to the dipole centre of the heart. A complete set of standard 12 lead recording arrangement of ECG is shown in Fig 2.5.

2.7.4 Orthogonal Leads

An ideal lead system for recording ECG and vector cardiogram(VCG) essentially consists of three leads with the following characteristics:

(a) The leads must be perpendicular to each other and also to the horizontal, vertical, and sagittal axis of the body.

(b) The amplitudes of the three leads would be equal from vectorial standpoint.

(c) All the three leads would have the same strength and direction, not only for a single point within the heart, but for all points in the heart where electromotive forces are generated. Such leads are called corrected orthogonal leads. Theoretically these leads should contain all the information present in the normal 12 lead ECG [40]. By convention X,Y and Z are referred to as, horizontal, vertical and sagittal axis and hence these are usually referred to as XYZ leads.
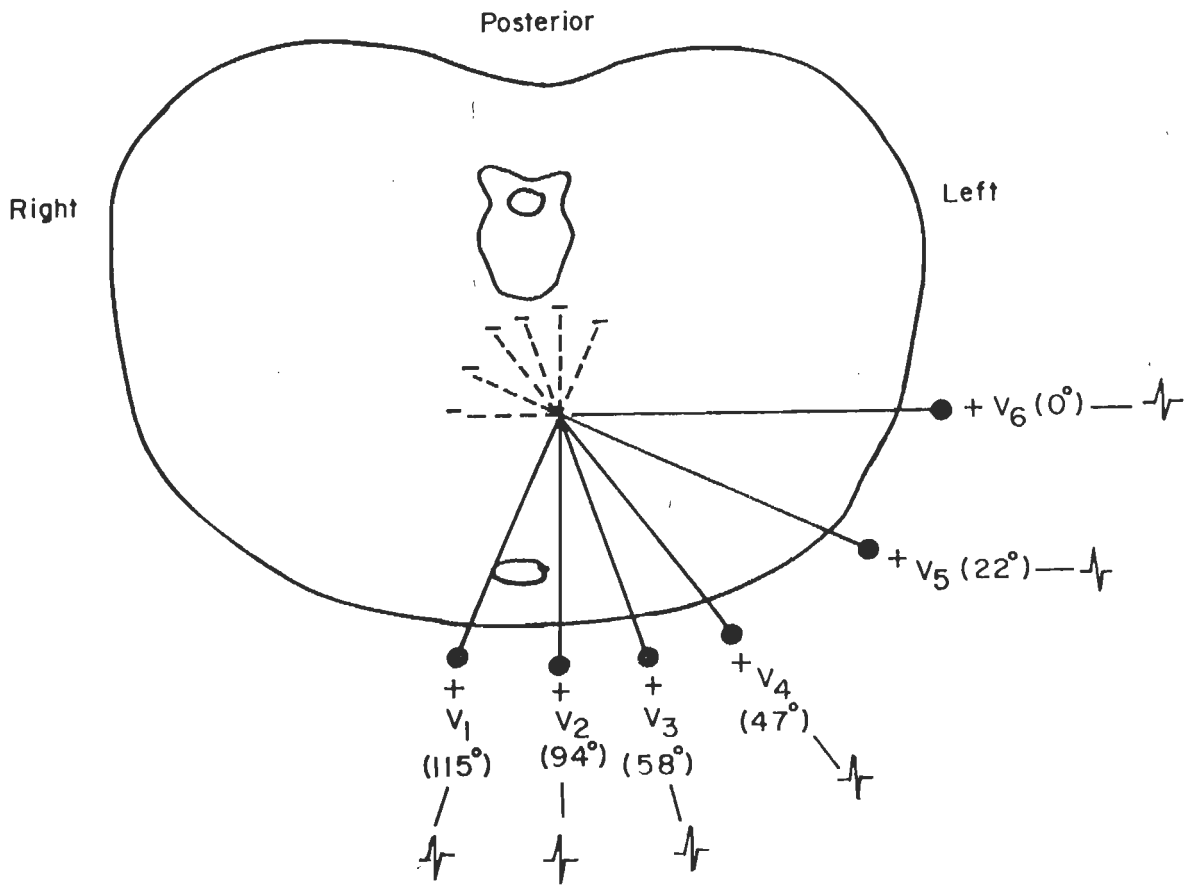
Fig. 2.7 Chest leads in horizontal plane

2.8   ECG Database

Over the last four decades, a rapid growth has taken place in computer ECG processing. Before 1980, there was no standard database available for computer assisted ECG analysis. There was a lack of agreed definition of waves, of common measurements, of standardized criteria for classification and common terminology for reporting. This hampered the exchange of diagnostic criteria and made evaluation studies on the utility and performance of ECG computer programs difficult. In the recent years, standard database has been developed to overcome some of these problems. At present three standard database are available, namely, American Heart Association (AHA), Common Standards for Quantitative Electrocardiography (CSE) and Massachusetts Institute of Technology / Beth Israle Hospital (MIT/BIH). In the present work, last two database have been used for testing the different algorithms developed for ECG processing. The details of two database are given below:

2.8.1   Common Standards for Quantitative Electrocardiography (CSE) [134]

The European community in the year 1980, started a project under the leadership of late J.L. Willems with an aim of establishing "Common Standards for Quantitative Electrocardiography (CSE)". The Working Party developed three CSE reference databases. Two have been developed for the testing and development of ECG measurement programs: the first for ECGs in which three leads have been recorded simultaneously in the normal standard sequence, that is lead group I, II, III; leadgroup aVR, aVL, aVF; leadgroup V_1, V_2, V_3; leadgroup V_4, V_5, V_6 and finally the Frank leads XYZ.

The second database contains all leads, that is the twelve leads plus the three Frank leads have been recorded simultaneously. The third CSE database has been developed for the assessment of diagnostic ECG and VCG programs. This database also contain multilead recording both of the standard ECG and the VCG. Each data set contains 125 records. The data for this library were sampled at 500 Hz with a resolution of at least 10 bits and a minimum quantization level of 5 μv. They were recorded with equipment meeting AHA standards.

The three lead CSE measurement database consists of 250 original and 310 artificial ECG recordings. They have been divided into two equal sets, that is data set 1 (CSE-DSI) and data set 2 (CSE-DSII).The multilead measurement database also contains original and artificial ECG recordings. This data base has been divided into two equal sets that is data set three (CSE-DSIII) and data set four (CSE-DSIV).

The enlarged selected beats as well as the entire tracings are given for each ECG of data set, three of the CSE multilead measurement library and is named as training set. Time locations are shown for the overall onset and offset of P, QRS and T. The referee results are also available on the enlarged beats. The referee have analysed a random sample that is, every fifth case, as well as for some other measurement where the individual program results were too scattered. In addition to the plots of median results, all individual referee and program results are also presented. Finally diagnostic database (named as data set five (CSE-DSV)) only digitized ECG data are given but clinical validated diagnostics is not available. This database has been developed primarily for testing the performance of diagnostic ECG and VCG programs.

2.8.2   Massachusetts Institute of Technology - Beth Israle Hospital (MIT/BIH) |98|

The source of the ECGs included in the MIT/BIH Arrhythmia database contain a set of over 4000 long-term Holter recordings that were collected by the Beth Israle Hospital Arrhythmia Laboratory between 1975 to 1979. About 60% of these recordings were obtained from inpatients. The database consists of two groups, namely 100 and 200 series.The first group contains 23 records (numbered from 100 to 124 inclusive with some missing numbers) chosen at random from this set, and second group has 25 records (numbered from 200 to 234 inclusive, again with some numbers missing) chosen from the same set to include a variety of rare but clinically important events. Each of the 48 records is slightly over 30 minutes in length.

The first group is intended to serve as a representative samples of the variety of waveforms and artifacts that an arrhythmia might encounter in routine clinical practice. Records in the second group on the other hand, were chosen to include complex ventricular, junctional and supraventricular arrhythmia and conduction abnormalities. Several of these records were selected because features of rhythm, QRS morphology variation or signal quality can be expected to present significant difficulty to arrhythmia detector.

In majority of the records, the upper signal is a modified limb lead II (ML II), recorded by placing the electrode on the chest. The lower signal is usually, a modified lead V_1 (occasionally V_2 or V_5 and in one case V_4); as for the upper signal, the electrodes are also placed on the chest. This configuration is commonly followed by the BIH Arrhythmia Laboratory. Normal QRS complexes are usually prominant in the upper signal. The lead

axis for the lower signal may be nearly orthogonal to the mean cardiac electrical axis.

The ECG signals are sampled at 360 Hz. The ADC is unipolar, with 11 bit resolution over ± 5 mV range. The annotations generally appear at the R-wave peak, and are located with sufficient accuracy to make the reference annotation files usable for studies requiring waveform averaging and for heart rate variablity studies. The database contains about 1,09,000 beats. The diseases included in this database are different 35 types of important arrhythmias such as Normal sinus rhythm, paced beats, Premature Ventricular Contraction (PVC), Atrial Premature Contraction (APC), Bradycardia, Bigeminy, Trigeminy, AV blocks, Ventricular flutter and fibrillation etc.

CHAPTER - 3

HARDWARE REALIZATION OF
AMBULATORY MONITOR

CHAPTER - 3

HARDWARE REALIZATION OF AMBULATORY MONITOR

3.1   Introduction

Ambulatory monitors are in common use to monitor ECG of an ambulatory patient for the detection and analysis of cardiac arrhythmias. It provides continuous real-time information about the condition of the patient. In the present application the monitor is developed with an aim to provide efficient health care service to cardiac patients on way to hospital. The monitor placed in the ambulance records arrhythmias and conduction disturbances of interest. When a premonitory arrhythmia or conduction disturbance occurs, the monitor records it. An alarm alerts the paramedical staff, to provide necessary preliminary resuciation to the patient. The recorded data can be stored and transmitted to the hospital for expert opinion. The unit should be portable, light in weight, battery powered and can be conveniently placed in the ambulance. For the successful use in the real-time environment, the data acquisition system and other hardware and software must be compatible to each other. Moreover, the selection of processor and analog-to-digital converter and their operating periods are very crucial, so that data acquisition, processing and data compression are to be completed within the sampling interval.

Having considered the above requirement the design was initiated, with an objective of meeting optimal level of performance and possible upgradation in future.

Ambulatory ECG monitor has been developed using Intel 8088 microprocessor based hardware. The system has been designed in modules so as to make any future expansion easy. The system has the following five main modules:

1.   Data Acquisition Module

2.   Microprocessor Module

3.   Memory Module

4.   Digital Input/Output Module

5.   Display and Indication Module

Details of each module are presented in the following sections, after a brief discussion on design consideration and selection of microprocessor for the job.

3.2   Basic Design Considerations

The guiding considerations in the design of ambulatory ECG monitoring system are:

(a) Good performance to meet the requirement of an ambulatory monitor.

(b) Small size.

(c) Low power consumption and

(d) Low cost of the system hardware.

The cost of the system is governed by the cost of the components. High stability close tolerance components are comparatively costly and so they are used only where their values are critical for circuit operation. The

second consideration is the hardware reliability, which increases when the component count is low. This has been accomplished through the use of large and very large scale integrated (LSI and VLSI) chips. The monitor draws its d.c. power from batteries. In order to maintain constant power supply over extended periods of monitoring, the system should be designed with low power consumption chips. This has been achieved by using low power consumption integrated circuit chips.

3.3 Selection of Microprocessor

In view of the sophisticated arrhythmia analysis it has to perform, a fairly large number of instructions will have to be executed by the micropro-cessor in real-time environment, demands utmost care in its selection. The selection of microprocessor is based on the technical characteristics such as speed, word length, on chip registers, programmability etc [71]. Other fac-tors, which should be considered are the availability of processor, its sup-port chips and peripheral chips. A general consideration in the selection of microprocessor is presented below [124]:

(a)   For the real-time implementation instruction cycle or clock speed is one of the important parameter for the selection of processor. The ambulatory monitor needs higher speed version of the processor.

(b)   Word size directly has the impact on the precession of the processor, therefore, depending on the degree of precession, a choice should be made between 8 and 16 bit processor. Although 8 bit processor can be used to give moderate accuracy, but that would increase the complex-ity of the system and computational time involved will also increase.

(c)   On chip registers allow immediate data transfer between the registers during calculation rather than requiring external references to memory for temporary storage. This facility available in the processor increases the throughput.

(d)   A major consideration in the processor selection is the availability of compatible support chips, such as clock generator, memory and peripheral chips.

(e)   Yet, another consideration being the availability of processor chip, this aspect should also be taken into account while making the final selection of the processor.

(f)   Lastly, programming is yet another important consideration. The architecture of each microprocessor determines its instruction set. Generally, efficient programmes can be written for the processors having large number of instructions with many addressing modes and various types of memory referencing schemes. This improves execution time considerably and reduces the memory space requirement.

On the basis of the foregoing considerations, microprocessor 8088 has been selected for the present application. The 8088 processor has 16 bit internal data bus and 20 bit address bus; it has however 8 bit external bidirectional bus to make it upward compatible with its 8085 predecessor. It has four groups of registers (Total 14) accessible to the user and has addressing capability of 1 M byte of memory [15,48,61,62,63,84,147]. It can address up to 64K bytes wide input/output ports using isolated I/O scheme. The internal architecture provides for Minimum/Maximum mode operations, efficient interrupt management using maskable and non-maskable external interrupts

alongwith software interrupt instructions. The functions of these interrupts can be defined by the user. Instruction set of 8088 microprocessor includes instructions for multiplication and division too

3.4   System   Schematic

The motivation for developing medical emergency ambulatory monitoring system (MEAMS) described below is to create means for reliable arrhythmia analysis, generate alarm in case of lethal arrhythmia and to establish communication link between the cardiac centre and the cardiac patient. A block diagram of the whole system is shown in Fig. 3.1. The monitor will be placed in an ambulance to monitor the ECG.

MEAMS is intended to monitor the ECG of the patient on way to the hospital. The construction of the monitor is rugged taking into consideration the rough handling ,it might be subjected to while in use in the ambulance. The system has been made ergonomic by providing minimum number of switches on the front panel of the monitor. To operate this monitor the attending staff manning the ambulance has to just press three switches.These switches are start/stop, display next and transmit/receive. The system consists of three independent signal conditioner channel.The ECG signals are collected through these channels by placing electrodes on the patients body using standard lead system (refer Fig 2.5,chapter2). These channels are interfaced with microprocessor. The differential ECG signal, picked up by the surface electrodes placed on the human body, is amplified in the signal conditioning unit to obtain an adequate voltage level.The amplified ECG signal, which may be corrupted by the noise and powerline interference is filtered
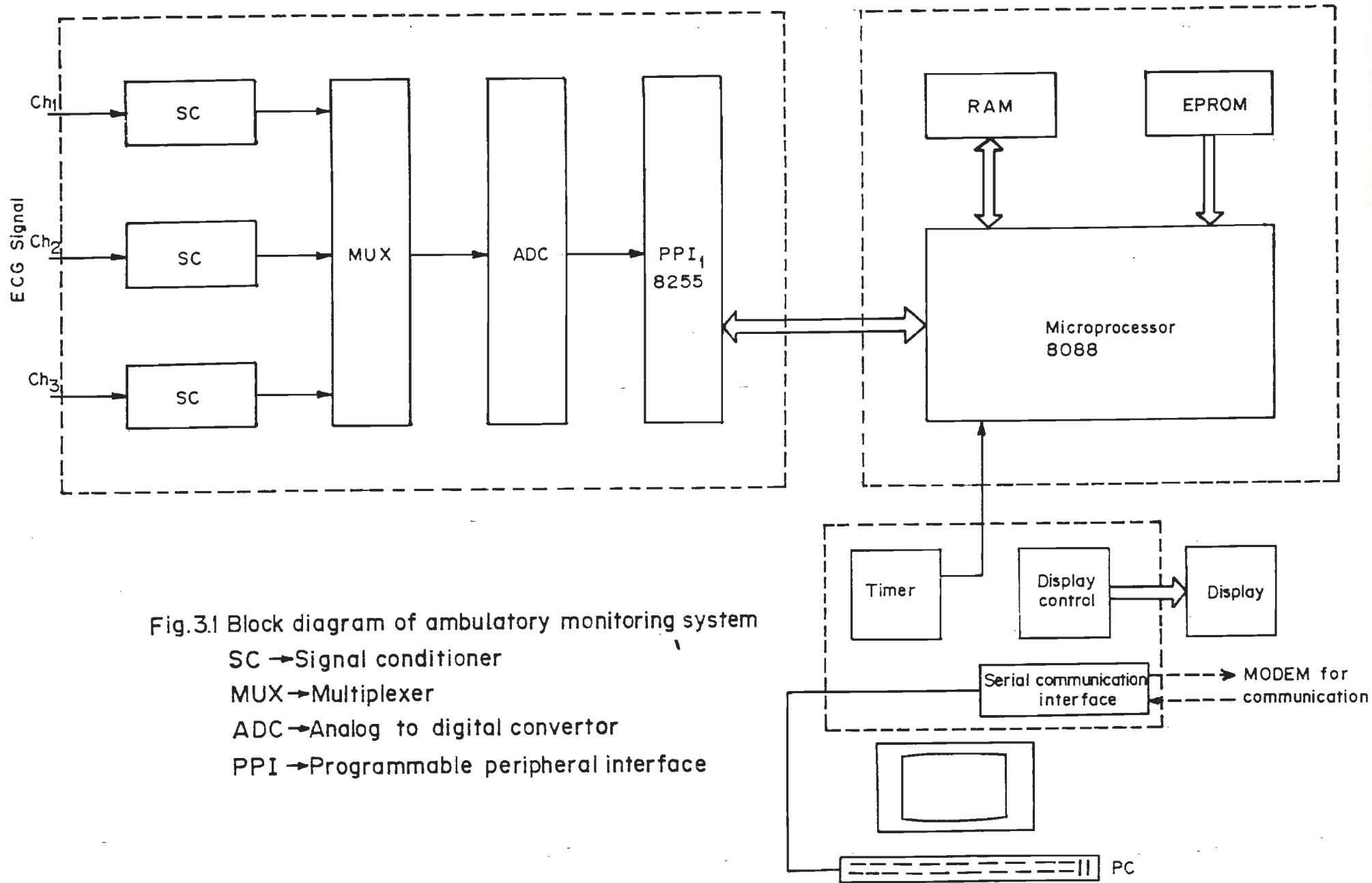
Fig.3.1 Block diagram of ambulatory monitoring system

    SC → Signal conditioner
    MUX → Multiplexer
    ADC → Analog to digital convertor
    PPI → Programmable peripheral interface

-42-

for improving the signal to noise ratio. A three-to-one channel multiplexer presents the signal conditioned ECG to a high precision 12 bit ADC (AD574) one by one. The digitized signals thus available are used for processing and storage. If there is an abnormality in the signal it is compressed and then transmitted to the cardiologist for expert opinion or it may be stored in the RAM for off-line analysis. The software to operate the whole system has been written in assembly language and stored in an EPROM. The software also performs self test on the system after the power is switched on.

3.5 Data Acquisition Module

Interpretation of the electrocardiogram (ECG) requires that the signal be quantified for extracting useful features needed for diagnosis. For the feature extraction, the signal should be processed suppressing the unwanted noise. Earlier, improvements in ECG recorders were aimed at reducing the size and weight of the recorder and cutting down the recording period [32]. Multi-channel ECG recording has been in use for several years, but its importance is appreciated more now [24,118]. Multi-channel detection and analysis leads to considerable improvement in ECG recorders performance although a huge quantity of data has to be processed. Noise and artifacts often tend to occur intermittently at the time of recording. Such events usually appear independently in different channels, so multi-channel record-ing can give high immunity to these disturbances [70,92,151]. Although all 12-leads can be recorded simultaneously, three channel recording remains popular because of the following reasons.

(a)   12-lead recording is very expensive. Using only two frontal plane leads and one chest lead, all the 12-leads can be synthesized [122].

-43-

(b) To obtain the vector cardiography or orthogonal lead recording, only three simultaneous channels are necessary.

(c) Generally, single lead is sufficient for arrhythmia analysis but simultaneous three channel recording improves the analysis by gathering more information. Moreover, selection of the single lead out of the three for extracting the parameters can be made on the basis of the noise level present in the signal.

The data acquisition module has three channels of signal processing circuitry. The block diagram of the circuit is shown in Fig. 3.2. The study of ECG signal gives a picture of slow varying of low amplitude waveform, which is susceptible to various kinds of noises. To extract the useful signal from the spectrum, it is required to optimize

(i) The gain of the amplification unit
(ii) The frequency range of interest

3.5.1 Amplifier

The ECG signal generally lies in the range of ± 2.5 mV. This level is very low, as most of the analog-to-digital converters work in the range of ± 5V or ± 10 V. In the present system AD 524 (Analog Devices) has been used. The amplifier is capable of providing pin programmable gain up to 10,000. Also if the resistances are properly matched, high Common Mode Rejection Ratio (CMRR) can be achieved. The gain and linearity of the amplifier are fixed over the entire frequency range of interest and stable over the working temperature range [10]. In the present application gain is adjusted to be 2000.
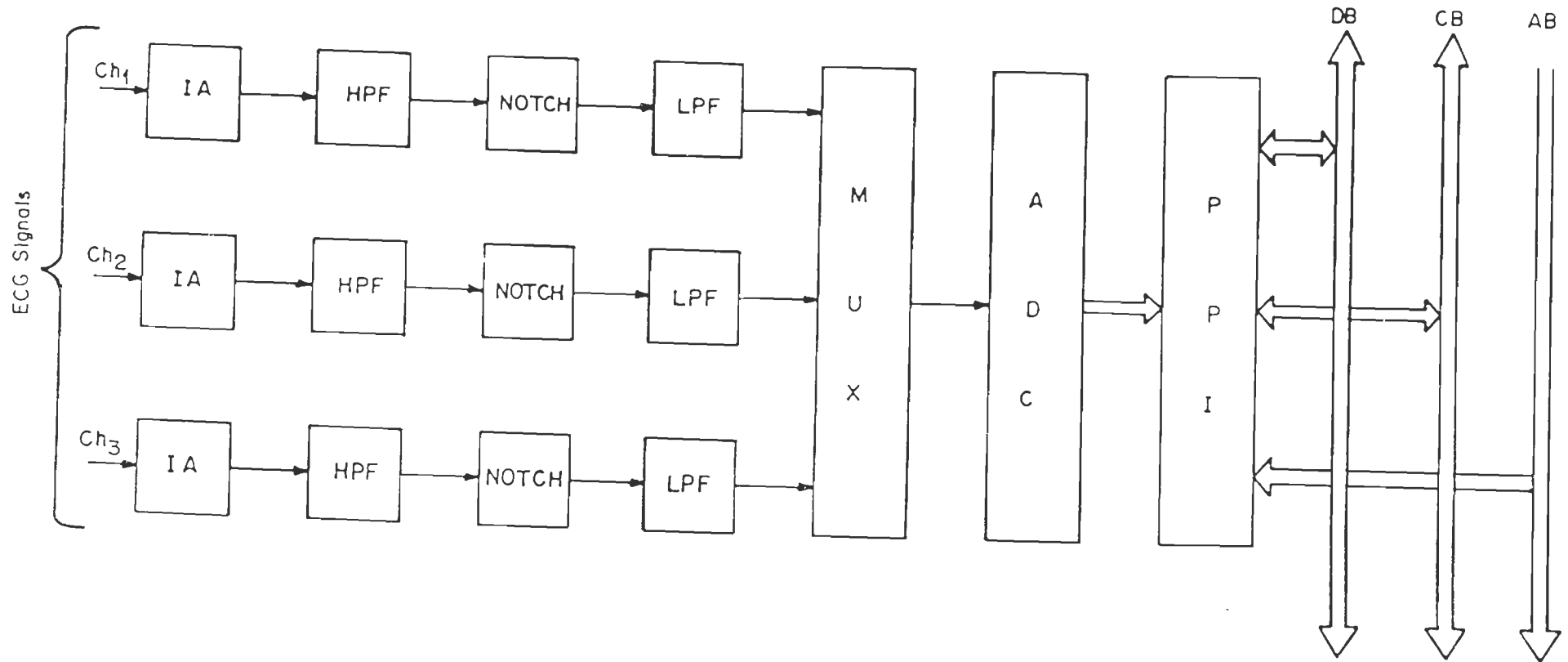
Fig.3.2 Block diagram of data acquisition module
IA→Instrumentation amplifier, HPF → High pass filter
LPF→ Low pass filter, MUX → Multiplexer
ADC→Analog to digital convertor, PPI→ Programmable peripheral interface
DB → Data bus, CB — Control bus, AB →Address bus

3.5.2   Filters

Most of the diagnostic information present in the ECG signal is specified up to 30 Hz. But in the QRS complex ,some higher frequency signals are also present which when neglected may cause some error. So the frequency range of the ECG signal is considered up to 100 Hz. Further, due to muscle artifacts and somatic tremor, baseline wander is found to be an extremely low frequency signal, which can be eliminated if the system rejects frequencies below 0.05 Hz.

The powerline interference is one of the important artifacts which must be eliminated by special means. The powerline frequency has a narrow bandwidth around 50 Hz. (in India). So a 50 Hz notch filter will be sufficient to eliminate any powerline frequency component still present, as most of it is rejected because of the high CMRR of the amplifier.

(a)   High Pass Filter

Extraneous low frequency components can severly affect the visual as well as computer based interpretation of the ECG signal [126]. Therefore it is necessary to eliminate baseline wander present in the ECG signal to reduce changes in beat morphology without disturbing the clinical information. Respiration and electrode impedance changes due to prespiration are the common sources of baseline wander. The frequency of the baseline wander is usually in the range well below 0.05 Hz. In the present application an active high pass filter with a cutoff frequency of 0.05 Hz is used and is configured with a unity gain. Two second order filters with a roll off 40 dB/decade, are arranged in cascade to make a fourth-order filter [96].

(b)   Notch Filter

A notch filter working in a matched tee configuration is used here. At resonance, the impedance of the tee-branches match and output is sharply reduced. At all other frequencies, the impedance in the tee results in significant potential output [83]. The active notch filter has a narrow band rejection and has a high attenuation of the tuning frequency.

(c)   Low Pass Filter

After the high-pass and notch filters, the signal may contain harmonics of the power frequency i.e. 100 Hz, 150 Hz and so on, and high frequency noise from the sources like radio frequency interference and electromagnetically induced pickup [59]. A low pass filter attenuates higher frequency noise and also serves as antialising filter. Two low pass filters, each of second order with a roll off of 40 dB/ decade, are used in this application. In order to preserve the nature of the ECG signal, cutoff frequency of 100 Hz is selected which helps to retain the highest frequency components of the ECG signal. The fourth order low pass filter effectively eliminate electromyographic (EMG) and other high frequency noise.

3.5.3   Multiplexer

In this system, a eight to one channel analog multiplexer, AD 7503, is used to multiplex three input signals for presenting one by one to ADC 574. The AD7503 multiplexer (Analog Devices) is selected on the basis of high degree of isolation, low turn-on resistance and fast switching. The on-resistance is of the order of 200 ohms while the off resistance is several megaohms range. The inter-channel capacitance is of the order of 30 pF. [10].

3.5.4   Analog-to-Digital Converter

The analog-to-digital converter (ADC) digitizes the signal and makes it readable by the processor. As per American Heart Association (AHA) standards, the ADC should be of 10 or 12 bit resolution. The selection of ADC is made on the basis of its conversion speed and resolution. The effect of quantization error in conversion will have direct effect on the ECG recording system. Another factor influencing the choice of ADC is its capability to operate in bipolar mode [10,65]. This is needed in this application as the ECG signals are bipolar in nature. The error accounted with 12 bit ADC is of the order of 1 in 4000 which is quite small; the cost of 14 and 16 bit ADC's are relatively very high. Therefore , AD 574 (Analog Devices) 12 bit ADC has been selected for this application. Besides the output data of AD 574 is buffered and can be tristated. This reduces the requirements of an additional buffer.

3.6   Microprocessor Module

The block diagram of microprocessor module is shown in Fig.3.3. It consists of an 8088 microprocessor configured in minimum mode and permanently disabling the nonmaskable interrupt . Clock is provided by 10 MHz crystal through clock generator 8284, this resulted in 3.333MHz processor clock and 1.667 MHz peripheral clock. Buffers and latches namely 74LS244, 74LS245, and 74LS373 clock frequency divider for providing a clock of lesser frequency to chips like timers and USART, decoders for providing chip select signals to the I/O chips in the system and for memory selection are used. The microprocessor module has an 8 Kbytes EPROM
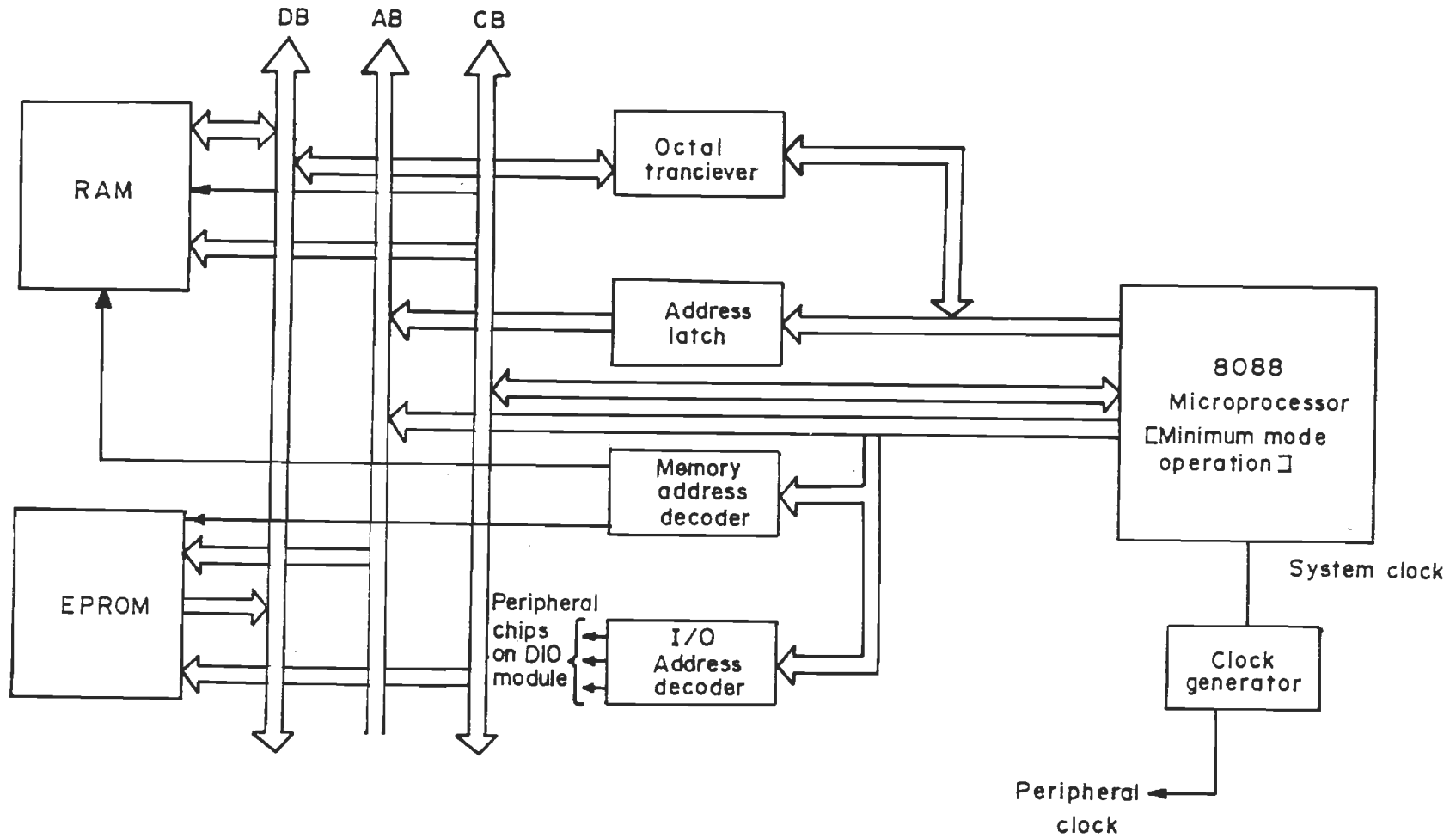
Fig.3.3 Block diagram of 8088 microprocessor module

monitor containing system software and 768 Kbytes RAM for storing the acquired data. The system contains the following common signals.

Address bus : A0-A19

Data bus : D0-D7

Control signals ALE, READY,IO/$\overline{M}$ $\overline{WR}$, $\overline{RD}$

Power supply lines : +5, GND, -12, +12 Volts.

3.7 Memory Module

32 Kbytes high speed static CMOS RAM (62256) chips which operates on +5V supply is used in the memory module. These chips are directly TTL compatible. In the present application, the demand for memory space is fairly large and around 1.44 MB memory is required to store one hour ECG data acquired from single channel (Lead II). The 8088 microprocessor can support maximum of 1 MB of SRAM. The memory module constructed for use has 768 KB RAM. Fig. 3.4 shows the block schematic of the memory module for 768 KB capacity. Twentyfour 62256, 32 Kx8 static RAMs are interfaced to the 8088 microprocessor starting from the memory location 00000H. This module makes use of three decoders (74LS138) to select the twentyfour different RAM memory components and a fourth one is used for generating the necessary chip enable signals for these three, 3 to 8 line decoders. Twenty four 32K RAMs fill memory from location 00000H through location BFFFFH, for 768K bytes of memory. This capacity is not quite adequate, but it is sufficiently large enough to indicate that, with suitably compressed ECG signal, twentyfour numbers of 32K RAM devices would be sufficient to store one hour data recorded during the period in

248/99
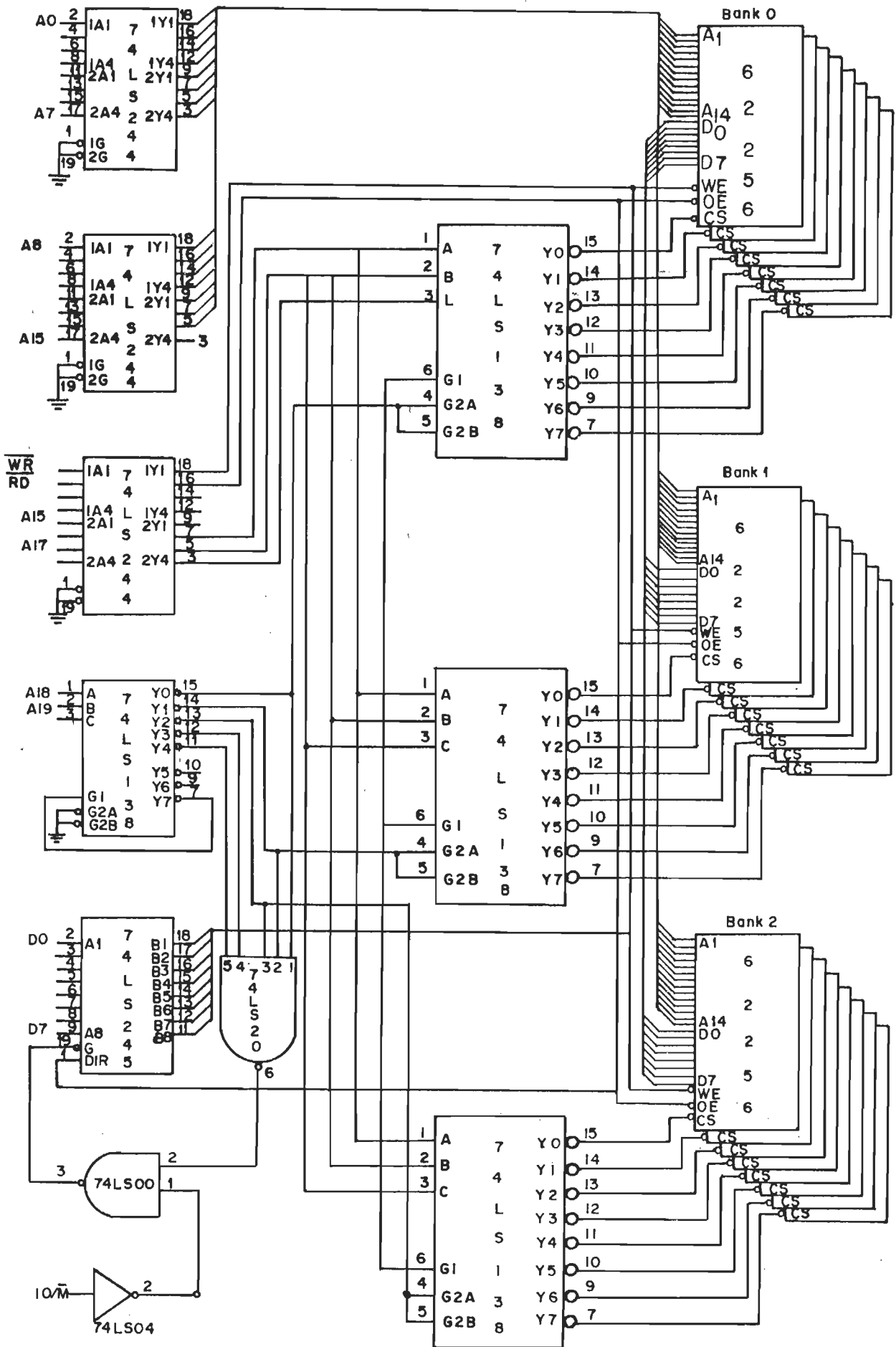
Fig.3.4 Block schematic of 768 KB Memory module

-51-

which patient is shifted from remote place to the hospital. Therefore suitable direct data compression techniques have been developed for ECG signal and are presented in chapter 6.

3.8   Digital Input/Output Module   (DIO)

The block diagram of DIO module is shown in Fig.3.5. It consists of four programmable I.C. chips interfaced to the system bus; these are 8255 PPI, 8279 keyboard controller, 8253 PIT and 8251 USART. The 8255 has three programmable ports one of which is used as an output port for providing signals to various LEDs and another is used as an input port for inputing system control signals such as start/stop, transmitt, download and so on. 8251 (USART) chip has been provided for communication purpose or it can also be used for down loading the various data acquired to PC through the RS232C protocol. 1488 and 1489 are provided for converting the TTL level signals into RS232C level and vice versa. A timer chip 8253 (PIT) has been provided for getting the required delays. A 74LS125 chip has been provided for the self test of the system.

3.9   Display and Indication Module

The various timers, counters, flags and other parameters are required to be displayed on-line. For this purpose, a keyboard and display controller chip 8279 (part of DIO module discussed in section 3.8) has been interfaced with the microprocessor module. Various outputs from 8279 i.e. digit lines, scanlines have been brought out to this module. A 5x5 membrane type keypad and a 10+6 digit seven segment display is mounted on this module.
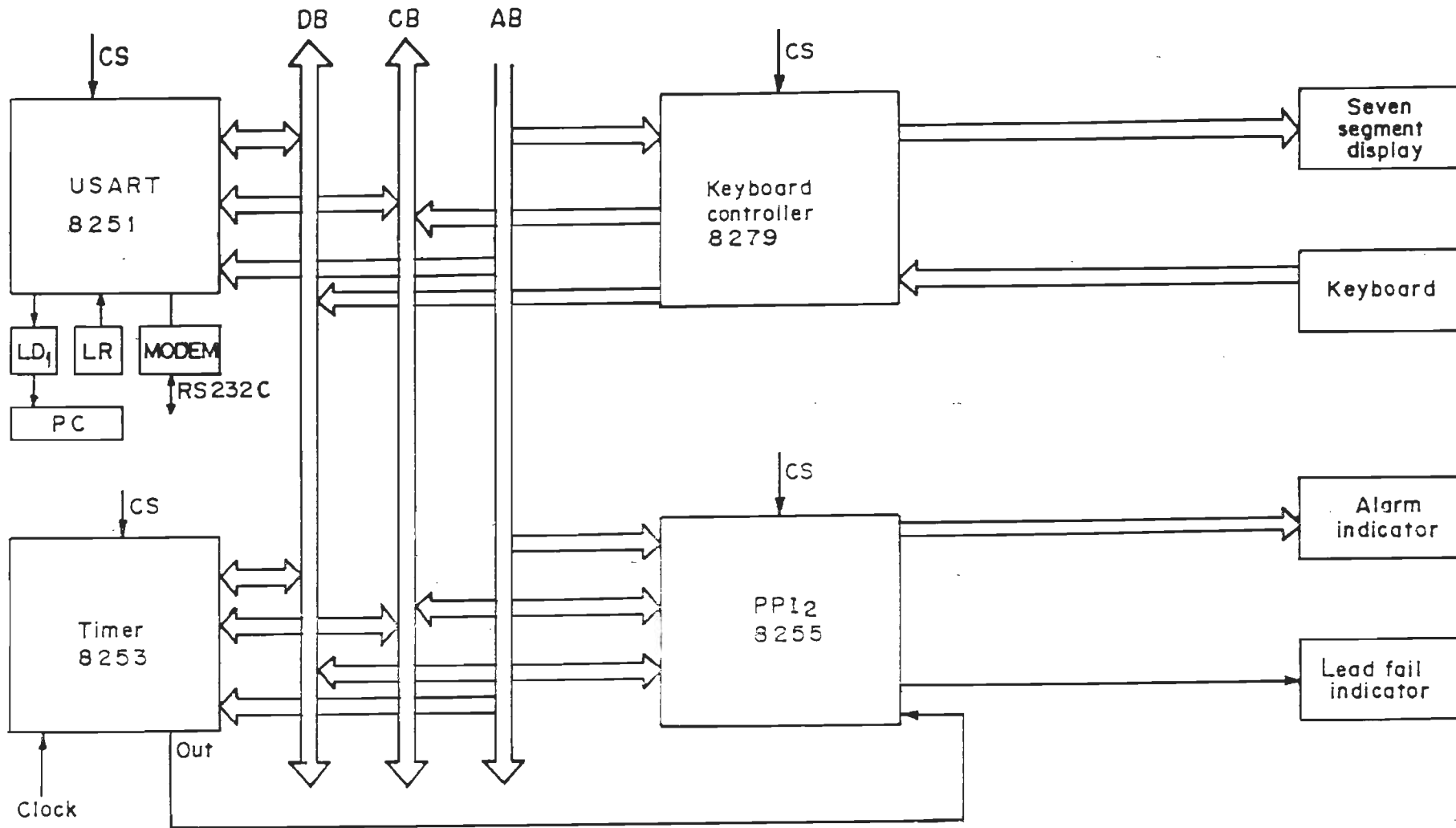
Fig.3.5 Block diagram of DIO module

The block schematic of the display and indication module is shown in Fig.3.6.

The four scan lines are decoded using a 4x6 line decoder (74LS154). The active low outputs of decoder are inverted using 7404 inverter. These outputs then connected to a transistor array which sinks the current from the selected FND543 common cathode type seven segment display. The digit outputs which are coming from the digit lines (A0-A3, B0-B3) are first inverted using 7405 and then fed to array of PNP transistor (SK100) and connected to each digit of display. Each character in the seven segment LED display unit can display a digit from '0' through '9' or an alpha character 'A' through 'F'. A 5x5 keypad is interfaced to input parameters and active various display menues.

3.10   Mother   Board

The mother board integrates the processor module, DIO module, Data acquisition module using 64 pin EURO connectors. There is a common connection between all three modules containing the control bus, data bus, chip select signals and power supply lines. The power supply connections are brought into the mother board by means of heavy duty connectors. The RS232C connections between DIO module and modems or the PC are also made in this module itself. The mother board after integration along with the display and indication module would complete the hardware of the ambulatory monitor.

3.11   Novel   Features

The hardware for ambulatory monitor is built around 8088 micropro-cessor. The signal conditioner module consists of an amplifier with high

Segment O/P from 8279 A_0-A_3 B_0-B_3 →/8→ Invertor 7405 →/8→ PNP Transistor SK 100 →/8→ a,--f, dp 16 Seven segment displays common cathodes K_1 K_2 ... K_{16}

Scan lines SLO-SL3 →/4→ 4 to 16 line decoder 154 →/16→ Invertor 7404 →/16→ NPN Transistor array 2003 →/16→
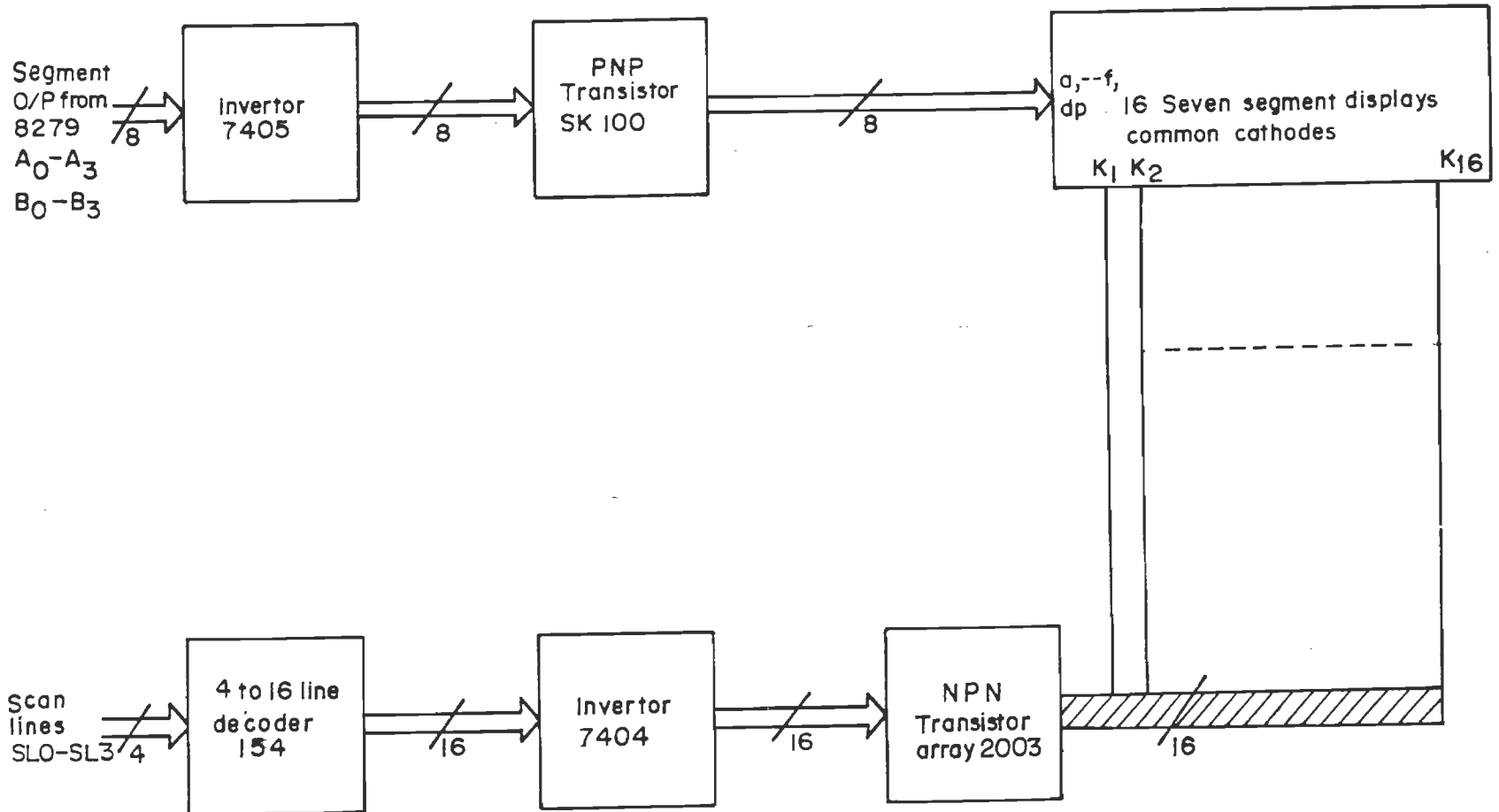
Fig.3.6 Block diagram of display and indicating module

CMRR has been used to amplify the ECG signal without distorting the morphology of the waveform. In addition, to minimize all unwanted artifacts and interferences, three filters are used. A multiplexer with high degree of isolation, low turn on resistance and fast switching has been used for channel selection. The selection of ADC fullfills the requirements of American Heart Association (AHA) recommendations. The selection of microprocessor is made on the basis of speed and powerful instruction set. The digital input/output module consists of general purpose peripheral chips which have been used for different purpose. A display and indicating module provides necessary indications and displays during monitoring. The hardware designed is completely software controllable. The following are the novel features of the proposed system.

1. The system is capable of recording three channels simultaneously.

2. The monitor meets the performance standards of the American Heart Association (AHA).

3. The input channels are isolated from each other with least interference.

4. The selection of channels and sampling frequency are software controllable.

5. The hardware filtering largely eliminates, baseline wander, powerline frequency EMG and high frequency noise present in the signal.

6. A provision is provided to establish radio link between monitor and hospital through MODEMS using RS232C serial port interface.

7. Indication and display facility is provided to display the events during monitoring.

8. The system can be operated by the attending staff manning the ambulance easily.

CHAPTER-4

ECG WAVE RECOGNITION AND CHARACTERISTIC POINT DETECTION

CHAPTER-4

ECG WAVE RECOGNITION AND CHARACTERISTIC POINT DETECTION

4.1   Introduction

In chapter 3 a detailed description has been given for the hardware of ambulatory monitoring system based on minimum mode 8088 microprocessor system. This unit will be placed in the ambulance carrying the patient to the hospital. The on-line data acquired using ambulatory monitor, are to be studied, analyzed and decisions taken in variety of ways. The ECG analysis can be done both on-line and off-line. The on-line analysis is absolutely essential to take emergency measures to save the patient on the way to the hospital. The off-line analysis of the data becomes necessary for clearly identifying the disease, the patient may have. Besides, the data so acquired will become very useful for future use as database. In this chapter, a detailed analysis of the ECG wave is done off-line to determine amplitudes and the characteristic points (or boundaries) of P wave, QRS complex and T wave. The characteristic points thus located will be used for computing intervals and segments. This information is used for disease classification. Interpretation of arrhythmias and techniques for ECG data compression will be taken up in the subsequent chapters.

In the context of arrhythmia analysis the importance of reliable ECG wave recognition and delineation is always stressed [28,80], since it forms the front end of any ECG measurement or analysis program. The main objective of this processing is to identify the P, Q, R, S and T waves and to locate the characteristic points P_{on}, P_{off}, QRS_{on}, QRS_{off}, and T_{end} in each cycle. After identifying the ECG waves their respective amplitudes are measured with respect to the base line. Based on the characteristic points of each wave, measurements of the interwave, segments and intervals are then made. These parameters will be further used for classifying the arrhythmias. Further, two important algorithms, namely, preprocessing (noise filtering)

algorithm and ECG wave recognition and characteristic point detection algorithm are developed for off-line analysis of the ECG signal. The performance of these algorithms have been tested on the standard MIT/BIH Arrhythmia database. The details of the algorithm along with their software implementation is explained in the following sections.

4.2 Preprocessing

This section describes application of digital filter for the removal of powerline interference and baseline wander. Interference from 50 Hz (in India) AC, some times referred to as AC pickup or hum can pose problem while recording ECG. The source for this interference being the AC line potential (voltages) that is unavoidably present in any clinical situation, if for no other purpose than to light the room or power the recording unit. Baseline wandering in the ECG records produces artifactual data when measuring ECG parameters. Particularly, ST segment measures are strongly affected by this wandering. Respiration rate and electrode impedance changes due to prespiration are important sources of baseline wander in most types of ECG recordings. The frequency content in the baseline wander is usually below 0.5 Hz.

4.2.1 Necessity for Preprocessing

The best performance of an ECG processing system can be achieved if the input data is free from noise. Artifacts in ECG can arise from different sources in a recording or monitoring system [60]. During recording, the signal get contaminated by the noise such as powerline interference and baseline wander. Their removal is important not only for computer processing but also for visual examination of ECG waveform. Digital filtering is used to eliminate powerline interference and baseline wander.

Digital filtering can be achieved either by frequency domain approach or time domain methods. Frequency domain filtering introduces a large amount of delay in arriving at noise free ECG signal because of the fact that, the time domain signal has to be first transformed into frequency domain signal, filtered and retransformed to the time domain results into large

computational time. Hence , this method of filtering is not suitable for this particular application. Further, filters must be designed in such a fashion that morphological features are retained without loosing diagnostic information [117]. Only a few methods are available for the removal of baseline drift and powerline interference from ECG signals [4,42,86,143]. Although some of them are novel in their approach, their major draw back is the large computational time. Finite impulse response (FIR) filters are commonly employed for noise removal from the ECG as they introduce minimum signal distortion because of their inherent linear phase characteristics [148].

4.2.2   Modification of Lynn's Subtraction Filter

A method was described by Lynn wherein the elimination of powerline interference was carried out using subtraction filter [86]. In Lynn's method sharp notch filter was used by subtracting the output of a bandpass filter from the noisy input ECG signal. This approach is also computationally slow. Hence in the present work bandpass filter is replaced by multiband filter known as extraction filter which reduces computational time considerably. The reduction in computational time is essentially due to the use of integer arithmetic in the present approach, rather than a complex mathematical calculations involved in the Lynn's method. It eliminates both powerline interference and baseline wander to a considerable extent. The extracted signal is subsequently subtracted from the noisy signal as shown in Fig. 4.1. This method dictates that the extraction filter be a linear phase FIR filter because it has to introduce a constant delay into all the extracted frequency components. The noisy ECG samples are also delayed by the same value before subtraction.

From Fig. 4.1

$$W(z) = z^{-K} X(z) - Y(z)$$

$$= z^{-K} X(z) - H(z) * X(z) \qquad 4.1$$
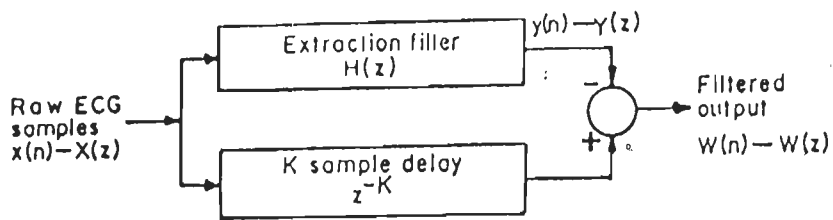
Fig 4. 1. Block diagram of the subtraction
filter.
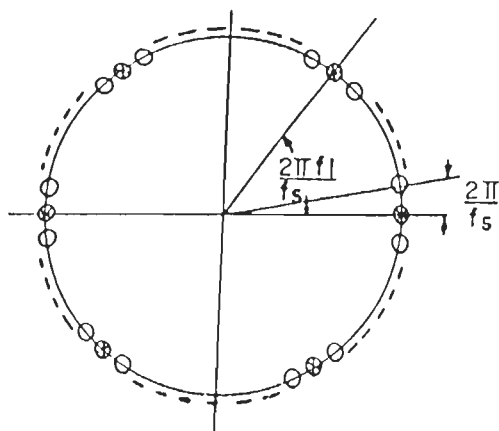
Fig 4.2.(a) Pole zeros of H(z)
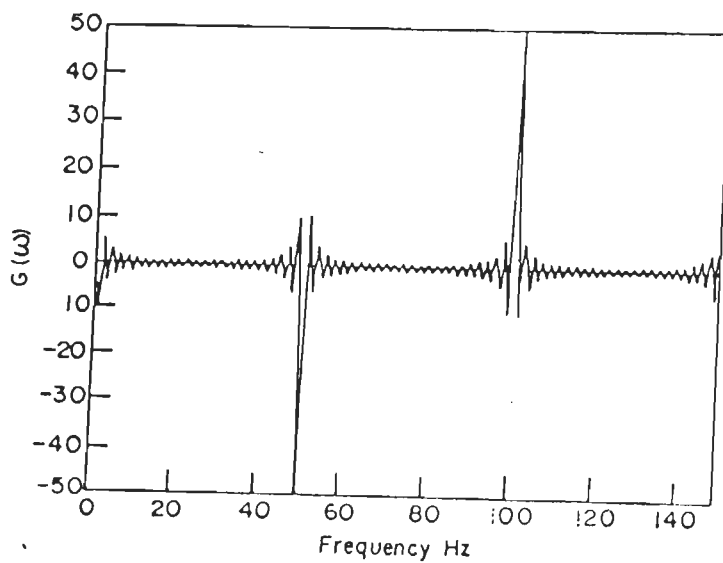
Fig 4. 2.(b). Plot of G(ω) with frequency.

The pulse transfer function is then

$$P(z) = z^{-K} - H(z) \qquad\qquad 4.2$$

where $P(z) = \dfrac{W(z)}{X(z)}$, k is number of sample delays

4.2.3   Filter Design

The design of the extraction filter $H(z)$ is illustrated by assuming a sampling frequency 'fs' and powerline frequency 'fl'. The frequency content of the baseline is usually in a range well below 0.05Hz. Hence for the removal of baseline drift, the cutoff frequency selected here is approximately 0.05Hz [4,93]. Thus fs number of zeros are placed around the unit circle in the z-plane at every 1 Hz and fs/fl poles at angles of $(2\pi^* \ fl/fs)$ from zero as shown in Fig.4.2 (a). Note that the pole zero cancellation at fs/2 Hz does not affect the signal as it is band limited to twice the powerline frequency before sampling.

The pulse transfer function referred to Fig 4.2. (a) is given by

$$H'(z) = \dfrac{1 - z^{-fs}}{1 - z^{-R}} \qquad\qquad 4.3$$

Where $R = fs/fl$. $\qquad\qquad$ 4.4

Expressing equation 4.3 in a recursive form

$$H'(z) = 1 + z^{-R} + z^{-2R} + \dots z^{-(fs-2R)} + z^{-(fs-R)}$$

$$= \sum_{k=0}^{fl-1} z^{-Rk} \qquad\qquad 4.5$$

or

$$H'(e^{j\omega T}) = \sum_{k=0}^{fl-1} e^{-jRk\omega T}$$

The value of the maximum gain $H(e^{j\omega T})$, which occurs at $\omega T = (2\pi*fl)/fs$, corresponding to angles of pole zero cancellation is given by

$$\sum_{k=0}^{fl-1} 1 = fl \qquad\qquad 4.6$$

The frequency response of equation 4.3 is given by

$$H'(e^{jwT}) = e^{-j((fs-fs/fl)/2)\omega T} \frac{Sin\,(fs\omega T/2)}{Sin\,(R\omega T/2)}$$

$$= e^{-j((fs-fs/fl)/2)\omega T} G(\omega) \qquad\qquad 4.7$$

The plot of $G(\omega)$ with frequency is shown in Fig. 4.2(b). It may be noted that an extra 180^0 phase-shift is introduced in the fl extracted component, this leads to an error in the subtraction. This error can be overcome by either squaring $H'(z)$ or by multiplying $H'(z)$ by a factor such as $(1 \pm z^{-R})$. Squaring will result in a maximum filter gain of square of the powerline frequency. Therefore using the first option the transfer function of the filter is obtained as

$$H(z) = \frac{(1-z^{-fs})\,(1+z^{-R})}{(1-z^{-R})} \qquad\qquad 4.8$$

The frequency response of H(z) is given by

$$H(e^{j\omega T}) = 2e^{-(fs/2)\omega T} \frac{\text{Sin}(fs\omega T/2)\cos(\omega TR/2)}{\text{Sin}(\omega TR/2)} \qquad 4.9$$

From equations 4.6, 4.7 and 4.9 it is clear that $H(e^{jwT})$ has a maximum gain of 2 fl in the passband. The maximum side lobe level in the stopband of H(z) is cbserved to be very low. It is evident from equation 4.9 that the filter introduce a constant delay (fs/2) samples in the stopband. To obtain the difference equation for implementing P(z), equation 4.8 is written as

$$H(z) = \frac{Y(z)}{X(z)} = \frac{1+z^{-R} - z^{-fs} - z^{-fs-R}}{1 - z^{-R}} \qquad 4.10$$

y(n) and w(n) are obtained from equation 4.10 and 4.1 as follows

$$y(n) = x(n) + x(n-R) + x(n-fs) - x(n-fs-R) + y(n-R) \qquad 4.11$$

$$w(n) = x(n-fs/2) - y(n)/2fl \qquad 4.12$$

Note that the gain of 2fl is introduced by the extraction filter is taken into account in equation 4.12 by dividing y(n) by 2fl.

4.2.4   Implementation, Results and Comments

The algorithm for filter implementation has been developed using 'C' language and the flowchart for the same is shown in Fig. 4.3.

The algorithm has been tested for powerline interference on different ECG signal recorded in the laboratory sampled at 200Hz frequency. On the other hand

Start

Initialise variables
and arrays

Read the data from
input file & store
in an array.

Get sampling frequency
& powerline frequency

Compute
y[n]=X[n]+X[n-R]+
X[n-fs]-X[n-fs-R]+
y[n-R]
and w[n]=X[n-fs/2]
-y[n]/2 *f1

Store filtered data
in the output file

All
data
over

No

Yes

Stop
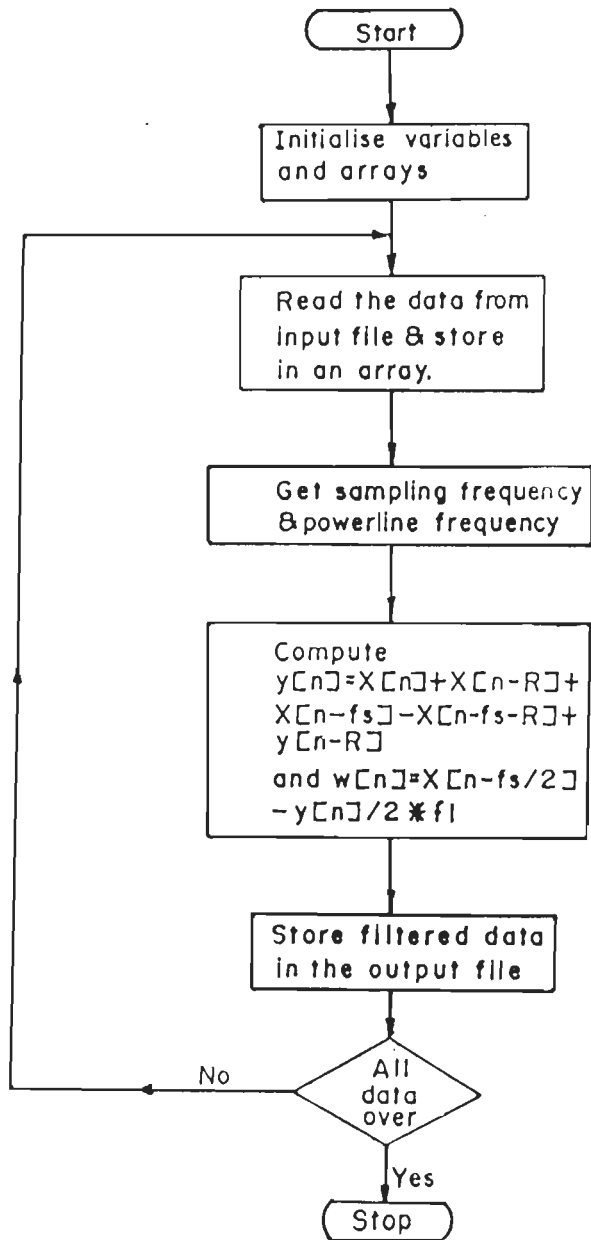
Fig. 4.3 Flow chart for the removal of
powerline interference and.
baseline wander.

baseline wander evaluation has been carried out using data from different records of MIT/BIH database library, the samples are taken at different sampling frequencies. Results for one representative case for each are presented to show the efficiency of the algorithm. Fig. 4.4 (a) shows the original noisy signal containing powerline interference and Fig. 4.4(b) the corresponding signal after filtering. Similarly two cases have been selected from the MIT/BIH database in order to show that the algorithm efficiently works for different sampling frequencies by modifying the equations 4.10 and 4.11. Figs. 4.5(a) and 4.6 (a) are the original signals with baseline wander, former is sampled at 250Hz and latter is taken at a sampling rate of 360 Hz. The corresponding filtered outputs are presented in Figs. 4.5(b) and 4.6(b) respectively after the removal of baseline wander.

The performance of the filter shows that it works satisfactorily over a range of 100 to 500Hz sampling frequency by modifying the transfer function. The filter has been designed using a pulse transfer function of the form $(1 \pm Z^{-n})$ and appropriately cancelling all zeros at the frequency of interest. Further, the filter presented here, has the advantage of having linear phase response and sharp notch characteristics. The visual examination of the filtered output shows that the signal distortion is minimum.

4.3   ECG Wave Recognition

Over the past two decades a good amount of work has been made for the development of computerized processing of electrocardiograms. Computerized ECG processing systems, like manual ECG processing system, carry out two distinct tasks. The first is concerned about the ECG wave recognition and parameter measurement. The second is an interpretation task, which makes use of the results of the first task [125,140]. The ECG waveform consists of several deflections, that represents the electrical activity of the heart. The principle component waves are P, QRS and T. These three complexes together is known as PQRST complex.

A fundamental approach for ECG analysis is to identify P,Q,R,S and T waves accurately and to measure amplitude, duration and segments of interest [77,103]. Time intervals defined from onset and offset of different waves are significant in electrocardiographic diagnosis. The most important
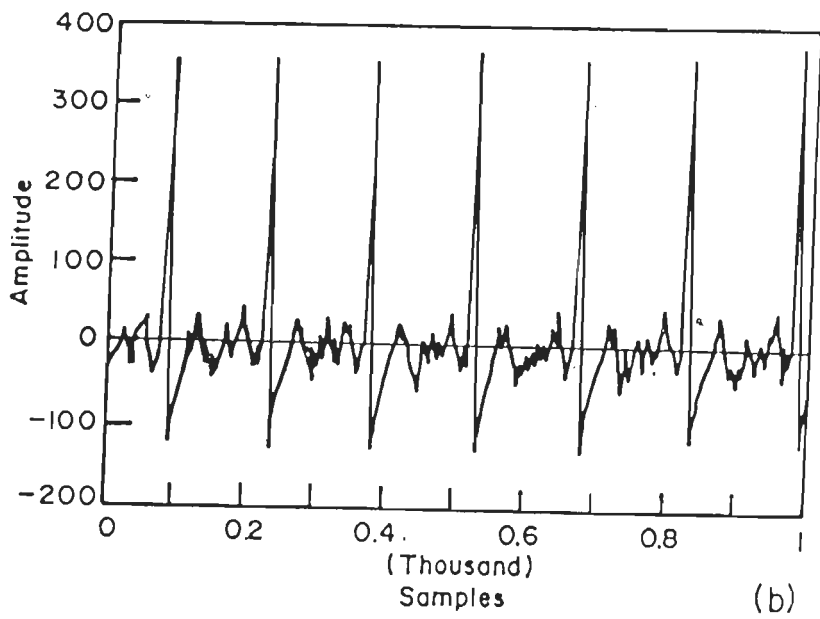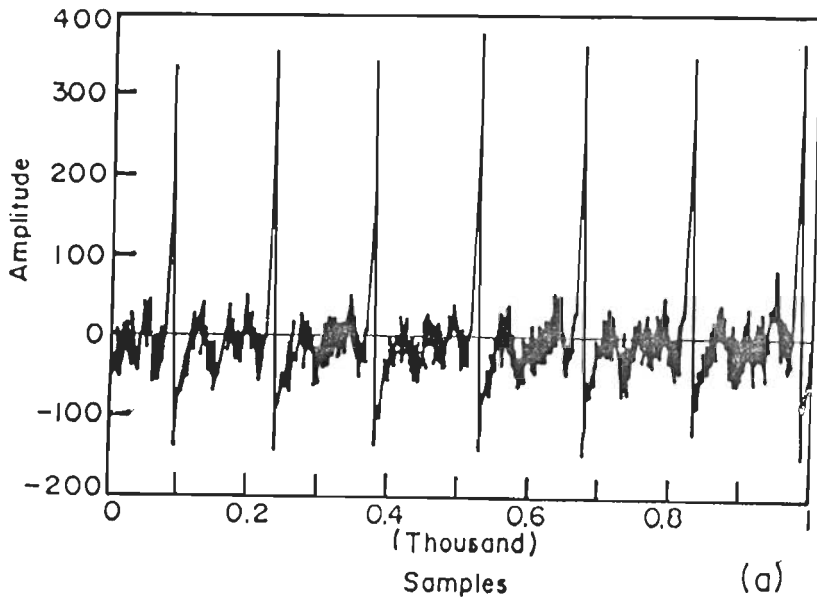
Fig4.4 Sample of power line interference
    (a) Noisy ECG signal sampled at 200 Hz
    (b) Filtered output
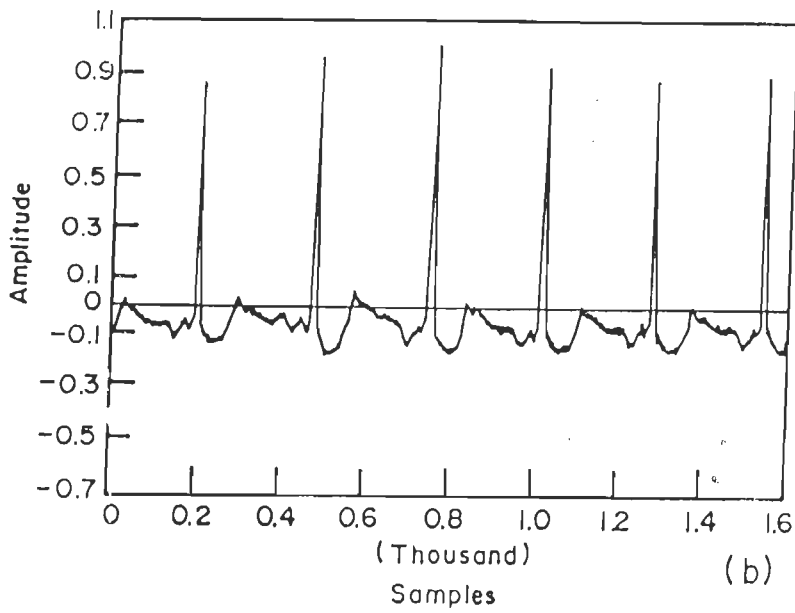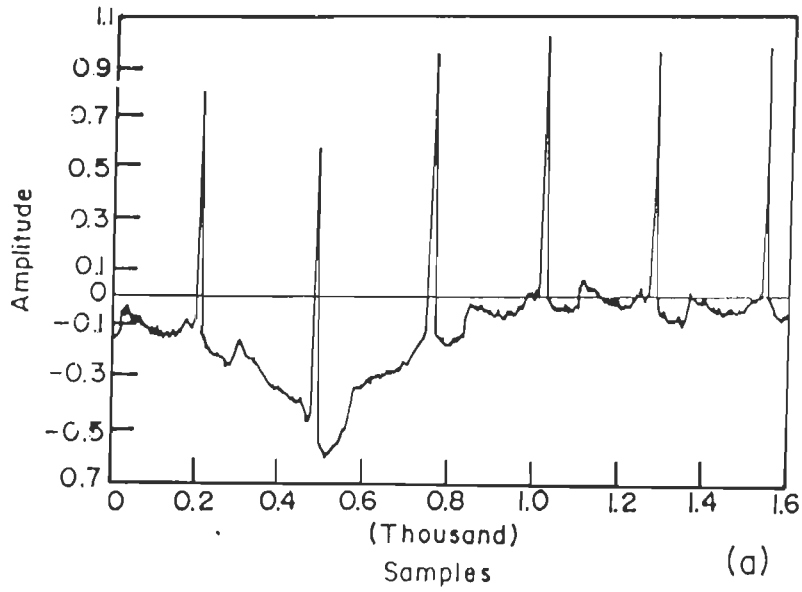
Fig.4.5 Sample of baseline wander removal
for 250 Hz sampling frequency.

(a) Noisy ECG signal R. no. Cu-01 MIT/BIH database
(b) Filtered output
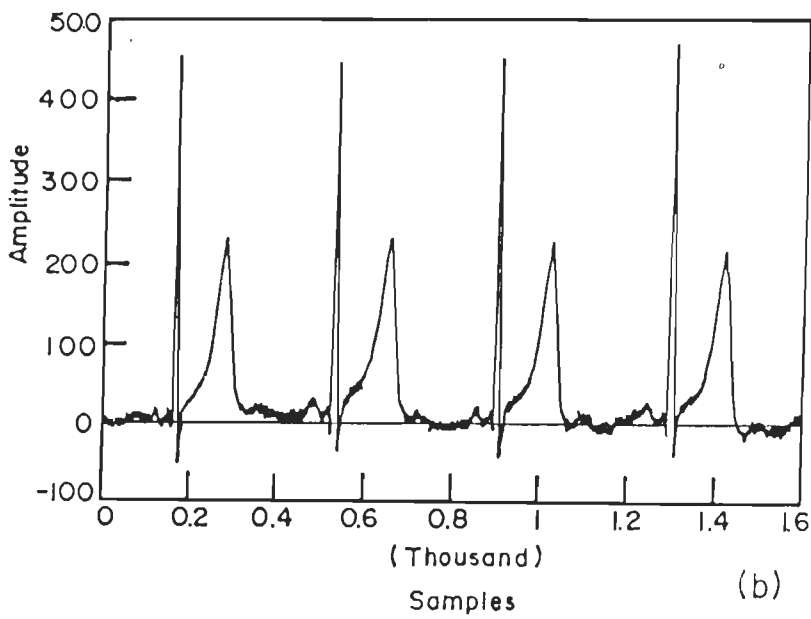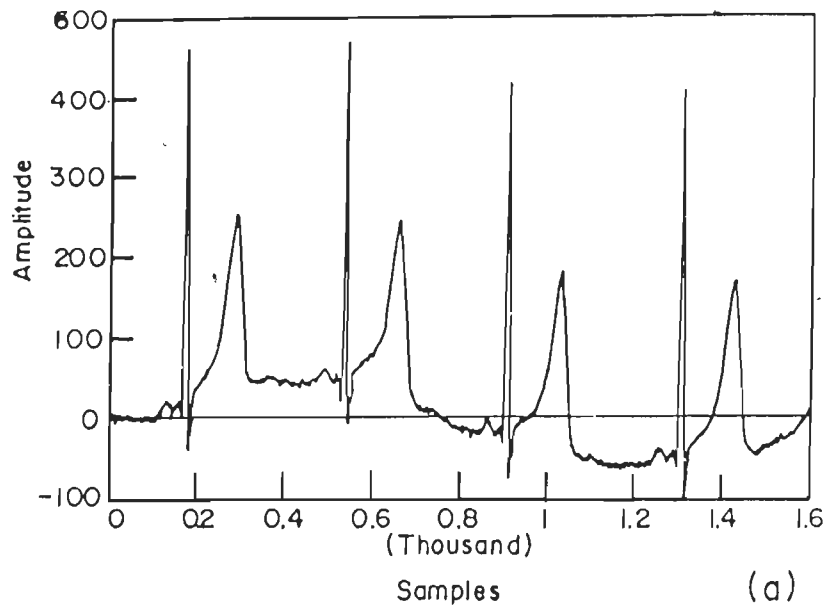
Fig 4.6 Sample of baseline wander removal for
        360 Hz sampling frequency.
    (a) Noisy ECG signal R.no 113 MIT/BIH database
    (b) Filtered output

intervals are RR,PR,QRS and QT [78]. Thus P,QRS and T wave onset and offset must be determined properly because other parameters are derived from this information. The performance of the detection algorithms will have direct impact on the performance of the interpretation programs [129]. This section of the chapter presents a general method for determining the peaks, onset, and offset of P, QRS and T waves along with the software implementation. Selection of algorithm for this particular task is decided based on the simplicity of mathematical calculations involved and computational efficiency both for on-line and off-line applications.

4.3.1   QRS   Detection

In the ECG signal, the most prominent feature is the QRS complex. A fiducial marked on the QRS complex sets the process of more detailed examination of the ECG signal in order to study the complete cardiac cycle. Hence in almost all the ECG interpretation methods the identification of QRS complex forms the starting point [7,107,127,139,142]. Extraction of QRS complex from the cardiac cycle is complicated due to the presence of noise in the ECG signal, the amplitude of T wave becoming comparable to that of the R wave and wide variations in the amplitude, duration and morphology of QRS complex [109].

The software techniques of QRS complex detection can be classified into three categories, namely, nonsyntactic, syntactic and hybrid techniques [47,51,81]. The algorithms based on syntactic approach are time consuming due to the use of grammar for each class of patterns. On the other hand nonsyntactic approach is relatively simple and makes use of integer arithmetic that needs lesser computation time. This aspect make them more suitable for real-time implementation . A good number of QRS detection algorithms have been reported in the literature, yet there is a clear scope for improvement in detection and measurement of QRS complex [39].

A simple technique for QRS detection was proposed by Holsinger et.al [55]. In this method ECG signal is digitally differentiated using the first difference and then its comparison with the threshold provide, an effective method of detecting the QRS complex in the presence of P and T

waves. A modification of this approach for the detection of R wave was proposed by Bolton and Coleman. The QRS detector used by them is quasi-static in nature and hence requires frequent adjustment for adoption to the varying nature of the input signal. Another limitation with this method being its tendency of aggravating noise in the signal. Alternatively, refinement over the first difference came in the form of central difference and five point parabolic fit. Amplitude response of the three point digital differentiation along with the two point and five point approaches are shown in Fig.4.7 . The response in case of 3-point and 5-point algorithms goes to zero at nyquist frequency where as for the 2-point difference it does not. Further the response is ideal upto about 20 Hz and deviates a little from ideal between 20 Hz and 30 Hz. Although latter method gives adequate noise suppression but its performance at low frequency is not good. It is computationally slow. On this background the three-point central difference approach gives much better performance besides being computationally fast and hence used in the present work.

QRS complex consists of three waves and among them R wave is the most prominent and is characterized by steep up and down slopes and large amplitude (in standard lead II). The steep positive slope of the R wave and the duration for which it continues to rise may provide strong basis of detection of the QRS complex. Moreover, in case the P, R and T waves have same order of amplitude it is only the slope feature that can help in identifying the QRS complex. The onset of the QRS complex is marked by a small downward deflection in terms of Q wave followed by a very rapidly rising R wave which after reaching maximum value returns towards the baseline with a similar slope. The complex terminates in S wave representing the depolarization of the ventricles. A number of researchers have used negative slope feature for identifying the R-wave. However, positive slope is less affected due to distortion in the event of morphological changes. Because of this reason the positive slope of R-wave has been chosen here in order to characterize the QRS complex. The complex has a narrow frequency band in the range of 10 to 25 Hz.

Recognition of QRS complex becomes difficult because of the presence of noise and P and T waves of the cardiac cycle. Discrimination
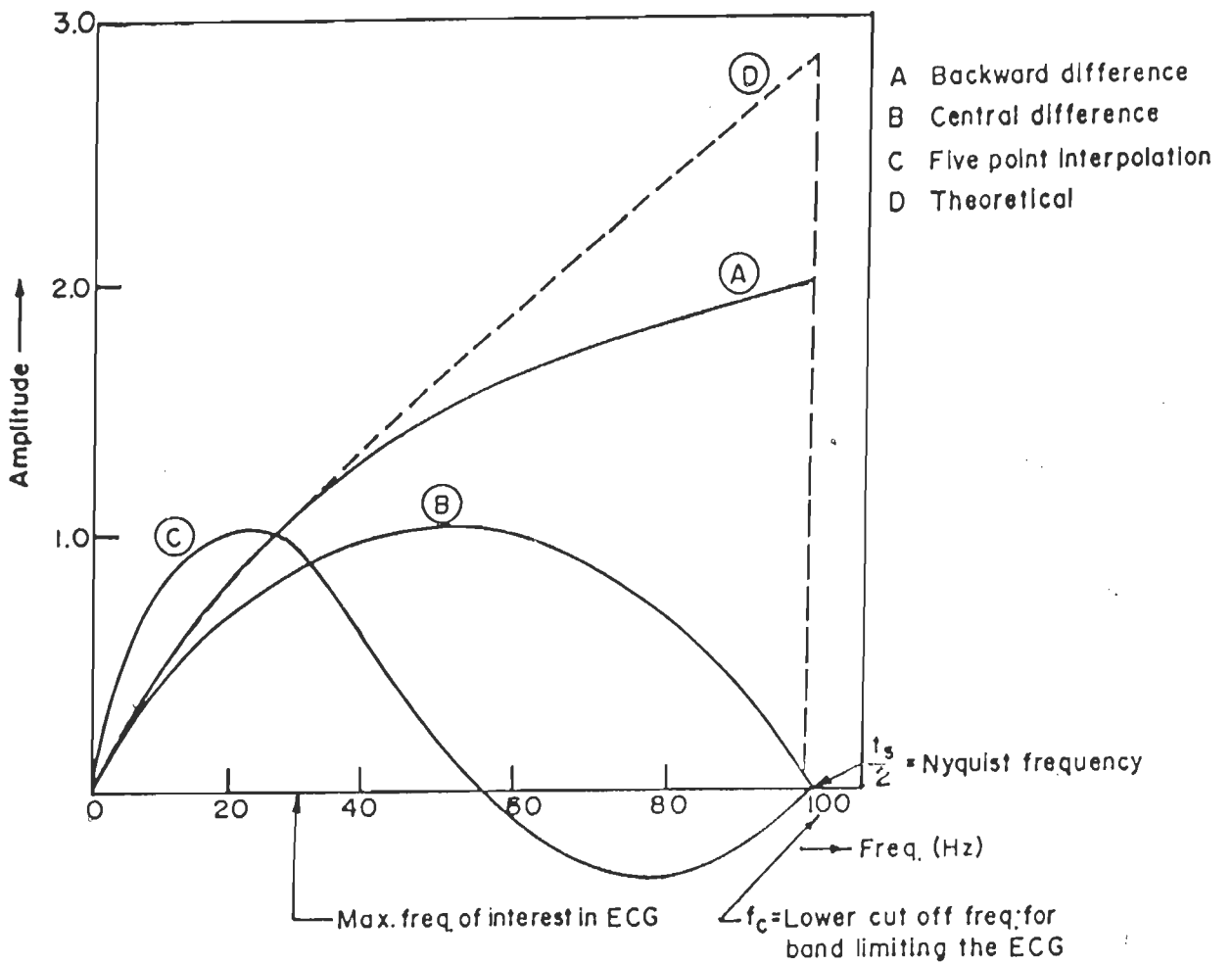
Fig.4.7 Amplitude response of digital
differentiator

between the noise and QRS complex is achieved by setting the upper threshold on the positive slope of R-wave. The value exceeding this threshold is rejected as noise. It is also possible that R-wave itself is mixed with noise spikes. This has been taken care by checking the sequence of slope polarities for five successive samples. A lower threshold on the positive slope has been set in order to differentiate between P and T waves and the R-wave. The variation in the QRS complex and the R-wave amplitude has been taken into account by adaptively adjusting the slope thresholds. To effect this, thresholds are updated continuously on the basis of sliding average value of the peak amplitude of the R-wave calculated at the occurrence of each QRS complex. R-peak is identified by a change of slope from positive to negative using first difference.

The central difference algorithm for digital differentiation uses sampled data with equal sampling interval 'T'. To obtain the derivative at a sample X(KT) the resulting difference equation is written as

$$y(KT)) = \frac{1}{2T} [X(KT) - X(KT-2T)] \qquad 4.13$$

where, y(KT) represents the derivative or slope of the ECG signal at sample X(KT) and X(KT-2T) represents the sample 2T intervals before the current one. A detection function D(KT) has been selected as equal to 2T times y(KT), thus,

$$D(KT) = X(KT) - X(KT-2T) \qquad 4.14$$

For detection of QRS complex ,the detection function D(KT) is computed using relation (4.14) at every sample and then the computed value is compared with the upper and lower limits of its normal distribution which were already set up on the basis of the spectral information of the ECG signal.

Thus, when D(KT) satisfies the condition

$$S_L < D(KT) < S_U \qquad\qquad 4.15$$

it is concluded that the samples at which the function has been computed lie on the upslope of the R-wave.

The procedure for setting up of the thresholds which has been adopted begins with finding out on the basis of statistical data, the range of slope distribution and the normal deviation. Using these values an interactive analysis has been carried out with wide range of inputs and the response of the algorithm was observed. The procedure for setting up of initial limits on the thresholds, in which D(KT) should lie for detection of QRS complex, is explained below.

The parameters of ECG wave, in respect to the QRS complex are the R-peak or peak-to-peak of the QRS complex and its duration. These two parameters vary in the range 0.5 to 3.5 mV and 0.05 to 0.1 second. On the basis of this range of slope distribution has been computed and which is found to lie between 16.7 μV/ms and 40 μV/ms. These values represents the maximum and minimum rate of rise on the positive slope of the R-wave. Slope values that are computed if lie outside the upper limit then they are considered to be corresponding to the noise spikes. On the other hand those lying outside the lower limit are considered to be corresponding to the P and T waves. In case of P wave 2% of the maximum value of QRS complex is chosen and for T wave it is 4% of the maximum value of QRS complex.

These slope values when held constant will not differentiate between large R-wave and noise spikes and small R-wave and P and T waves, when the patients ECG shows appreciable fluctuation of the R-wave amplitude. To overcome this problem the R-wave amplitude variations, the slope thresholds are continuously updated on the basis of running average of R-wave amplitude over four beats.

This algorithm fails in situation where the QRS complex and the noise frequency-band overlap. In this situation the algorithm has to be modified on the basis that the QRS-complex and noise spikes lying in the same slope bounds can be isolated from one another if the duration for which slope continues to be positive is also monitored. A lower bound on this duration will eliminate the noise in favour of the R-wave.

Thus, the algorithm for QRS detection is finally written in the form,

$$S_L (KT-T) \leq D(KT) \leq S_U (KT-T)$$

$$\text{and } D(KT) > 0 \qquad\qquad 4.16$$

Equation (4.16) should be satisfied together with at least 5 successive sampling intervals for positive identification of the QRS complex. While checking the conditions (4.16), it may happen that $D(KT)$ changes sign once in five successive intervals. If such a change of sign occurs more than once "QRS-found" decision is reverted and again a new search is initiated, because in this case the processed samples might be those lying on noise spikes.

4.3.2   R-peak Detection

An algorithm to locate the peak of the detected R-wave, which checks the point of inflexion on the R-wave slope has been developed. While the QRS detection algorithm uses the central difference, the R-peak detection used the first difference since only point of inflex is to be determined but not the slope value.

The digital differentiation is continued with first difference and the change in its sign is observed. At the point inflexion the sign of the derivative changes from positive to negative. The detection algorithm for R-peak is thus represented by

$$D(KT) = [X(KT) - X(KT-T)]$$

$$> 0 \text{ on R-wave upslope} \qquad\qquad 4.17$$

$$< 0 \text{ on R-wave down slope.}$$

The point of transition is the R-peak.

It is likely that the R wave slope get mixed with sharp noise spikes and in consequence the detection of R peak becomes difficult. The noise spikes introduce points of inflexion at places other than R peak and the attempts of locating the actual R peak thus get foiled. This problem has been overcome by checking the slope polarity over four successive sampling interval. If the slope is negative for two successive sampling interval then location of R peak is confirmed otherwise it is noise spike.

4.3.3   QRS Onset and Offset Detection

After the detection of R peak, the onset and offset of QRS complex are to be determined. The onset of the QRS complex is defined as the beginning of Q wave (or R wave when Q wave is absent and offset of QRS complex is defined as end of S wave (or R wave when S wave is absent) [8,57,78,79,81,121]. To determine the R-position(R_p); The R wave has the highest slope in the QRS complex; thus R wave peak will be the maximum slope value on either the upward going side or downward going side of the R wave. The other highest slope of the R wave will be either Q peak or S peak, depending which has the larger absolute value. Then R position (R_p) is located as the zero crossing between R peak and the highest absolute value of Q peak or S peak. A backward search from R_p position is carried out in a window of 80 ms, the first zero crossing preceding the R_p position is the Q position (Q_p). If there is no zero crossing within this window the Q wave is absent. In the next stage QRS onset is to be identified. The position of Q and R wave have already been detected. From Q_p (or R_p) point a backwards search is carried out to locate Q_i (or R_i) point of maximum slope in the signal. From Q_i (or R_i) a backward search is carried out using threshold to locate threshold crossing point. This point is the QRS onset. Similar procedure is used for detecting QRS offset. In this case a forward search is carried out from R_p position in a window of 80 ms, the first zero crossing following the R_p position is the S position S_p. If there is no zero crossing within this window, the S wave is absent. In the next step QRS offset is to be identified. From S_p (or R_p) point, a forward search is initiated

to locate S_i (or R_i) point of maximum slope in the ECG signal. From this point forward search is carried out using threshold to locate threshold crossing point. This point is the QRS offset. In this way QRS fiducials are identified.

4.3.4   P and T Wave Detection

Next step after determining QRS fiducials is to identify P and T waves. These waves have lower frequency components than the QRS complex, therefore detection of P and T waves is a difficult task [57,78,79,81,121]. A window of 150 to 200 ms is defined before R-peak position. This window is shortened when T or next Q peaks are present in it. In this window a search is performed to find the maximum and minimum value. If these values exceeds 2% of the maximum slope of the QRS complex it confirms the presence of P wave, otherwise P wave is absent [78]. P wave position is considered in the zero crossing between the maximum and minimum values of slopes in the window. After the detection of P wave its onset and offset are detected by searching backwards and forwards from P peak respectively to find the maximum value of slope. In order to detect T wave a window is defined which is a function of heart rate. In this window again a search is carried out to find maximum and minimum values of slope. According to their relative position and value of slope, different shapes of T wave are identified such as regular, inverted biphasic. T wave position is located in the zero crossing adjacent to the maximum and minimum value. T wave onset and offset are obtained in a similar fashion as in the case of P wave but the search in this case is carried out from T wave backwards and forwards respectively.

4.3.5   Algorithm

Software for identifying peaks, onsets and offsets of various waves in ECG signal has been developed using 'C' language based on the discussion presented in sections 4.3.1 to 4.3.4. The flow chart for implementation of the algorithm is shown in Fig. 4.8. The CSE Working Party has given certain definitions with regards to the baseline, onset and offset for each wave [134]. The recommendations are followed here too for measurements.

```
                    ┌─────────┐
                    │  Start  │
                    └────┬────┘
                         │
              ┌──────────▼──────────┐
              │ Read data from input│
              │ file and store in array│
              └──────────┬──────────┘
                         │
   ┌───┐      ┌──────────▼──────────┐
   │ B │      │ Detect QRS complex  │
   └───┘      │ using slope threshold criteria│
              └──────────┬──────────┘
                         │
              ┌──────────▼──────────┐
              │ Identify R peak using│
              │ first difference and │
              │ locate R peak position│
              │ by change of slope.  │
              └──────────┬──────────┘
                         │
              ┌──────────▼──────────┐
              │ Detect Qp by searching│
              │ back wards from R peak│
              │ in order to find the │
              │ zero crossing        │
              └──────────┬──────────┘
                         │
                    ╱─────────╲
          No       ╱    If      ╲      Yes
      ◄───────────  Rp−Qp>80ms  ───────────►
                    ╲           ╱
                     ╲─────────╱
                         │
   ┌──────────┐                      ┌──────────┐
   │ Qp absent│                      │ Qp present│
   └────┬─────┘                      └─────┬────┘
        │      ┌──────────────────┐        │
        └─────►│ Locate QRS onset │◄───────┘
               │ searching backwards│
               │ from Qp or Rp for max.│
               │ slope.           │
               └────────┬─────────┘
                        │
              ┌─────────▼──────────┐
              │ Indentify Sp by carrying│
              │ out search forwards │
              │ from R peak.        │
              └─────────┬──────────┘
                        │
                   ╱─────────╲
         No       ╱    If      ╲      Yes
     ◄───────────  Rp+Qp<80 ms ───────────►
                   ╲           ╱
                    ╲─────────╱
                        │
  ┌──────────┐                      ┌──────────┐
  │ Sp absent│                      │ Sp present│
  └────┬─────┘                      └─────┬────┘
       │       ┌──────────────────┐       │
       └──────►│ Detect QRS offset│◄──────┘
               │ searching forwards│
               │ from S peak for max.│
               │ slope            │
               └────────┬─────────┘
                        │
                    ┌───▼───┐
                    │   A   │
                    └───────┘
```

Fig.4.8 Flow chart for ECG wave recognition and characteristic point identification

The first and foremost step in the algorithm is the identification of the QRS complex, and then the R-peak is obtained. This has been achieved by using the standard slope criteria. The next step is to determine the Q and S peaks. This is achieved by searching backwards and forwards to find the respective peaks from the R peak. Then fiducial points for the QRS complex is determined using slope threshold criteria in a similar fashion alongwith search method. Finally, P and T waves are located once again using slope criteria. To facilitate analysis, the horizontal segment preceding the P wave is designated as the baseline for P wave measurements. Similarly PR segment has been used as the baseline for QRS complex and T wave measurements. The amplitude (voltage) for each wave, that is P, Q, R, S and T, are measured from the baseline. The onsets and offsets are marked 20 μV above the baseline as per the recommendations made by the CSE Working Party [134] this is shown in Fig. 4.9. The next step is to find the P_{on}, P_{off} and T_{end}. This has been accomplished by searching forwards and backwards; from P peak using slope criteria, the onset and offset are located. The case for T_{end} is similar. In this case the search is carried out forwards from T peak to locate T_{end} using the same criteria. All the peaks P,Q,R,S and T and the boundaries P_{on}, P_{off}, QRS_{on}, QRS_{off} and T_{end} are stored in an output file for further calculations and diagnosis. From this information other parameters are derived for disease classification.

4.3.6   Results and Discussions

First the algorithm has been validated using 25 records of third data set of CSE database for which measurement results and referee results are given in the database. The measurement results obtained by the developed software for these 25 records are presented in Table 4.1. The results show that the algorithm works satisfactorily on majority of these records but fails only on 4 records out of 25 records. This is because of low amplitude P waves and QRS complex mixed with the noise makes difficult to identify these waves. In the present work QRS complex has been detected using slope threshold criteria. The slope threshold values change with sampling frequency. This aspect has been taken into account by updating slope thresholds using first two seconds of the ECG recording.
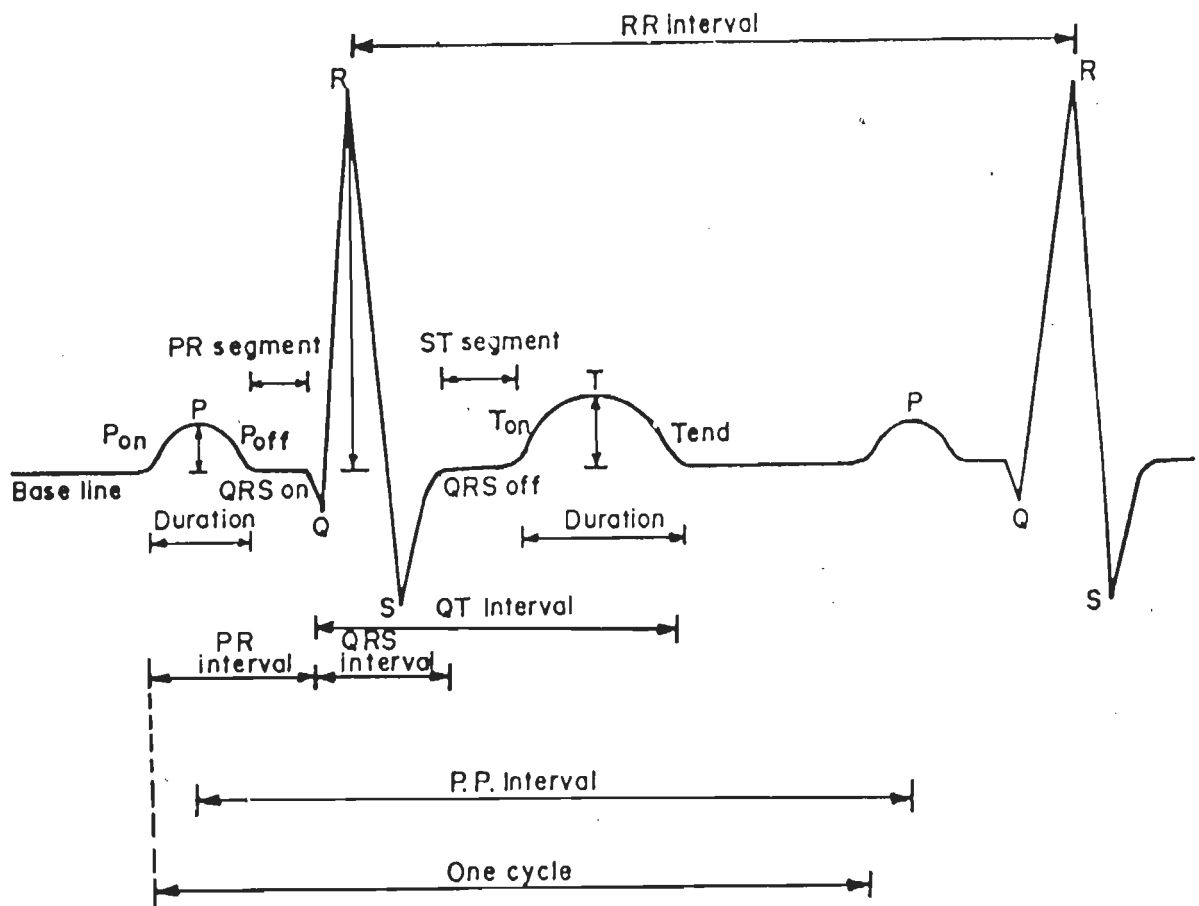
Fig.4.9 A typical ECG waveform.

Table 4.1   Measurement results of 25 records of CSE III data set

Record No.	Onsets and offsets in ms.				
	P_{on}	P_{off}	QRS_{on}	QRS_{off}	T_{end}
1	25	90	133	200	360
6	25	70	131	135	270
11	23	74	98	148	295
16	36	80	99	147	287
21	102	162	181	229	402
26	50	129	141	223	367
31	48	100	121	175	324
36	51	103	127	179	304
41	52	101	125	198	332
46	28	84	106	176	345
51	12	64	93	138	252
56	80	134	172	216	400
61	56	125	168	214	375
66	61	124	139	195	360
71	46	94	118	165	306
76	38	104	126	201	314
81	50	108	124	182	330
86	40	93	118	190	380
91	36	98	123	190	384
96	30	90	114	168	340
101	22	78	91	139	280
106	68	124	128	180	350
111	Ab	Ab	94	148	315
116	52	111	122	168	318
121	23	87	122	185	330
125	51	92	110	160	314
Referee Deviation in ~~sec.~~ mS.	8	12.8	7.8	12.4	32.8

After the validation, the algorithm is applied to MIT/BIH Arrhythmia database [98]. This database contains 48 records, each of 30 minutes duration and sampled at 360 Hz. Each record contains two signals namely signal (0) and signal (1). Signal (0) has been used for testing the algorithm in the present work. Though the algorithm has been tested on all the records but the results for five representative cases are summarized in Table 4.2 to 4.6. The table contains the amplitudes, positions and characteristic points for P wave, QRS complex as well as for end of T wave respectively. The results obtained by the software were also varified using manual measurements made using ECG plots. The algorithm works satisfactorily on the majority of the records for QRS detection. The algorithm produced 396 false positives and 293 false negative beats and a total failure of 0.67% .The detector produced a positive predictivity of 99.6 %.The detector performance has also been compared with the annotated results available in the MIT/BIH Arrhythmia database. The algorithm fails to identify QRS complexes on some of the records, because of presence of very high noise or long episodes of flutters and fibrillation, baseline wander and other artifacts. Record number 102 contains paced beats which leads to higher percentage of detection failures. Record number 200 and 232 contains non QRS complexes with unusual morphologies. This results in large percentage of failures on these records. Some other records namely 116, 117, 205, 211, 220 and 230 contains more noise and motion artifact, therefore, percentage of failures is high on these records.

The algorithm developed also detects QRS fiducials, P &T waves and their respective onsets and offsets. From the results obtained for all records it is observed that in few records the detection of onsets and offsets P & T wave are not being done accurately. These are the cases where the signals are highly influenced seriously by noise or baseline drift or their amplitudes are too small. One such case of record number 113 for which results are given in Table 4.7. The reason for failure is that the P wave amplitude is very small and mixed with noise. The percentage of P wave detection is found to be 65% and that for T wave the detection is 75%. The deviations in the onset and offset for P wave, QRS complex as well as T_{end} are within the tolerance limit recommended by the CSE Working Party [Table 4.1] [134]. Similarly, the deviation observed from the manual measurement also confirms the same.

Table 4.2: Peak and Boundary Measurement Results for Record No. 100 of MIT/BIH Arrhythmia Database

P_{on}	P_{pos}	Ppeak (mV)	P_{off}	R_{pos}	Rpeak (mV)	QRS_{on}	QRS_{off}	T_{on}	T_{pos}	Tpeak (mV)	T_{end}
0124	0148	0.023	0168	0206	0.239	0185	0215	0277	0316	-0.02	0358
0394	0427	0.025	0448	0479	0.242	0455	0487	0547	0586	- 0.02	0628
0670	0700	0.022	0718	0755	0.236	0736	0766	0829	0866	- 0.02	0909
0970	0980	0.021	1000	1039	0.272	1018	1049	1099	1138	-0.024	1180
1233	1259	0.022	1277	1319	0.307	1295	1331	1392	1430	-0.021	1474
1498	1527	0.025	1546	1589	0.271	1564	1598	1656	1695	-0.023	1737
1779	1808	0.025	1829	1862	0.237	1841	1872	1932	1970	-0.022	1995

Table 4.3: Peak and Boundary Measurement Results for Record No. 101 of MIT/BIH Arrhythmia Database

P_{on}	P_{pos}	Ppeak (mV)	P_{off}	R_{pos}	Rpeak (mV)	QRS_{on}	QRS_{off}	T_{on}	T_{pos}	Tpeak (mV)	T_{end}
0245	0265	0.027	0282	0313	0.35	0294	0332	0381	0420	0.037	0464
0571	0598	0.026	0619	0656	0.37	0636	0679	0717	0756	0.035	0797
0930	0952	0.027	0973	1008	0.369	0990	1028	1083	1122	0.036	1163
1314	1344	0.027	1363	1395	0.362	1377	1417	1475	1514	0.036	1558
1644	1674	0.025	1692	1728	0.349	1707	1748	1809	1844	0.037	1888

Table 4.4: Peak and Boundary Measurement Results for Record No. 103 of MIT/BIH Arrhythmia Database

P_{on}	P_{pos}	Ppeak (mV)	P_{off}	R_{pos}	Rpeak (mV)	QRS_{on}	QRS_{off}	T_{on}	T_{pos}	Tpeak (mV)	T_{end}
0014	0022	0.022	0032	0073	0.387	0051	0084	0138	0165	0.089	0209
0296	0324	0.025	0345	0385	0.394	0362	0396	0450	0484	0.09	0528
0619	0650	0.021	0669	0700	0.412	0679	0712	0762	0801	0.091	0845
0938	0970	0.02	0986	1024	0.406	1000	1036	1085	1124	0.091	1163
1267	1287	0.025	1304	1347	0.385	1323	1360	1403	1442	0.088	1482
1585	1615	0.026	1628	1667	0.41	1646	1679	1721	1760	0.089	1801

Table 4.5: Peak and Boundary Measurement Results for Record No. 111 of MIT/BIH Arrhythmia Database

P_{on}	P_{pos}	Ppeak (mV)	P_{off}	R_{pos}	Rpeak (mV)	QRS_{on}	QRS_{off}	T_{on}	T_{pos}	Tpeak (mV)	T_{end}
0009	0040	0.02	0065	0104	0.206	0083	0124	0181	0215	0.07	0254
0322	0354	0.03	0383	0423	0.207	0402	0442	0506	0545	0.08	0589
0633	0665	0.03	0694	0733	0.201	0712	0753	0800	0828	0.06	0872
0945	0977	0.04	1002	1042	0.217	1021	1063	1124	1163	0.08	1207
1264	1295	0.02	1324	1362	0.204	1342	1381	1436	1474	0.09	1515
1576	1606	0.04	1631	1670	0.205	1650	1689	1748	1786	0.06	1827
1870	1903	0.04	1931	1970	0.207	1949	1989	1993	2016	0.07	2057

Table 4.6: Peak and Boundary Measurement Results for Record No. 232 of MIT/BIH Arrhythmia Database

P_{on}	P_{pos}	Ppeak (mV)	P_{off}	R_{pos}	Rpeak (mV)	QRS_{on}	QRS_{off}	T_{on}	T_{pos}	Tpeak (mV)	T_{end}
0079	0090	0.011	0118	0170	0.225	0137	0183	0244	0276	0.066	0319
0919	0941	0.014	0969	1008	0.21	0980	1021	1074	1113	0.072	1157
1845	1862	0.011	1891	1932	0.196	1906	1944	1993	2016	0.067	2060

Table 4.7: Peak and Boundary Measurement Results for Record No. 113 of MIT/BIH Arrhythmia Database

P_{on}	P_{pos}	Ppeak (mV)	P_{off}	R_{pos}	Rpeak (mV)	QRS_{on}	QRS_{off}	T_{on}	T_{pos}	Tpeak (mV)	T_{end}
0077	0106	0.013	0126	0163	0.44	0143	0170	0226	0265	0.21	0304
0336	0369	0.018	0390	0429	0.471	0407	0439	0502	0534	0.214	0574
0582	0611	0.007	0631	0670	0.472	0648	0679	0736	0775	0.19	0819
0869	0900	0.023	0918	0960	0.482	0936	0971	1034	1073	0.183	1116
1235	1268	0.007	1289	1330	0.467	1307	1339	1395	1434	0.153	1478
1607	1628	0.014	1649	1685	0.452	1665	1693	1755	1791	0.219	1834

CHAPTER - 5

INTERPRETATION OF ARRHYTHMIAS

CHAPTER - 5

INTERPRETATION OF ARRHYTHMIAS

5.1   Introduction

When the heart rate, rhythm, or conduction fails to confirm to normal standards, the resulting disorder is called Arrhythmia. Because of wide acceptance and common usage, the terms arrhythmias and dysarrhythmias are used interchangeably with disorder of heart beat, even though semantically the two terms imply an irregularity in rhythm. Arrhythmias may occur without noticeable symptoms or cause, the severe symptoms that accompany an exteremly low cardiac output or myocardial ischemia . These disorders can be identified by electrocardiogram analysis.

In this chapter detailed arrhythmia classification based on two different mechanisms and also based on prognosis or seriousness is presented. Lead selection and length of recording have been discussed in brief. A six step logical procedure used for off-line interpretation of arrhythmias is given here. The diseases considered in the present work are briefly explained in this chapter. The algorithm developed for arrhythmia interpretation has been tested for its performance on the different records of MIT/BIH Arrhythmia database.

5.2   Classification of Arrhythmias

Arrhythmias can be broadly classified in two alternate ways namely, according to their underlying mechanism and according to the prognosis or seriousness of the disease [68]. In the first method of classification according to the underlying mechanism of arrhythmia, it can be of two types:

(a) Disturbances in impulse formation

(b) Disturbances in impulse conduction

5.2.1.   Disturbances in Impulse Formation

Under the normal circumstances the sinoatrial (SA) node [Fig 2.2] serves as the pacemaker for the heart and it generates impulses regularly at a rate of 60 to 100 beats/minute. If the normal sinus rhythm is disturbed either due to the SA node discharges abnormally or because a pacemaker at another site gains control of the heart beat, the resulting disorder is termed as disturbance in impulse formation.

Arrhythmias that fall under this category are classified according to the site of impulse formation as follows :

1. Disturbances arising in the SA node (sinus rhythms)
2. Disturbances arising in the atria (atrial arrhythmias)
3. Disturbances arising in the AV junction (AV junctional arrhythmias)
4. Disturbances arising in the ventricle (ventricular arrhythmias)

These disorders of impulse formation may be further subclassified according to the mechanism of the arrhythmia. There are six major arrhythmic mechanisms as follows :

1.   Tachycardia
2.   Bradycardia
3.   Premature beats
4.   Escape beats
5.   Flutter
6.   Fibrillation

5.2.2.   Disturbances in Impulse Conduction

A conduction disturbance refers to a block or abnormal delay in the passage of cardiac impulses from the SA node through the AV node and

left and right bundle branches and to the purkinje fiber system in the ventricles [Fig 2.2.]. Blocks may occur at any point along the course of the conduction system but it is customary to classify these disorders according to three main anatomic sites as follows :

1.   Blocks within the SA node or atria (sinoatrial blocks)
2.   Blocks between the atria and ventricles (atrioventricular blocks)

This is further subclassified as :

(a)   First degree AV block
(b)   second degree AV block
(c)   Third degree (Complete) AV block

3.   Blocks within the ventricles (intraventricular blocks)
This is further subdivided as:

(a)   Left bundle branch blocks
(b)   Right bundle branch blocks
(c)   Bilateral bundle branch blocks
(d)   Ventricular asystole

5.3   Arrhythmia Classification Based on Prognosis

In addition to the methods described above, arrhythmias can also be classified in a general way according to their seriousness or prognosis. This classification is helpful for the staff manning the ambulatory monitor, since it considers relative importance of various arrhythmias from clinical point of view. Using this classification the following three prognostic categories of arrhythmias can be established.

5.3.1   Minor Arrhythmias

These disorders are not of immediate concern because they usually do not affect the circulation nor do they warn of the development of more serious arrhythmias.

5.3.2.   Major Arrhythmias

These disturbances either reduce the pumping efficiency of the heart or herald the onset of lethal arrhythmias. They require prompt treatment.

5.3.3.   Lethal Arrhythmias

These arrhythmias require immediate resusciation in order to prevent death of the patient.

The classification of arrhythmias according to their seriousness or prognosis is presented in Table 5.1.

5.4   Lead Selection and Length of Recording.

Cardiac monitors can record one or more electrocardiographic leads. Lead II is often selected as a monitoring lead because of the fact that the normal axis of cardiac depolarization is in the same direction as the axis of this lead. Both atrial and ventricular depolarization are clearly seen in lead II . A chest electrode V_1 is used as a second monitoring lead or as an alternate lead. This lead is particularly useful for monitoring ischemic changes in myocardium. While lead II and V_1 are the most useful leads for detecting the majority of arrhythmias, there can be no means to reveal all disturbances in cardiac rhythm. It is important to recognize this limitation of cardiac monitoring, and to understand that when the interpretation of an arrhythmias is in doubt, the chest leads may have to be repositioned or a 12 lead ECG is recorded so as to gather more diagnostic information from the other leads.

In most instances in order to arrive at diagnostic decision based on rhythm disturbances , length of electrocardiographic tracing equivalent to 15 to 30 seconds will be sufficient, but occasionally however, tracings of 60 to 120 seconds duration or more will be necessary in complex arrhythmia diagnosis [58,68,94].

Table 5.1 Classification of Arrhythmias based on Prognosis [67].

Minor	Major	Lethal
*Sinus tachycardia *Sinus bradycaradia *Sinus arrhythmia *Wandering pacemaker *Premature atrial con traction *Premature junctional contraction *Premature ventricular contraction.	* Sinus tachycardia (when per sistent) * Sinus brady cardia (rate <50/ minute) * Sick sinus syndrome * Sinoatrial arrest (and SA block) * Proxysmal superventricular tachycardia * Atrial flutter. * Atrial fibrillation * Premature junctional contrac tions * Junctional rhythm * Paroxysmal junctional tachy cardia * Nonparoxymal junctional tachycardia * Premature ventricular con structions * Accelerated adioventricular rhythm First-degree AV heart block * Second-degree AV heart block * Third -degree Av heart block Intraventricular blocks, bandle branch blocks.	* Ventricular tachycardia * Ventricular fibrillation * Ventricular asystole.

5.5   Interpretation of Arrhythmias

In general, the problem of ECG interpretation can be tackled by two complementary approaches First one is based on the experience in the interpreting the ECG by directly mapping ECG strips into the event domain. The other approach uses knowledge such as physiology and anatomy in guiding the interpretation. Cardiologist use both the approaches for interpreting ECG which may lead to different diagnosis. The expert builds his own rules to establish a direct mapping between symptoms and diagnosis. The ECG literature contains a lot of information of this type as a result of decades of compiled clinical experience. A rule-based system can be derived from the relation between physiological events and ECG patterns.

ECG interpretation of arrhythmias requires analysis of cardiac rate, rhythm and conduction. Criteria for the classification of the single beat and the analysis of the rhythm were defined by experts in the field of cardiology, who have also supported with their valuable experience in terms of heuristic rules. Criteria for interpretation actually depends on the specific leads which are recorded. In the present work lead II has been used, since it is commonly used for ambulatory ECG monitoring.

Each beat is classified taking into account the QRS morphology, the presence of P wave and intra and inter-beat intervals [128]. Next rhythm is analysed on the basis of previous beat information. Most of the arrhythmias can be correctly identified by the six basic steps described below [68]. An attempt to interpret arrhythmias without adhering to this type of orderly process can only lead to confusion and error.

Step 1   Determine RR Interval

First locate R peaks. The time duration between two successive R peaks gives RR interval in seconds. This information can be directly used for calculating the heart rate either looking at the standard table or by calculating the same using mathematical formula.

Step 2   Determine the Regularity (Rhythm) of the R Wave

This is obtained by simply observing the ECG. If the RR intervals are same, without much variation in their length, it can be concluded that the ventricular rhythm is regular. In many situations, however, visual observation is unreliable and it is necessary to measure RR interval precisely in order to know about the regularity of the R waves. When the difference between consecutive RR intervals exceeds 0.12 sec the ventricular rhythm is described as abnormal or irregular. Many arrhythmias are characterized on the basis of regular or irregular rhythms and this single finding is therefore an important step in the process of interpreting arrhythmias.

Step 3   Identify and Examine P Wave

P wave often provide more information than any other ECG wave form about the type and mechanism of a cardiac arrhythmia. Because of this reason it is mandatory to search for P waves and examine their size , shape and position . A normal P wave (as seen in lead II) is upright, smoothly rounded and precedes each QRS complex. These findings indicate that the heart beat originates in the SA node and sinus rhythm is present. On the other hand, the absence of P waves or an abnormality in their configuration or position indicates that impulses are arising outside the SA node and that an ectopic pacemaker is in control of the heart rhythm.

Step 4   Meausure PP Interval.

It is similar to RR interval. First locate the P peaks and the time duration between two P peaks positions gives PP interval. This information is used for calculating atrial rate in the same fashion as that of ventricular rate. This parameter is most useful in atrial related diseases. Such as atrial flutter, tachycardia and fibrillation. In normal case PP and RR intervals will have the same value.

Step 5   Measure PR Interval.

Normally the duration of this interval should be between 0.12 to 0.2 sec.Prolongation of the PR interval beyond 0.2 sec indicates a delay in the passage of impulses from the SA node to the ventricle. On the other hand if PR interval is less than 0.12 sec indicates that the SA node impulses are reaching the ventricles sooner than expected, through an abnormal pathway.

Step 6   Measure QRS Duration.

The width of the QRS complex represents the time required for a stimulus to activate both ventricles. The normal duration of the QRS complex is not more than 0.12 sec. If there is an obstruction in one of the bundle branches, activation of the ventricles will be delayed, as manifested by the width of the QRS complex exceeding the limit of 0.12 sec.

Based on the above 6 steps a diagnostic disease classification for most common arrhythmias is presented in Table 5.2.

5.6   Arrhythmia Classification Program

Computer program using 'C' language has been developed for arrhythmia interpretation based on the algorithm discussed in section 5.5. The flow chart for the implementation of the algorithm is shown in Fig. 5.1. The arrhythmias are generally classified on the basis of timing interval. The input to the interpretation program is the output file obtained from the parameter extraction [section 4.3.5] software . This file contains onset and offset of P and QRS waves. The other parameters such as P-duration PR-interval, QRS-duration, PP and RR interval are derived from the above measured parameters . The classification program uses ECG features computed for each beat. The diagnostic rules have been applied to classify different arrhythmias. Brief, description of the five different types of arrhythmias alongwith their salient features that have been considered in the present work is given below:

TABLE 5.2 Arrhythmia Classification Table

Disease	Atrial interval (PP-INT in sec.)	Ventricular interval (RR-INT in sec.)	P wave Morphology	A-V delay (PR-INT in sec.)	Ventricular Morphology (QRS-DUR in sec.)	Comments
1) Sinus arrhyth-mia	Normal (1.0 to 0.65)	Normal (1.0 to 0.65)	Normal Upright, smoothly rounded and preceeds each QRS complex.	Normal (0.12 to 0.2)	Normal (0.04 to 0.12)	It is characterized by normal P-QRS-T complexes with alter-nating periods of grad-ually lengthening and shortening PP & RR in-tervals
2) Sinus Brady-cardia	Normal	1.5 to 1.0	Normal	Normal	Normal	It is characterized by normal P-QRS-T com-plexes, which are re-corded in slow succes-sion. It is commonly associated with respi-ratory sinus arrhythmia
3) Sinus Tachy-cardia	Normal	1.0 to 0.4	Normal	Normal	Normal	It is characterized by normal P-QRS-T com-plexes, which are re-corded in rapid suc-cession It varies with emotion, respiration and exercise. If this persists at rest then it is disorder.

Disease	Atrial interval (PP-INT in sec.)	Ventricular interval (RR-INT in sec.)	P wave Morphology PR-INT in sec.)	A-V delay	Ventricular Morphology (QRS-DUR in sec.)	Comments
4)Prematu -re Atrial Contraction (PAC)	Short	Usually normal	Either abnormally placed or inverted and different from normal P-wave	Usually normal but may be short or prolonged	Usually normal	It occurs when the premature impulse does not interfere with the sinus node cycle. The time dura- tion between the P- QRS preceeding and the P-QRS following the premature beat is less than two normal cycle.
5)Normal Sinus rhythm	Normal	Normal	Normal	Normal	Normal	The rhythm is normal and originates from the S.A. node.
6)Atrial flutter	0.24 to 0.15	1 to 0.38	Rather than P waves there are characteris- tic oscillation called saw tooth waves	PR interval absent	Normal	The resulting dispar- ity between atrial and ventricular rate is described as atrial flutter with 2:1, 3:1 or 4:1 block.

Disease	Atrial interval (PP-INT in sec.)	Ventricular interval (RR-INT in sec.)	P wave Morphology	A-V delay (PR-INT in sec.)	Ventricular Morphology (QRS-DUR in sec.)	Comments
7) Atrial Fibrillation	0.15 to 0.1	Normal rapid or slow 1 to 0.6	P waves are absent. Replaced small irregular rapid oscillation called 'f' waves	PR-Interval absent	Normal but occurs at irregular intervals	The characteristic feature is the irregular absence of P waves confirms the diagnosis.
8) Premature ventricular contraction (PVC)	Normal	Often normal but occur at any rate	P wave is usually hidden in QRS complex	Absent	QRS complex is widened and distroted in shape	PVCS are the most common of all arrhythmias associated with AMI.
9) Bigeminy	Normal	Normal	Not seen in PVCS	Absent	Grossly distorted	It may warn of more dangerous ventricular arrhythmia
10) R on T Pattern	Normal	Normal	Not seen in PVCS	Absent	Two beats are distorted and have different configuration	This indicate high risk of precipitating ventricular flutter
11) Venticular Tachy-cardia	variation in PP interval	0.66 to 0.27	No relation between P and QRS complex	Absent	wide, slurred complexes typical of repetitive PVCs.	If this persist for longer period it can generate ventricular fabrillation

(Contd....)

Disease	Atrial interval (PP-INT in sec.)	Ventricular interval (RR-INT in sec.)	P wave Morphology	A-V delay (PR-INT in sec.)	Ventricular Morphology (QRS-DUR in sec.)	Comments
12)Ventricular Fibrillation	—	—	—	—	—	It is characterized by rapid, repetative `f' waves originating in the ventricles. PQRST waves can not be clearly seen.
13) First degree A-V-block	Normal	Normal	Normal	Prolonged PR interval beyond 0.20	Normal	It usually indicate injury to the A-V nodal area and may warn for 2nd & 3rd degree A.V. block.
14.Second degree block Mobiz type I	Changes	Progressively decreasing	No. P waves always exceed the QRS complexes	Progressive Prolongation	Normal	It is usually caused by ischemic injury to A-V node & lead to 3rd degree block.
15. Second degree block Mobiz Type -II	Greater than 0.43	Normal	More P waves than the QRS complexes	Constant	widened	It may lead to complete heart block or ventricular stand still.

Disease	Atrial interval (PP-INT in sec.)	Ventricular interval	P wave Morphology (RR-INT in sec.)	A-V delay (PR-INT in sec.)	Ventricular Morphology	Comments (QRS-DUR in sec.)
16. Third degree block	Normal	1.2 to 0.1 sec.	P waves are more in number compared to QRS complexes	No relation between P & QRS complex	Normal or widened and distorted	It causes marked reduction in cardiac output. The ventricular rate is 30 to 40 beats/min. & can not increase to meet blood circulation de mands.
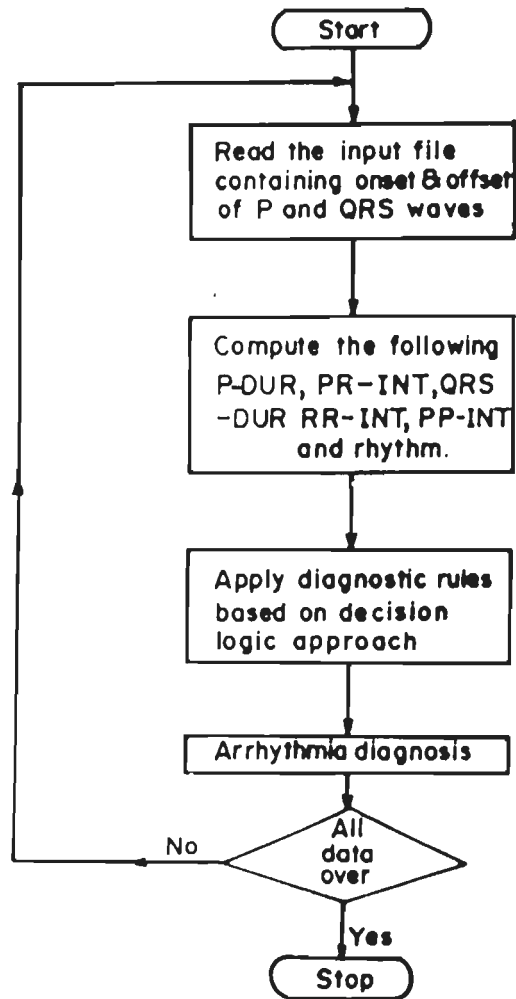
Fig. 5.1 Flow chart for arrhythmia Interpretation algorithm.

5.6.1.   Sinus Arrhythmia

It is most common phenomena found in children and tends to disappear with advancing age, but some times it may also be observed in adults. It is often but not always , related to the respiratory cycle. Characteristic of sinus arrhythmia is a normal sinus pacemaker which alternatively slows and speeds up. Normal atrial depolarzation (i.e normal P waves), normal AV conduction (i.e. normal PR and normal QRS) configuration are present. This arrhythmia involves only the rate of impulse formation by the cells of the sinus node. Thus the PP and RR intervals are equally affected in each cycle and of equal duration in any given cycle. The minimal variation in cycle length between the shortest and the largest cycle is 0.12 second.

5.6.2   Sinus Bradycardia

It is defined as a heart rate of less than 60 beats per minute with a normal sinus mechanism. It is a normal varient in well conditioned athelets at rest and in normal sleep in healthy individuals. The electrocardiographic findings include a normal P wave, normal QRS complex and a normal PR interval with a PP and RR interval of greater than 1.00 second.

5.6.3.   First Degree AV Block

This is a prolongation of the conduction time across the AV junction and is manifested electrocardiographically as a constant prolongation of the P-R interval in all complexes, as measured from the onset of the P wave to the first deflection of the QRS complex. The normal upper limit for the PR interval varies some what with age and with heart rate. The normal upper limit in the adult patient is 0.28 seconds and is lower in children . The normal upper limit also varies with heart rate, tending to be shorter with more rapid rates in normal persons.

5.6.4   Atrial Premature Contraction (APC)

These are common and occur both with and without identifiable heart disease. Frequent APC often precede the onset of atrial tachycardia or

atrial flutter or fibrillation. Electrocardiographically, the APC is recognized as an early P wave, frequently different in configuration from the normal P waves. Conduction of the premature impulse with a resulting QRS complex may or may not occur. The premature P: QRS is followed by a pause. It may be a compensatory or non compensatory.

5.6.5   Normal Sinus Rhythm.

It is observed in the normal individual, the rhythm is normal and originates from the SA node. The characteristic features are normal P wave normal PR -interval, PP and RR intervals are normal and QRS duration is also normal.

5.7   Results and Discussion

Evaluation of the software developed has been carried out on different records of MIT/BIH Arrhythmia database. The database also contains beat-by-beat anotated results for variety of arrhythmias. This helps to compare the performance of the software. A 12 sec ECG strip is extracted from each record based on the presence of particular type of arrhythmia for classification. In the present work five diseases have been considered and tested extensively on the MIT/BIH Arrhythmia database. The diseases considered are Normal sinus rhythm, Atrial premature contraction (APC); Sinus arrhythmia, First degree AV block and Sinus bradycardia. Though the algorithm has been tested on different records but the results for one representative case for each disease are presented as sample examples. The output produced by the interpretation program is given in Fig. 5.2 to 5.6. Because of space constraint only 6 sec record is given in each case and the detailed results for single beat where the abnormality has occured is presented. In Fig. 5.2 a portion of the record number 100 containing Normal sinus rhythm is given. It contains in all 16 beats, all these beats have been classified by the software as Normal sinus rhythm beats. Fig. 5.3 shows ECG strip of record number 101 containing Normal sinus rhythm and Atrial premature beats. In all ,there are 12 beats out of which 11 are Normal sinus rhythm beats and one beat
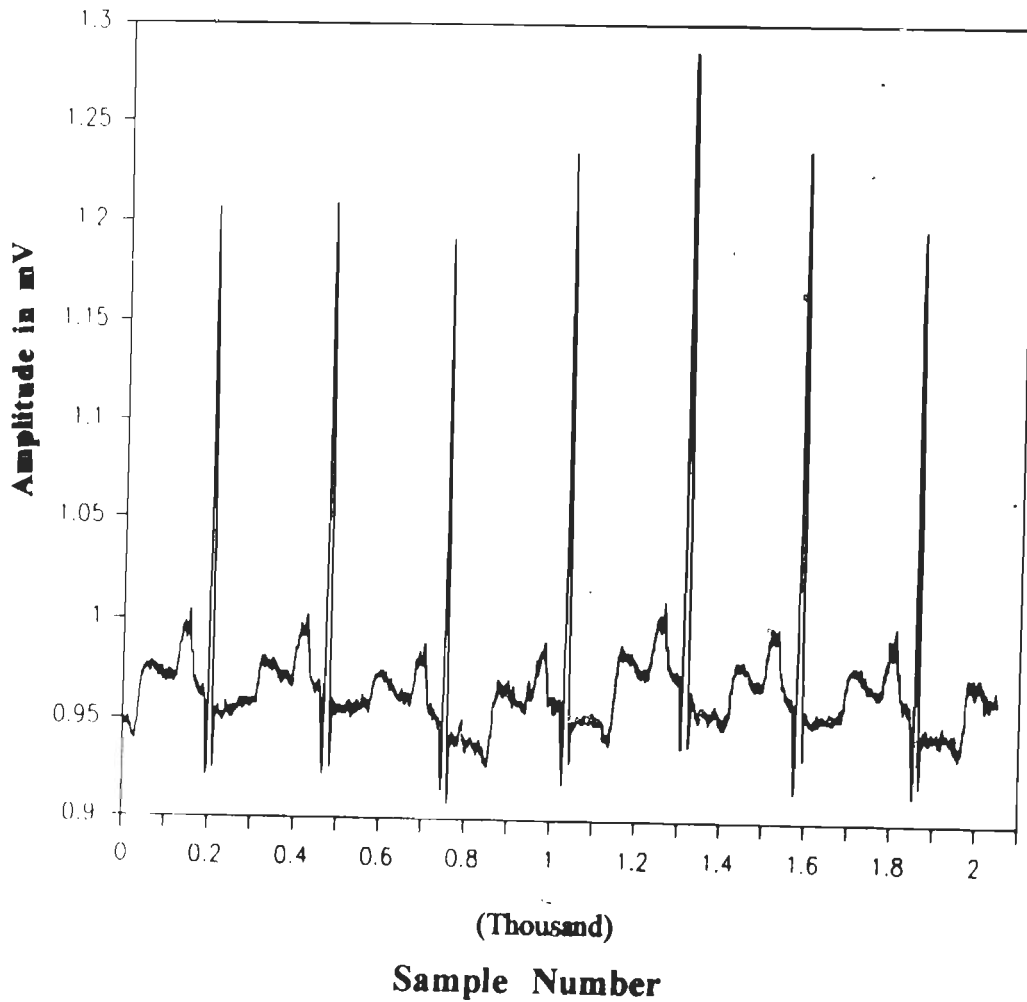
PR_interval in sec	= 0.174	Normal
QRS_duration in sec	= 0.087	Normal
P_duration in sec	= 0.140	Normal
RR_interval in sec	= 0.756	Normal
PP_interval in sec	= 0.748	Normal
Normal rhythm		

Normal Sinus Rhythm

Fig.5.2   Output from the Arrhythmia Interpretation Program for Record
No. 100 (for the 5th Beat) of MIT/BIH Arrhythmia Database

(Thousand)

Sample Number
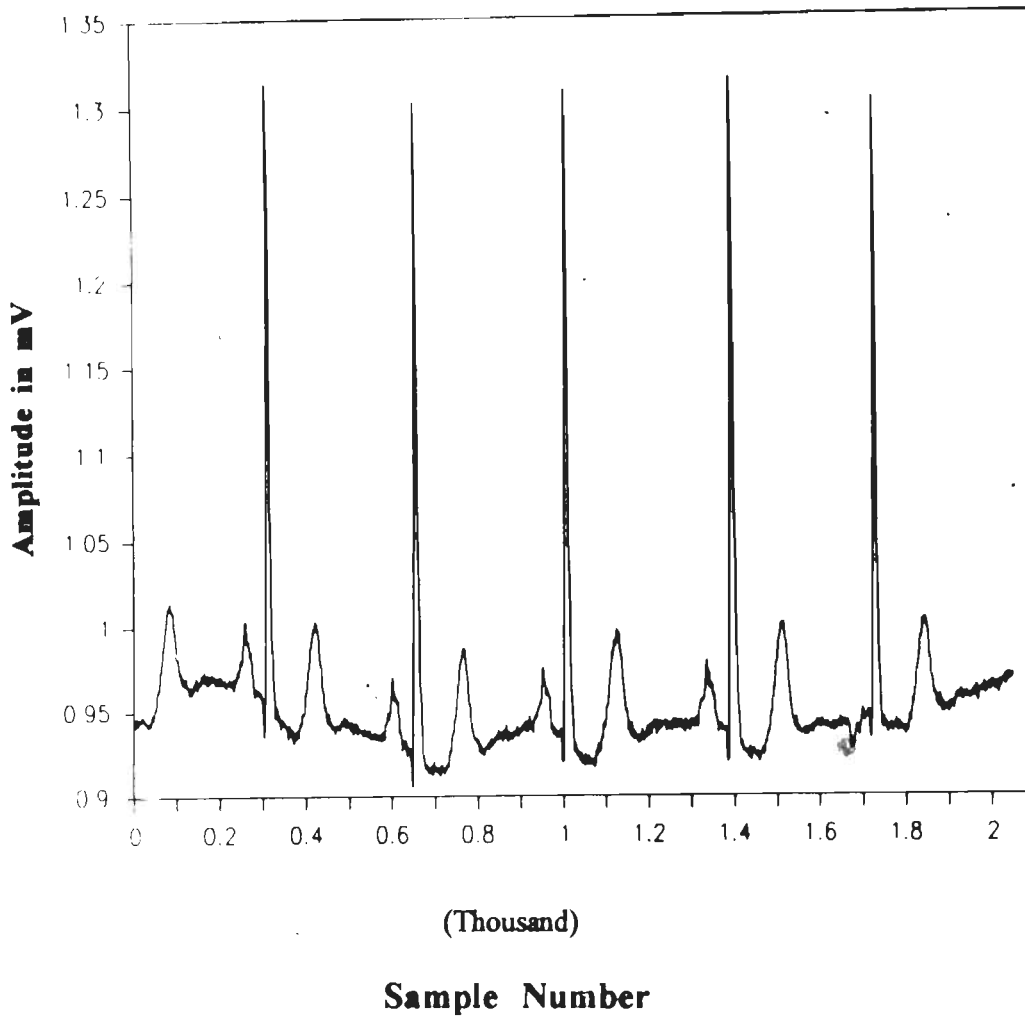
PR_interval in sec	= 0.176	Normal
QRS_duration in sec	= 0.115	Normal
P_duration in sec	= 0.134	Normal
RR_interval in sec	= 1.159	Abnormal
PP_interval in sec	= 1.193	Abnormal
Normal rhythm		

Atrial Premature Contraction

Fig.5.3   Output from the Arrhythmia Interpretation Program for Record No. 101 (for the 5th Beat) of MIT/BIH Arrhythmia Database

is identified as APC. Fig. 5.4 is a case of Sinus arrhythmia present in record 103. This strip contains 14 beats all these beats are classified as Sinus arrhythmia beats. A case of first degree AV block is presented in Fig. 5.5. The strip contains 14 beats out of which 6 beats are Normal sinus rhythm beats and remaining 8 beats show the presence of first degree AV block. Record number 232 is a case of Bradycardia shown in fig.5.6. The strip has 6 beats all of them show the presence of Sinus bradycardia. The results thus obtained by the software were then compared with those given in the database. It is observed that in majority of cases the result matches with MIT/BIH Arrhythmia diagnosis, but in few cases the algorithm fails in classifying atrial arrhythmias. One such example is given in Fig. 5.7. In this case P wave has not been detected accurately [Table 4.7] therefore the interpretation program wrongly classified the disease as Normal sinus rhythm but the case is of Sinus arrhythmia.

(Thousand)

Sample Number

PR_interval in sec	= 0.162	Normal
QRS_duration in sec	= 0.078	Normal
P_duration in sec	= 0.118	Normal
RR_interval in sec	= 0.952	Normal
PP_interval in sec	= 0.941	Normal
Irregular rhythm		
Sinus Arrhythmia		

Fig.5.4   **Output from the Arrhythmia Interpretation Program for Record No. 103 (for the 5th Beat) of MIT/BIH Arrhythmia Database**

(Thousand)

Sample Number

PR_interval in sec	= 0.218	Abnormal
QRS_duration in sec	= 0.109	Normal
P_duration in sec	= 0.168	Abnormal
RR_interval in sec	= 0.862	Normal
PP_interval in sec	= 0.871	Normal
Normal rhythm		

Normal Sinus Rhythm
First Degree A-V Block

Fig.5.5   Output from the Arrhythmia Interpretation Program for Record No. 111(for the 5th Beat) of MIT/BIH Arrhythmia Database
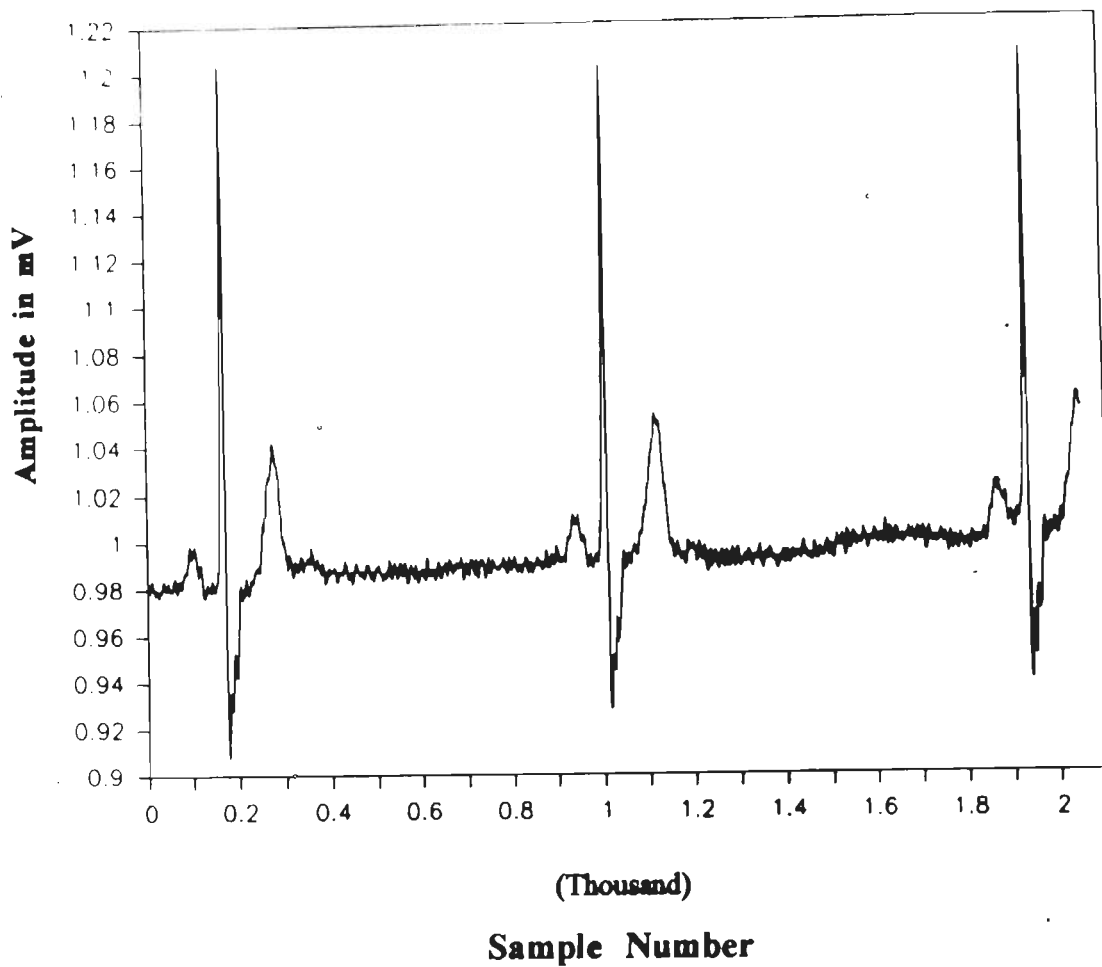
PR_interval in sec	= 0.171	Normal
QRS_duration in sec	= 0.115	Normal
P_duration in sec	= 0.140	Normal
RR_interval in sec	= 2.587	Abnormal
PP_interval in sec	= 2.579	Abnormal
Normal rhythm		
Sinus Bradycardia		

Fig.5.6   Output from the Arrhythmia Interpretation Program for Record No. 232 (for the 2nd Beat) of MIT/BIH Arrhythmia Database

(Thousand)

Sample Number

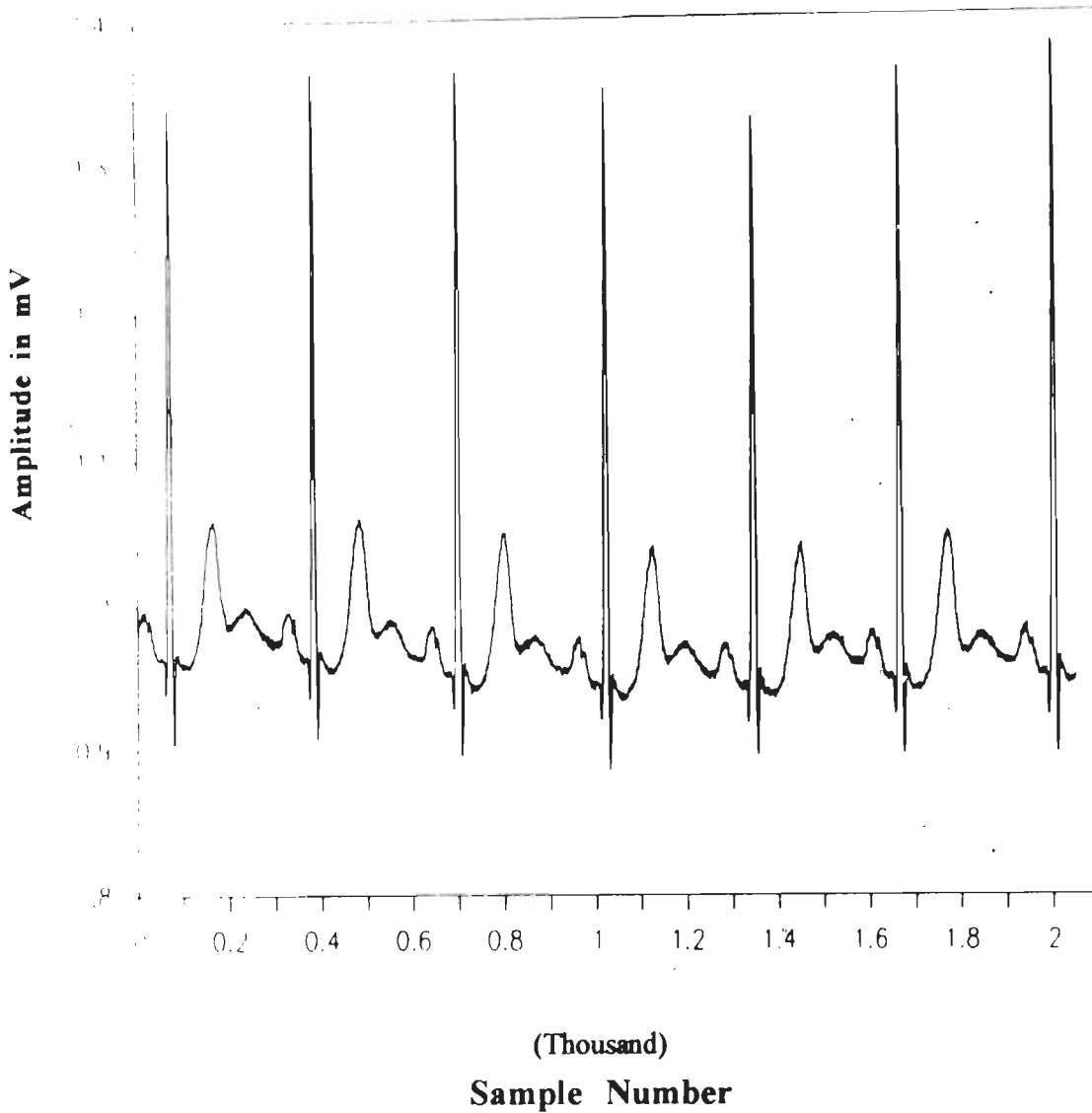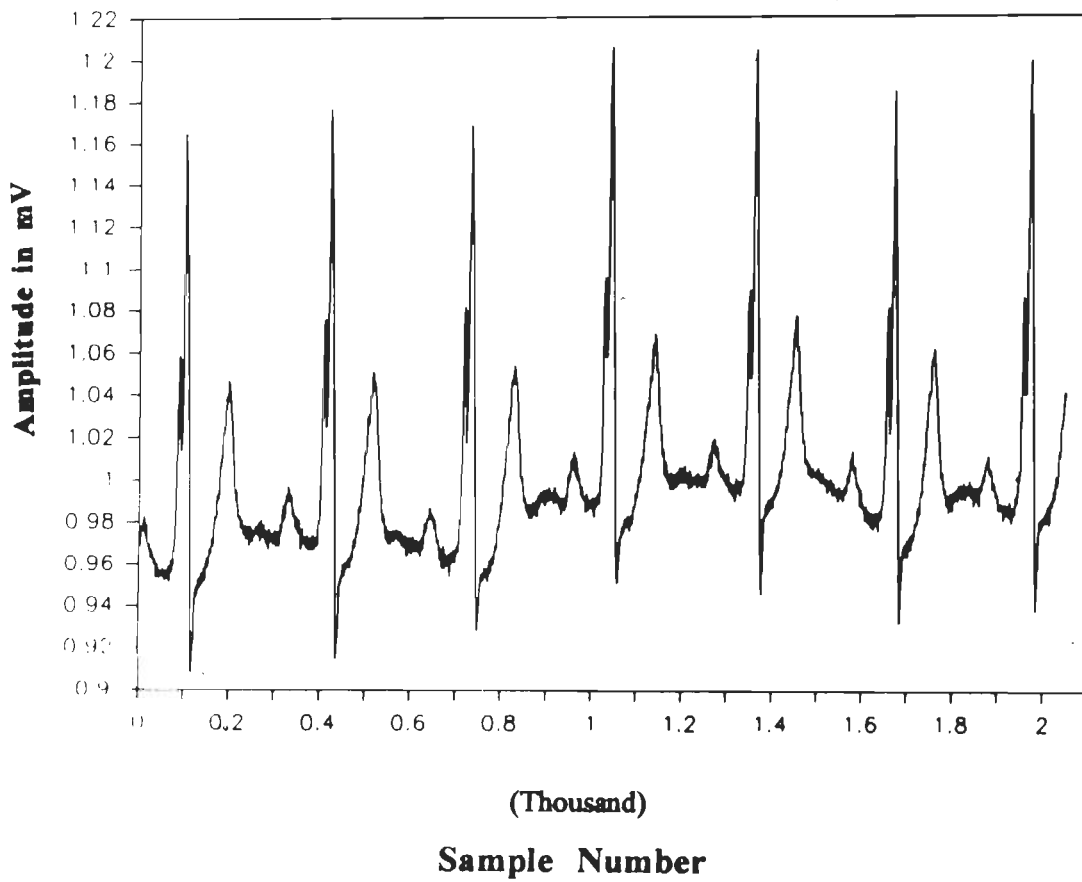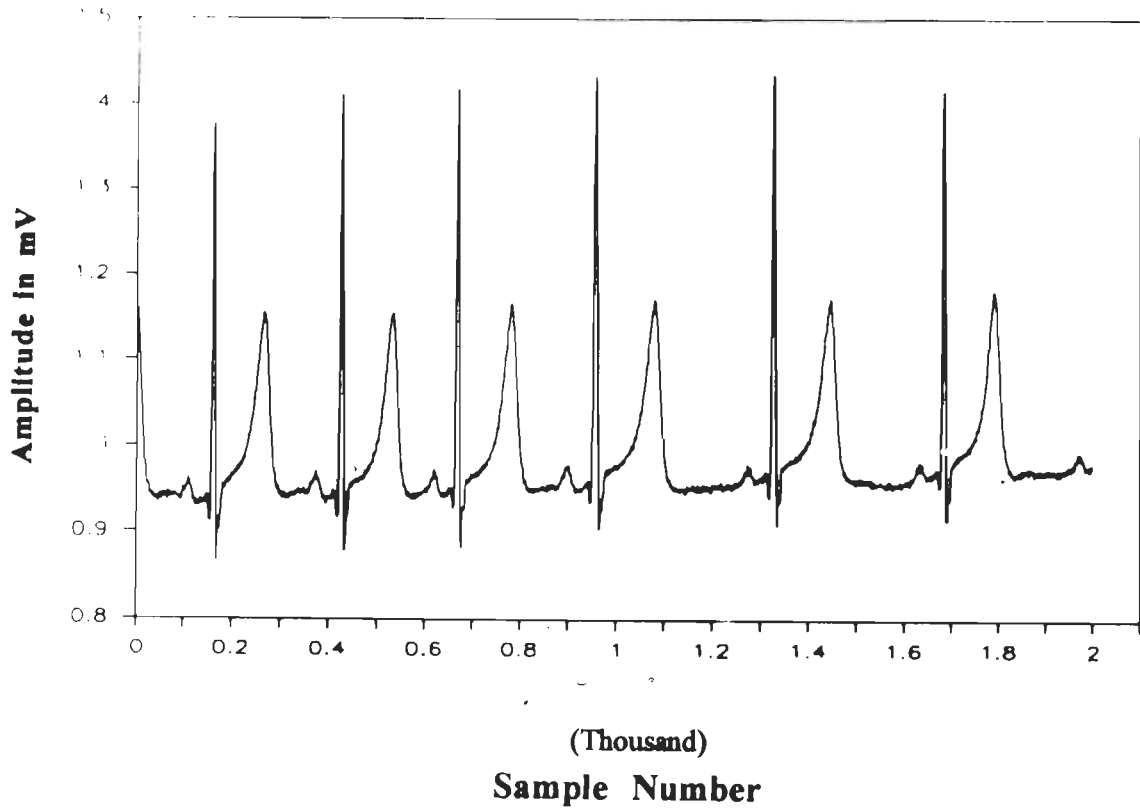|		
PR_interval in sec	= 0.180	Normal
QRS_duration in sec	= 0.090	Normal
P_duration in sec	= 0.134	Normal
RR_interval in sec	= 0.994	Normal
PP_interval in sec	= 1.008	Abnormal
Normal rhythm		

Normal Sinus Rhythm

Fig.5.7   **Output from the Arrhythmia Interpretation Program for Record No. 113 (for the 5nd Beat) of MIT/BIH Arrhythmia Database**

CHAPTER - 6

DIRECT ECG DATA COMPRESSION

CHAPTER - 6

DIRECT ECG DATA COMPRESSION

6.1 Introduction

One of the common problems addressed in the ambulatory ECG monitor is the efficient handling of large quantities of data. This system stores or transmit in real-time large volumes of ECG data. Use of suitable data compression techniques can give better utilization of memory or storage space in them and also save on the data transmission time. This demands accurate, reliable and efficient ECG data compression techniques without loosing clinical information. Data compression essentially involves a trade off between compression ratio and the clinical information content of the signal [41,52]. Different direct data compression techniques suitable for ambulatory monitor are presented in this chapter. The techniques have been tested for their performance on the standard database in terms of compression ratio, percent root-mean-square difference (PRD)and fidelity.Further, in order to know the extent to which clinically important information is preserved in the reconstructed signal, peak and boundary measurements were made both on the reconstructed and original ECG signal and compared. This clearly establishes the clinical acceptability of the compression techniques . In addition,effect of sampling frequency on the performance of the DDC techniques is also made. This is the major contribution of the thesis in this chapter.

Techniques for ECG data compression can be grouped into three categories namely, direct data compression, transformation compression and parameter extraction. In direct data compression, data reduction is achieved by discarding digitized samples that are not important for subsequent clinical interpretation. The second category algorithms compress the data under certain mathematical rules, so that the data can be recovered under inverse mathematical rules, operating within predefined error limits. In the third group, a preprocessor is used to extract some features that are latter used to

reconstruct the signal. The techniques in the first two categories are more commonly used as they use reversible processes which allow an easy reconstruction of the original signal from the compressed data [73].While DDC techniques is discussed fully in this chapter,the transformation compression technique is delt with in the subsequent chapter.

6.2 Techniques and Algorithms

The direct data compression (DDC) schemes are based on the detection of redundancies from the direct analysis of the actual signal samples. Most of the DDC schemes use prediction or interpolation algorithms. They attempt to reduce data sequence by examining the successive samples. A prediction algorithm utilizes a prior knowledge of both the previous and the future samples. These methods are generally preferred for on-line real-time application, because they are easy to implement and the computation time required is also small. In the paragraphs to follow five important DDC schemes are discussed briefly.

6.2.1 Turning Point Technique

The turning point (TP) technique was developed basically for reducing the sampling frequency without diminishing the elevation of large amplitude QRS complex of the ECG signal. It has the greatest ease of implementation and requires the least amount of computation. It analyses the trends of sample points and stores any one of each pair of consecutive points. The peak and valley points at which the slope of the signal changes or turns are retained these points are known as turning points [2,74].

As for its implementation compression is accomplished by considering a trend among three consecutive data points, a reference X_0 point and the two following points X_1 and X_2. Either of X_1 or X_2 is retained depending on which point preserves the slope of the original signal segment X_0-X_1-X_2 [74,102]. Fig. 6.1 illustrates the flow-chart of the TP algorithm. The algorithm begins with reading the first sample from the input file containing ECG samples and is assigned as X_0. Then next two samples are read as X_1 and X_2. The slope S_1 and S_2 are computed between X_0 & X_1 and X_1 & X_2
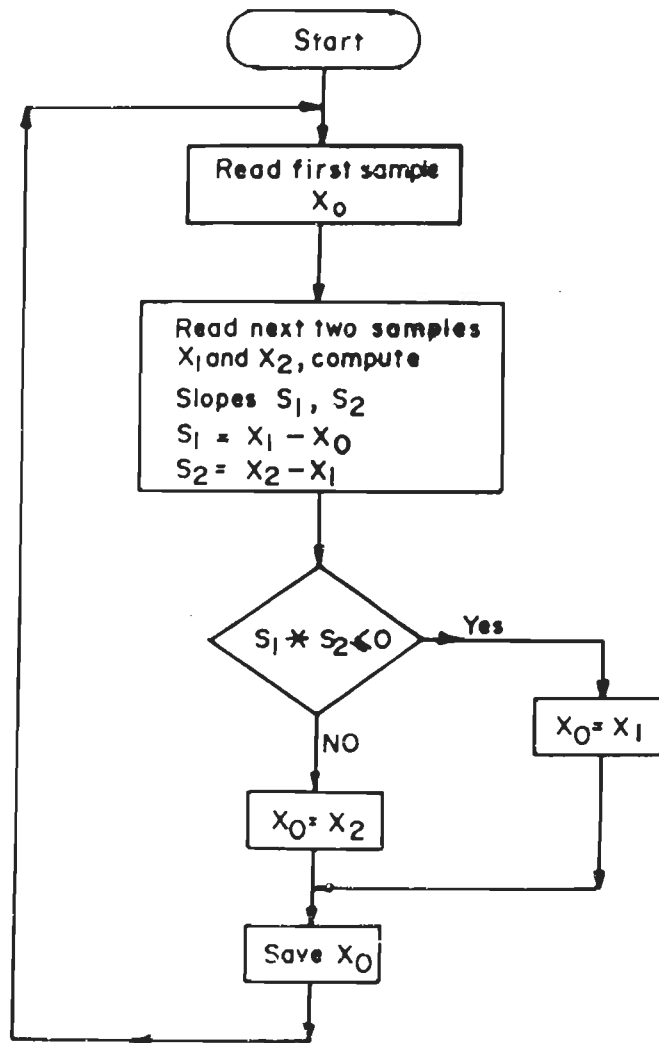
Fig. 6.1 Flow chart for turning point algorithm

respectively. When the following condition is satisfied a turning point is stored as X_0

$$\text{If } (S_2 * S_1) < 0 \quad X_0 = X_1 \qquad\qquad 6.1$$

and

$$\text{If } (S_2 * S_1) > 0 \quad X_0 = X_2 \qquad\qquad 6.2$$

Further next two samples are read, their values are assigned as X_1 and X_2 and this process is repeated till all samples in the data file are over.

The reconstruction of the original signal from the data compressed is quite simple and is achieved by linear interpolation [2].

6.2.2   AZTEC Technique

The amplitude-zone-time-epoch coding (AZTEC) technique, consists of splitting the given signal into horizontal lines and slopes [27]. The horizontal lines are produced on the principle of zero order interpolation (ZOI), and the information is stored in respect of its magnitude, and the length in terms of the number of samples. A slope is selected whenever the number of samples needed to form a horizontal line is less than three. A slope is stored as its duration (the number of samples) and the elevation of the last point [66].

Fig. 6.2 shows flow-chart of the AZTEC algorithm. The first step in the algorithm is to read the first sample and initalize it to X_{max} (maximum value) and X_{min} (for minimum value). The next sample is then compared with X_{max} and X_{min}. If the sample is greater than X_{max} then X_{max} is made equal to the present value of the sample. On the other hand, if the sample is less than X_{min} then X_{min} is made equal to the current sample. This process is repeated until either the difference between X_{max} and X_{min} is larger than a predefined threshold X_{th} or more than 50 samples have been read. Either event produces a line. To store this line, previous to this sample is saved as T_1 (time or length of the line). Then the values of X_{max} and X_{min}, previous to

```
                    ( Start )
                        │
                        ▼
          ┌──────────────────────────┐
          │ Read first sample $X_1$   │
          │ and set $X_1 = X_{max} = X_{min}$ │
          └──────────────────────────┘
                        │
                        ▼
          ┌──────────────────────────┐
          │   Read next sample X      │
          └──────────────────────────┘
                        │
                        ▼
          ┌──────────────────────────┐
          │   Num = Num + 1           │
          │   $X_{max} = X_{max_1}$   │
          │   $X_{min} = X_{min_1}$   │
          │   $X = X_1$               │
          └──────────────────────────┘
                        │
                        ▼
                  ◇ Num > 50 ◇ ──── Yes ────┐
                        │                    │
                        No                   │
                        ▼                    │
                  ◇ $X_{max} < X$ ◇ ── Yes ──┐│
                        │                    ││
                        No          ┌────────┴┴┐
                        │           │ $X_{max_1} = X$ │
                        │◄──────────└──────────┘
                        ▼                    │
                  ◇ $X_{min} > X$ ◇ ── Yes ──┐│
                        │                    ││
                        No          ┌────────┴┴┐
                        │           │ $X_{min_1} = X$ │
                        │◄──────────└──────────┘
                        ▼                    │
    Yes ◄──── ◇ $X_{max_1} - X_{min_1} < X_{th}$ ◇
     │                  │
     │                  No ◄──────────────────┘
     │                  ▼
     │       ┌──────────────────────────┐
     │       │   Calculate              │
     │       │   $T_1 = Num - 1$        │
     │       │   $X_1 = (X_{max} + X_{min})/2$ │
     │       └──────────────────────────┘
     │                  │
     ▼                  ▼
    ( B )              ( A )
```
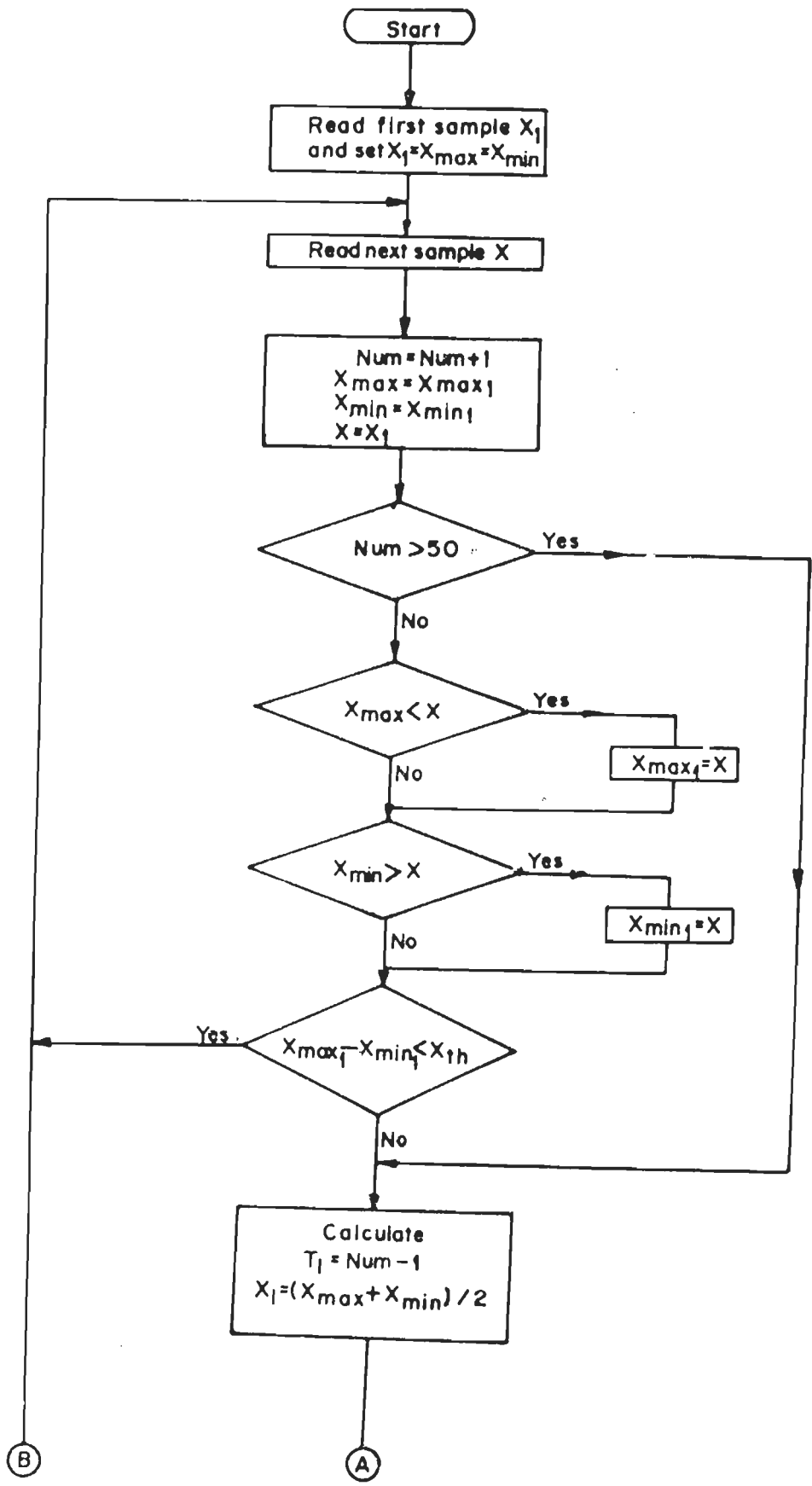
Fig.6.2 Flow chart for AZTEC algorithm.

the current sample are averaged and assigned as X_1 which is saved (i.e. values of the line $X_1 = (X_{max}+X_{min})/2$ at time t-1). X_{max} and X_{min} are then set equal to the current sample and the process is continued. If the number of samples required to produce a line is less than three a slope is produced. Now the algorithm starts computation of slope. First the value of the line is set to X_{s1} (value of slope). Second the length of the line is assigned as $T_{s1}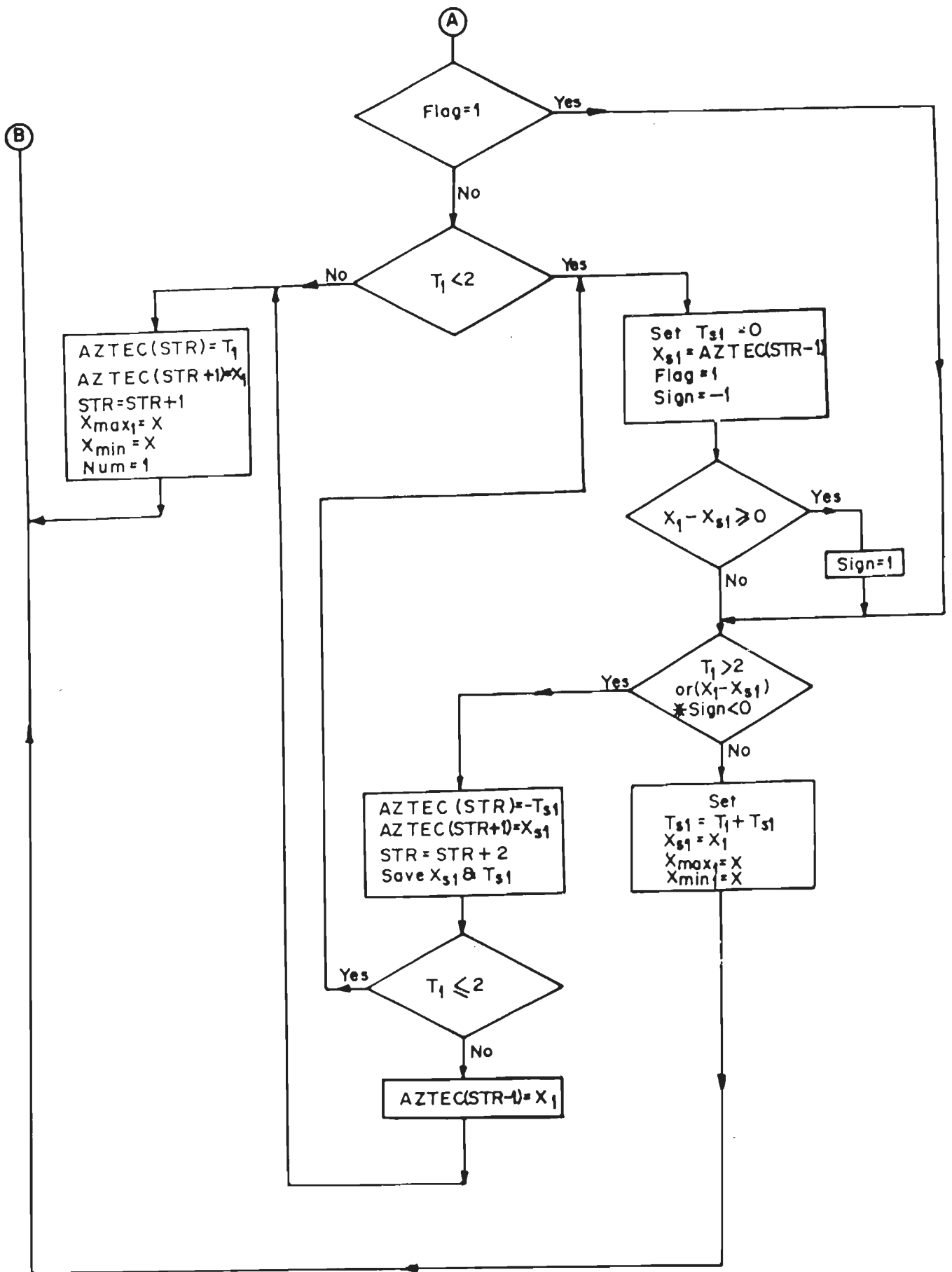$ (time or length of the slope). The direction of the slope (+ or -) is also recorded. The algorithm returns to the line direction beginning with initialization for X_{max} and X_{min} equal to the current sample. When the next line is produced, a decision is arrived at whether or not the slope data to be updated or terminated. This is achieved if the length of the new line is greater than two or if the direction of the slope is changed, the slope is terminated. Otherwise, the slope is updated X_{s1} is made equal to the value of the new line and the length of the line is added to T_{s1}. After this the algorithm returns to the line direction.

When the slope is finally terminated, the slope parameters are determined and saved. First T_{s1} is multiplied by -1 and stored. If the slope was terminated by a change in direction and the line length is less than three a new slope X_{s1} is saved, T_{s1} is made equal to the line length X_{s1} is made equal to terminating line amplitude and the algorithm returns to sample for a new line but is producing a new slope. If the slope was terminated by a change in direction and/or the terminating line length is more than two, the amplitude of that line is saved, then the length of that line and finally the amplitude of the line is saved again in other words, the updated T_{s1} times -1, X_{r}, T_1 and X_1 are saved in this order. After all the four values are stored, the algorithm returns to reinitialize X_{max} and X_{min} and begins to produce a new line.

The signal reconstruction is obtained by expanding the horizontal line and slope data into respective sets of discrete points. Parabolic fitting is then used for smoothing the signal using a set of seven points in order to make the signal acceptable to a cardiologist for visual examination [2,75,135].

6.2.3   CORTES Technique

The coordinate-reduction-time-encoding-system (CORTES) is the combination of the AZTEC and turning point (TP) techniques. This technique takes advantages of the strength of each technique while side-stepping their weakness [2]. In this technique AZTEC is applied to isoelectric regions and the TP technique to clinically significant high frequency regions of the ECG signal. The AZTEC and TP algorithms are applied in parallel to the incoming sampled ECG data. Whenever an AZTEC line is produced, a decision based on the length of the line is used to determine whether to save AZTEC data or TP data. If the line is longer than an empirically determined threshold, the AZTEC line is saved otherwise TP data are saved. To speed up the process, the TP data stored into the compressed array. By the use of two array pointers P_1 & P_2, the difference between probationary and permanent data is determined. A marker is used to identify transition between AZTEC and TP data.

The flow chart for the implementation of CORTES algorithm is shown in Fig. 6.3. The first ECG sample read from the file is set equal to X_{max}, X_{min} and X_0. The first CORTES array location is made equal to the marker P_1 and is set equal to 1 and P_2 is set equal to 2. Finally, the flags are initialized.

The second sample is made equal to X_1 and compared with X_{max} and X_{min}. The third sample is set equal to X_2 and compared to the AZTEC window limits. X_0 is then stored and P_2 is incremented. This continues until AZTEC line is found. If the line is longer than X_{ln}, an AZTEC line is stored and the pointers are moved. If the line is not long enough, then TP data are made permanent. After the data are stored (pointer P_1 is moved forward), the algorithm begins to produce another line while storing TP data on a probationary status at the same time.

If the produced AZTEC line is too short to be stored and the present data point was set equal to X_1, then the next data sample must be read before the TP data can be made permanent. This is done so that new data sample can be made equal to X_2 and a determination of the new value for X_0

Start

Read first sample
Initialise to X_{max} & X_o
Flag1, 2, = 0

Read next sample

Flag = 1

Yes
$X_2 = 1$
$F_2 = 1$

No

$X_1 = X$
$F_1 = 1$

Set
$X_{max.} = X_{max1}$
$X_{min} = X_{min.1}$
$Num = Num + 1$

$Num > 50$ Yes

No

$X_{max} < X$ Yes $X_{max1} = X$

No

$X_{min} > X$ Yes $X_{min1} = X$

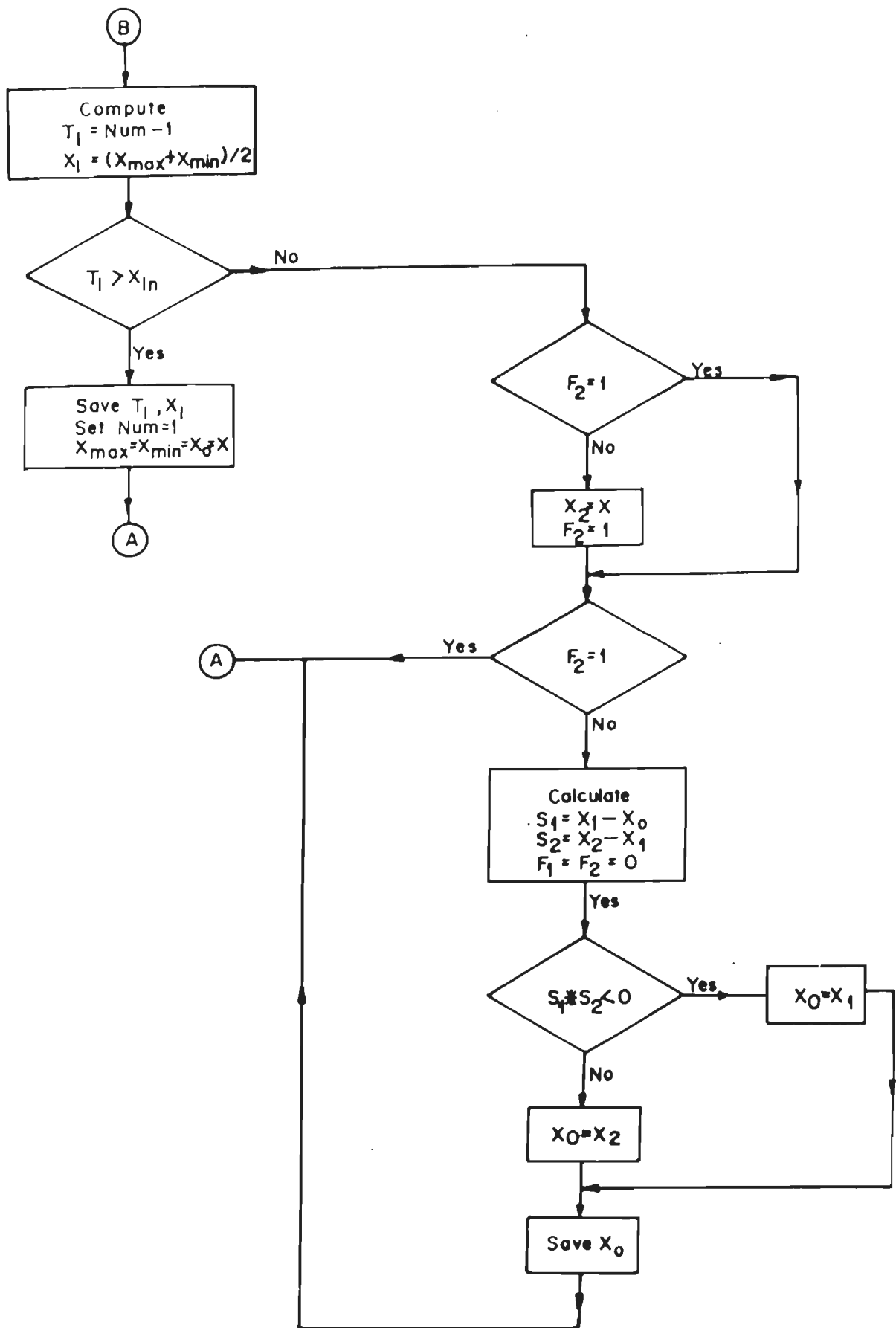No

Yes $X_{max1} - X_{min1} < X_{th}$ No

A

B
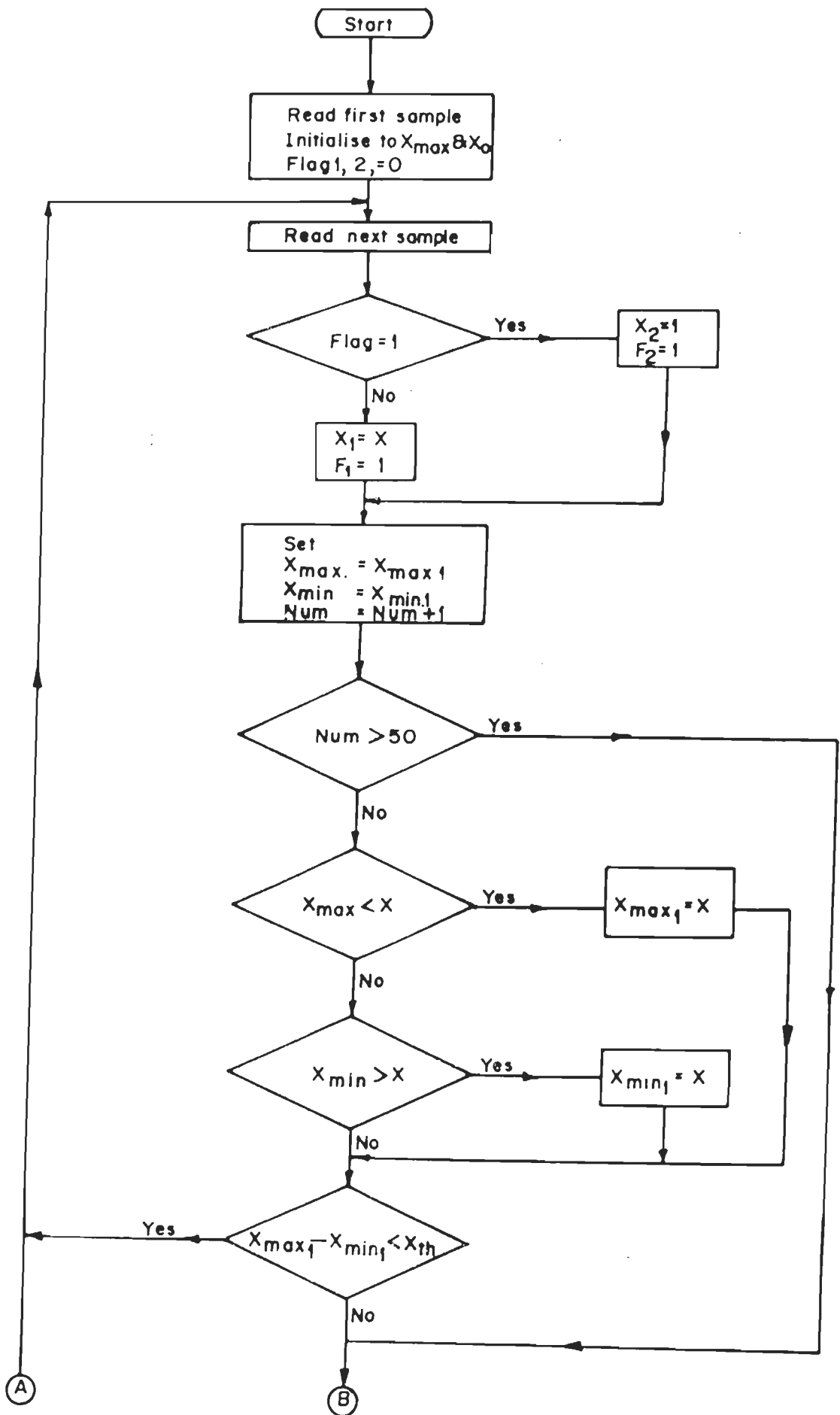
Fig. 6.3 Flow chart for CORTES algorithm

-118-

can be made. This new value is required, since X_{max1} and X_{min1} are made equal to the new X_0 and the new location of P_1 points to X_0. Therefore, if the next line is long enough, it will over write the beginning of the TP data it is supposed to represent and will keep the correct time base.

The reconstruction of the signal is achieved first by expanding AZTEC data into discrete data points and the interpolation is carried out for each pair of TP data points. Lastly, parabolic smoothing is carried out to make the signal compatible for visual interpretation [75,135].

6.2.4   Modified AZTEC Technique

The technique is a modification of the AZTEC technique, wherein the error threshold for zero order interpolation of the AZTEC algorithm is made adaptive to the ECG signal variations [41]. It calculates some statistical parameters of the signal to be compressed and adapts to the nature of the signal by reestimating the threshold value. The compression algorithm consists of the following steps.

Step 1:   The algorithm reads raw ECG data and produces short lines similar to the AZTEC algorithm. Let X_i denotes a sequence of input samples, where $(i = 1, 2 . . .)$ and X_{max} and X_{min} are the maximum and minimum values respectively. The initial value assigned for X_{max} and X_{min} are set to be equal to the first sample X_1. The subsequent samples are compared with X_{max} and X_{min}. If the current sample is greater than X_{max}, then X_{max} is made equal to the value of the present sample. On the other hand if the sample is less than X_{min} then X_{min} is set equal to the value of the present sample. This process is repeated until the difference $X_{max}-X_{min}$ is greater than a threshold value T_k. In case of AZTEC algorithm, threshold value is predetermined and can not be changed when the compression is in progress, while in the present algorithm the threshold represents y_i, $(i=1,2 . .)$ and it is computed in real-time.

Step 2 :   If the condition $X_{max}-X_{min} > T$ is satisfied, the line is stored using two data points (X,t) where X is the amplitude of the line calculated as the average value of the samples X_i in the current region, while t is the length of the line that corresponds to the number of samples in the region.

Step 3: The variable threshold T_i depends upon the nature of the signal. The threshold values for the isoelectric regions will be more than the threshold values for high frequency regions. In this way the algorithm adapts to the nature of the signal region itself.

Step 4: In order to find out the regions and switch over from one region to another, the algorithm calculates the statistical parameters of the signal, which are then used for reestimating the threshold value.
The parameters are defined as follows:

$$\text{Mean value} \quad \overline{X} = \frac{1}{n} \sum_{i=1}^{n} X_i \qquad\qquad 6.3$$

$$\text{Standard deviation} \quad \sigma = \sqrt{\frac{1}{n} \sum_{i=1}^{n} (X_k - \overline{X})^2} \qquad\qquad 6.4$$

$$\text{and third moment} \quad M = \left[\frac{1}{n} \sum_{i=1}^{n} (X_k - \overline{X}^3) \right]^{1/3} \qquad\qquad 6.5$$

The standard deviation (σ) of the signal represents the deviation of sample from the mean value. This information is used to distinguish between low information and high information signal regions. In some cases it fails to detect short picks. Therefore, the algorithm calculates the third moment and uses this additional criterion for calculating the threshold.

The statistical parameter $\overline{X}, \sigma$, and M are to be computed dynamically. Therefore from equation 6.3 to 6.5 the following recursive formulas are derived:

Mean value $\overline{X}_k$ $= \dfrac{(k-1)\overline{X}_{k-1} + X_k}{k}$ 6.6

Standard deviation $\sigma_k = \sqrt{(k-1)\,\sigma^2_{k-1} + (X_k - \overline{X}_k)^2}$ 6.7

and Third moment $M_k = \left[\dfrac{(k-1)M^3_{k-1} + (X_k - \overline{X}_k)^3}{k} \right]^{1/3}$ 6.8

where $\overline{X}_k$, σ_k and M_k are the mean value, the standard deviation, and third moment, respectively, after k samples. The $\overline{X}_{k-1}$, σ_{k-1} and M_{k-1} are the values after (k-1) samples, and X_k is a sample at the kth time interval.

Using the recursive formulas of equation 6.6 to 6.8, a new sample of the signal will immediately update the statistical parameters and therefore any change in the signal will be identified quickly.

Step 5: After each sample, a criterion function CF_k is calculated by using the following formula:

$$CF_k = c_1\,(\sigma_k + M_k)$$ 6.9

On the basis of the criterion function, the threshold is continuously updated by the following equation

$$T_k = T_{k-1} - c_2(\,CF_k - CF_{k-1}\,)\,T_{k-1}$$ 6.10

The constants c_1 and c_2 can be obtained empirically.

The flow chart of the algorithm is shown in Fig. 6.4. The compression algorithm begins with an initial value for the threshold, and then criterion functions are applied after each sample is read from the input file containing the ECG data to update threshold T until the difference $(X_{max} - X_{min})$ is more than the present T_k. When the condition $(X_{max} - X_{min}) > T_k$ is satisfied, the line is stored by using the data points (x,k), and the procedure is repeated.

The method for reconstruction of the ECG signal is similar to that used with the AZTEC technique.

6.2.5   SAPA Technique

The scan-along-polygonal approximation (SAPA) technique is based on the principle of first-order interpolation with two degrees of freedom (FOI-2DF) [66]. In this technique, an approximation of the ECG is achieved by piecewise linear segments inside the corridor formed by the two functions, which are less than and greater than the given waveform by amounts ε as illustrated in Fig. 6.5 (a). This concept yields polygonal curves for which the maximum difference between the given waveform and the polygonal approximation is equal to or less than a specified value [64].

To explain the polygonal approximation algorithm the following notation is followed. The original samples data to be approximated are represented by the discrete sequence (k,t), where the integer t is the sample number. The allowable error in the approximation is $\pm\varepsilon$ chosen by the user. The polygonal approximation will allow reconstruction of the original data within $\pm\varepsilon$ and a specific reconstruction is symbolized by the discrete sequence k(t) for which $|k(t) - \overline{k}(t)| \varepsilon$, t = 1, 2, 3 . . . .

The approximations themselves are described by a subset of the original data in which a number of original data points have been discarded. If the original data contain (sample number, amplitude) pairs

$$\{(t, k(t), \quad t = 1,2,3 . . . . \}$$

the approximation is represented for the compressed data
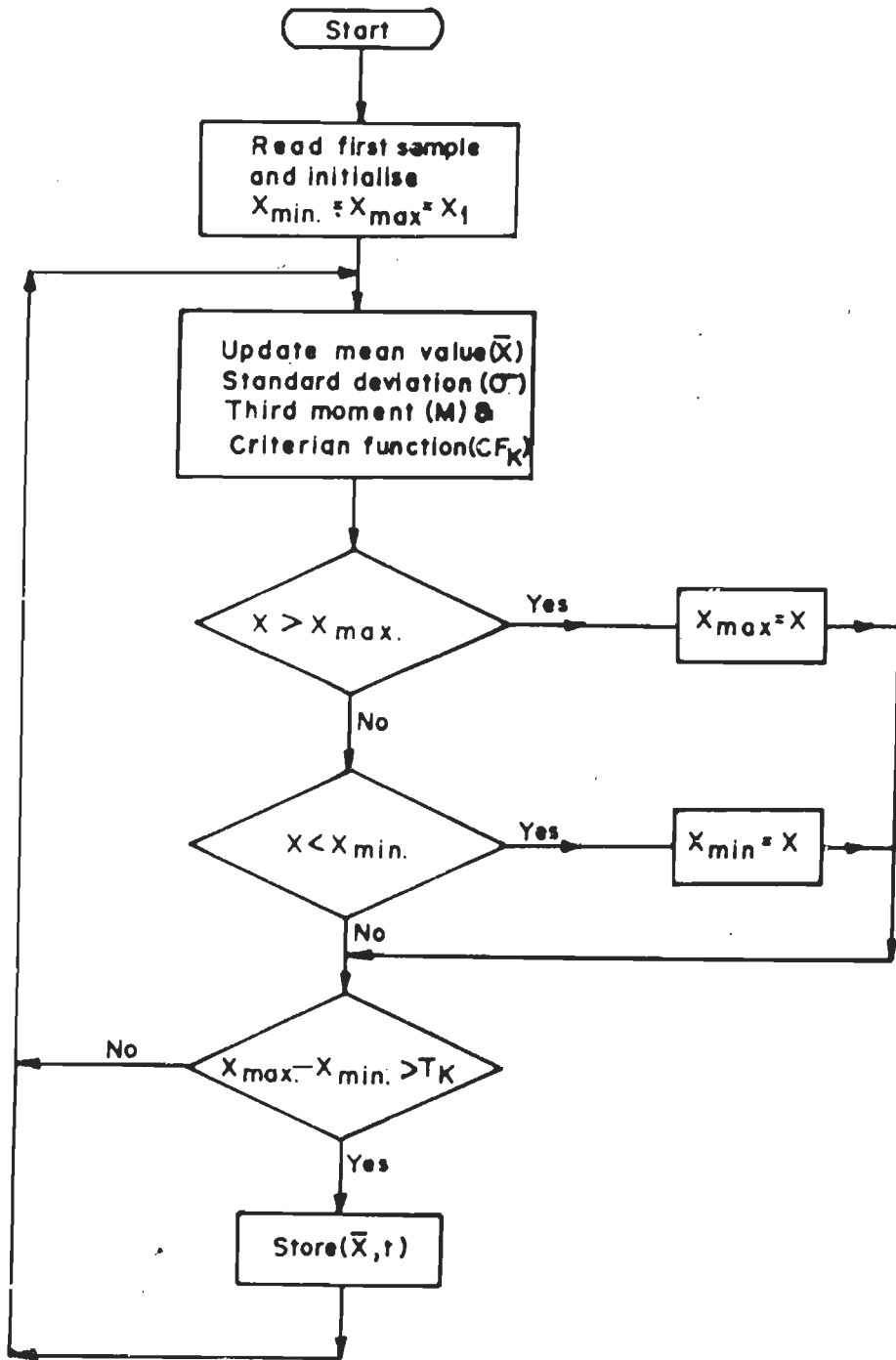
Fig.6.4 Flow chart for MAZTEC algorithm.
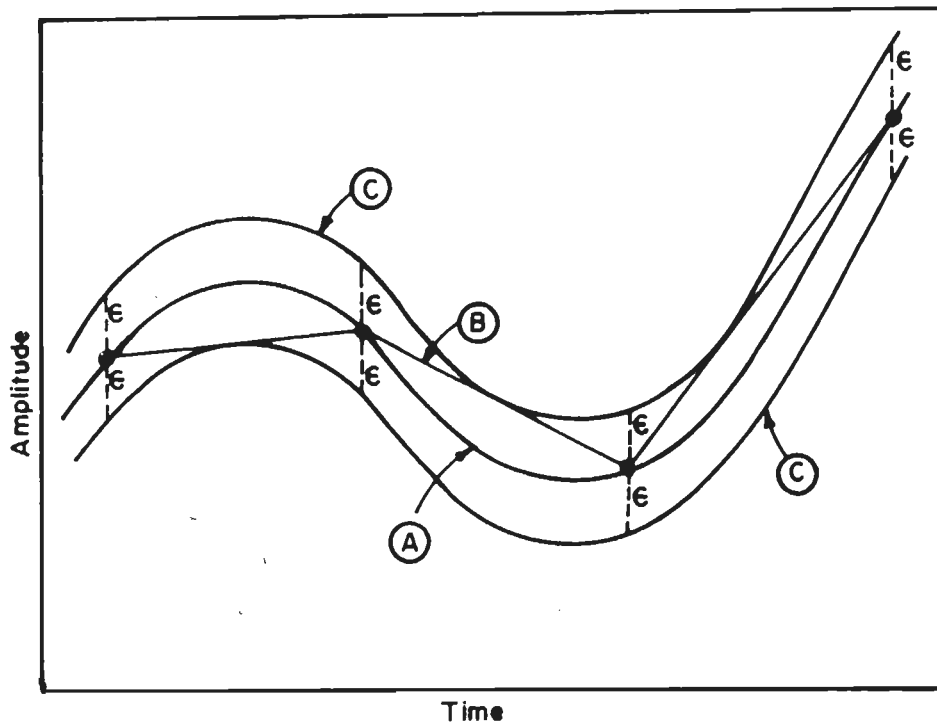
Fig.6.5 (a) Basic concept of polygonal approximation
(A) Original signal (B) Straight line approximation
of original signal (C) Approximation error
boundary.

$$\{t, k(t) \; , \qquad t = n1, n2 \; . \; . \; . \; .\}$$

when n1, n2 . . . . are the sample numbers in the compressed data sequence.

The (sample number, amplitude) pairs of the compressed data are termed vertices of the original data. Between any two vertices, the data are approximated by the points on the straight line joining the two vertices.

Let t=n represent the sample number of the most recently found vertex of the data. At the start of the algorithm the first sample in the data set is a vertex. Upon the receipt of the next sample at t=c, the normalized slopes of the two lines joining starting (k(n) to k(c)+ε) and ending (k(c) - ε) points are calculated. These slopes are

$$h(c, \varepsilon) = \frac{(k(c) + \varepsilon) - k(n)}{c-n} \qquad\qquad 6.11$$

and

$$h(c, -\varepsilon) = \frac{(k(c) - \varepsilon) - k(n)}{c-n} \qquad\qquad 6.12$$

This is shown in Fig. 6.5 (b).

As each new data point being processed, the current smallest value of $h(c, \varepsilon)$ is stored as M_1 and current largest value of $h(c, -\varepsilon)$ is stored as M_2. The numbers M_1 and M_2 thus store the maximum and minimum slopes that a line from n may have and still pass within ±ε of subsequent data points. Whenever $M_2 > M_1$ as is the case shown in Fig. 6.5(b) at t = c+i, the immediately previous sample is selected as a vertex. This process is repeated for all the data points.
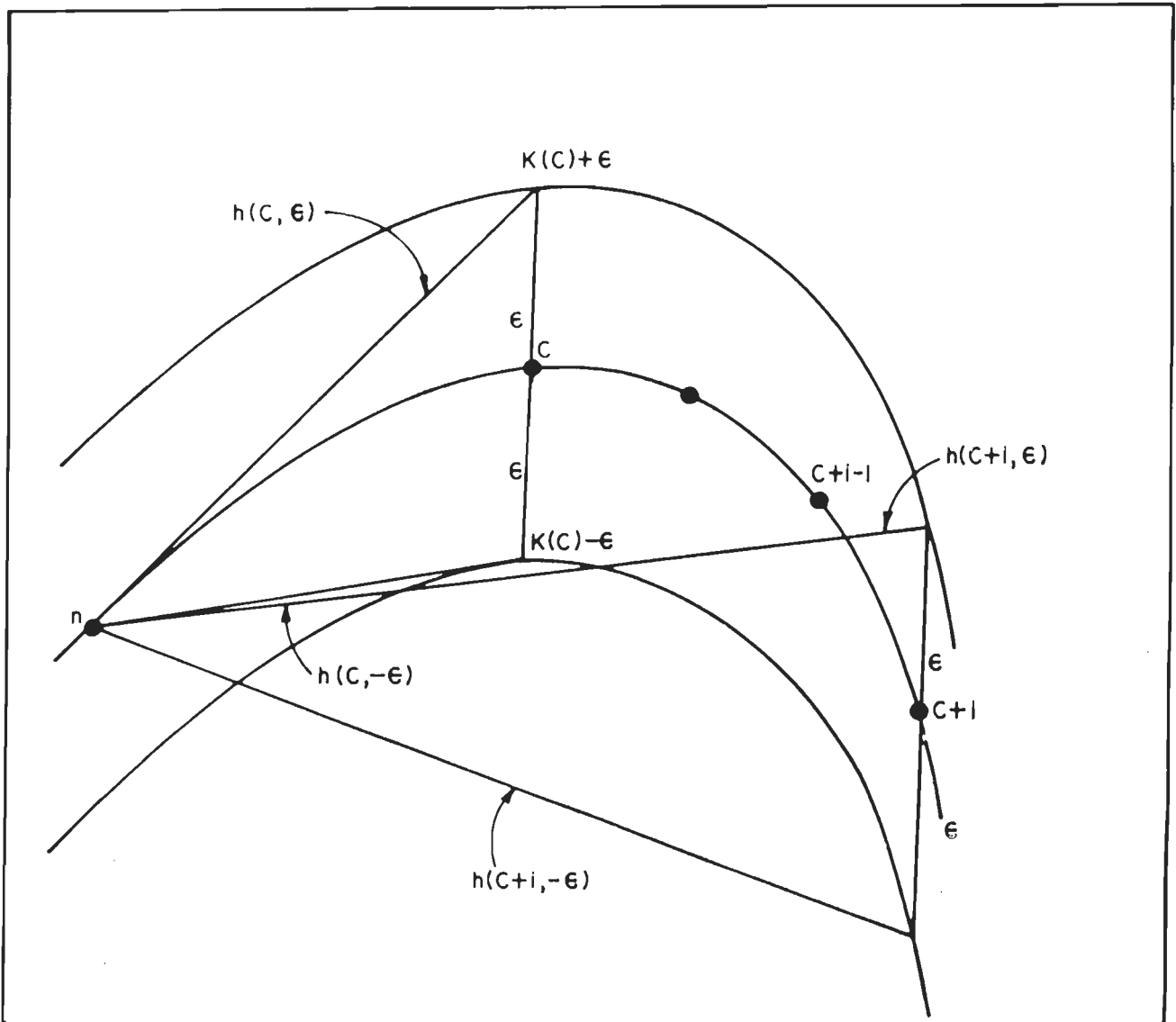
Fig.6.5 (b) Illustration of SAPA−1 algorithm.

The flow-chart for implementation of the algorithm is shown in Fig. 6.6. The algorithm starts by retaining the first sample as the vertex. The next step is to set upper and lower limit index n=c. After this, next sample is read and upper and lower slopes computed. This slope is compared with the set values of M_1 and M_2 and slopes are updated. Further if $M_1 < M_2$ condition is satisfied, store the previous sample number and its amplitude otherwise read next sample. This process is repeated till all the samples are processed.

The reconstruction of the signal is achieved by linear interpolation. Two successive samples are averaged and the averaged value is inserted between the samples. This is called linear interpolation.

6.3   Performance Evaluation

The performance of the proposed data compression techniques are measured in terms of three important indices namely, compression ratio (CR) the percent root-mean-square difference (PRD), loss in diagnostic information besides the fidelity of the reconstructed signal is also used.

6.3.1   Compression Ratio (CR)

The amount of compression is very often represented in terms of compression ratio (CR) and is defined as the ratio between the number of samples in the original data to that in the compressed data. It is a dimension less quantity. It is dependent on the sampling frequency and the nature of the ECG data in addition to the technique used [6]. In a transformation method the compression ratio varies inversely with the number of coefficients to be retained in the compressed signal.

6.3.2   Percent root-mean-square Difference (PRD)

For the quantitative comparison of the distortion in the reconstructed signal, many researchers have used percent root-mean-square difference (PRD) as the index.
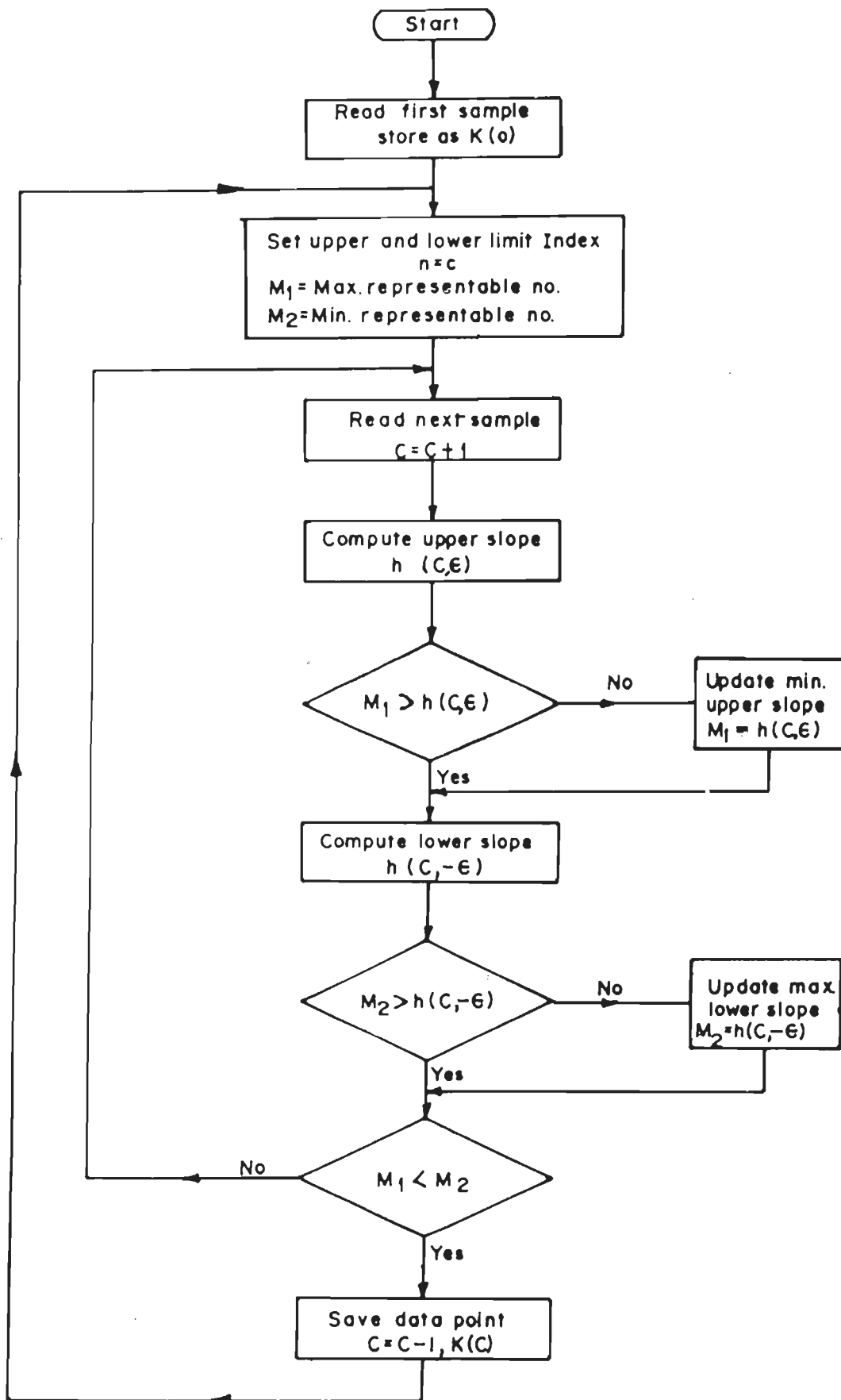
Fig.6.6 Flow chart for SAPA algorithm

The PRD is defined as

$$PRD = \sqrt{\frac{\sum\limits_{i=1}^{n} (X_{org} - X_{recon})^2}{\sum\limits_{i=1}^{n} (X_{org})^2}} \times 100 \qquad\qquad 6.13$$

where X_{org} and X_{recon} are the samples of the original and reconstructed signals, respectively. This index represents an average potential error for the signal on the whole. It is easy to calculate the index and it does not penalize one algorithm in favour of another. For these reasons, this index has been used for a quantitative comparison here too.

6.3.3   Loss in Diagnostic Information

ECG recording, unlike text storage, does not require "lossless" compression. The only requirement is that the difference between a reconstructed signal and the original signal has no bearing on the clinical interpretation. A compressed ECG signal can be clinically acceptable despite the large PRD values. Clinically acceptable quality is neither guaranteed by low PRDs nor ruled out by higher ones [99]. PRD alone cannot reveal the extent of loss of information in the reconstructed signal. Therefore, some researchers have proposed a determination of the onset and end-points and the measurement amplitudes (peak values) of P,Q,R,S and T waves, and have compared them with the corresponding information in the original signal [64,67,75]. This helps to decide the extent to which the algorithm is capable of preserving the diagnostic information.

6.3.4   Fidelity

There are several methods of evaluating the performance of the compressed data. An effective evaluation however, requires that the signal be

reconstructed from the compressed data and then compared with the original signal. The comparison can be made either visually or by calculating a suitable index, such as the corelation coefficient, error power to signal power ratio etc [85]. The former method is commonly used by cardiologists and has therefore been selected here for evaluation.

6.4   Results

Results of five DDC techniques as well as effect of sampling frequency on performance of DDC techniques are given in this section.

6.4.1   Performance

The five DDC techniques have been implemented here using C-language and tested on 25 records of 30 seconds strip from the MIT/BIH Arrhythmia database [98]. But the detailed results of one representative case record number 103 (signal 0) of MIT/BIH database taken at a sampling frequency of 360 Hz are presented here.

The TP algorithm produces a fixed compression ratio of 2:1. It can be increased to 4 if the compression algorithm is applied twice. The other algorithm produce compression ratio that vary with the threshold or allowable error limit (in case of SAPA). Table 6.1 shows the results of comparison of five DDC techniques. AZTEC, CORTES, MAZTEC techniques produced variable compression ratio in the range 3.23 to 8.57. On the other hand SAPA technique produced a compression ratio in the range 2.95 to 9.57 as shown in column number two of Table 6.1.

From third column of Table 6.1 it is clear that PRD values in case of turning point method are 0.24 and 1.54 for the compression ratios of 2 and 4 respectively.But on the other hand the PRD values vary with compression ratio depending on threshold or allowable error limits. In case of AZTEC,CORTES,MAZTEC PRD values vary in the range from 1.42 to 14.56. But in case of SAPA the PRD values are different and lies in the range from 2.83 to 6.67 for the compression ratio varied over the same range in each case.

Table 6.1   Comparison of Five Direct Data Compression Techniques

Method	Compression ratio	PRD	Errors in peaks values in percentage					Errors in onset and end points (no.of samples)				
			P	Q	R	S	T	P_{on}	P_{off}	QRS_{on}	QRS_{off}	T_{end}
TP	2.0	0.24	-0.1	0	0.4	0	-0.2	1	1	0	0	0
	4.0	1.54	0.3	0	0.4	0	0.6	1	2	1	1	4
AZTEC	3.23	3.20	-0.1	0	0.04	0	0.1	1	2	1	2	4
	6.38	13.80	0.9	0	0.4	0	-0.2	2	3	1	2	3
	8.69	14.65	1	0	0.5	0	-0.3	7	4	2	4	5
CORTES	3.26	1.42	0.8	0	0.2	0	0.2	1	2	1	0	5
	6.31	11.19	0.2	0	0.1	0	0.2	2	3	2	0	4
	8.69	14.91	1.1	0.4	0.5	0	0.3	8	6	6	0	7
MAZTEC	4.44	5.42	0.2	0	0.4	0	0.3	1	2	2	2	4
	6.97	11.37	0.4	0	0.5	0	0.4	1	2	0	0	6
	8.57	14.07	1.2	0.2	0.45	0	0.5	1	0	7	8	6
SAPA	2.95	2.83	0.2	0	0.5	0	0.3	1	2	1	2	7
	6.12	6.03	0.5	0.2	0.6	0.3	0.4	2	1	2	3	5
	9.52	6.67	1.2	0.4	2.0	0.4	1.5	8	5	4	6	6

For visual comparison, signals have been reconstructed from the compressed data obtained from each algorithm. The reconstruction method used were as explained in section 6.2. The reconstructed signals have been plotted with the original signal for different compression ratios as shown in Figs. 6.7 (a) to (e) on a common horizontal axis for the visual comparison. The observations made from the visual comparison are that in case of TP algorithm the reconstructed signal resembles the original signal with very little distortion for a compression ratio of 2. But if the compression ratio is increased to 4, the distortion also increases. The algorithm is generally not applied more than twice in that case the reconstructed signal will loose its morphology. On the other hand in case of AZTEC, CORTES, MAZTEC and SAPA methods the reconstructed signals suffers from some discontinuities and distortions in the isoelectric regions at higher compression ratios.

Finally, the peak and boundary measurements were made both on the original and reconstructed signal for each technique to find out the errors in peaks and boundaries. These errors reveal the clinical information preserved in the reconstructed signals. The errors in peaks and boundaries for different compression ratios and for different methods are summarizingly presented in fourth and fifth columns of Table 6.1. It is clear that in case of TP method the errors in peaks and boundaries are negligibly small. But for AZTEC, CORTES, MAZTEC methods the error in the peaks and boundaries increases as the compression ratio is increased. The errors are more in P,R & T waves and Q&S peaks are not affected. Similarly the onset and end points of P & QRS waves are more affected when the compression ratio is made maximum i.e ten and are clinically not acceptable. On the other hand in case of SAPA method the errors in the peaks P, R and T including Q and S peaks are large for higher compression ratio and the onset and end points lie outside the tolerable limits and makes it clinically un-acceptable.

Five different types of DDC tecniques presented here are suitable for online application. But the selection of the technique depends on the application.In the present work the intersample interval is 5ms therefore the processing and data compression are to be completed within this period.Hence
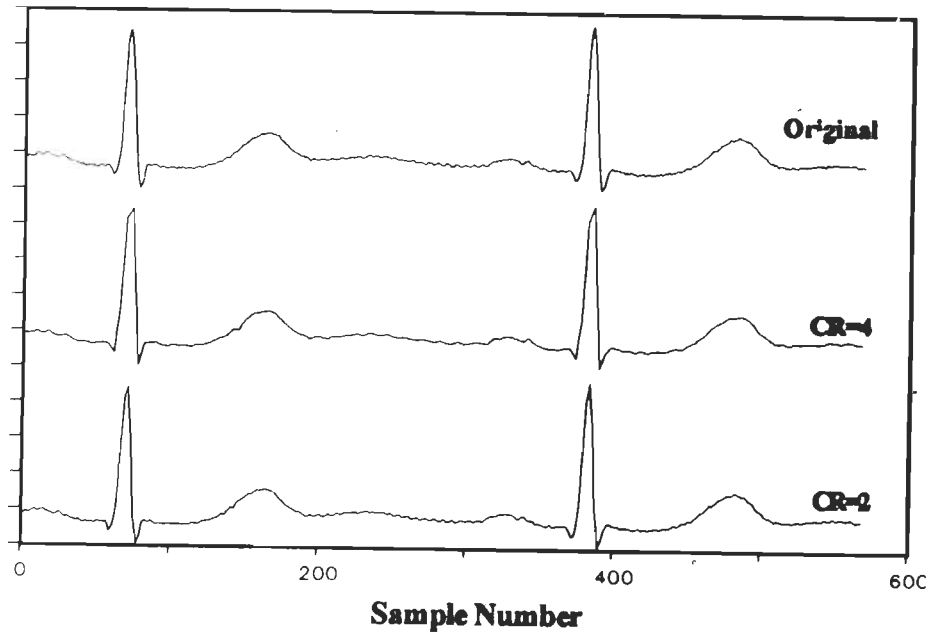
(a)
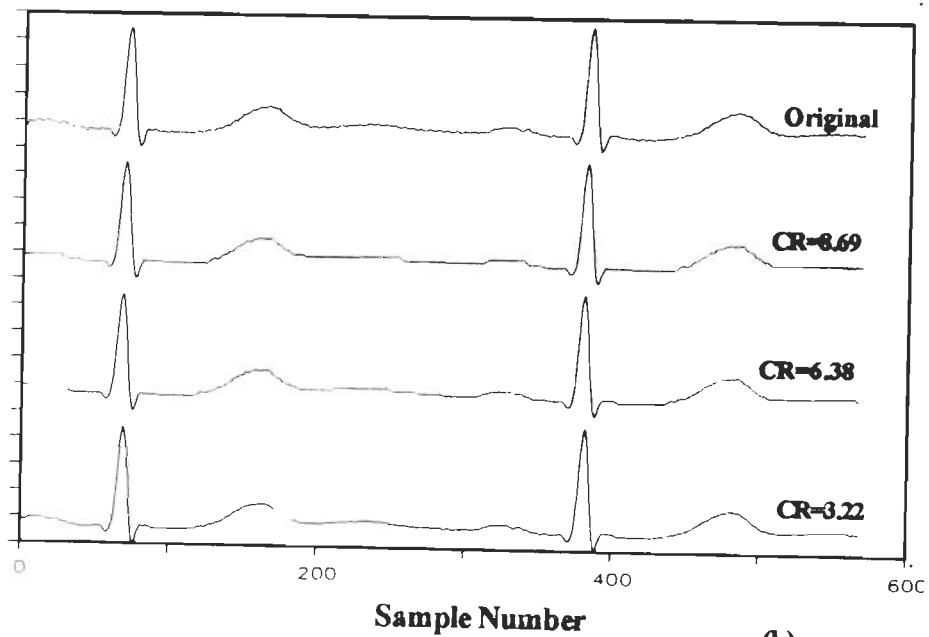
(b)

Fig. 6.7   Original and Reconstructed Signals for Record No. 103 of MIT/BIH
Arrhythmia Database for Different Compression Ratios
(a) Turning Point Method (b) AZTEC Method

Fig. 6.7   Original and Reconstructed Signals for Record No. 103 of MIT/BIH
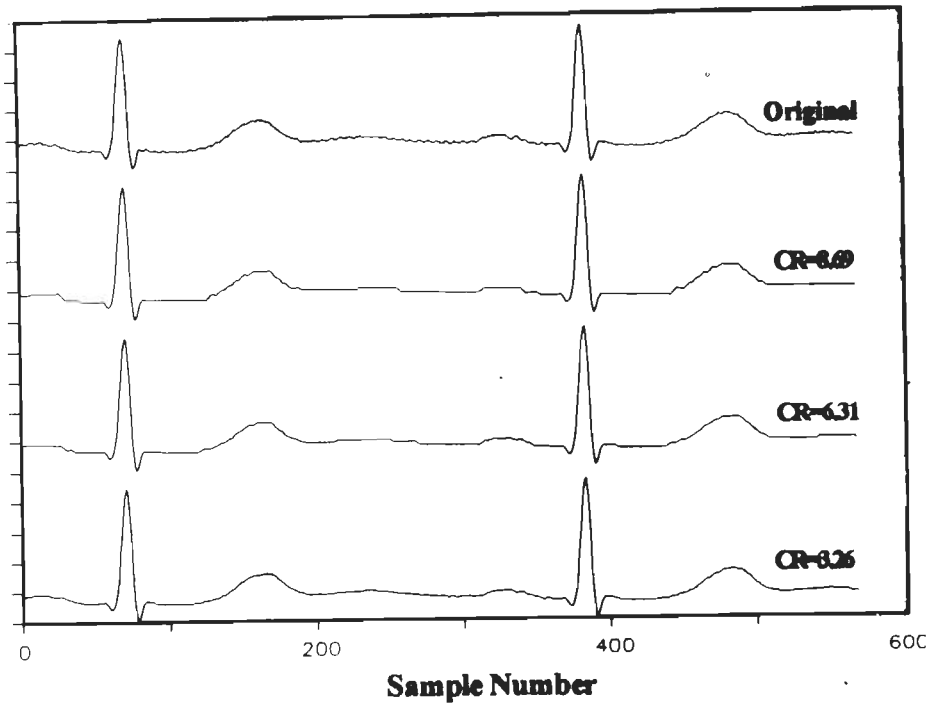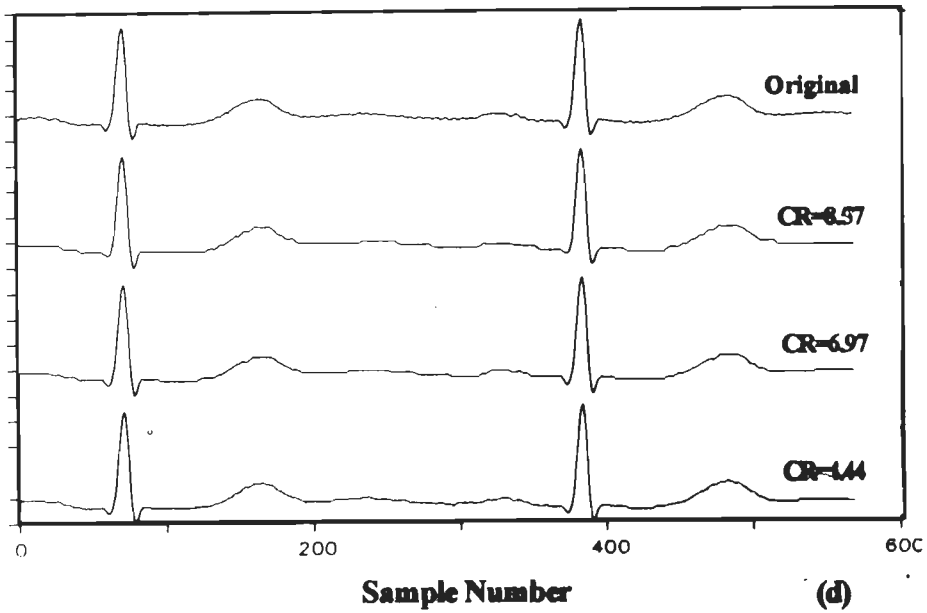Arrhythmia Database for Different Compression Ratios
(c) CORTES Method (d) MAZTEC Method
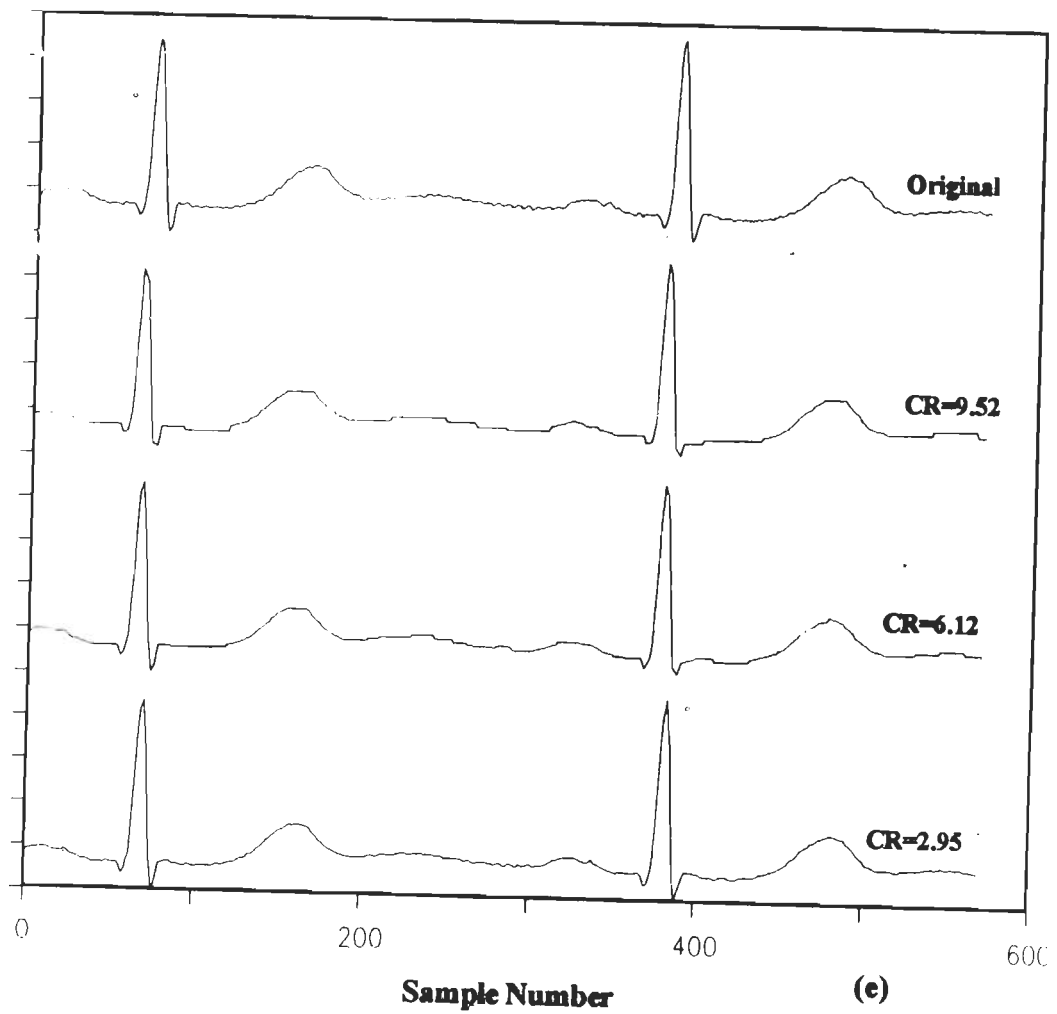
Fig. 6.7   Original and Reconstructed Signals for Record No. 103 of MIT/BIH Arrhythmia Database for Different Compression Ratios (e) SAPA-I Method

it is proposed that among the five DDC techniques turning point technique is best suited for the present application.Despite computationally very efficient and can be implemented on microprocessor without the use of coprocessor.

6.4.2   Effect of Sampling Frequency on Performance

The effect of an important parameter, like the sampling frequency on the performance of the direct data compression techniques has not been studied so far. This section reports the effect of this parameter on compression ratio, percent root-mean-square difference, fidelity, peaks, onset and end points. The techniques described in section 6.2 have been tested for their performance on 125 records of the third set of CSE database library. The samples are taken at a sampling frequency of 500Hz. In order to show the effect of sampling frequency on the performance of DDC tecniques different data sets sampled at different sampling frequencies are required.Therefore as the CSE data is sampled at higher sampling frequency and meaurement results are also available for comparison hence this database is selected [134]. Detailed results are presented for record number 01L2, which pertains to a normal case. There is no data set available at sampling frequencies, for the case at 125 Hz and 250 Hz. The two sets of data have been generated here through software by taking alternative samples from the original signal. This is done in order to evaluate the performance of all the algorithms presented here on the same set of data for different sampling frequencies.

Fig. 6.8 illustrates the variation of compression ratio with respect to the threshold or allowable error limit (in the case of SAPA) for different sampling frequencies. From these graphs it is evident that, as the sampling frequency is increased, the compression ratio increases.The compression ratio in the case of AZTEC, CORTES and SAPA techniques is in the range of 2.3 to 10 for 500 Hz sampling frequency, 1.69 to 6.94 for 250 Hz and 1.34 to 4.8 for a sampling frequency of 125 Hz. but in the case of the modified AZTEC technique the corresponding compression ratio values are 2.41 to 7.69, 1.76 to 5.43 and 1.37 to 3.78 respectively.
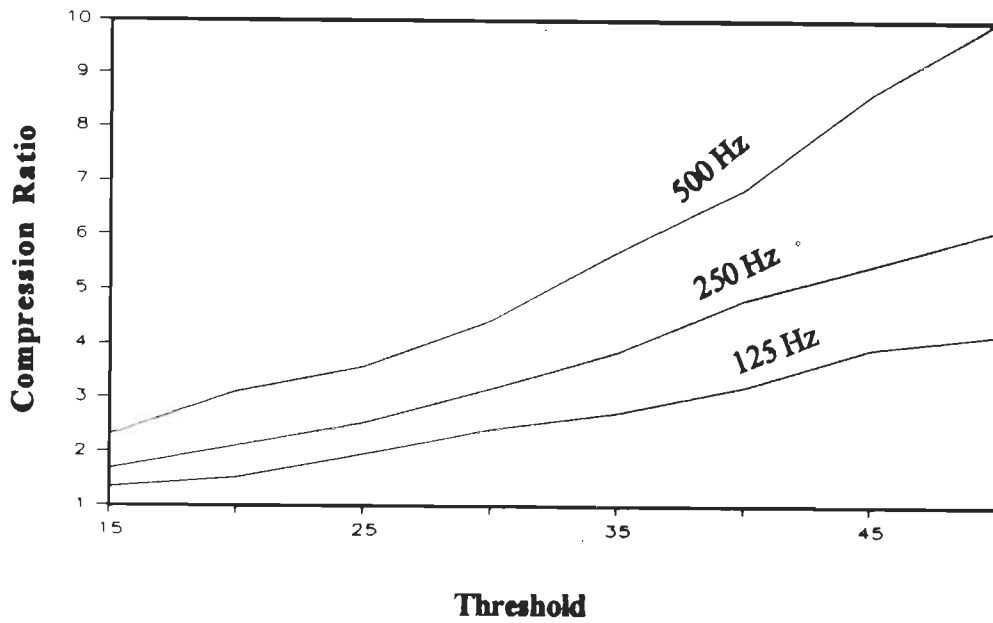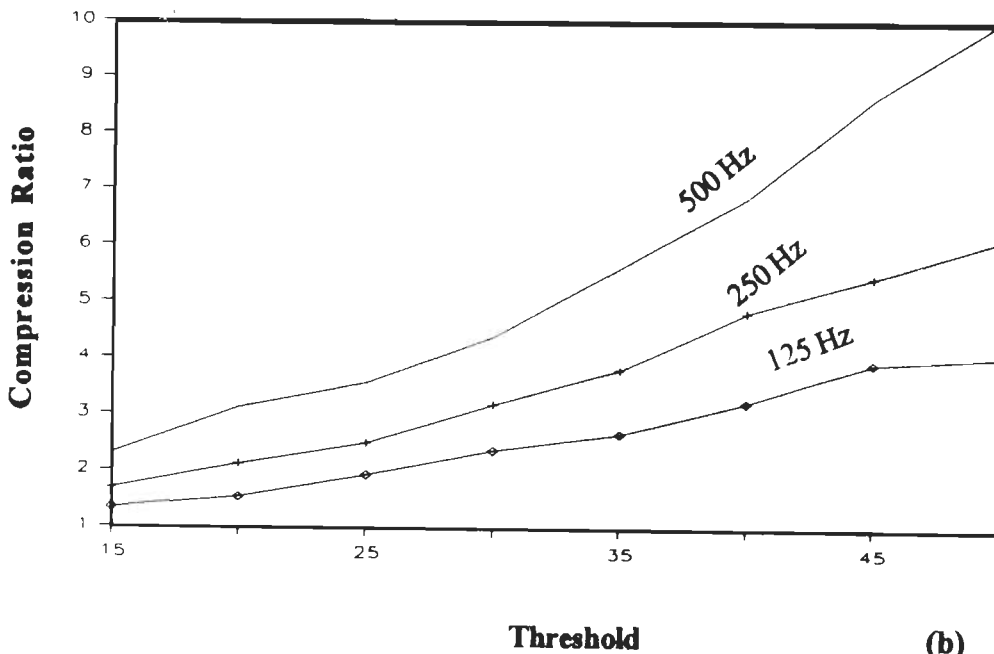
Fig. 6.8   Variation of Compression Ratio for Record No 0112 CSE Database

(a) AZTEC Method (b) CORTES Method
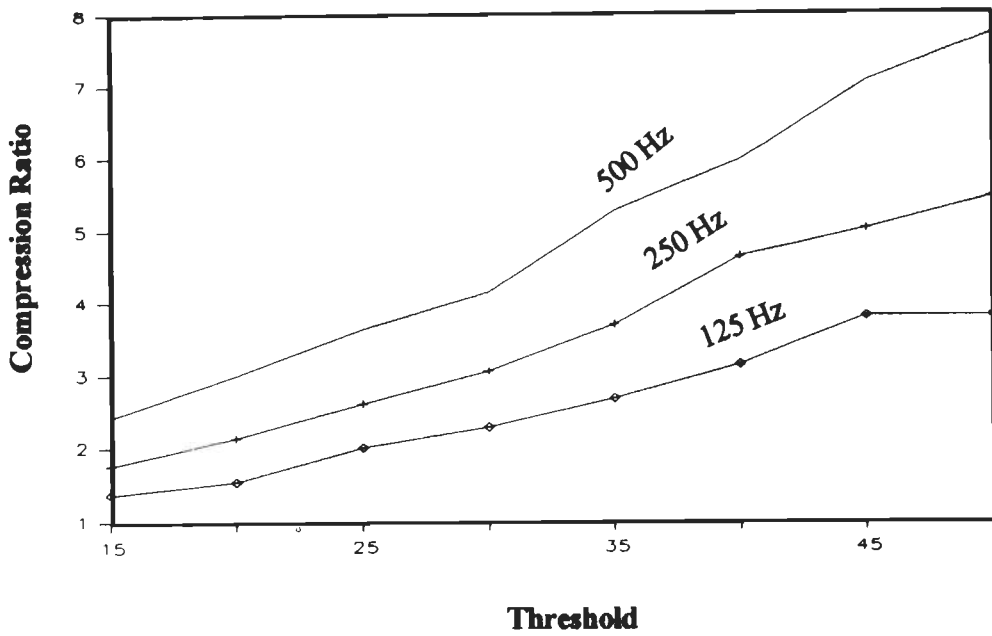
(c)
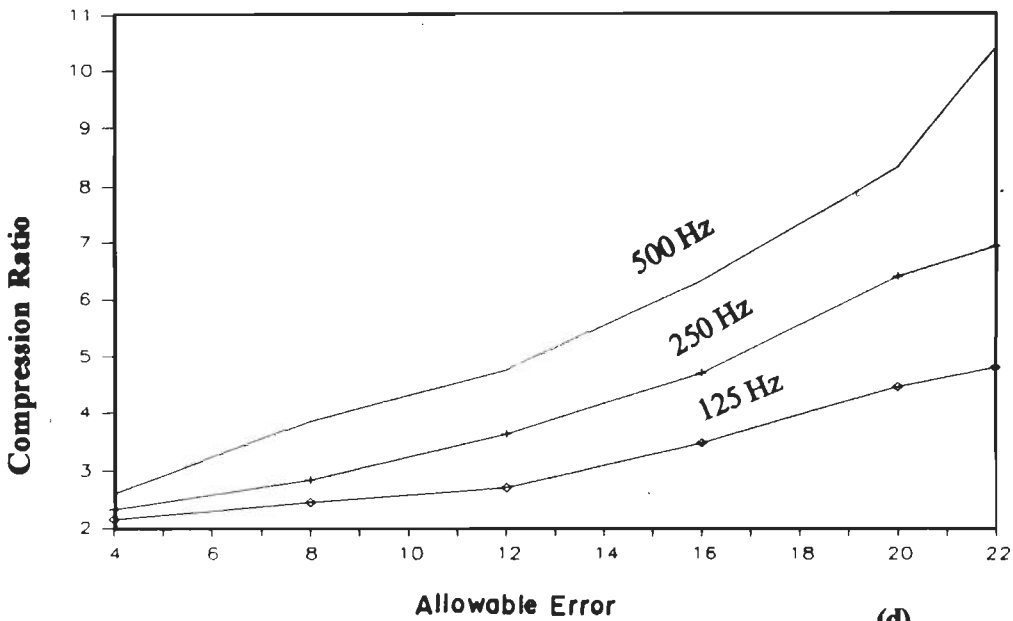
(d)

Fig 6.8   **Variation of Compression Ratio for Record No 01l2 CSE Database (c) MAZTEC (d) SAPA-I**

Fig. 6.9 shows the effect of sampling frequency on PRD. The graphs indicate the variation of PRD with respect to threshold/allowable error limit. It is noticed that, as one would expect, the PRD decreases as the sampling frequency is increased. However, the PRD values are different for each algorithm.

The reconstructed signals are plotted along with the original signal on a common horizontal axis to facilitate comparison. The reconstructed signals are shown in Figs. 6.10 and 6.11. The selection is based on the basis of a compromise between compression ratio and PRD. Moreover, results of only two sampling frequencies that is 500 Hz and 125 Hz, are shown, the reason being that the results of 250 Hz lie between these values. Furthermore, the AZTEC, CORTES and modified AZTEC techniques produce similar morphologies of the wave with small changes and they operate on a common selected threshold. Therefore, the results for the AZTEC method above are presented. SAPA operates on a different principle and therefore graphs for this method are also shown.

The following observations are made from the graphs. With a sampling frequency of 500 Hz, the reconstructed signal obtained is of high quality, having larger bandwidth and higher resolution. This results in insignificant loss of clinical information in the reconstructed signal, which is essential for certain diagnosis. Examples of such a class of diseases are ventricular hypertrophy and myocardial information etc. As the sampling frequency is decreased it is observed that the reconstructed signal quality deteriorates. This amounts to a loss of clinical information, that is loss of amplitude information in different ECG peaks. This loss is acceptable in the majority of arrhythmia cases . Therefore, the selection of sampling frequency is application dependent. It is also observed from the graphs that the high frequency signal is rejected because of smoothing. This helps in reducing the electromyographic (EMG) noise.

Peak and boundary measurements are made using separate software implemented in 'C' language as explained in section 4.3.5 has been used here. The limits for onset and end-points are followed here according to the
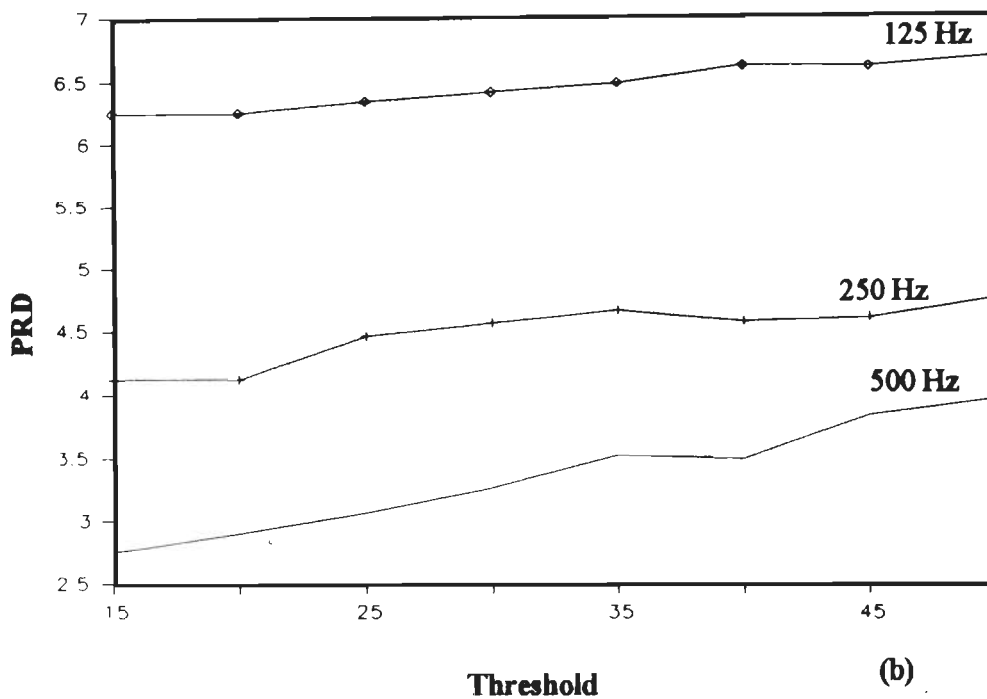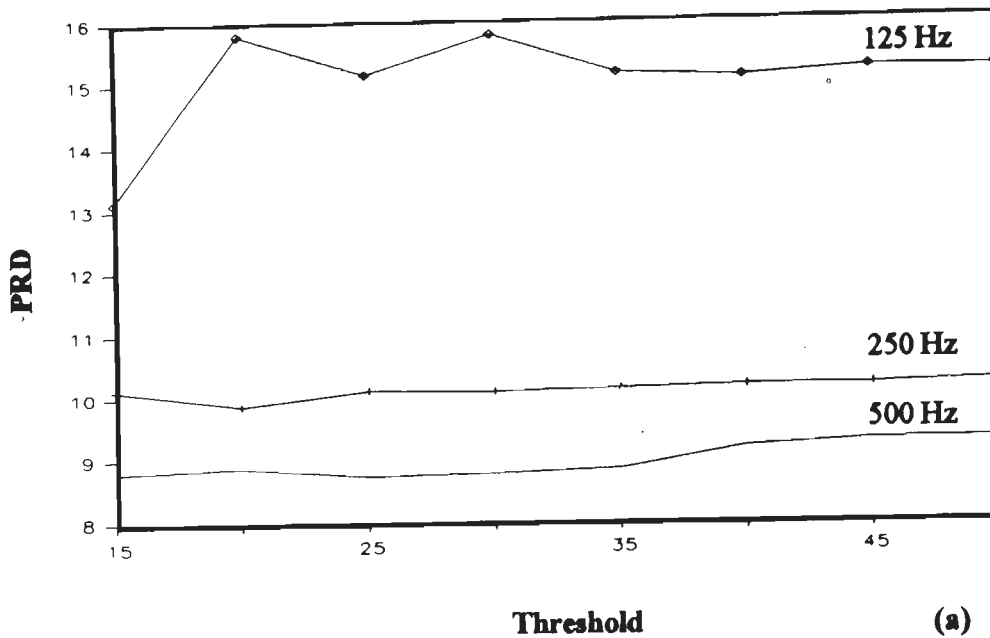
Fig 6.9   Variation of PRD for Record No 01l2 CSE Database (a) AZTEC Method (b) CORTES Method
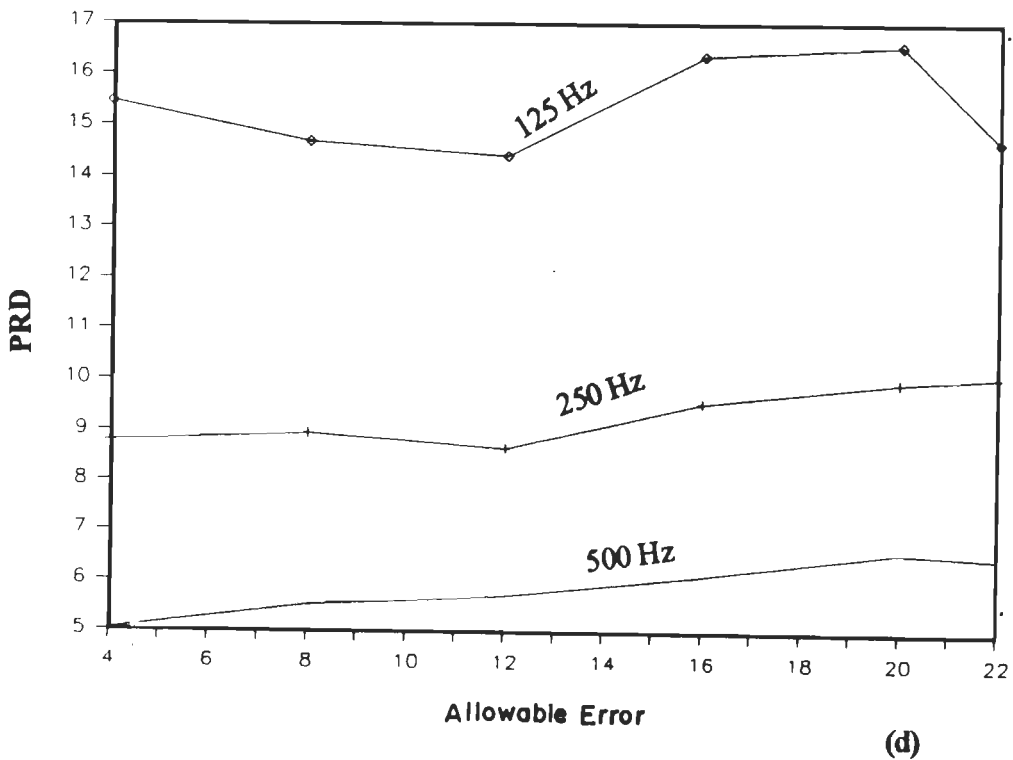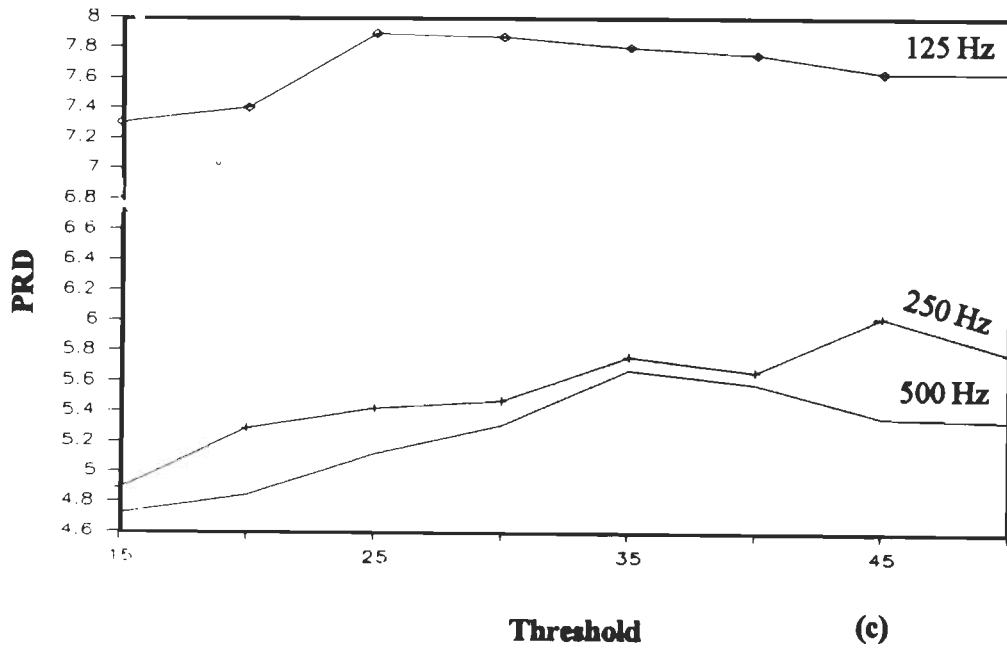
Fig 6.9   Variation of PRD for Record No 0112 CSE Database
(c) MAZTEC Method (d) SAPA-I Method
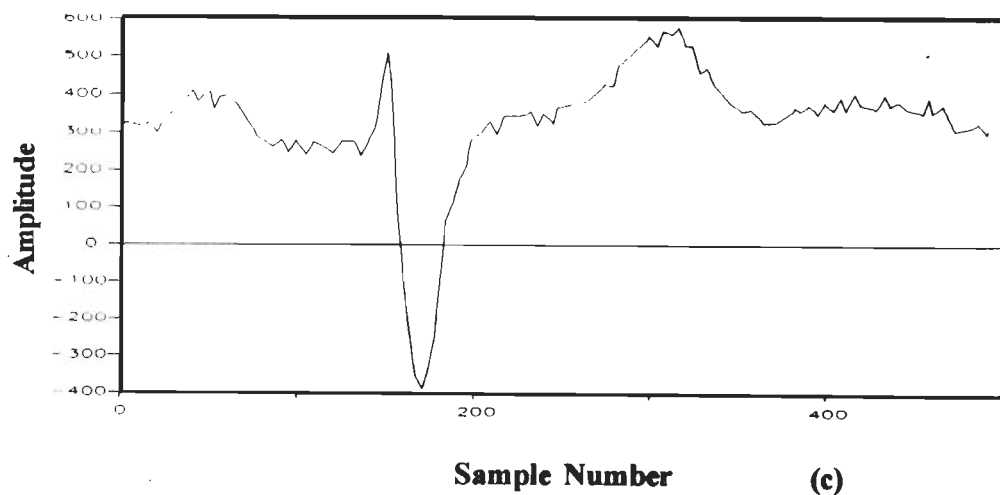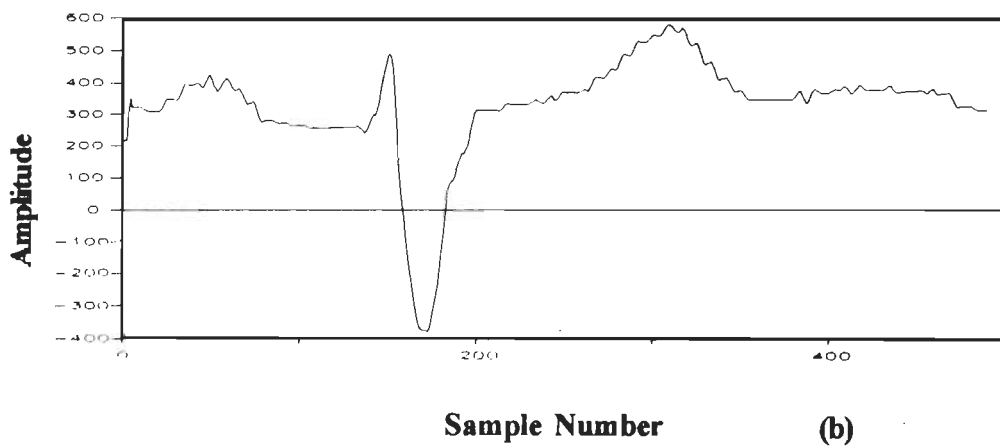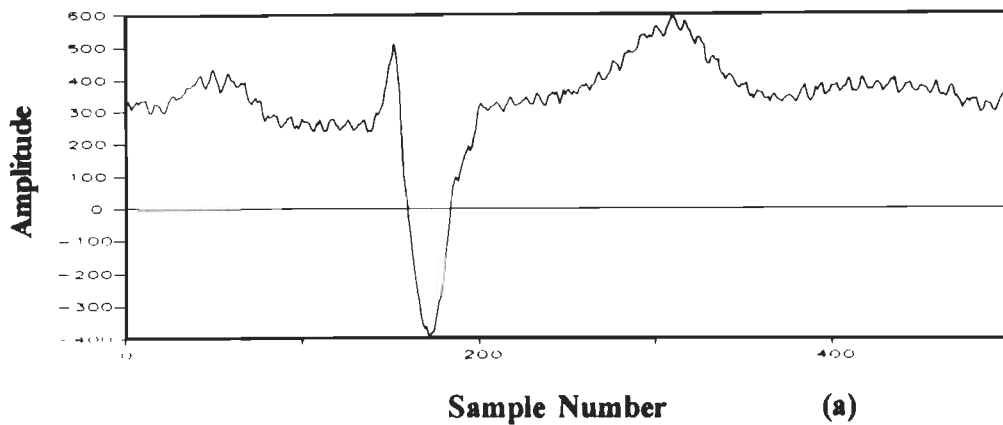
Fig 6.10   Original and Reconstructed ECG Signal for 500 Hz Sampling
Frequency for Record No. 01L2 CSE Database
(a) Original (b) AZTEC (c) SAPA-I Methods
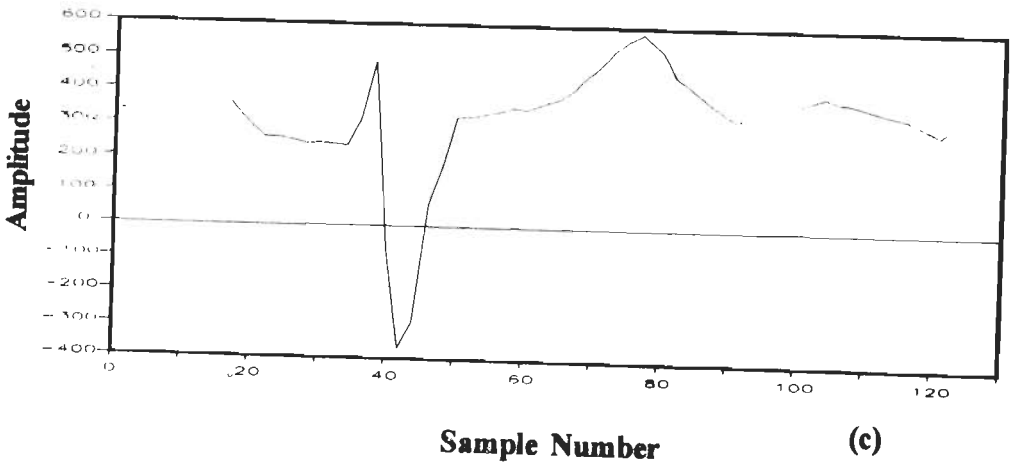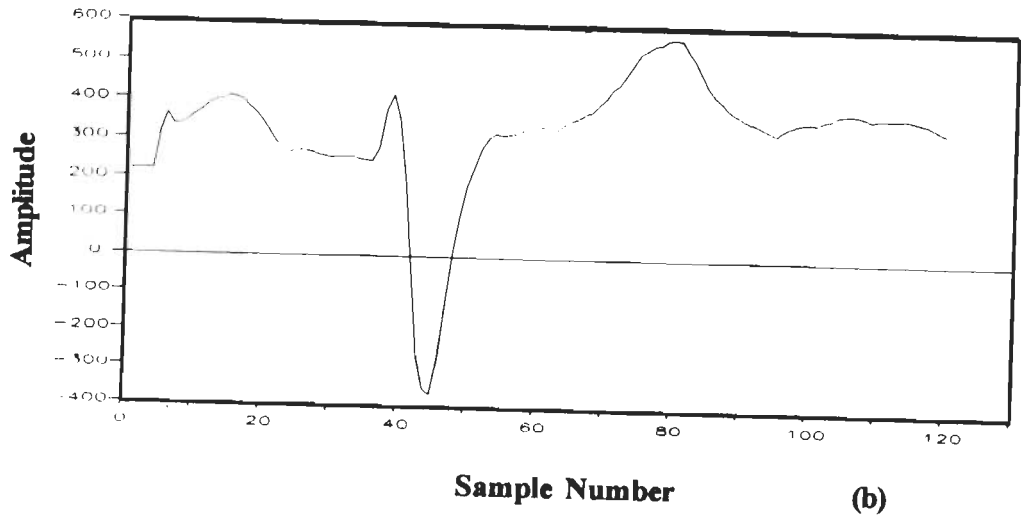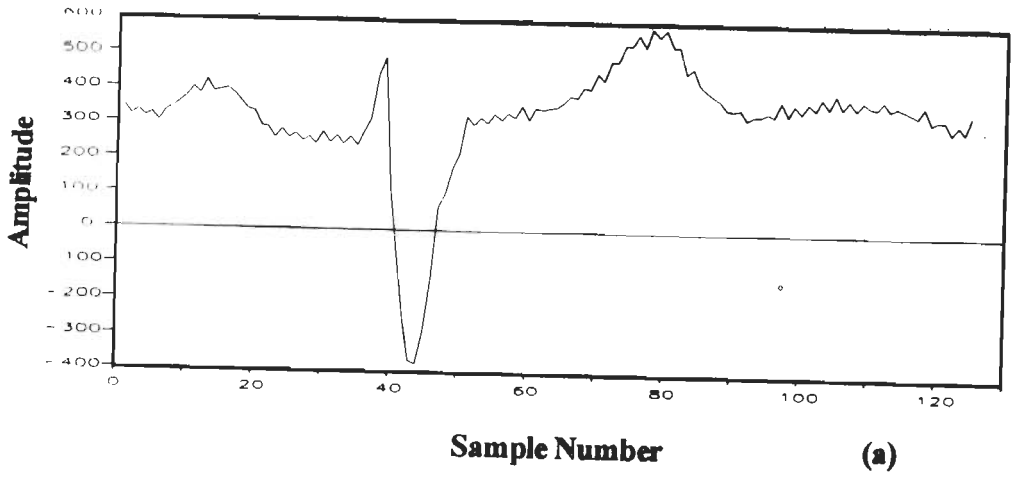
Fig 6.11 Original and Reconstructed ECG Signal for 125 Hz Sampling Frequency for Record No. 01L2 CSE Database (a) Original (b) AZTEC (c) SAPA-I Methods

guidelines recommended by the CSE Working Party [134]. In the case of AZTEC, CORTES and MAZTEC, the results in the third column of Table 6.2 show that the errors are higher in P, R and T peaks compared with Q and S peaks. But, among the three peaks, the R peak generally has the largest error because it is the highest frequency component in the ECG signal. The interval information gets changed because of changes in the onset and end-points lie outside the limits as indicated in fourth column of Table 6.2 for a compression ratio of 10. In the CORTES method, the error in the R peak is slightly less as compared with the AZTEC at 500 Hz sampling frequency. However, it remains the same for 250 Hz and 125 Hz sampling frequencies. In the MAZTEC method compression ratio obtained is less, hence the peak errors are small, as compared with AZTEC. The reconstructed signal is morphologically better than that obtained with the AZTEC methods. In all the three methods as expected, the error in the R peak increases as the sampling frequency is reduced this is observed in fifth column of Table 6.2.

The SAPA method works on a different principle, therefore, at low compression ratio the loss in peak information is small and the onset and end-points lie within the limits, in the reconstructed signal. As the compression ratio is increased the error in the 'Q' peak increases. However, for a compression ratio of 10 the 'Q' peak is lost, errors in P, R, S and T peaks are unacceptably large and their respective onset and end-points lie outside the limits shown in Table 6.2. The CSE Working Party has recommended the tolerance limit for onset and offset for P wave, QRS complex as well for T end for 500 Hz sampling frequency. Correspondingly for 360 Hz sampling frequency, the limits were modified and used for comparing the results obtained by the software.

6.5   Comments

A comparison of five DDC techniques prepared on the basis of compression ratio, PRD and errors in the peaks and the characteristic points is presented in Table 6.1. The compression ratio for TP technique is fixed, but in case of AZTEC, CORTES, MAZTEC methods it varies with the threshold or allowable error limit in case of SAPA technique. The PRD generally

Table 6.2 Results of Effect of Sampling Frequency on Performance of DDC Methods

Method	Sampling frequency (Hz)	Compression ratio	Errors in peak values Percentage					Errors in onset and end-points (No. of Samples)				
			P	Q	R	S	T	P_{on}	P_{off}	QRS_{on}	QRS_{off}	T_{end}
AZTEC	500	2.31	-0.3	-0.1	2.5	0.1	1.1	0	1	3	2	6
		4.42	1.5	-0.4	2.9	1.3	0.6	1	1	3	1	5
		10.00	1.7	-2.0	2.9	1.7	2.5	7	11	4	0	9
	250	1.69	1.5	3.0	3.4	-0.4	1.3	1	2	3	4	5
		3.16	1.7	3.1	3.4	0.1	1.5	2	0	2	5	0
		6.90	1.7	-1.5	3.2	0.1	1.7	1	2	1	5	5
	125	1.34	-0.3	-0.8	9.6	1.1	1.3	2	1	1	2	2
		2.71	-0.8	-1.2	9.6	1.1	1.4	1	3	1	4	2
		4.16	0.7	-1.4	9.6	0.9	1.4	2	1	1	3	2
CORTES	500	2.30	-0.5	-0.1	1.8	0.1	1.1	2	5	3	5	6
		5.61	-0.2	-0.3	2.4	1.2	1.4	3	6	2	2	7
		10.00	0.7	-0.3	2.4	1.1	2.2	7	7	4	2	2
	250	1.68	1.5	-1.6	3.4	-0.4	1.3	2	1	3	2	0
		3.78	1.6	-1.4	3.4	-0.4	1.9	3	2	2	5	2
		6.09	1.7	-1.4	3.2	0.1	1.7	0	1	1	5	8
	125	1.34	-0.3	-1.9	9.6	1.1	1.5	2	2	3	2	2
		2.65	-0.8	-0.8	9.6	1.1	1.4	1	1	1	3	2
		4.03	-1.1	-1.4	9.6	0.9	1.4	1	3	3	0	4
MAZTEC	500	2.41	0.6	0.0	2.0	0.1	1.0	0	4	1	1	6
		5.26	0.5	0.5	2.2	0.1	1.0	3	3	3	0	0
		7.60	0.1	1.2	2.2	0.1	0.8	3	5	1	1	6
	250	1.76	1.5	0.6	3.5	-0.5	1.6	1	3	3	4	5
		3.67	0.0	1.6	3.2	-0.5	1.2	1	2	3	4	2
		5.43	-0.5	1.3	3.2	-0.5	2.3	1	2	1	5	5
	125	1.37	-0.2	-0.1	9.7	1.1	1.6	2	1	1	2	2
		2.66	-1.8	-0.1	9.8	1.1	0.7	1	3	1	3	2
		3.78	-2.1	-0.8	9.8	1.1	0.5	2	1	1	3	2
SAPA	500	2.60	1.7	0.0	0.0	1.0	1.0	2	1	1	1	6
		6.33	0.2	0.5	0.0	0.0	2.4	3	1	1	1	6
		10.40	0.2	lost	5.6	5.9	2.4	7	1	5	2	2
	250	2.33	0.0	0.1	0.0	1.5	0.5	1	2	2	1	2
		4.71	0.0	0.2	0.6	2.9	2.5	1	4	1	3	7
		6.94	2.9	lost	0.0	0.0	0.5	2	3	4	2	9
	125	2.15	-2.3	0.0	0.0	1.0	0.0	1	1	1	2	2
		3.47	-2.3	0.0	0.9	1.0	0.0	0	3	3	1	0
		4.80	-2.3	lost	0.0	0.0	0.0	1	1	5	2	4

increases as the compression ratio is increased. Among the five methods, TP produced least PRD values. AZTEC, CORTES, MAZTEC produced more or less the same order of PRD but, it is smaller in case of SAPA method. Visual comparison reveals the quality of the reconstructed signal obtained by TP method is good. But, for other methods at higher compression ratio step like discontinuities appear in the reconstructed signal. The errors in peaks and boundaries are negligibly small in case of TP but on the other hand they increase as the compression ratio is increased .These errors are tolerable up to certain value of compression above which they are clinically unacceptable. In case of SAPA technique, the values of Q and S peaks are also affected to a greater extent, when the compression ratio is increased. All the five methods are suitable for on-line ECG data compression

The effect of sampling frequency on the performance of five DDC methods has been studied. From the results obtained, it is evident that, as the sampling frequency is increased, the compression ratio increases, correspondingly the PRD value also increases. With a higher sampling frequency, the reconstructed signal obtained is of high quality having larger bandwidth and higher resolution. It is also noticed that for different sampling frequencies the errors in peaks and boundaries are tolarable up to certain compression ratio. Beyond which, they are clinically unacceptable. The selection of sampling frequency is application dependent and the sampling rate usually ranges from 125 Hz to 500 Hz. It has been observed that even a sampling frequency of 125Hz is adequate to retain the diagnostic information in the reconstructed signal for arrhythmia classification.

CHAPTER - 7

TRANSFORM BASED ECG DATA COMPRESSION

CHAPTER - 7

TRANSFORM BASED ECG DATA COMPRESSION

7.1   Introduction

A wide variety of techniques are available for ECG data compression. Orthogonal transforms have been used for data compression but they are not commonly used in applications requiring real-time implementation, because of computational complexity. Using Orthogonal transforms in data compression, only a subset of the coefficients in the transform of the input signal is selected, with which the signal is reconstructed without loosing clinical informations. Transform compression schemes, based on the application of linear operators, provide high quality of the reconstructed signal and the compression ratio obtained is also resonably high. Because of the foresaid reasons these methods are better suited for off-line data compression. The following are the applications wherein these methods can be effectively applied for ECG data compression.

(i)   The need for efficient utilization of memory space for permanent storage of ECG's as data base requires compact data storage with easy retrieval without loosing clinical information.

(ii)   Economical rapid transmission of off-line ECG's over public telephone line from a remote place to a interpretation centre for expert opinion.

In the current chapter two transform based techniques are developed and proposed for off-line ECG data compression. The techniques have been tested for their performance on CSE and MIT/BIH Arrhythmia database. The performance evaluation has been made using two important parameters, namely, compression ratio and PRD, besides visual comparison. Further, in order to know the clinical acceptable quality of the reconstructed signal, peak and

boundary measurements were made on both the reconstructed and the original signal of the same record for comparison.

7.2   FFT-Based Algorithm

The Fourier descriptor has been earlier used for ECG data compression where the cardiac cycle is separated into two parts, namely the high frequency QRS complex and the rest of the cycle [114]. Then a fast Fourier transform (FFT) is applied to different segments after determining fiducial points. Although the idea of treating two parts of the ECG differently is novel, it requires an extra algorithm for QRS complex detection . On the other hand, the technique being proposed here is simple and straight forward and the algorithm is very efficient.

An algorithm based on fast Fourier transform applied to ECG data compression is presented in this section. It is based on the principle of successive doubling method [45] . It is so named because of the fact that a two point transform is obtained from two one-point transforms, a four-point transform from two two-point transforms and so on.

Let us first consider the discrete Fourier transform (DFT), which is represented by a pair of equations 7.1 and 7.2 given below:

$$F(u) = \frac{1}{N} \sum_{x=0}^{N-1} f(x) \exp[-j2\pi ux/N] \qquad 7.1$$

for u = 0,1,2,......N-1

and

$$f(x) = \frac{1}{N} \sum_{u=0}^{N-1} F(u) \exp[j2\pi ux/N] \qquad 7.2$$

-148-

for $x = 0, 1, 2 \ldots\ldots, N-1$

where F(u) Fourier transform , f(x) a discrete signal in time domain and $N = 2^n$ where n is a positive integer.

The number of complex multiplications and additions required for implementing equation (7.1) is proportional to N^2. The algorithm is made faster by reducing this number to $N \log_2 N$ using a decomposition procedure, called as fast Fourier transform (FFT). The following equations are obtained for calculating FFT :

$$F(u) = 1/2\{ F_{even}(u) + F_{odd}(u)\, W^u_{2m}\} \qquad\qquad 7.3$$

$$\text{and } F(u+M) = 1/2\,\{F_{even}(u) - F_{odd}(u)\, W^u_{2m}\} \qquad\qquad 7.4$$

where $M = N/2$, $u = 0, 1, 2 \ldots N/2 - 1$ and

F(u) denotes one dimensional Fourier transform.

A computer program has been written in 'C' langauge using the method discussed above and the flow chart is given in Fig. 7.1. First the data samples are read from the file and then computation of the FFT begins. In the first part of the algorithm the input data is reordered as even and odd arguments. In the second part successive doubling calculations are performed. The last step divides the result by N. The output file contains the same number of FFT coefficients as the number of samples in the input signal. Only lower order coefficients are retained and rest higher order coefficients are set to zero. The data, thus stored in the array, is used for reconstructing the signal from the compressed data [76].

Fig.7.1 Flow chart for FFT−based ECG
data compression algorithm.

The reconstruction of the signal is obtained by the reverse process called inverse transform. Input to this transform is the FFT coefficients stored in the array of compressed signal.

7.3   FWT-Based Algorithm

Researchers have developed different algorithms for the discrete Walsh transform, generally by modifying the Cooley-Tukey fast Fourier transform (FFT) algorithm. This is the simplest way of obtaining the Walsh transform which yields the coefficients in the natural or hadamard order [123]. In this section of the chapter fast Walsh transform (FWT) algorithm based on successive doubling principle is presented.

The one dimensional discrete Walsh transform is expressed by a general relation

$$W(u) = \sum_{x=0}^{N-1} f(x) \, g(x,u) \qquad\qquad 7.5$$

where $W(u)$ is the transform of $f(x)$ and $g(x,u)$ is the forward transformation kernel, and 'u' assumes values in the range 0,1.., N-1. Similarly, the inverse transform is given by

$$f(x) = \sum_{x=0}^{N-1} W(u) \, h(x,u) \qquad\qquad 7.6$$

where $h(x,u)$ is the inverse transformation kernel and 'x' assumes values in the range 0,1,....,N-1.

When $N=2^n$, the discrete Walsh transform of a function $f(x)$, denoted by $W(u)$, is obtained by substituting the kernel

$$g(x,u) = \frac{1}{N} \prod_{i=0}^{n-1} (-1)^{b_i(x) \, b_{n-1-i}(u)} \qquad\qquad 7.7$$

into equation 7.5, which results in

$$W(u) = \frac{1}{N} \sum_{x=0}^{N-1} f(x) \prod_{i=0}^{n-1} (-1)^{b_i(x) \, b_{n-1-i}(u)} \qquad\qquad 7.8$$

The values of g (x,u), excluding the constant term 1/N , are given in Table 7.1 for length N =8. The array formed by the Walsh transformation kernel is a symmetric matrix whose rows and columns are orthogonal. These properties, which hold in general, lead to an inverse kernel that is similar to the forward kernel, except for the constant multiplication factor 1/N, that is

$$h(x,u) = \prod_{i=0}^{n-1} (-1)^{b_i(x) \, b_{n-1-i}(u)} \qquad\qquad 7.9$$

Thus the inverse Walsh transform is given by

$$f(x) = \sum_{u=0}^{N-1} W(u) \prod_{i=0}^{n-1} (-1)^{b_i(x) \, b_{n-1-i}(u)} \qquad\qquad 7.10$$

It is worth noting that, unlike Fourier transform which is based on trigonometric terms, the Walsh transform consists of a series expansion of basis functions whose values are +1 or -1. It is also of interest to note

-152-

Table 7.1 Values of Walsh transformation kernel for N=8

u \ x	0	1	2	3	4	5	6	7
0	1	1	1	1	1	1	1	1
1	1	1	1	1	-1	-1	-1	-1
2	1	1	-1	-1	1	1	-1	-1
3	1	1	-1	-1	-1	-1	1	1
4	1	-1	1	-1	1	-1	1	-1
5	1	-1	1	-1	-1	1	-1	1
6	1	-1	-1	1	1	-1	-1	1
7	1	-1	-1	1	-1	1	1	-1

from equations 7.8 and 7.10 that the forward and inverse Walsh transform transforms differ only in respect of the term 1/N Thus any algorithm for computing the forward transform can be used directly to obtain the inverse transform simply by multiplying the result of the algorithm by N.

The Walsh transform can be computed by fast algorithm similar to the successive doubling method given in for the fast Fourier transform (FFT) [45]. The only difference between these two algorithms is that all exponential terms are replaced by one in the case of fast Walsh transform (FWT). Finally the following equations are obtained for calculating FWT:
:

$$W(u) = 1/2 \ \{W_{even} \ (u) + W_{odd}(u)\} \qquad\qquad 7.11$$

and

$$W(u + M) = 1/2 \ \{W_{even}(u) - w_{odd}(u)\} \qquad\qquad 7.12$$

Where $M = N/2$, $u = 0,1,2,\ldots\ldots$, $N/2\text{-}1$ and $W(u)$ denotes one dimensional Walsh transform.

The operation of an algorithm for ECG data compression is explained as follows: the input to compressor is a digitized ECG signal. When this signal is operated upon by the forward transform, Walsh coefficients are produced. The software for data compression using FWT method discussed above has been implemented here using `C' language and flow chart is shown in Fig. 7.2. The algorithm starts with reading the data samples from the input file then computation of FWT begins. In the first stage of the algorithm performs reordering of the data into even and odd arguments. The second stage does the successive doubling calculation and in the final stage the result obtained is divided by N.
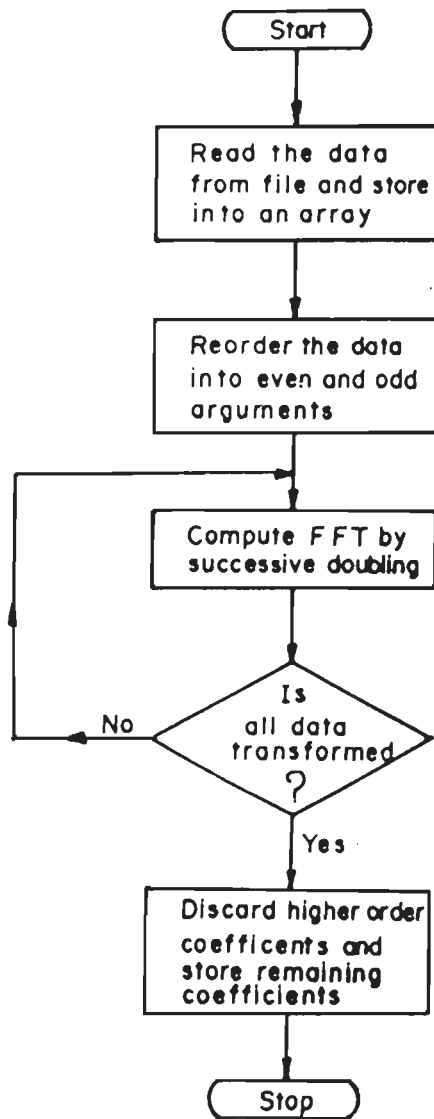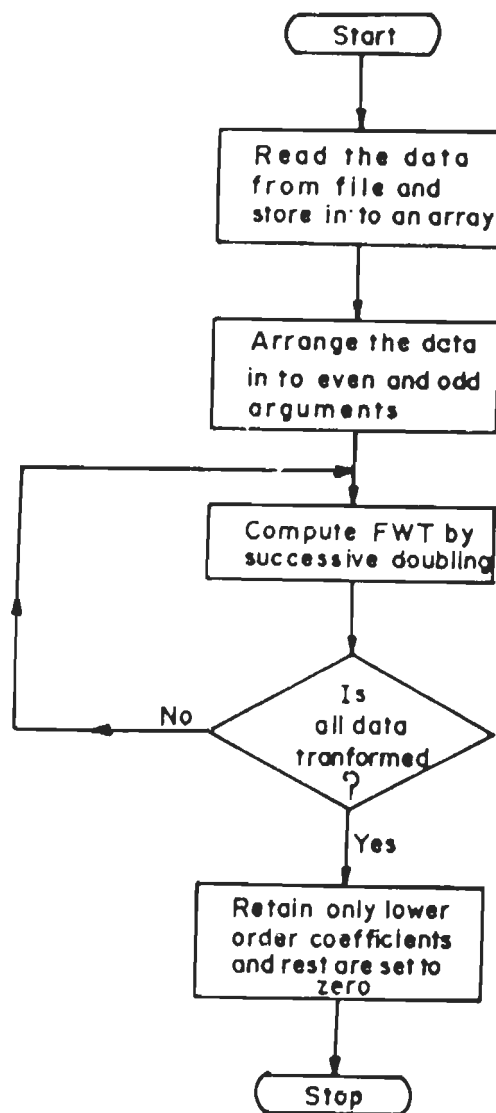
Fig.7.2 Flow chart for FWT-based ECG
data compression algorithm.

The reconstruction of the signal is effected by using the reverse process called inverse transform. Input to this transform is the FWT coefficients stored in the array of compressed signal. The inverse FWT is obtained using same algorithm with a little modification. The reconstructed signal obtained by this process contains some step like discontinuities which are not acceptable to the cardiologist for visual interpretation. Therefore the signal is smoothened using least-square polynomial curve fitting technique.

The least-square polynomial filtering technique is an easy and fast method to smoothen the signal [135]. It is a low-pass nonrecursive filter which approximates sets of points in the input sequence by a parabolic polynomial. The smoothening has been tried out with three versions, namely five point, seven point and nine point filters. Fig .7.3 shows the smoothened waveforms for different filters. Finally it has been decided to use seven point filter because the smoothening effect of the five point filter is not adequate and, on the other hand, in the nine point filter the amplitude deviations are too large (Fig 7.3). Smoothening produces a new waveform that contains little noise and has no step like discontinuities. An additional advantage of smoothening is that it eliminates the artifacts such as electromyographic (EMG) noise due to its smoothening effect.

7.4   Results

The performance of both FFT and FWT algorithms for ECG data compression are measured using important parameter, namely, compression ratio, percent root-mean-square difference besides visual comparison. Further, in order to know the clinical acceptable quality of the reconstructed signal peak, boundary and interval measurements were made both on the original and the reconstructed signal of the same record for comparison. These parameters have been explained in section 6.3. The algorithm has been tested on 125 records of CSE third data set and 25 records of 20 sec length of MIT/BIH Arrhythmia

Sample Number
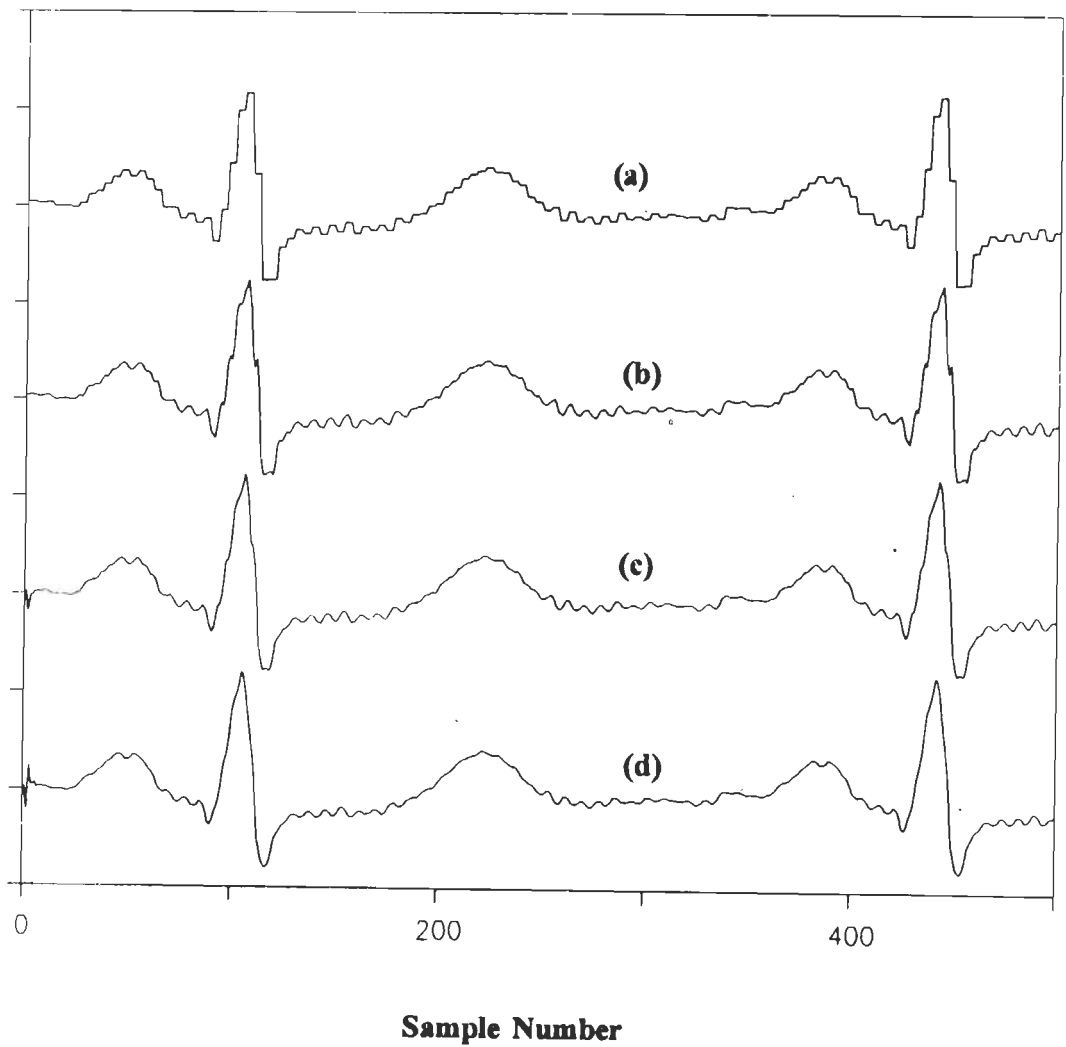
Fig. 7.3   Reconstructed   ECG signals
(a) Without filtering
(b) Using five point filtering
(c) Using seven point filtering
(d) Using nine point filtering

database. For peak and boundary measurements, the software implemented in ` C 'language as given in section 4.3.5 has been used here.

7.4.1   FFT

The results for one representative case from each database are presented here. In Tables 7.2 and 7.8 the first three columns show that the variation of compression ratio and PRD with the number of FFT coefficients. The difference between the peaks of the original and reconstructed signals have also been determined and are summarizingly presented for P, Q, R, S and T peaks in Tables 7.2 and 7.8. It is evident that the difference in amplitudes of various peaks in original ECG and the amplitudes of corresponding peak in the reconstructed signal (expressed as the percentage of the former) is more for R peak than for the other peaks. Moreover as the number of coefficients retained are increased the   difference reduces.

The peak information is important in certain cardiac diseases, such as myocardial infraction LVH, RVH, although it is not so important in most of the arrhythmia analysis. There is no standard data available for clinically acceptable deviations in peaks between original and reconstructed signals. This issue has been discussed with a group of cardiologists, according to their view the deviation of 15% in R peak, 10% in P and Q peaks and 12% in S and T peaks is acceptable [73,76]. The results presented in Tables 7.2 and 7.8 for specific cases and that listed in Table 7.3 for ten representative cases of CSE database are well within the acceptable range.

Figs. 7.4   and 7.5 show the original and reconstructed ECG signals plotted on a common horizontal axis for the ease of visual comparison. From the figures it is clear that morphology of the waveform is disturbed when the number of FFT coefficients are reduced to 48. It can also be observed that the signal get smoothed as the number of FFT coefficients are reduced due

Table 7.2   Compression ratio and Deviation in Peaks for Different Number of FFT Coefficients (CSE Data set III Rec.No 22L2)

No. of FFT coefficients	Compression Ratio	PRD	Deviation in peaks in %				
			P	Q	R	S	T
48	10.6	22.03	2.9	-4.2	16.4	0.1	1.8
64	8.0	13.86	-1.6	3.5	7.5	-3.4	1.5
80	6.4	10.60	-1.2	1.2	3.7	-5.5	1.2
128	4.0	4.90	-0.6	1.1	-0.4	-0.2	1.6
256	2.0	2.91	0.4	0.1	-0.5	0.21	-0.2

Table 7.3   Percentage Errors in Peaks for 64 FFT Coefficients (Ten Cases of CSE Data set III)

Record No.	PRD	Deviation in different peaks in %				
		P	Q	R	S	T
6	18.41	1.4	9.0	-6.0	4.5	-1.1
11	7.12	-1.1	-0.1	1.7	0.8	2.4
16	3.46	1.9	1.8	10.2	-1.9	1.4
22	13.86	-1.6	3.5	7.5	-3.4	1.5
31	10.61	-0.3	0.2	4.9	0.8	2.0
41	11.41	3.4	-6.1	13.9	-7.0	-3.4
46	3.62	-0.8	-1.0	-3.5	0.7	-0.4
51	5.50	6.7	0.2	-0.4	7.4	3.8
66	15.61	-2.5	0.9	-2.6	10.3	9.7
71	6.60	-3.4	-3.2	10.0	5.8	-4.2

Table 7.4   Boundary Measurements for Original and Reconstructed ECG (CSE Data Set III Rec.No.22L2) with Referee Tolerance

Signal	No. of coefficients	Onset and Offset for each wave in ms.				
		P_{on}	P_{off}	QRS_{on}	QRS_{off}	T_{end}
(A) Original	512 samples	36	152	276	376	660
(B) Reconstructed	48	30	143	274	380	664
	64	32	148	276	374	658
	80	36	152	272	374	658
	128	36	150	274	372	656
	256	36	152	276	376	660
Referee deviation in ms. for limb leads		8	12.8	7.8	12.4	32.8

Table 7.5 Results for inter and intra-peak intervals in ms. (CSE Data set III Record No. 22 L2)

Number of coefficients	P-DUR	QRS-DUR	PR-INT	QT-INT
A. Original(512)	116	100	240	384
B. Reconstructed				
48	113	106	244	390
64	116	98	244	382
80	116	102	236	386
128	114	98	238	382
256	116	100	240	384

Sample Number
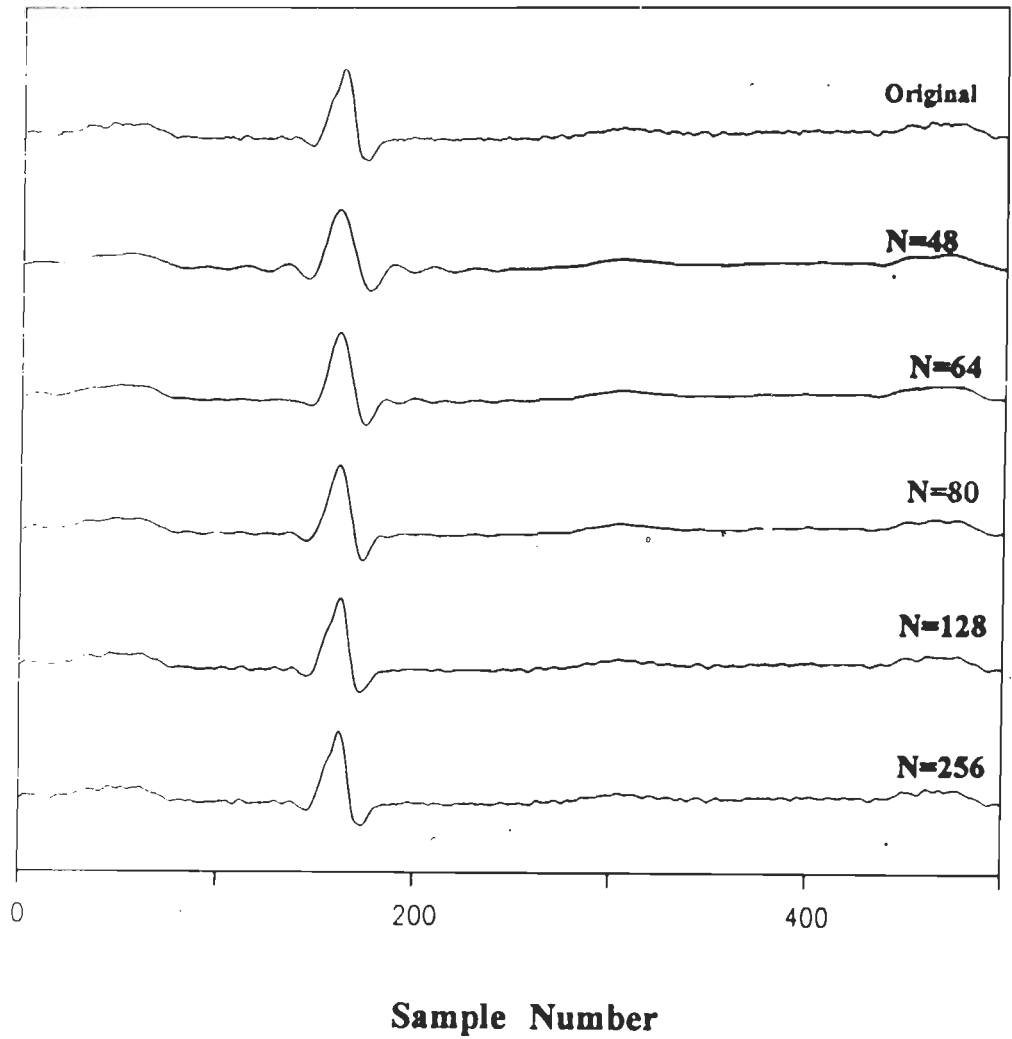
Fig. 7.4   Original and Reconstructed ECG Signal for Different Number of
                FFT Coefficients (N) (CSE III Data set Record No. 22L2)
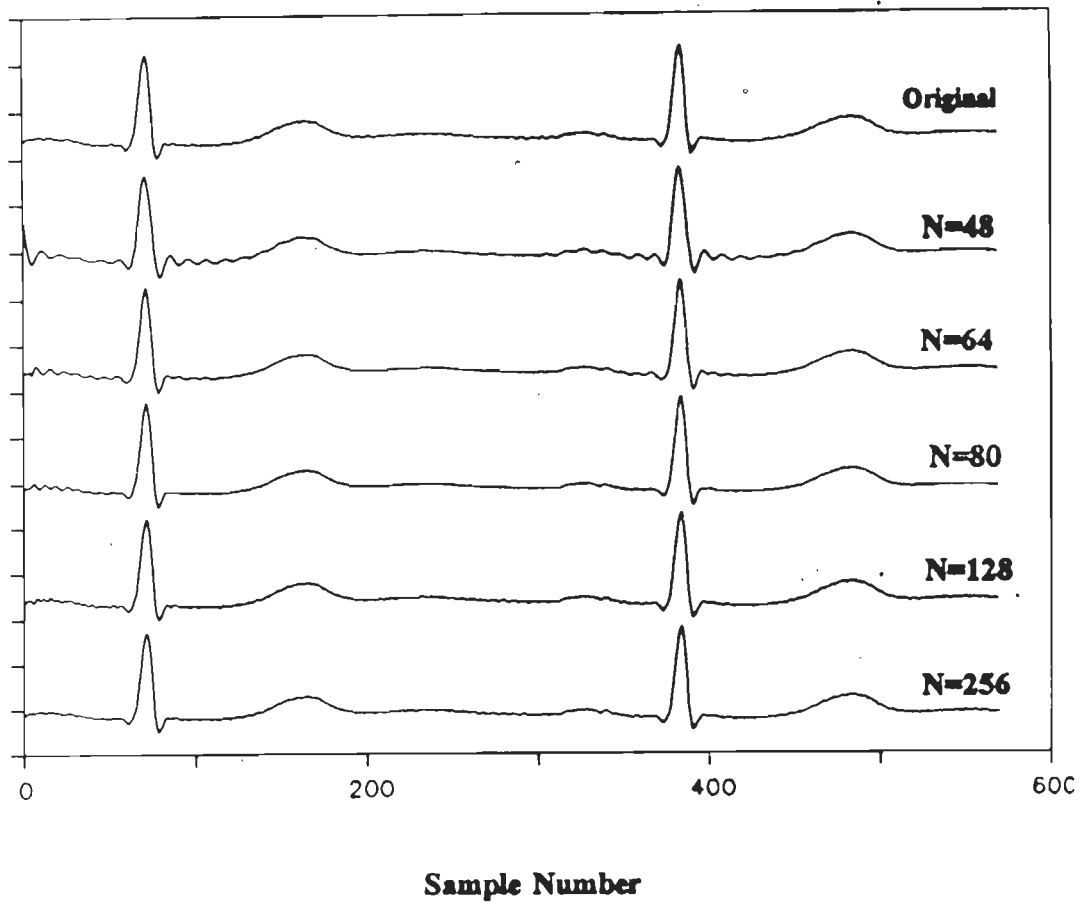
Fig. 7.5 Original and Reconstructed ECG Signal for Different Number of FFT Coefficients (N) (MIT/BIH Arrhythmia Database Record No. 103)

to elimination of high frequency noise present in the original signal . This amounts to the reduction of electromyographic (EMG) noise.

Boundary measurements in terms of onsets and offsets were also made for both the original and the reconstructed ECG signals. The algorithm for determining characteristics points (onset and offeset) for P, QRS & T waves is given in section 4.3.5 has been validated with the CSE multilead measurement database [134]. The results obtained by the software developed has also been compared with manual measurements . The detailed results for one representative case from each database is given in Tables 7.4 and 7.9. It is noticed from Tables 7.4 and 7.9 that errors in P-wave onset and offset increases with the reduction in coefficients compared to QRS and T waves. A minimum of 64 coefficients are required to keep the onsets and offsets well within the permissible range as recommended by the CSE Working Party [134]. On the other hand if the coefficients are reduced to 48 it is clear from Tables 7.4 and 7.9 that the errors in the characteristic point increases and lie outside the tolerance limit. Hence retaining only 48 coefficients is not clinically acceptable.

Results are also presented for significant interval values: P-duration (P-DUR), PR-interval (PR-INT) QRS- duration (QRS-DUR) and QT-interval (QT-INT) are presented in Tables 7.5 and 7.10. These results also confirm that a minimum of 64 coefficients are necessary while retaining the diagnostically important parameters well within the acceptable range [152].

The results given in Table 7.6 for ten representative cases also show that the characteristic points are well within the limits as specified by the CSE Working Party. Similarly Table 7.7 presents the interval information for P,QRS and T waves for the same ten records. In these cases also the intervals are well within the permissible limits.

Table 7.6   Errors in Onset and End-points for 64 FFT Coefficients in ms. (CSE data set III for Ten Cases)

Record No.	Onset and offset for each wave in msec.				
	P_{on}	P_{off}	QRS_{on}	QRS_{off}	T_{end}
6	4	12	6	0	32
11	0	0	6	4	8
16	8	2	2	2	32
22	4	4	0	2	2
31	8	-2	-2	0	32
41	8	10	6	-6	-12
46	8	8	0	0	0
51	4	10	6	12	4
66	8	10	6	4	-4
71	2	4	0	-12	-12

Table 7.7   Results for inter and intra peak intervals for 64 coefficients in ms. (CSE Data set III for Ten Cases)

Record No.	P-DUR	QRS-DUR	PR-INT	QT-INT
6	-0.18	-0.08	0.04	0.28
11	0.00	0.02	-0.06	0.14
16	-0.16	0.00	-0.16	0.30
22	0.00	0.02	0.04	0.02
31	-0.32	0.02	-0.32	-0.32
41	0.18	-0.16	0.18	-0.22
46	-0.06	0.00	0.14	0.00
51	-0.02	0.00	0.06	-0.14
66	-0.02	-0.06	-0.02	-0.14
71	0.02	-0.18	-0.02	-0.12

Table 7.8 Compression Ratio and Deviation in Peaks for Different Number of FFT Coefficients (MIT/BIH Arrhythmia Database Record Number 103)

Number of FFT coeffi-cients	compression ratio	PRD	Deviation in peaks in percentage				
			P	Q	R	S	T
48	10.6	1.15	3	0.1	17.5	1.2	4.5
64	8.0	0.81	1.0	0.05	3.0	0.2	1.2
80	6.4	0.67	0.5	0.02	1.0	0.1	0.6
128	4.0	0.43	0.05	0.0	0.2	0.0	0.2
256	2.0	0.013	0.1	0.0	0.2	0.05	0.1

Table 7.9   Boundary measurements for original and reconstructed signal (MIT/BIH Arrhythmia database record no 103)

Signal	NO. of FFT coefficients	Onset and offset for each wave in ms				
		P_{on}	P_{off}	QRS_{on}	QRS_{off}	T_{end}
A. Original	512	70	154	174	268	638
B. Reconstructed	48	58	146	172	255	630
	64	67	151	171	267	634
	80	68	150	172	268	636
	128	68	152	172	266	634
	256	70	154	173	268	636

Table 7.10 Results for inter and intra-peak intrevals in ms   (MIT/BIH Arrhythmia database for record no 103)

Signal	No. of coefficients	P-DUR	QRS-DUR	PR-INT	QT-INT
A. Original	512	84	94	104	464
B. Reconstucted	48	88	84	197	458
	64	84	90	104	463
	80	82	97	104	465
	128	84	94	104	462
	256	84	96	102	464

7.4.2   FWT

Results for one representative case tested on CSE and MIT/BIH database are given here. Tables 7.11 and 7.17 show detailed results of a specific case showing the variation of compression ratio and PRD with respect to the number of coefficients in the compressed signal and corresponding variation in the different ECG peak amplitudes (P,Q,R,S and T). From column number two of Tables 7.11 and 7.17 it is clear that the compression ratio decreases as the number of coefficients in the compressed signal are increased, correspondingly the PRD value as expected decreases as indicated in column three of Tables 7.11 and 7.17 and the quality of the reconstructed waveform improves as shown in Figs. 7.6 and 7.7. Results for ten representative cases from CSE database are also presented in Table 7.12 and 7.14 for a compression ratio of 4.

The guidelines for peak deviations are followed here as explained in section 7.4.1. The results given in Tables 7.11 and 7.17 for specific case reveals that as the compression ratio increases the deviations in the peaks of ECG (i.e. P,Q,R,S and T) also increases. It is observed from column five of Tables 7.11 and 7.17, that the deviation is found to be maximum in the R-peak compared to other ECG peaks. Because QRS complex being the highest frequency component of the ECG cycle. A minimum of 128 coefficients are required in order to preserve the morphology and to keep errors in the peaks within the tolerable limit. However, if the coefficients are reduced below 128 the errors in the ECG peaks are large and they are clinically not acceptable. The reconstructed signal shown in Figs. 7.6 and 7.7 also indicates that the morphology of the waveform get changed for 100 coefficients.

For the purpose of visual compression the reconstructed and original ECG signal for different number of coefficients are plotted on a common horizontal axis as shown in Figs. 7.6 and 7.7 for ease of comparision. From figure

-167-

Table 7.11. Compression ratio and deviation in peaks for different no. of FWT coefficients (CSE Data set III Rec.no 6L$_2$)

Number of coefficients	Compression Ratio	PRD	Deviation in peaks in percentage				
			P	Q	R	S.	T
100	5.12	22.8	8.5	8.4	19.4	2.2	-7.9
128	4.00	12.29	0.8	4.8	-6.1	10.3	-12.1
192	2.66	7.52	0.9	4.0	-8.6	9.5	12.2
256	2.00	5.4	0.01	5.2	-1.9	3.9	-9.7

Table 7.12 Percentage errors in peaks for 128 FWT coefficients (Ten Cases CSE Data Set III)

Record Numbers	PRD	Deviation in different peaks in percentage				
		P	Q	R	S	T
6	11.29	0.8	4.8	-6.1	1.3	-12.1
11	15.97	1.4	-0.5	3.5	0.5	1.8
16	6.13	3.9	2.0	9.4	1.0	4.7
21	7.59	-0.2	3.6	10.6	-2.1	0.1
22	12.09	-1.6	3.1	10.0	6.5	1.2
31	8.34	-1.0	1.4	2.8	4.2	-4.3
41	19.61	7.2	0.3	11.6	4.1	-0.8
46	5.05	0.7	5.4	0.6	0.9	0.5
66	6.32	-2.9	-1.9	6.5	-4.5	-1.5
71	11.58	5.1	5.9	11.9	-2.5	2.8

Table 7.13 Onset and end-points of original and reconstructed signals in ms. (CSE Data set III Record number 06L$_2$).

Signal	Number of coefficients	Onset & off set of each wave in msce.				
		P_{on}	P_{off}	QRS_{on}	QRS_{on}	T_{end}
(A) Original	512 samples	50	138	166	258	578
(B) Reconst-ructed	100	62	160	182	260	606
	128	46	138	166	260	574
	192	44	138	166	260	574
	256	50	150	168	258	576
Accepted tolerance for Limb lead in mses.		8	12.8	7.8	12.4	32.8

Table 7.14 Percentage errors in onset and end-points for 128 FWT coefficients (Ten Cases of CSE Data set III)

Record Number	Onset and end-points for each wave in msec.				
	P_{on}	P_{off}	QRS_{on}	QRS_{off}	T_{end}
6	4	0	0	2	4
11	0	-8	0	2	2
16	2	0	2	2	4
21	2	2	6	-4	-4
22	2	0	0	4	4
31	8	-4	-4	-8	16
41	0	12	6	-2	26
46	8	12	6	-4	32
66	0	6	2	12	16
71	0	-6	-4	-6	0

Table 7.15 Results for inter and intra-peak intervals in ms.
(CSE Data Set III Record No. 06L2)

Signal	No. of FWT coefficients	P-DUR	QRS-DUR	PR-INT	QT-INT
A. Original	512	88	92	116	412
B. Reconstructed					
	100	98	78	120	424
	128	92	94	120	408
	192	94	94	122	408
	256	100	90	118	408

Table 7.16 Results for inter and intra peak intervals for 128 coefficients in ms. (Ten Cases of CSE Data Set III)

Record No.	P-DUR	QRS-DUR	PR-DUR	QT-INT
6	-0.04	-0.02	-0.04	0.04
11	-0.08	0.02	0.0	0.02
16	-0.02	-0.04	0.0	0.02
22	0.0	0.0	0.02	0.0
31	-0.08	-0.04	-1.8	0.2
41	0.1	-0.11	-0.9	0.03
46	-0.02	-0.08	0.01	-0.12
51	0.02	-0.08	0.08	0.04
66	0.03	0.06	0.01	0.08
71	-0.03	-0.01	-0.02	0.02

Table 7.17 Compression Ratio and Deviation in Peaks for Different Number of FWT Coefficients (MIT/BIH Arrhythmia Database Record Number 103)

No. of coefficients	Compression ratio	PRD	Deviation in peaks in %				
			P	Q	R	S	T
100	5.12	28	10	4	30	8	15
128	4.00	6.9	1.2	2	5.4	3	2.1
192	2.66	2.07	0.6	1.2	3.4	2.5	1.5
256	2.00	1.84	0.1	0.2	2.0	1.6	1.0

Table 7.18 Boundary Measurements for Original and Reconstructed ECG (MIT/BIH Arrhythmia Database Record Number 103)

Signal	No. of FWT coefficients	Onset and offset for each wave				
		P_{on}	P_{off}	QRS_{on}	QRS_{off}	T_{end}
A Original	512	70	154	174	268	638
B. Reconstructed						
	100	50	124	170	250	600
	128	64	150	172	268	630
	192	68	152	172	265	630
	256	68	150	172	265	634

Table 7.19 Results for inter and intra peak intervals in ms. (MIT/BIH
Arrhythmia Database Record Number 103)

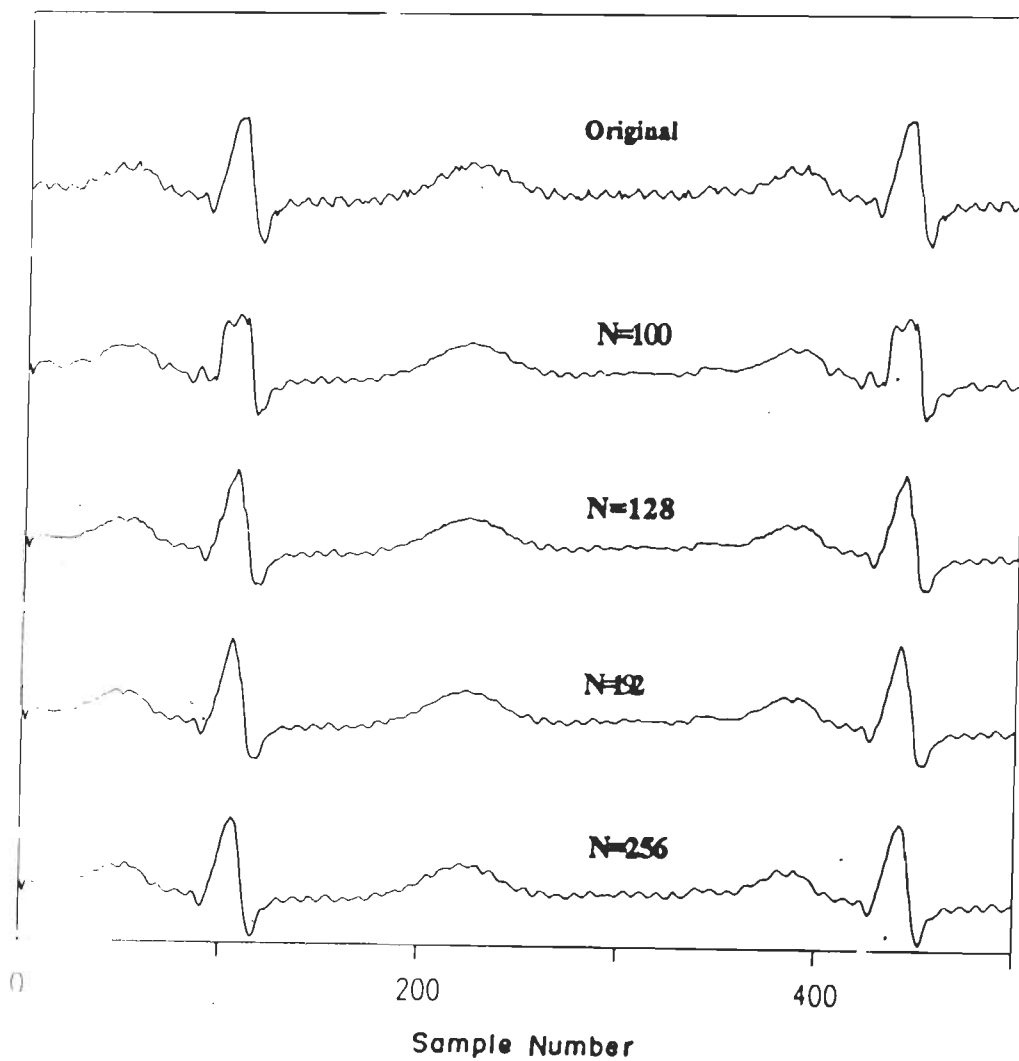| Signal	No.of coefficients	P-DUR	QRS-DUR	PR-INT	QT-INT
A. Original	512	84	94	104	464
B. Reconstructed					
	100	74	80	120	458
	128	86	96	108	458
	192	84	93	104	458
	256	82	94	104	462

Fig. 7.6 Original and Reconstructed ECG Signal for Different Number of FWT Coefficients (N) (CSE III Data set Record No. 06L2)
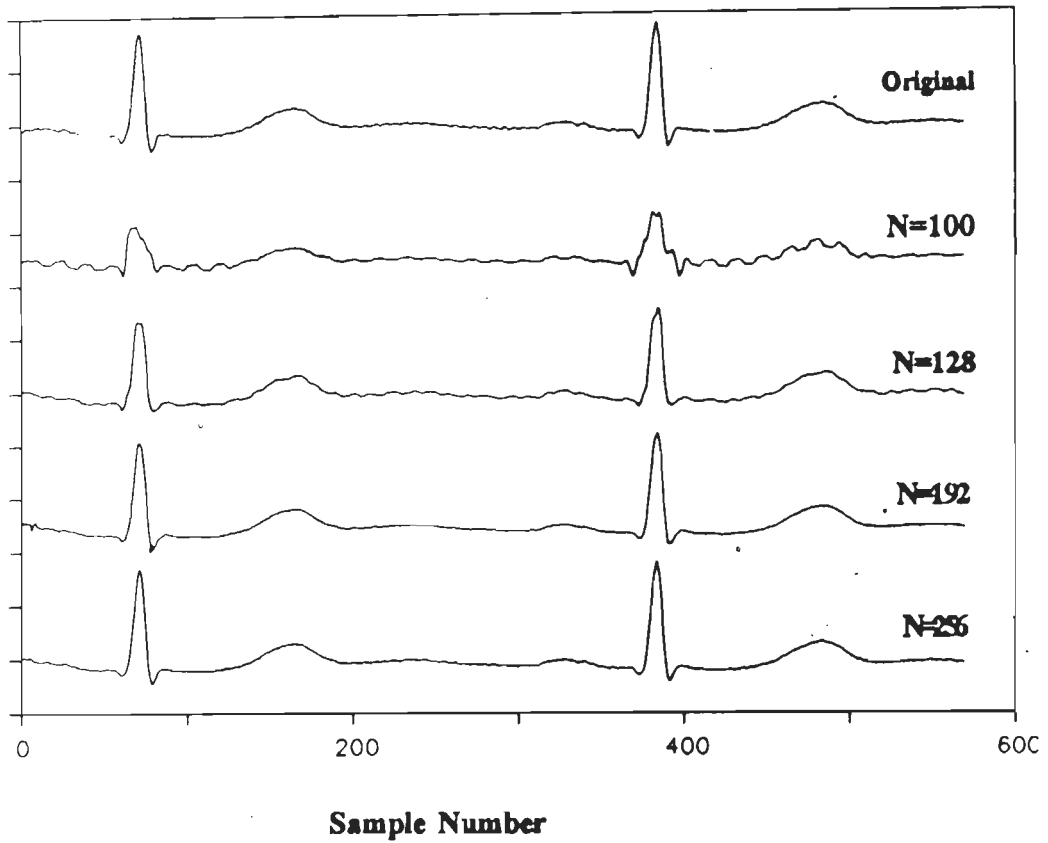
Fig. 7.7   Original and Reconstructed ECG Signal for Different Number of FWT
Coefficients (N) (MIT/BIH Arrhythmia Database Record No.103)

it is evident that the number of coefficients in the compressed signal are increased the reconstructed signal closely resembles the original signal. Tables 7.13, 7.14 and 7.18 shows the results of boundary detection in terms of onsets and offsets for P wave , QRS complex as well as for the T_{end}. These measurements have been made both on the original and the reconstructed signal using the software given in section 4.3.5 and then the results were compared with the tolerance limits recommended by CSE Working Party [134]. The results presented in Tables 7.13 and 7.18 for specific case, reveals that as the coefficients in the compressed signal are reduced the deviations in the onset and offset of P wave increases sharply as compared to QRS complex and T wave. Therefore a minimum of 128 coefficients are required while keeping the onsets and offsets well within the tolerable limits. On the other hand if the coefficients are reduced below 128 the results presented in Tables 7.13 and 7.18 for 100 coefficients shows large errors in the onset and offsets of each wave and they are not clinically acceptable.

The inter and intra peak interval results are given in Tables 7.15 and 7.19 .These results also demonstrate that a minimum of 128 coefficients are required in order to retain the clinically important parameters well within the acceptable limits [152]. Similarly, Table 7.16 shows the interval information for ten representative cases expressed as percentage error between original and the reconstructed signals for 128 coefficients.

7.4.3   Comparison

As both the algorithms have been tested on the same database, it is convinent to compare the performance. The following comparision can be made with the help of the results presented in section 7.3. The comparison is made on the basis of compression ratio, percent root-mean-square difference, fidelity and computation time.

(a) In case of FFT the compression ratio is double than that of FWT technique. This is because the number of coefficients retained in the compressed signal are less in case of FFT. The maximum compression ratio obtained is 8 in case of FFT while retaining the clinical information and wherein the compression ratio is 4 in case FWT technique.

(b) The PRD value in case of FWT is high. This is due to the fact that it operates only on real values, therefore, the reconstructed signal contains some step like discontinuities. On the other hand, FFT reconstructed signal quality is good, therefore PRD value is less

(c) As far as the fidelity is concerned the reconstructed signal obtained after inverse FFT produces a good quality of the signal. This is due to the fact that FFT has an important property of forming the mirror image. But however, in case of FWT the reconstructed signal which is obtained after inverse FWT is not of good quality. It contains discontinuities therefore, it is not acceptable to cardiologists, hence filtering is required to make the signal compatable to cardiologist for visual interpretation .

(d) The computation time required for FFT technique is more because, it involves $Nlog_2N$ complex multiplications and additions. But on the other hand FWT technique requires $Nlog_2N$ simple additions/subtractions results in a lesser computation time than FFT. Therefore FWT algorithm is computationally fast .Where as, FFT technique is more suitable for off line ECG data compression which is very much useful in database management .

7.5   Comments

Fast Fourier transform based on successive doubling principle is described in this chapter. It has been tested on 125 records belonging to the third set of CSE database library and 25 records of 20 sec length of MIT/BIH database. A compression ratio of 8 has been achieved while preserving the clinical information. Visual comparison reveals that the reconstructed signal contains negligible amount of noise, because of inherent smoothing

by the algorithm. This inturn reduce electromyographic (EMG) noise. The results presented in the text reveals that peak, boundary and interval measurements confirms the clinical acceptability of the compression scheme, given that the results are within the acceptable tolerance.

ECG data compression using fast Walsh transform (FWT) based on successive doubling method is presented here. The performance of the algorithm has been evaluated on 125 records belonging to third set of CSE database and 25 records of 20 seconds length of MIT/BIH library. A compression ratio of 4 has been obtained while retaining the clinically important information. Peak, boundary and interval measurements confirms the clinical acceptability of the algorithm, because the results are within the tolerance limits. Reconstructed signal requires smoothing in order to remove discontinuities, high frequency noise and to make the signal suitable for visual examination by the cardiologists. This process also helps in removing artifacts such as electromyographic (EMG) noise.

ECG data compression using fast Fourier transform is suitable for off-line data compression in order to store large amount of data for further use as database . As this scheme has high compression ratio and good quality of the reconstructed signal is obtained after inverse transform. On the other hand fast Walsh transform method of compression can be used to transmit the ECG data off-line over a public telephone from a remote place to interpretation centre for expert opinion.

CHAPTER-8

SOFTWARE FOR AMBULATORY MONITOR

CHAPTER-8

SOFTWARE FOR AMBULATORY MONITOR

8.1   Introduction

The software for the ambulatory monitor is written with an objective of its implementation in real-time. In order to minimize the execution time, programs are written in assembly language of 8088. Due care has been taken in writing programs to make effective use of the capabilities of the developed hardware presented in chapter 3. In previous chapters (4, and 6) algorithms were proposed for QRS detection, R peak location and ECG data compression. These algorithms can be used for both off-line and online applications. The algorithms have been tested for their performance on the CSE and MIT/BIH Arrhythmia database. However, based on the simplicity and computational efficiency of the algorithms, turning point technique for data compression and slope threshold technique for QRS detection have been selected for online implementation in ambulatory monitor. The software for ECG processing include, data acquisition, data compression, QRS detection and arrhythmia interpretation programs.

The performance of each algorithm has been evaluated separately. The data acquisition algorithm has been tested in real-time by acquiring ECGs from different subjects. While the other algorithms have been evaluated using data from the standard library MIT/BIH Arrhythmia database. As this database contains variety of arrhythmias and it also contains beat-by-beat annotated results. This facilitates to compare the performance of the algorithm with the results available in the database. The detailed implementation of each algorithm are explained in the following sections.

8.2   Data Acquisition Algorithm

On power up, the system software takes control of the system hardware. The first step in the data acquisition algorithm is to initialize the

programmable chips for their respective operations. The data and stack segments are also initialized. Since there are three channels to be scanned, the data from the three channels are stored in three different locations in the RAM. For each channel 250 k bytes of memory has been reserved and thus the data from the three channels occupy about 750k of RAM locations. The remaining 18k bytes of the RAM is used for the storage of the temporary data and for stack operation. Approximately 10 minutes of ECG data per channel can be stored in the RAM. The RAM is configured cyclically and as it gets full, the old data are deleted to make way for the new data. This process continues until the acquisition is stopped.

The flow chart for the algorithm implementation is shown in Fig. 8.1. The microprocessor selects required channel by outputting the appropriate address through PPI, which in turn selects the input channel of the analog multiplexer,and the conversion process is initiated. After the conversion is over, the data are read and stored in the respective memory location. When all the three conversion are over, the timer output is checked if it is high the next cycle to acquire data is initiated. The data stored in the RAM can be down loaded to PC using RS232C serial communication interface if required.

8.3   Data Compression Algorithm

The various data compression algorithms for real-time application are discussed in section 6.2 and their performance has been tested on standard data base. Among the five algorithms turning point (TP) algorithm has the advantage of ease of implementation on microprocessor and computationally fast for real-time application. The speed requirement is critical in this application because of the fact that the ECG processing should be completed within the sampling interval. Therefore, TP technique has been selected in the present work for on - line ECG data compression.

For the purpose of arrhythmia analysis, single lead (lead II) generally is used to classify the disease, hence single lead data compression algorithm is presented in this section. The flowchart for the implementation of the algorithm is shown in Fig. 8.2. The algorithm starts by acquiring the first sample and it is stored in the buffer as 'X_0' . After this, two more samples are
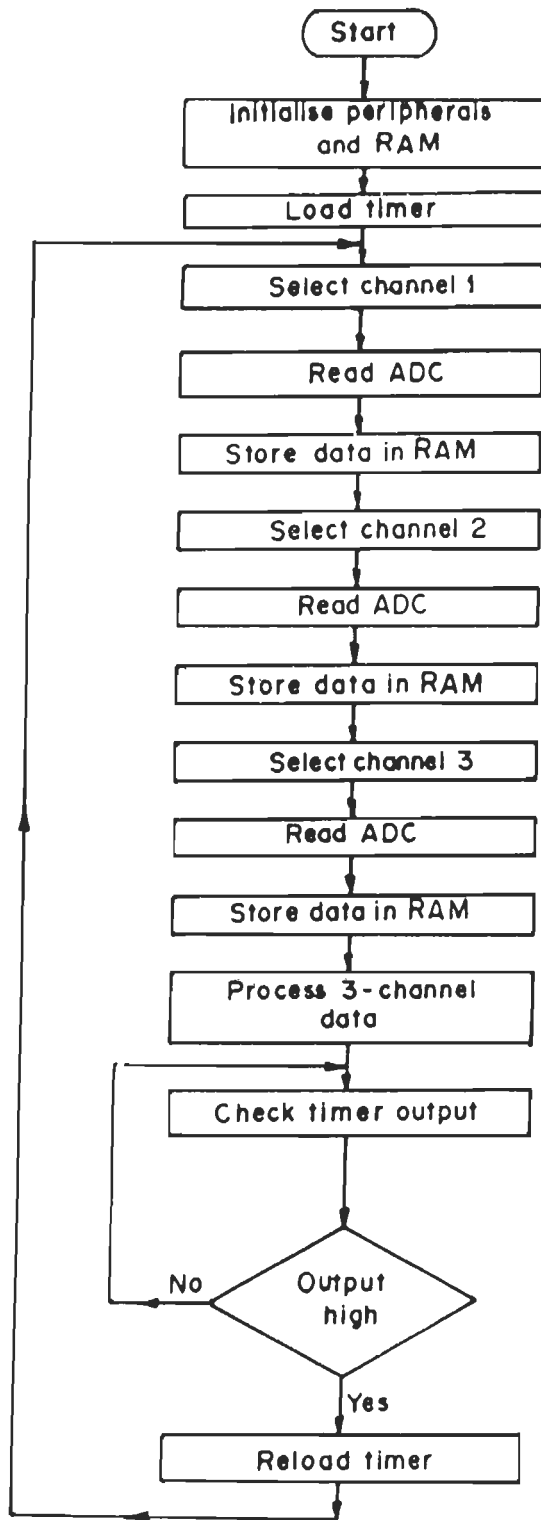
(a) Main program
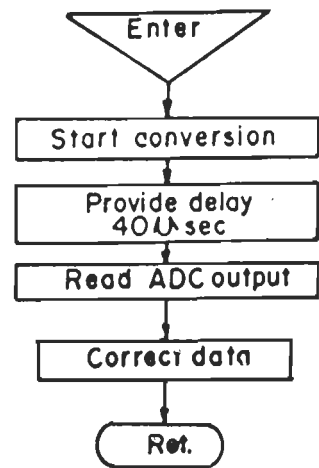
(b) Read ADC subroutine

Fig. 8.1 Flow chart for 3−channel simutaneous ECG recording

Fig. 8.2 Flow chart for real time implementation of turning point algorithm.

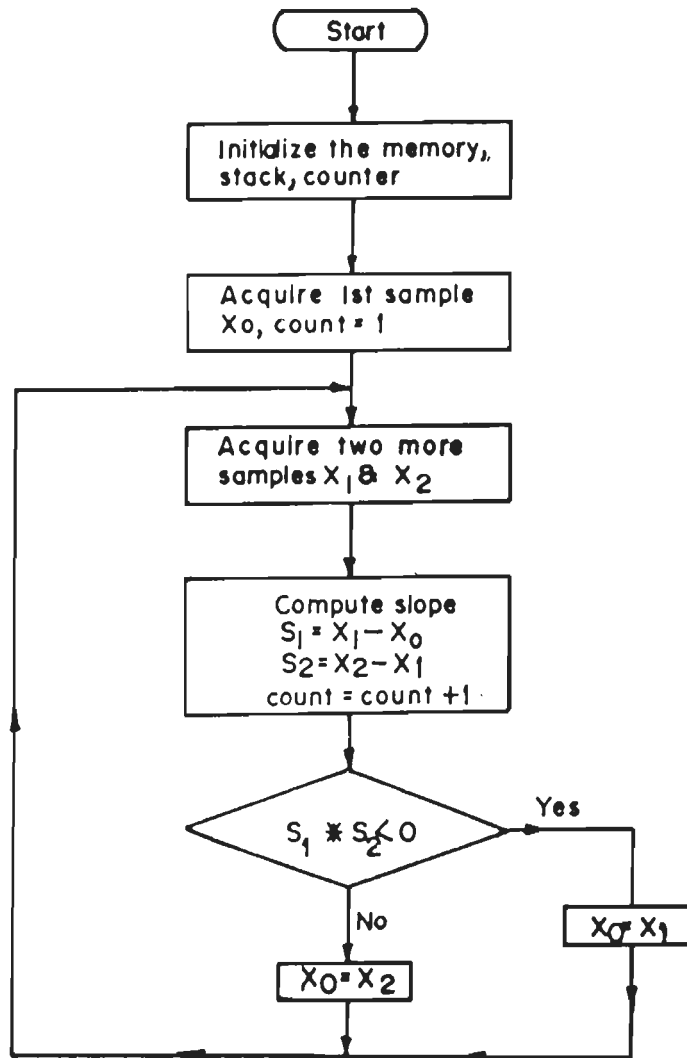acquired and stored in the buffer as 'X_1 and X_2'. The computation of slope S_1 and S_2 is carried out by subtracting 'X_0' from X_1 and X_1 from X_2 respectively. The product of two slopes are then compared, in order to find whether the slope is positive or negative. If product of slopes S_1 and S_2 is negative or zero X_0 is taken equal to X_1, otherwise X_0 is taken as X_2. This process is repeated till all the samples are over.

8.4 QRS Detection Algorithm

The QRS detection algorithm for off-line analysis is presented in section 4.3. The same algorithm is used for online application because of the fact that, the algorithm is simple, efficient and is easy to implement on microprocessor. The hardware schematic for QRS detector is shown in Fig. 8.3. The digital signal available on the CD ROM of MIT/BIH Arrhythmia database is converted into analog form using a 14-bit digital to analog convertor (DAC). Then this signal is passed through analog processing circuit consisting of amplifier and filters in order to remove high frequency noise, powerline interference and other artifacts. The analog to digital conversion is carried out using 12 bits analog to digital convertor (ADC). The samples are taken at a sampling frequency of 200 Hz, this allows 5 ms to complete the processing. After this the signal is processed by processor module for QRS detection.

Integer arithmatic has been used so that the algorithm can work in real-time. The flowchart of the algorithm implementation is shown in Fig. 8.4. First initialization of peripherals and data locations is made. A start conversion is issued to mark the instant of sampling and to initiate analog to digital conversion of the sample. A two second strip of ECG samples is stored in the RAM. These samples are then searched in order to find their maximum and minimum amplitudes. The difference between these values determines the peak-to-peak amplitude of the stored ECG. Under extremely low heart rate conditions, the two second interval ensures storage of at least one cardiac cycle. The peak-to-peak value obtained is now used for updating the positive slope thresholds which were selected initially on the basis of average value of the rate of rise of R-wave.
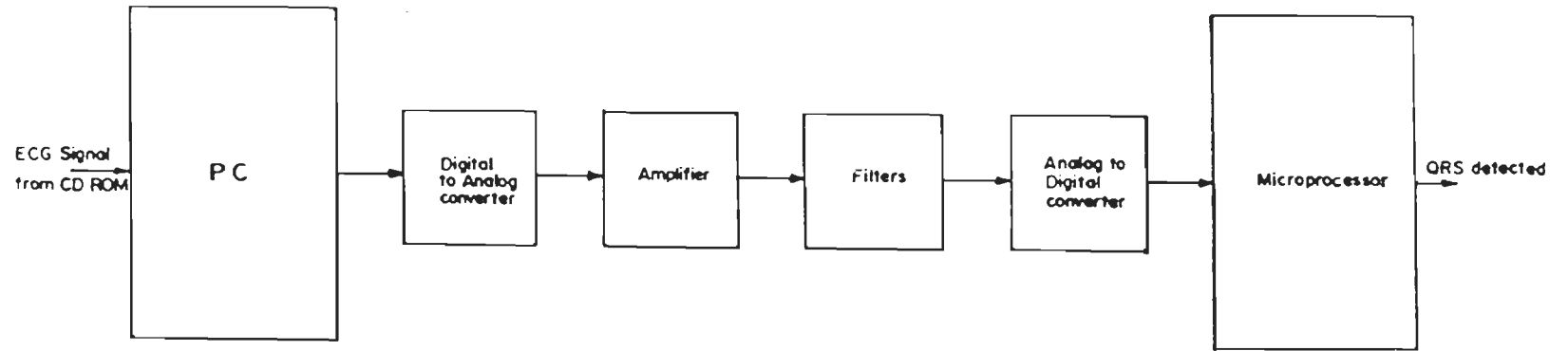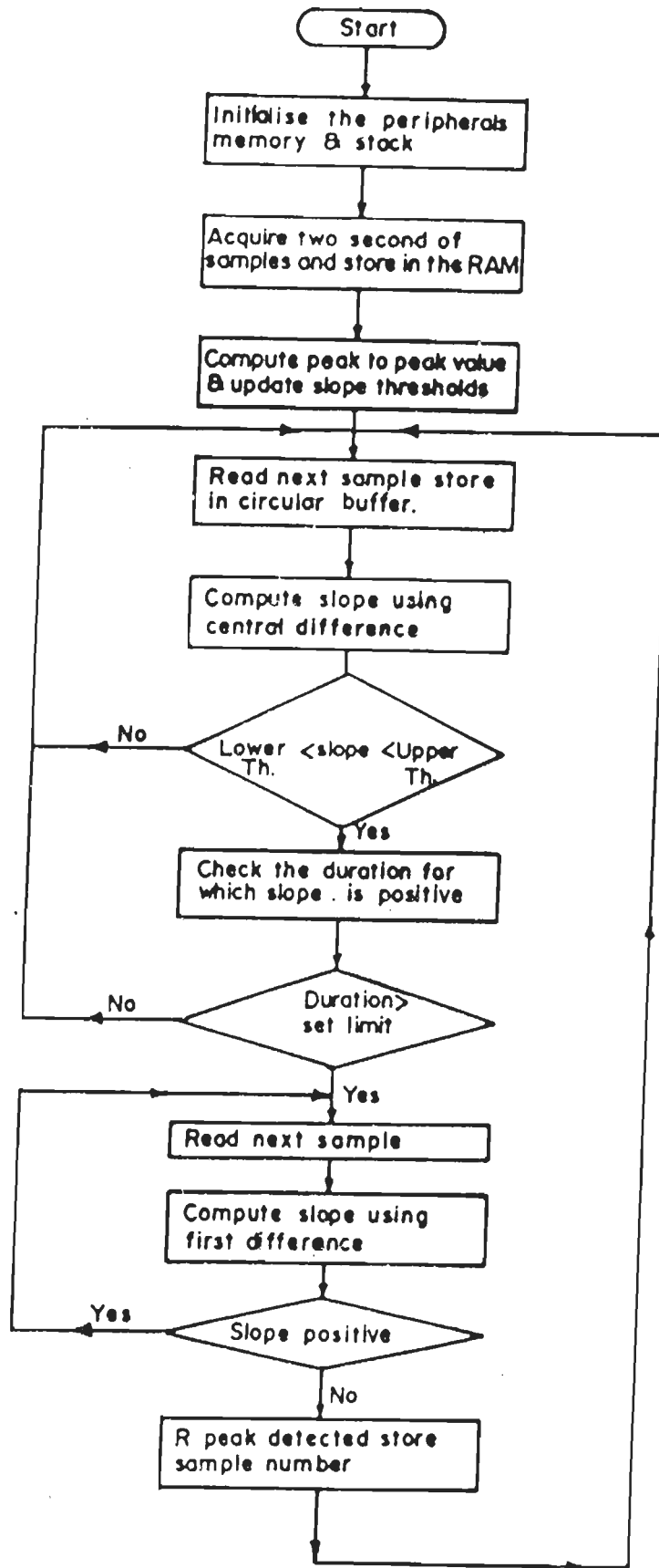
Fig.8.3 Block diagram of QRS detector

Fig. 8.4 Flow chart for QRS detection algorithm

Thereafter, the computation of slope starts using central difference technique. To reduce unnecessary processing the slope computation is initiated only after an upward deflection in the wave is detected. The computed slope is then compared with the upper and the lower limits and the decision is taken as to whether the samples lie on the R wave or otherwise. A buffer has been created for storing two previous samples at every sampling instant. When the computed slope falls within the set limits, a preliminary decision is taken that the samples might be lying on the R-wave. A deterministic decision is subsequently arrived at by checking the duration for which the positive slope continues. If the slope continues for more than a preset duration, it is confirmed that the samples currently acquired are on the R-wave. Computations of the slope continues until the R peak is identified as the point at which the slope changes from positive to negative .Sample number corresponding to this R peak is stored in RAM for further analysis

8.5   Algorithm for Arrhythmia Interpretation

For arrhythmia interpretation decision logic approach has been used in the present work based on RR interval and average of eight RR intervals. This approach is selected because of the fact that it is easy to implement on microprocessor, and its high computational efficiency. The arrhythmias that have been selected are identified primarily using RR interval and rhythm information the detailed discussion on interpretation of arrhythmias are presented in chapter 5.

The flow chart for the real-time implementation of the algorithm is given in Fig. 8.5. When power is switched on and the reset button is pressed the system enters into the main program. At initialization, the microprocessor clears the data buffer, sets the programmable timer to the proper sampling frequency and initializes software flags. After this Read-ADC subroutine is called to acquire ECG samples at a rate of 200 Hz. During the first two second of the ECG acquisition the samples are stored and searched for determining peak-to-peak amplitude of the signal for setting up of R wave slope threshold values. On the basis of these slope threshold the incoming
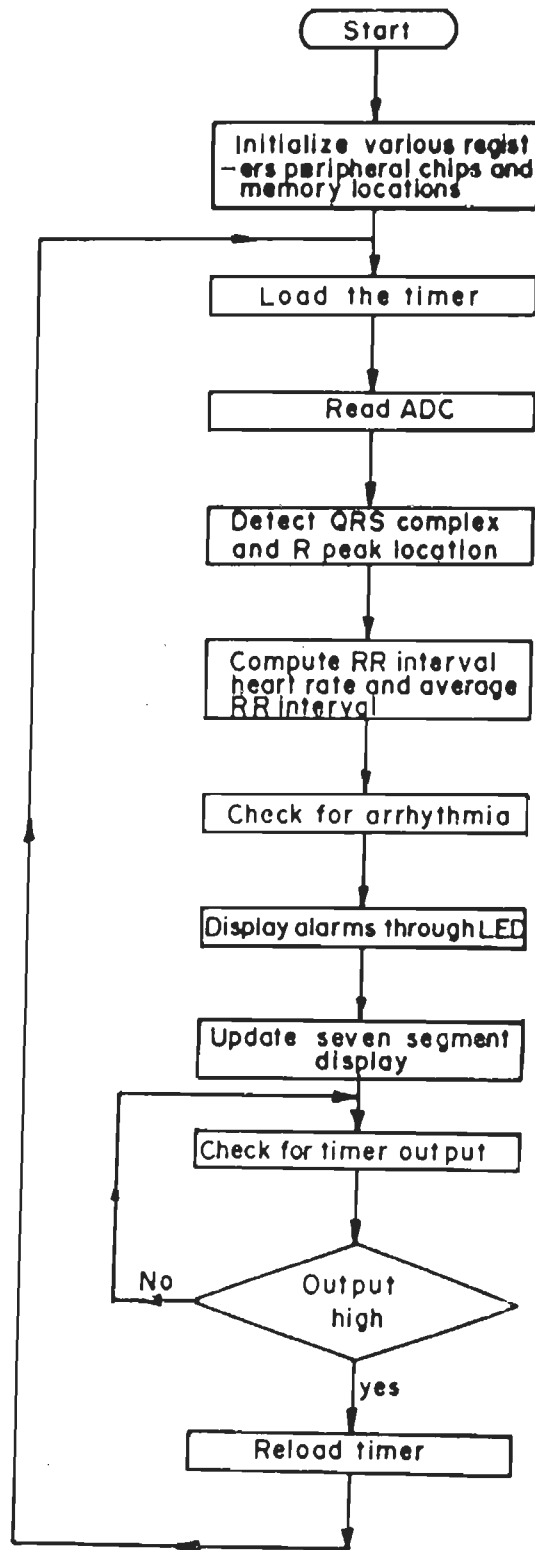
Fig. 8.5 Flow chart for arrhythmia
interpretation program.

samples are processed for identifying the QRS complex in each cardiac cycle. QRS complex is detected using slope threshold criteria. After this R peak is located, for time reference. R peak location is then used for computing RR interval and when two R peaks are located in succession completion of one cardiac cycle is considered. Some of the arrhythmias can be identified on the basis of heart rate alone. So when RR interval is computed, it is then compared with upper and lower limits and decision is arrived at on the basis of the heart rate falling below the lower limit and rising above the upper limit. These conditions are indicated using LED display provided on the front panel of the monitor. The algorithm for QRS detection is given in section 8.4. In this program it has been used as subprocedure.

8.5.1 Heart Rate Subroutine [Fig.8.6]

A counter which is incremented every time a sample is gathered when read between two R peak location gives the count of samples corresponding to the RR interval. When multiplied by 5 ms, the intersample interval, the result is RR intervals in ms. Inverting the RR interval gives the instantaneous heart rate, which is then converted to represent it in terms of beats per minute. The consecutive values of instantaneous heart rate are compared with each other and the variation in their change is computed and converted into percentage values and stored in the memory. The values are said to follow a particular trend i.e. increasing difference or decreasing difference, when continue to do so over at least four beats. This trend information is indicative of sinus arrhythmia

8.5.2 Display and Indication Subroutine [Fig.8.7]

Average heart rate or instantaneous heart rate are displayed on a 7-segment LED displays using 16 digit display unit. The alarms which are indicated by visual flashings, independently for each type of condition. Fig. 8.7 shows display and indication subroutine which triggers alarms on bradycardia or tachycardia.
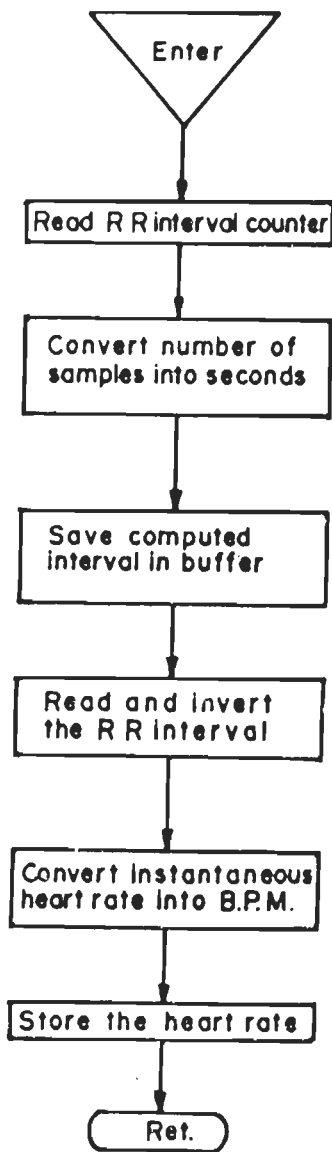
Fig. 8.6 Subroutine for R-R interval and
heart rate measurement
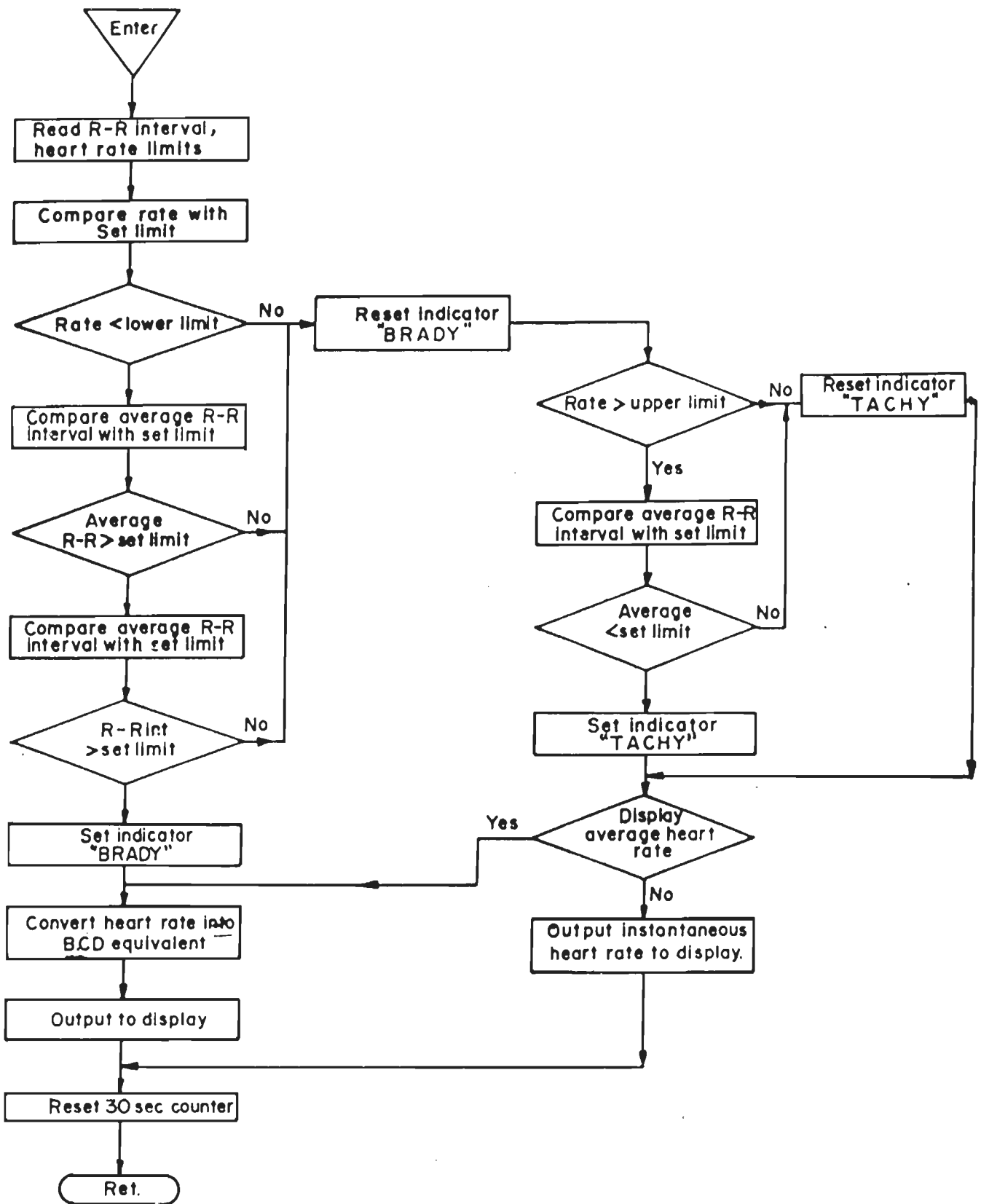
Fig. 8.7 Subroutine for display and indication (BRADY & TACHY)

8.6   Results and Discussion

The performance evaluation of all the four algorithms are presented in this section.

8.6.1   Simultaneous Three Channel Data Acquisition System

The amplifier AD524 was tested with a signal of 1mv and measured on a precision digital multimeter. The output was observed to be 1.98 V with a programmed gain of 1984. The input was varied over a range of 0.2mV to 2mV and the output variation was found to be fairly linear. The programmed gain depends on the resistance of the amplifier and therefore high precision high stability resistances have been used. The gain characteristic of the amplifier is shown in Fig. 8.8.

Each filter was supplied with a sinusoidal signal of 5V peak-to peak. The frequency range of the waveform was varied in the range of 0.1 to 600 Hz. Each filter response was measured individually. Finally the experiment was repeated with all filters arranged in cascade fashion. The combined filter response is shown in Fig. 8.9. The performance of the filter section closely matched the expected (Theoretical) response.

The analog-to-digital converter is a fast and precision device. The conversion time of the device is 24 μs, but to be on safer side the time delay to allow analog to digital conversion was kept at 40 μs. The ADC was tested on a signal varied from -5V to +5V to check the error. The maximum error was observed to be three LSB's.

The overall performance of the system was tested in a real-time environment. ECG signals of lead I,II,III were fed to three input channels . The following observations are made from the results which are presented in Fig. 8.10.
1.   All the three complexes, namely P, QRS and T are clearly visible.
2.   The powerline interference is completely eliminated
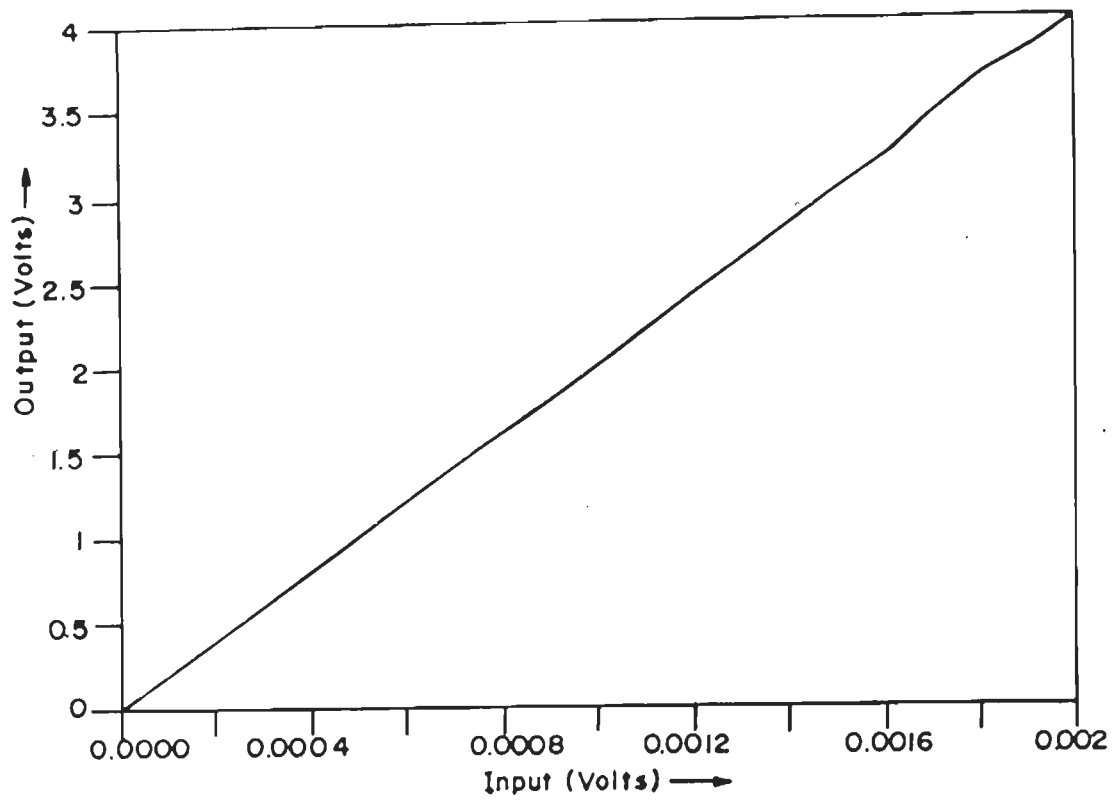
Fig.8.8 Amplifier response
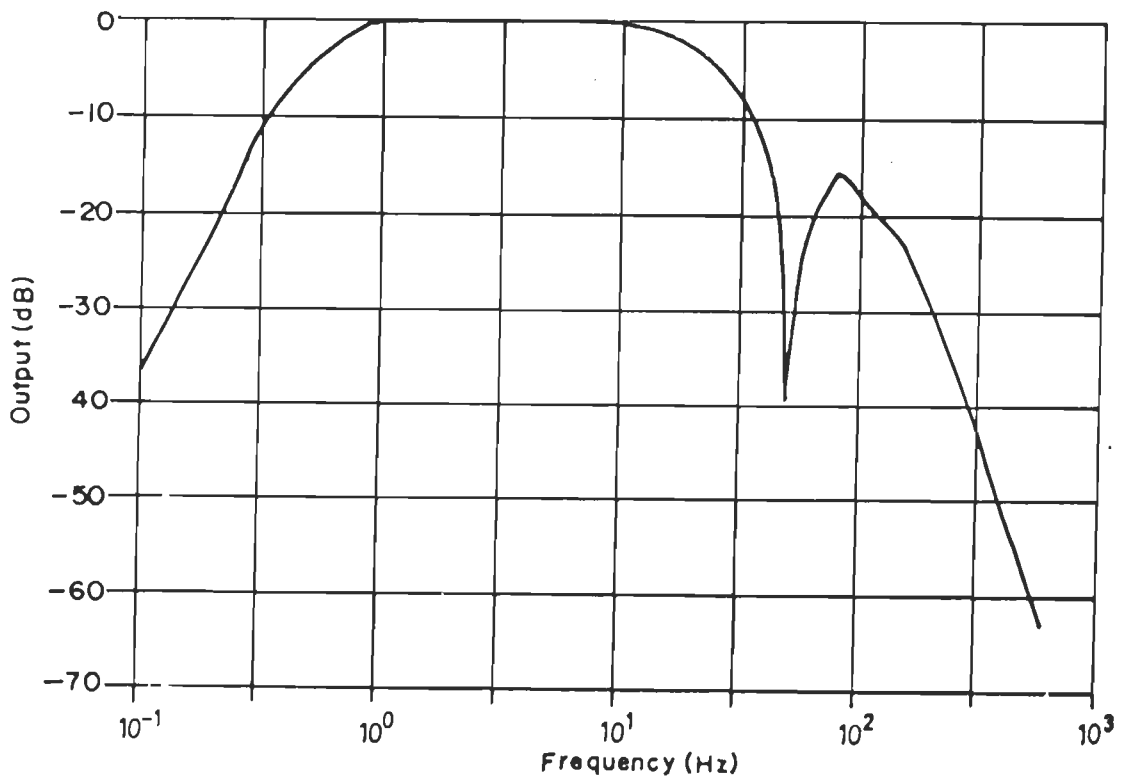
Fig.8.9 Combined filter response
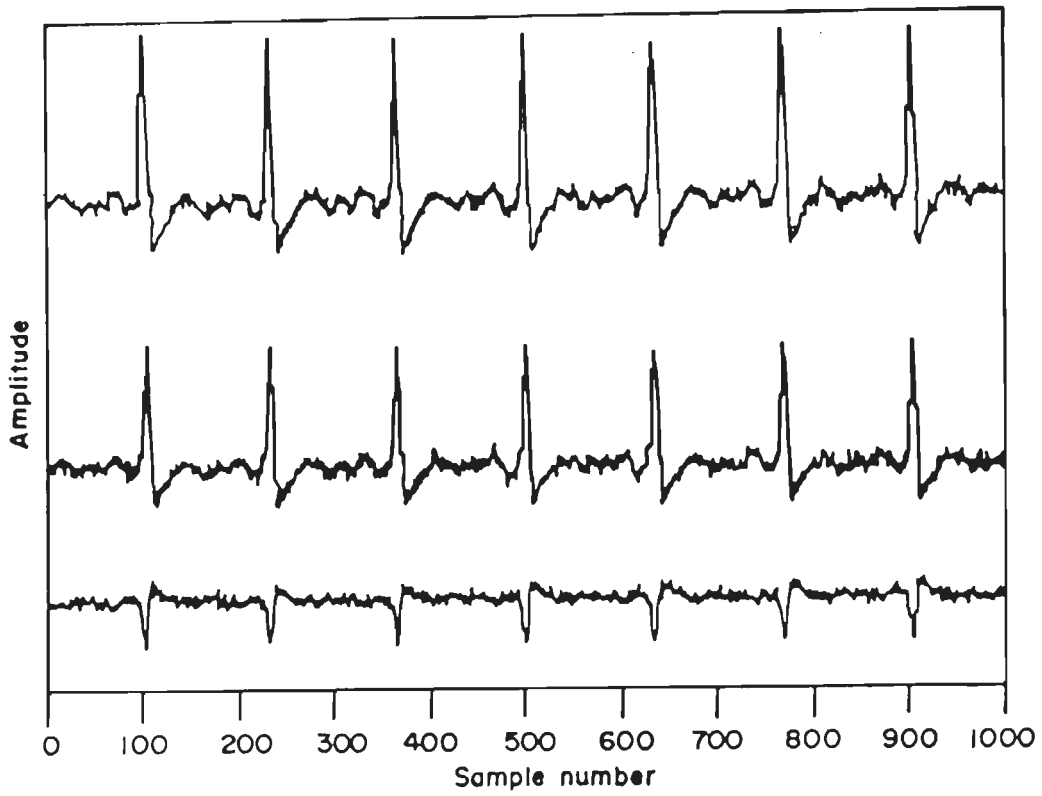
Fig.8.10 Simultaneous 3-channel output from the system obtained at 200Hz sampling frequency

3. High frequency noise present in the signal is highly attenuated. Its peak -to-peak amplitude is less than 0.16 % of the peak-to-peak value of the signal.

4 Q and S waves are very clear which makes it easy to mark the ·QRS fiducials.

5 Motion artifacts are very smooth. These can be reduced further by proper skin preparation and placement of electrodes.

8.6.2   Data Compression

Real time test results obtained by turning point-technique are quite similar to those given in section 6.4.1.

8.6.3   QRS Detector Performance

The performance of the QRS detector has been tested using channel 1 of the two channels ECG signal in the MIT/BIH Arrhythmia database .Table 8.1 present the summary of results in terms of false positives (FP's), and false negatives (FN's) and total detection failures. The algorithm produced 396 false positive beats and 293 false negative beats and a total failure of 0.67. The detector has a positive predictivity of 99.6% and a sensitivity of 99.71%.

The detector performance has been compared with the annotated results given in the MIT/BIH arrhythmia database. Some of the tapes in the database pose problems in identifying QRS complex because of presence of very high noise or long episodes of flutters and fibrillations, baseline wander and other artifacts. Record number 102 contains more number of paced beats which leads to a higher percentage of detection failures. Record number 200 and 232 have some non QRS complexes with unusual morphologies. This results in large percentage of failures on these records. Some other records, namely 116, 117, 205, 211, 220 and 230, contain more noise , therefore percentage failures is high on these records.

Table 8.1 Summary of Results for QRS detector tested on the MIT/BIH Arrhythmia Database

Tape Number	Total Beats	False detection		Total failures	
		FP Beats	FN Beats	Beats	Percentage
100	2273	1	1	2	0.08
101	1865	3	4	7	0.37
102	2187	13	10	23	1.05
103	2084	0	0	0	0.00
104	2230	11	10	21	0.94
105	2572	1	0	1	0.03
106	2027	13	8	21	0.64
107	2137	5	8	13	0.60
109	2532	4	2	6	0.23
111	2124	8	6	14	0.66
112	2539	2	5	7	0.27
113	1795	0	2	2	0.11
115	1953	3	5	8	0.40
116	2412	14	12	26	1.07
117	1537	30	26	56	3.06
118	2288	1	0	1	0.04
119	1987	0	0	0	0.00
121	1863	0	0	0	0.00
122	2476	0	0	0	0.00
123	1518	6	4	10	0.65
124	1619	5	5	10	0.61
200	2601	36	10	46	1.76
201	2000	12	9	21	1.05
202	2136	2	8	10	0.46
203	2980	6	4	10	0.33
205	2656	27	25	52	1.95
208	2955	12	6	18	0.61
209	3004	14	16	30	0.99
210	2650	4	2	6	0.22
212	2748	2	3	5	0.18
213	3251	3	1	4	0.12
214	2261	3	2	5	0.22
215	3363	8	12	20	0.60
219	2287	20	8	28	1.22
220	2048	12	9	21	1.02
221	2427	6	3	9	0.37
222	2483	7	4	11	0.44
223	2605	17	6	23	0.88
228	2053	11	10	21	1.02
230	2256	18	12	30	1.33
231	1573	7	8	15	0.95
232	1780	40	25	65	3.65
233	3079	8	2	10	0.32
234	2753	1	0	1	0.03
Totals	101965	396	293	689	0 67

(1) Positive pridictivity = $\dfrac{\text{True Positive}}{\text{True Positive} + \text{False Positive}} \times 100 = \dfrac{101965}{101965 + 396} \times 100 = 99.6\%$

(2) Sensitivity = $\dfrac{\text{True Positive}}{\text{True Positive} + \text{False Negative}} \times 100 = \dfrac{101965}{101965 + 293} \times 100 = 99.71\%$

It is difficult to compare the performance of different QRS detectors, as they are designed for different applications, though they may have been tested on the same database. A comparative statement is presented in Table 8.2 on the basis of the results reported in the literature.

The algorithm based on linear and nonlinear filtering methods requires 19 multiplications and 15 additions [51]. This leads to more computation time. The other algorithm presented by Hamilton et.al. is also based on the linear and nonlinear filtering but it is an improvement over the previous algorithm in the sense that it requires 17 multiplication and 11 additions [110]. These two algorithms have been implemented for on-line applications. A genetic algorithm reported recently requires 10 multiplication and 9 additions for processing one sample [113]. Among the five algorithm listed in Table 8.2 , the algorithm based on Wavelet transform has good results but it requires more computation time (0.4ms to process each sample), as it involves more complex mathematical calculations [81]. Hence it is not suited for real-time application. On the other hand, the algorithm presented here requires only 8 additions and it requires 7.2 μs to process each sample. Therefore the algorithm is computationally fast compared to the other algorithm.

8.6.4   Arrhythmia Interpretation

The performance evaluation of the algorithm has been carried out on the 12 sec. of ECG strips selected from the MIT/BIH Arrhythmia database. The test was carried out on 5 records. The diagnosis given by the proposed algorithm for the four diseases namely, Normal sinus rhythm, Sinus arrhythmia, Tachycardia and Bradycardia are found to be in conformity with standard results given in the MIT/BIH Arrhythmia database. The summary of results are given in Table 8.3.

8.7   Comments

The software developed for ambulatory monitor is written in assembly language and tested for their performance on the standard MIT/BIH database. From the results it is clear that the algorithms developed work satisfactorily for different tasks.

Table 8. 2 Comparative Statement

Sl..No	Authors	Application	computations/ time		sensitivity	positive pridictivity
			multiplication	addition		
1	Pan . et.al	real-time	19	15	99.76	99.56
2	Hamilton et.al	real-time	17	11	99.69	99.77
3	Li et al.	off-line	0.4 ms/sample		99.94	99.90
4	Pol i et.al	real-time	10	9	99.60	99.51
5	Present algorithm	real-time	- 7.2 μ sec	8	99.60	99.71

Table 8.3 Summary of Results for Arrhythmia Classification

Tape number	Total beats	Normal sinus rhythm	Sinus arrhythmia	Bradycardia	Tachycardia
100	16	14	-	-	-
101	12	9	-	-	-
103	14	-	12	-	-
214	14	6	-	-	2
232	6	-	-	-	6
Totals	58	29	12	6	2

CHAPTER - 9

CONCLUSION AND SCOPE FOR FUTURE DEVELOPMENT

CHAPTER - 9

CONCLUSION AND SCOPE FOR FUTURE DEVELOPMENT

The work was initiated with an objective of providing emergency medical care to cardiac patients away from the hospital. A portable instrument capable of real-time ECG rhythm analysis and potential to provide the physician with readily available, quantitative reports at low cost is proposed in the present work. The prototype instrument uses a general-purpose microprocessor with specialized peripherals, powered by batteries and package for use in ambulatory environment is developed. The techniques and algorithms have been developed for the elimination of powerline interference and baseline wander, wave recognition and characteristic point location, arrhythmia classification and data compression.

9.1 Conclusions

The following are the conclusions drawn from the work presented in the thesis.

1. The hardware developed for ambulatory monitor meets the performance of standards of the American Heart Association (AHA). The input channels are isolated from each other with least interference. The monitor is capable of recording three channels simultaneously. The selection of channels and sampling frequency are software controllable. The hardware filtering eliminate EMG, high frequency noise, powerline interference and baseline wander to a considerable extent. The hardware developed is completely software controllable.

2. In order to filter out noise from ECG signal alongwith baseline wander and powerline interference, hardware as well as digital filters are used. The use of digital filters yields a reduction in hardware and overcome the limitations of hardware filters. The filter making use of subtraction method is described here. The filter has been tested for powerline interference on the ECG recorded in the laboratory with

200 Hz sampling frequency. But for the removal of baseline wander, the developed algorithm has been tested for different sampling frequencies using different records of MIT/BIH database. The performance of the filter shows that it works satisfactorily over a range of 100 to 500 Hz sampling frequency by modifying the transfer function. The filter has been designed using a transfer function of the form $(1 \pm Z^{-n})$ and approximately cancelling all zeros at the frequency of interest. Further, the filter presented here has the advantage of having linear phase response and sharp notch characteristics. The results show that the signal distortion is minimum .

3. The proposed technique for ECG wave recognition and characteristic point location is simple, efficient and fast. It is based on the slope threshold approach. It allows the measurement of all peaks and intervals clinically interesting in ECG records with good accuracy . The developed algorithm has been tested on the standard MIT/BIH Arrhythmia database. Before this, the validation of the algorithm has been carried out on the 25 records of CSE database for which measurement and referee results are available and to cross check the same, manual measurements were also made. The results indicate that the detection of R peak found to be 99.6%, P peak detection is 65 % and T peak detection found to be 75 %. From the results, it is also clear that the onset and offset of P and T waves has not been detected accurately in few cases, when they are influenced seriously by noise or baseline drift or their amplitudes are too small. The interval values, wave amplitudes, patterns of P and T waves and their presence or absence, could be used as inputs to a system that allows automatic diagnosis from ECG analysis.

4. For arrhythmia interpretation the diseases considered in the present work are those for which diagnostic rules have been clearly defined. In case of some other diseases these rules are ambiguous and therefore difficult to implement them using computer. The interval information has been used for classifying arrhythmia.An algorithm for this is developed.In this, six step procedure is followed which takes into account RR interval, PR interval, P-duration, PP interval, QRS

duration and rhythm for interpretation of arrhythmia. The algorithm has been tested on 20 records of each 12 sec.strip of the MIT/BIH arrhythmia database the results obtained by the algorithm are in conformity with the diagnosis made in the MIT/BIH Arrhythmia database.

5. Many direct data compression algorithms have been developed with an aim to use one of the algorithm for real-time implementation. The DDC techniques have been tested on the standard MIT/BIH and CSE database in terms of compression ratio, PRD, fidelity and clinical acceptability. The results show that compression ratio is 2 in case of turning point algorithm and for other methods compression ratio of 6.12 is achieved while preserving the clinical information. The effect of sampling frequency on DDC technique has also been studied. From the results it is evident that a sampling rate of 125 Hz is sufficient to store the diagnostic information in case of arrhythmia.

6. Off-line data compression algorithms have been developed for storing large amount of data recorded for the purpose of storage as database for future reference. Fast Fourier transform based on successive doubling principle is used for compressing the ECG signal. The scheme has been evaluated on 125 records belonging to the third data set of CSE database library and 25 records each of 20 second strip of MIT/BIH database. A compression ratio of 8 has been achieved while preserving the clinical information. Visual comparison reveals that the reconstructed signal contains negligible amount of noise, because of inherent smoothing by the algorithm. This inturn, reduce electromyographic (EMG) noise. The results presented here show that peak, boundary and interval measurements confirms the clinical acceptability of the compression scheme, given that the results are within the acceptable tolerance.

7. Another method for off-line ECG data compression based on successive doubling method has been presented. The performance of the algorithm has been tested on 125 records of third data set of CSE database library and 25 records of 20 second strip from the MIT/BIH database. A compression ratio of 4 has been obtained while retaining the clinically important information. Peak, boundary and interval

measurements confirm the clinical acceptability because, the results are within the tolerance limits. Smoothing of the signal is required to remove the high frequency noise and make the signal suitable for visual examination. This also removes the electromygraphic (EMG) noise present in the signal.

8. The software for simultaneous three channel data acquisition algorithms is written in assembly language of Intel 8088 for its real-time implementation. The performance of each stage that is amplifier, filters and multiplexer have been tested individually. The overall performance of the system was tested in real-time on different subjects. ECG signal recorded by placing electrodes on different locations of the body and connecting these electrodes to three input channels in bipolar standard limb lead configuration.The fidelity of the ECG signal obtained from data acquisition module is high therefore, the data can be used for analysis and disease classification straightway.

9. The algorithm for on-line ECG data compression using turning point technique gave results similar to those presented in section 6.4.1.

10. The QRS detector used for off-line analysis has been used for real-time application because it is simple to implement on microprocessor. It is based on slope threshold criterion. The algorithm uses integer arithmetic which makes it suitable for real-time implementation on microprocessor without the use of co-processor. The added advantage of this technique is that, it is immune to baseline wander, AC & DC drifts and amplitude variation in the ECG signal. It clearly discriminates between R wave and other components of ECG and noise. False positives and false negatives are minimized by adaptively updating slope thresholds based on the sliding average of actual R wave amplitude. Wide morphological changes in the ECG are handled without manual intervention. The error in identifying the position of R wave peak being very small (±5 ms), hence the diagnostic decision made on the basis of RR interval will be very reliable.

11.   The algorithm for classification of arrhythmia for real-time implementation has been developed on the basis of RR interval. Three diseases have been considered here namely, Normal Sinus rhythm, Sinus arrhythmia, Tachycardia and Bradycardia. The algorithm identified the diseases accurately considered in the present work for on-line classification. The performance was evaluated on a beat-by-beat basis, each beat is individually examined and compared against the results available in the MIT/BIH arrhythmia database. The results of the system are in good agreement with those reported in the data base.

Despite the proposed system classify only few arrhythmias on-line and other complex arrhythmia classification is done off-line. The implementation of a low cost system with these features would make ambulatory monitoring considerably more attractive as standard clinical practice.

9.2   Scope for Future Development

In the present work, ambulatory ECG monitor has been developed and tested successfully for the interpretation of arrhythmias. The facilities provided in the ambulatory monitor hardware are not fully used and the effectiveness of the software has to be improved further. Hence, there exists a scope for the improvements at various levels of the algorithms some of those are as follows.

(a)   The peak boundary, and characteristic point algorithm needs further improvement specially in case of detecting P wave and its onsets and offsets. This is very much essential because of the fact that majority of atrial arrhythmias are classified on the basis of P wave information.

(b)   In the present work only few arrhythmias are considered for classification,whose diagnostic rules are clearly defined. More number of diseases are to be added in the classification program so as to make it a general program for arrhythmia classification.

(c)   Only single lead information is used for classifying arrhythmia in the

present application. However, use of simultaneous three channel analysis significantly improves the sensitivity of the diagnosis by gathering more clinical information.

(d)   Implementation of complex algorithms such as Wavelet transform, Fuzzy set theory using microprocessor becomes difficult. Therefore use of digital signal processing chip allows easy implementation of these algorithms, which also increases the speed of the system.

(e)   On-line arrhythmia analysis is carried out in the present work using only RR interval and its rhythm QRS duration, PP and PR intervals should be added in the classification program so that classification of arrhythmias can be made more accurately.

(f)   A real-time ECG data can be transmitted to the hospital through MODEMS using RS232C serial port interface. This helps in getting experts opinion and future course of action can be given to paramedical staff, to provide necessary preliminary resuciation to the patient.

REFERENCES

REFERENCES

1. Abboud, S. and Sadeh, D.,
    "The waveforms alignment procedure in the averaging process for external recording of the His bundle activity", Comput. Biomed, Res., 15, pp. 212-219, 1982

2. Abenstein, J.P. and Tompkins. W.J.,
    "A new-data reduction algorithm for realtime ECG analysis", IEEE Transactions on Biomedical Engineering, , 29, pp. 43-48, 1982.

3. Ahlstrom, M.L. and Tompkins. W.J.,
    "Automated high speed analysis of Holter tapes with microcomputers", IEEE Transactions on Biomedical Engineering ,30, pp. 651-657, 1983.

4. Ahlstrom, M.L and Tompkins, W.J.,
    "Digital filters for real-time ECG signal processing using microprocessors", IEEE Transactions on Biomedical Engineering, 32, pp. 708-713, 1985.

5. Ahmed. N., Milne, P. and Harris. S.,
    "Electrocardiographic data compression via orthogonal transforms", IEEE Transactions on Biomedical Engineering , 22, pp. 484-487, 1975.

6. Akazawa. K., Uchiyama. T., Tanka, S., Sasamori. A., Harasawa. E.,
    " Adaptive data compression of ambulatory ECG using multi templates", Computers in Cardiology (Los Alamitos California U.S.A. IEEE, Computer society press), pp. 495-498, 1993.

7.   Akazawa. K., Motoda. K., Sasamori, A., Ishizawa. T., Harasawa, E., "Adaptive threshold QRS detection algorithm for ambulatory ECG". Computers in Cardiology (Los Alamitos California U.S.A. IEEE, Computer society press), pp.. 445-448, 1992.

8.   Akseriod, S., Norymberg, Peled. I, Karabelink. E. and Green. M.S., "Computerised analysis of ST segment changes in ambulatory electrocardiograms", Med. Biol. Eng. and Comput. Vol. 25, pp. 513-519, 1987.

9.   Amazeen, P.G., Moruzzi, R.L and Feldmann, C.L., " Phase detection of R- waves in noisy electrocardiograms", Ibid, Biomedical Engineering ,19, pp. 63-66, 1972.

10.   Analog Devices " Data Conversion Product Data Book". 1988.

11.   Anant. K., Dowla. F. and Rodrigue. G., "Vector Quantization of ECG Wavelet coefficients", IEEE Signal processing letters 2, pp. 129-131, 1995.

12.   Babskoy, E.H., Khodoror, B.I., Kositsky and Zubkov. A.A., "Human Physiology" Mir Publishers, 1970.

13.   Barbaro, V., Bartolini, P., Bolle, G., Ialongo, D., and Marielti. P., "Experience for recording electrical activity from His bundle by non-invasive method", Innov. Tech. Biol Med.,4, pp. 103-112, 1983.

14.   Bartoli, F., Cerutti, S. and Gatti. E., "Digital filtering and regression algorithms for an accurate detection of the baseline in ECG signals", Med. Inform., 8, pp. 71-82, 1983.

15. Barry. B.B.,

     "The Intel microprocessors 8086/8088, 8086, 80286, 80386 and 80486, Architecturs, Programming and Interfacing", Third Edition, Prentice Hall.

16. Bessette, F., Nguyen. L.,

     "Automated electrocardigram analysis: the state of the art", Med. Inform; 14, pp. 43-51, 1989.

17. Blazek, Z. and Janecek. J.,

     "Low cost micro-controller driven ECG", Journal of Microcomputer applications 17, pp. 311-315, 1994.

18. Bolton M.P. and Coleman. J.D.,

     "Detection of QRS complexes in ECG Signals and evaluation of instantaneous- heart rate. Proc. changes in Health Care Instrumentation due to microprocessor technology", pp. 249-256, Princiroli, p. and Anderson, J.(Eds) North Holland Pub. Co. Amsterdam, 1983.

19. Bradon, C.W. and Brody. D.A.,

     "A hardware trigger for temporal indexing of the electrocardiographic signal", Comput. Biomed. Res., 3, pp. 47-57, 1970.

20. Bradie. B.,

     "Wavelet packet based compression of single lead ECG", IEEE Transactions on Biomedical Engineering ,43, pp. 493-501, 1996.

21. Cameran, J.R. and Skofronick

     "Medical physics" A willey - Science publications.

22. Cashman, P.M.M.,

     "The use of R-R interval and difference histograms in classifying disorders of sinus rhythm", Journal of Medical Engg. and Technology, pp. 20-28, 1977.

23. Chen. J., Itoh, S. and Hashimato. T.,
"ECG data compression using Wavelet transform", IEICE Transactions on Information and Systems E76D, pp. 1454-1461, 1993.

24. Clark, K.W., Hitchens. R.E., Ritter, J.A., Rankin, S.L., Oliver, G.C., and Thomas L.J.,
ARGUS/2H : "A dual channel Holter tape analysis system" Computers in Cardiology (Los Alamitos California U.S.A. IEEE, Computer society press), pp.. 191-198, 1977.

25. Cohen. A., Poluta, P.M. and Scott- Millar. R.,
"Compression of ECG signals using vector quantization", In Proc. IEEE-90 S.A. Symp. Commun. Signal processing COMSIG-90, Johannesburg, South Africa.pp. 45-54, 1990.

26. Comerchero, H., Miller, A. and Ben Dzi, D.,
ARGUS/sentinel: "A computer assisted system for arrhythmia monitoring", Taylor & Francis Ltd., London, Medical data processing, pp. 684-695, 1976.

27. Cox, J.R., Nolle, F. M., Fozzard, H.A. and Oliver, G.C., "AZTEC a preprocessing programme for real-time ECG rhythm analysis", IEEE Biomedical Engineering, 15, pp.128-129, 1968.

28. Cox. J.R. Nolle, F.M. and Arthur, R.M.,
"Digital analysis of the electroencephalogram, the blood pressure and the electrocardiogram proc. IEEE, Vol. 60, pp. 1137-1164, 1972.

29. Craelius, W., Restivo M., Assadi - M.A. and EL-Sherif. N.,
"Criteria for optimial averaging of cardiac signals", IEEE Transactions on Biomedical Engineering ,33, pp. 957-966, 1983.

30. Craig. D. L.,

"Microprocessor heart rate histogram recorder for ambulatory monitoring of daily physical activity", Med. & Biol. Eng. & Comput, Vol.19, pp. 367-369, 1981.

31. Cromwell. L., Weibell. F.J. and Pfieffer. E.A.,

"Biomedical Instrumentation and Measurments", Second Edition, Prentice Hall, 1995.

32. De-maso, J., Myers. S., Sellers. C.,

"Disk-based high resolution ECG recorder for ambulatory monitoring", Computers in Cardiology (Los Alamitos California U.S.A. IEEE, Computer society press), pp.435-438, 1992.

33. Denniss, A.R., Richards, D. A., Farrow, R.H., Davison. A., Ross, D.L. and Uther, J.B.,

"Technique for maximizing the frequency response of the signal averaged Frank vector cardiogram", Journal of Biomed. Eng., 8, pp. 207-212, 1986.

34. Degani. R. and Bortolan, G.,

"Methodology of ECG interpretation in the Padova program", Meth. Information, Med. 29, pp. 386-392, 1990.

35. Fancott, T. and Wong, D.H.,

"A minicomputer system for direct high-speed analysis of cardiac arrhythmia in 24 hour ambulatory ECG tape recordings", IEEE Transactions on Biomedical Engineering, 27, pp. 685-693, 1980.

36. Feldman, C.L. and Hubelbank, M.,

"Cardiovascular monitoring in the coronary care unit", Med. Instrum., 11, pp. 288-292, 1977.

37. Ferrara, E. R. and Widrow, B.,
    "Fetal electrocardiogram enhancement by time sequenced adaptive filtering", IEEE Transactions on Biomedical Engineering, 29, pp. 458-460, 1982.

38. Fraden, J. and Neuman, M.R.,
    "QRS Wave detection",Med. & Biol.s Engg. & Comput.Vol. 18, pp. 125-132, 1980.

39. Friesen, G. M., Jannett. T.C., Jadallah, M.F., Yates, S.L., Quint, S.R., Nagle, H.T.,
    "A Comparision of the Noise sensitivity of Nine QRS detection algorithm", IEEE Transactions on Biomedical Engineering, 17, pp. 85-98, 1990.

40. Friedmen, H.
    "Diagnostic electrocardiography and vector cardiography". McGraw Hill, 1971.

41. Furht, B., and Perez. A.,
    "An adaptive real-time ECG compression algorithm with variable threshold", IEEE Transactions on Biomedical Engineering,35, pp. 489-494, 1988.

42. Furno, G.S., Tompkins, W.J.,
    "A learning filter for removing noise interference IEEE Transactions on Biomedical Engineering ,30 pp. 233-235,1983

43. Geddes. L.A. and Baker L.E.,
    "Principles of Applied Biomedical Instrumentation", John Willey and Sons Inc., New York, London,1968

44. Goldmann, M.J.,
    "Principles of Electrocardiography"Medical Publications, 1986.

45.   Gonzalez, R.C. and Paul Wintz.,
        "Digital Image Processing", Second (Addition) Edition Addison
        Wesely, pp. 102-115, 1987.

46.   Goovaerts, H.G., Ros, H.H., Akker, T.J. and Schneider, H.,
        "A digital QRS detector based on the principle of contour limit-
        ing", IEEE Transactions on Biomedical Engineering,23, pp. 154-
        160, 1976.

47.   Gritzali, R.,
        "Towards a generalized scheme for QRS detection in ECG wave
        forms", Signal processing, Vol. 15, pp. 183-192, 1982.

48.   Hall, D.V.,
        "Microprocessors and Interfacing, Programming and Hardware",
        Tata McGraw Hill, Reprint, 1992.

49.   Ham, F. M. and Han, S.,
        "Classification of Cardiac arrhythmias using FUZZY ARTMAP".
        IEEE Transactions on Biomedical Engineering, ,43, No. 4, pp.
        425-430, 1996.

50.   Hamilton, D.J., Thomson, D.C. and Sandham, W.A.,
        "ANN compression of morphologically similar ECG complexes",
        Med. Biol .Eng. & Comput. Vol. 33, pp. 841-843, 1995.

51.   Hamilton, P.S., Tompkins, W.J.,
        "Quantitative Investigation of QRS detection rules using the MIT/
        BIH Arrhythmia data base", IEEE Transactions on Biomedical
        Engineering, 33, 1157-1165, 1986.

52.   Hamilton, P.S.,
        "A Comparision of algorithms for ambulatory ECG compressor
        with fixed average data rate", Computers in Cardiology (Los
        Alamitos California U.S.A. IEEE, Computer society press), pp.
        683-686, 1992.

53. Hann, K.L.,
"Firmware for a patient monitoring station", Hewlett - packard, J., 31(11), pp. 23-28, 1980.

54. Hilton M.L.
"Wavelet and Wavelet packet compression of Electrocardiography", IEEE Transactions on Biomedical Engineering, 44, pp. 394-402, 1997.

55. Holsinger, W.P., Kempner, K.M. and Miller, M.H.,
"A QRS preprocessor based on digital differentiation" IEEE Transactions on Biomedical Engineering, 18, pp. 212-217, 1971.

56. Holter, N.J.,
"New methods for heart studies:continuous electrocardiography of active subjects", Science, Vol. 134, pp. 1214-1220, 1961.

57. Hung, T.L. William, C., Armand, M.M., Pottala, E.W. and Bailey, J. J.,
"Automated analysis of Rodent three channel ECG and VCGS", IEEE Transactions on Biomedical Engineering, 32, pp. 43-50, 1985.

58. Hurtes. J.W. and Myerburg, R.J.,
"Introduction to Electrocardiography"

59. Huhta. J.C., Webster, J.G.,
"Interference in bio-potential recordings in Biomedical Electrode Technology", Theory and Practice (Editions: New York Academic) pp. 129-142, 1974.

60. Huhta, J.C. and Webster J.G.,
"60 Hz Interference in Electrocardiography", IEEE Transactions on Biomedical Engineering, 20, pp. 91-101, 1973.

61. Intel 8086/8088 "User's manual Programmer's and Hardware Reference; U.S.A.,1989.

62. Intel "Microprocessor and Peripheral Hand Book, 1990.

63. Intel "Microprocessor", 1990

64. Ishijima, M., Shin, S., Hostetter, G.H. and Sklansky, J.,
    "Scan-along polygonal approximation for data compression of electrocardiograms", IEEE Transactins on Biomedical Engineering, 30, pp.723-729, 1983.

65. Jager. F.,Jaklic.A.,Koren.I,Gyergyek.L.,
    "A real-time personal computer based system for analysis of electrocardigrams",Computers in Cardiology (Los Alamitos California U.S.A. IEEE, Computer society press), pp. 497-500, 1989.

66. Jalaleddine, S.M.S., Hutchens, C.G., Strattan, R.D.,and Coberly.,W.A,
    "ECG data compression techniques- a unified approach", IEEE Transactions on Biomedical Engineering,37, pp. 329-342, 1990.

67. Jane, R., Olmas, S., Languna, P. and Caminal, P.,
    "Adaptive Hermite models for ECG data compression : Performance and evaluation with automatic wave detection",Computers in Cardiology (Los Alamitos California U.S.A. IEEE, Computer society press), pp. 389-392, 1993.

68. Kathileen, D.A. and Lange.,
    "Intensive coronary care a mannual for nurses" Fifth Edition, Prentice Hall, International (U.K.) Ltd., London, 1995.

69. Kempner, K.M.,
    "The continuous monitoring of cardiac arrhythmias" Proceeding of the 1976 IEEE National Conf. on Cybernetics and Society, pp. 214-218, 1976.

70. Klein, M.D., Feldman, C.L., Clark, A.P., Fessas, D.L., Ryan, T.J., and Perira, R.A.,
"Vectorial characteristic of ventricular extraseptoles stimulated during cardiac catheterization". Journal of Electrocardiography, 9, pp. 103-107, 1976.

71. Krishna Kant,
"Microprocessor Based Data Acquisition System Design", Tata McGraw Hill publishing Company Ltd., New Delhi, 1987.

72. Kuklinski, W.S.,
"Fast Walsh transform data compression algorithm: e.c.g. applications", Med. & Biol. Eng.and Comput., Vol.21, pp. 465-472, 1983.

73. Kulkarni, P.K., Vinod Kumar, Verma, H.K.,
"ECG data compression using fast walsh transforms and its clinical acceptability", Int. Journal of Systems Science, Vol. 28, No.8, Aug. '97.

74. Kulkarni, P.K., Vinod Kumar, Verma, H.K.,
"Direct Data Compression Techniques : compression ratio and PRD studies", National Systems Science Conference, pp. 546-550, 1995.

75. Kulkarni, P.K., Vinod Kumar, Verma, H.K.,
"Direct data compression techniques for ECG signals: Effect of sampling frequency on performance", Int. Journal of System Science, Vol. 28, No. 8, pp. 217-228, 1997.

76. Kulkarni, P.K., Vinod Kumar, Verma, H.K.,
"Diagnostic Acceptability of FFT-based ECG data compression", Journal of Medical Engg. and Technology, 1997.

77. Kyrkos, A., Giakoumakis, E.A., Carayannis, G.,
"QRS detection through time recursive prediction techniques"
Journal of Signal processing, Vol-15, pp. 429-436, 1988.

78. Laguna, P., Vigo, D., Jane, R., Caminal, P.,
"Automatic wave onset and offset determination in ECG signals validation with CSE database", Computers in Cardiology (Los Alamitos California U.S.A. IEEE, Computer society press), pp. 167-170, 1992.

79. Laguna, P., Thakor, N.V., Caminal, P., Jane, R., Hyung - Ro Yoon
" New algorithm for QT interval analysis in 24-hour Holter ECG", performance and applications Med.& Biol. Eng.& Comput. Vol. 28, pp. 67-73, 1990.

80. LeBlanc, A.P. and Roberge, F.A.,
"Present state of arrhythmia analysis by computer", C.M.A.J. pp. 1239-1251, 1973.

81. Li, C., Chong xun, Z. and Changfeng Tai,
"Detection of ECG characteristic points using wavelet transforms", IEEE Transactions on Biomedical Engineering, 42, pp. 21-28, 1995.

82. Lindecrantz, K.G. and Lilja, H.,
"New software QRS detector algorithm suitable for real-time applications with low signal to noise ratios", Ibid, 10, pp. 280-284, 1988.

83. Lenk J.D.,
"Handbook of integrated circuits for Engineers and Technicians", Reston publication company, Virginia, pp. 170-171, 1978.

84. Liu, Y., Gibson.,
"Microcomputer systems; The 8086/8088 family", Prentice Hall India, 1991.

85.   Lux, R.L., Smith, C.R., Wyatt, R.F. and Abildskov, J.A.,
      "Limited lead selection for estimation of body surface potential maps in electrocardiography", IEEE Transactions on Biomedical Engineering, 25, pp. 270-276, 1978.

86.   Lynn, P.A.,
      "On-line digital filters for biological signals: some fast design for small a computer", Med.& Biol Eng. & Comput. Vol. 15, pp. 534-540, 1977.

87.   Lyon, L.L.,
      "Basic Electrocardiography Handbook", Van Nostrand Reinhold Company, 1977.

88.   MacFarlane, P.W., Peden, J., Lennox, G., Watts, M.P. and Lawrie, T.D.V.,
      "The Glasgow System: In Proceedings of trends in computer processed electrocardiograms", Van Bemmel J.H. and Willems. J. L. (Eds) Norths- Holland, pp. 143-150, 1977.

89.   Mahler, Y., Setton, A., and Rogel, S.,
      "Computerised dynamic three - dimensional joint interval histogram display for arrhythmia monitoring", Med. & Biol. Eng. & Comput. 20, pp. 129-133, 1982.

90.   Mahoudeaux, P.M. Moreau, C., and Moreau, D.,
      " A simple microprocessor based system for on-line ECG arrhythmia analysis", Med. & Biol. Eng. & Comput.19, pp. 497-500, 1981.

91.   Makivirta, A., Estola, K.P., Saramaki, T., Kalli, S. and Jarvinen, K.,
      "Exercise ECG preprocessor with a high performance digital filter" Proc. 14th Int. conf. Med. & Biol. Engg., ESPOO, Finland, 11th - 16th Aug., pp. 629-630, 1985.

92. Mammen, C.P. and Ramamurthy, B.,

   "Vector quantization of multichannel ECG", IEEE Transaction on Biomedical Engineering.,37, pp. 821-825, 1990.

93. Marques De Sa, J.P.,

   "Digital FIR filtering for removal of ECG baseline wander", Journal of Clinical Engineering Vol. 8, pp. 235-240, 1982.

94. Marriott, H.J.L.,

   "Practical electrocardiography" Sixth Edition, The Williams and Wilkins co. Batimore, 1978.

95. Meyer, C.R. and Keiser, H.N.,

   "Electrocardiogram baseline noise estimation and removal using cubic splines and state space computation", Comput. Biomed. Res., 10, pp. 450-479, 1977.

96. Milliman, J. Halkias,

   "Integrated Electronics",MH International Singapore Ltd., pp. 552-556, 1987.

97. Mohammad - Djafari, A., Heron, F, Deperdu, R. and Perrin, J.,

   "Non-invasive recording of the His- purkinje system: Electrical activity by a digital system design", Ibid., 3, pp. 147-152, 1981.

98. Moody, G. B.,

   "ECG Database Applications Guide", Harvard Univ. MIT, Div. Health Sci. Technol., database available on MIT/BIH data base distribution MIT Cambridge - M.A. 1992.

99. Moody, G.B. Kambiz, S. and Mark - R.G.,

   "ECG data compression for tapeless ambulatory monitors", Computers in Cardiology (Los Alamitos California U.S.A. IEEE, Computer society press), pp. 467-470, 1988.

100. Mortara, D.,

   "Digital filters for ECG signals" Computers in Cardiology (Los Alamitos California U.S.A. IEEE, Computer society press), pp. 511-514, 1978.

101. Mortara, D.,

   "Source consistency filtering ; A new tool for ECG noise reduction", Computers in Cardiology (Los Alamitos California U.S.A. IEEE, Computer society press), pp. 125-128, 1992.

102. Muller, W.C.

   "Arrhythmia detection software for an ambulatory ECG monitor", Biomedical Science and Instrumentation 14, pp. 81-85, 1978.

103. Murthy I.S.N. and Durgaprasad, B.,

   " Analysis of ECG from pole zero models", IEEE Transactions on Biomedical Engineering, 39, pp. 741-751, 1992.

104. Murthy I.S.N. and Niranjan, U.C.,

   "Component wave delineation of ECG by filtering in the Fourier domain", Med. & Biol. Eng. & Comput. 30, pp. 169-176, 1992.

105. Niranjan, U.C. and Murthy, I.S.N.,

   "ECG component delineation by Prony's method", Signal processing, 31, pp. 191-202, 1993.

106. Nygards, M.E. and Sornmo, L.,

   "Delineation of the QRS complex using the envelope of the ECG" Med. & Biol. Eng. & Comput. 21, pp. 538-547, 1983.

107. Okada, M.,

   "A digital filter for the QRS complex detection", IEEE Transactons on Biomedical Engineering, 26, pp. 700-703, 1979.

108 Oliver, G.C., Kleiger, R.E., Krone, R.J., Martin, T.F., Miller, J.P., Nolle, F.M. and Cox J.R. (Jr),

"Applications of high speed analysis of ambulatory electrocardiograms" Proc. Comput. Cardiol, pp. 43-54, 1974.

109. Pahlm, O., and Sornmo. L.,

"Software QRS detection in Ambulatory monitoring:a review Med. & Biol .Eng. & Comput. 22, pp. 289-297, 1984.

110. Pan. J. and Tompkins, W.J.,

"A real time QRS detector algorithm" IEEE Transactions on Biomedical Engineering, 32, pp. 230-236, 1985.

111. Pande, V.N., Verma, H.K. and Mukhopadhyaya, P.,

"Bedside ECG monitor using a microprocessor", Med. & Biol. Eng., & Comput. 23, pp. 487-492, 1985.

112 Plonsy, R., and Fleming, D.G.

"Bioelectric phenomena" McGraw Hill Book Company, 1969.

113. Poli, R., Cagnonis. S. and Valli, G.,

"Genetic design of optimum linear and non-linear QRS detectiors." IEEE Transactions on Biomedical Engineering, 42 pp. 1137-1141, 1995.

114. Reddy, B.R.S., and Murthy I.S.N.,

"ECG data compression using Fourier - descriptors" IEEE Transactions on Biomedical Engineering, 33, pp. 428-433, 1986.

115. Ripley, K.L and Murray, A.,

" Introduction to automated arrhythmia detection", IEEE comput. soc., Long Beach, Ca. 1980.

116. Risso, W.L., Kempner. K., Owen, D., Gorlen, K., Holsinger, W., Mc Lantosh. C. and Syed. D.,

   "A post surgical intensive care computer system at the national institute of health", Computers in Cardiol, pp. 101-108, 1975.

117. Rossi, R., Castelli, A., Bertinelli. M.,

   "Fast FIR filters for a stress test system", Computers in Cardiology (Los Alamitos California USA computer society press). pp. 129-132, 1992.

118. Rosenberg, N.W. and Tartakovsky, M.B.,

   The Telaviv System; "A three channel evaluation of long term ECG records for atrial and ventricular identification and verification of arrhythmias",Computers in Cardiology (Los Alamitos California U.S.A. IEEE, Computer society press), pp. 29-32, 1979.

119. Ruiz, R., Hernandez, C., Mira.J.,

   "Method for mapping cardiac arrhythmia in real time using microprocessor based systems", Med. & Biol. Eng. & Comput. 22, pp. 160-167, 1984.

120. Ruttiman, U.E. and Pipberger.

   "Compression of the ECG by prediction or interpolation and entropy encoding", IEEE Transactions on Biomedical Engineering, 26, pp. 613-623, 1979.

121. Sahambi, J.S., Tandon, S.N. and Bhatt, R.K.P.,

   " Using Wavelet transforms for ECG characterization", IEEE Engg. in Medicine and Biol. pp. 77-83, Jan./Feb. 1997.

122. Scherer, J.A. and Williams, J.L.,

   "Evaluation of the 12-lead ECG synthesis using analysis measurements in 240 patients", Computers in Cardiology (Los Alamitos california U.S.A. IEEE, Computer society press), pp.. 41-94, 1992.

123. Shanks J.L.,

      "Computation of Fast Walsh Fourier Transform", IEEE Transactions on Comput, pp. 457-459, 1967.

124. Short, K.L.,

      "Microprocessor and programming logic", Prentice Hall Inc., 1981.

125. Skordalakis',E.,

      "Syntactic ECG processing: A review pattern recognition", Vol. 19, No. 4, pp. 305-313, 1986.

126. Sornmo. L.,

      "Time varying digital filtering of ECG baseline wander" Med. & Biol Eng. and Comput. 31, pp. 503-508, 1993.

127. Sornmo., L, Pahlmo, O, Nygards, M.,

      "Adaptive QRS detection: A study performance" IEEE Transactions on Biomedical Engineering , 32, pp. 392-401, 1985.

128. Taddie, A., Niccolai, M., Emdin, M., Marchesi C.,

      ABACUS: " A knowledge based system for the interpretation of arrhythmias in long term ECG", Computers in Cardiology (Los Alamitos California U.S.A. IEEE, Computer society press), pp.. 887-890, 1993.

129. Talman, J.L.,

      "Algorithm for the detection of events in ECG computers and programs", Bio-medicine 22, pp. 149-161, 1986.

130. Thakor, N.V. and Webster J.G.,

      "Electrode studies for the long term ambulatory ECG", Med. & Biol. Eng. and Comput. 23, pp. 116-121, 1985.

131. Thakor, N.V. and Webster J.G., Tompkins, W.J.,
" Design, Implementation and Evaluation of a microcomputer based ambulatory arrhythmia monitor", Med. Biol. Engg. & Comput. Vol. 22, pp. 151-159, 1984.

132. Thakor, N.V.,
"From Holter monitors to automatic defibrillators:Developments in ambulatory arrhythmia monitoring", IEEE transactions on Biomedical Engineering, 31, pp. 770-778, 1984.

133. Thakor, N.V.,
"Reliable R-wave detection from ambulatory subjects", Biomedical Science Instrumentation, Vol. 14, pp. 67-72, 1978.

134. The CSE Working Party
"Recommendations for measurement standards in qualitative Elecrocardiography." European Heart Journal. pp 815-820, 1985.

135. Tompkins and Webster.,
"Design of micro-computer based medical instrumentation", (Engle wood cliff NJ: Prentice Hall) pp. 433-451, 1981.

136. Tompkins, W.J.,
"A portable microcomputer based system for biomedical applications", Biomed. Sci. Instrum., Vol. 14, pp. 61-66, 1978.

137. Tompkins, W.J.,
" Trends in ambulatory electrocardiography" IEEE   Frontiers of Eng. in Health Care, pp .1-4 ,1982.

138. Tompkins, W.J.,
"Patient worn intelligent arrhymthmia systems", IEEE Engg. in Medicine and Biology magazine, pp. 38-42, 1985.

139. Trahanias, P.E.
"An approach to QRS complex detection using morphology."
IEEE Transactions on Biomedical Engineering, 40 pp 201-205,
1993.

140. Trahanias,P.E.,Skordalakis.E.,
"Bottom up approach to the ECG pattern recognition problem",
Med. Biol. Engg and comput. 27, pp. 221-219,. 1989.

141. Uijen, G.J.H., Deweerd, J.P.C. and Vendrik, A.J.H.,
"Accuracy of QRS detection in relation to the analysis of high
frequency components in the electrocardiogram" Med. Biol. Eng
& Comput., 17, pp. 492-502, 1979.

142. Urrusti, J. and Tompkins, W.J.,
"Performance evaluation of an ECG QRS complex detection al-
gorithm", Computers in Cardiology (Los Alamitos California
U.S.A. IEEE, Computer society press), pp. 800-801, 1993.

143. Van Alste. J.A., Schilder, T.S.,
"Removal of baseline wander and powerline interface from the
ECG by as efficient FIR filter with a reduced number of
taps".IEEE Transactions on Biomedical Engineering, 32, pp. 1051-
1060, 1985.

144. Van Alste, J., Vaneck, W. and Herrman, O.E.,
"ECG baseline wander reduction using linear phase filters", Com-
puter Biomed, Res. 19, pp. 417-427, 1986.

145. Wajszczuk, W.J., Stopczyk, M,J., Moskowitz, M.S. Zochowski, R.J.
Bauld, T., Dabos, P.L. and Rubenfire, M.,
" Non invasive recording of His purkinje activity in man by QRS-
triggered signal averaging", Circ, 58, pp. 95-102, 1978.

146. Walters, J.B.
          "Microprocesor based ambulatory EKG monitor", Proc. Annual
          conf. Eng. Med. Biol. 18, pp. 255, 1976.

147. Walter A. T, and Avtar Singh
          "The 8088 and 8086 Microprocessor, programming, Interfacing,
          Software, Hardware and Applications", Prentice Hall of India,
          1995.

148. Wariar, R and Eswaran, C.,
          "Integer coefficient bandpass filter for the simulataneous removal
          of baseline wander, 50 and 100 Hz interfernce from the ECG"
          Medical & Biol. Eng. & comput. Vol. 29, pp. 333-336, 1991.

149. Webster, J.G.,
          "An intelligent monitor for ambulatory ECGs", Biomed Sci.
          Instrum, Vol. 14, pp. 55-60, 1978.

150. Wiesspeiner, G., and Xu, W.,
          "Multichannel ambulatory monitoring of circulation related
          biosignals", Computers in cardiology (Los Alamitos California
          USA IEEE computer society press), pp. 457-460, 1992.

151. Zywietz ,C., Grabble W and Hampel, G.,
          "HES LKG a new program for computer assisted analysis of Holter
          electrocardiograms" Computers in Cardiology (Los Alamitos,
          California USA IEEE computer society press) pp. 169-172, 1981.

152. Zywietz, C. and Cellkag, D.,
          "Testing results and derivation of minimum performance criteria
          for computerzied ECG anlaysis"Computers in Cardiology (Los
          Alamitos, California USA IEEE computer society press) ,pp. 97-
          100, 1992.

LIST OF PUBLICATIONS BY THE AUTHOR

LIST OF PUBLICATIONS BY THE AUTHOR

1. "Direct data compression techniques : compression ratio and PRD studies", National Systems Science Conference, pp. 546-550, 1995.

2. "Direct data compression techniques for ECG signals: Effect of sampling frequency on performance", International Journal of Systems Science, Vol. 28, No. 3, pp. 217-228, 1997.

3. "Diagnostic acceptability of FFT-based ECG data compression", accepted for publication in the Journal of Medical Engg. and Technology, 1997.

4. "ECG data compression using fast Walsh transforms and its clinical acceptability", International Journal of Systems Science, Vol. 28, No.8, Aug. '1997.

5. "Removal of powerline interference and baseline wander using real-time digital filter", Proceedings of the International Conference on Computer Applications in Electrical Engg. Recent-Advances, pp.20-25, September 1997.

6. "Simultaneous three channel ECG data acquisition system and QRS detector for ambulatory monitor", revised and communicated to International Journal of Systems Science, U.K.